Terms and Conditions of Use of Digitised Theses from Trinity College Library Dublin

Copyright statement

All material supplied by Trinity College Library is protected by copyright (under the Copyright and Related Rights Act, 2000 as amended) and other relevant Intellectual Property Rights. By accessing and using a Digitised Thesis from Trinity College Library you acknowledge that all Intellectual Property Rights in any Works supplied are the sole and exclusive property of the copyright and/or other IPR holder. Specific copyright holders may not be explicitly identified. Use of materials from other sources within a thesis should not be construed as a claim over them.

A non-exclusive, non-transferable licence is hereby granted to those using or reproducing, in whole or in part, the material for valid purposes, providing the copyright owners are acknowledged using the normal conventions. Where specific permission to use material is required, this is identified and such permission must be sought from the copyright holder or agency cited.

Liability statement

By using a Digitised Thesis, I accept that Trinity College Dublin bears no legal responsibility for the accuracy, legality or comprehensiveness of materials contained within the thesis, and that Trinity College Dublin accepts no liability for indirect, consequential, or incidental, damages or losses arising from use of the thesis for whatever reason. Information located in a thesis may be subject to specific use constraints, details of which may not be explicitly described. It is the responsibility of potential and actual users to be aware of such constraints and to abide by them. By making use of material from a digitised thesis, you accept these copyright and disclaimer provisions. Where it is brought to the attention of Trinity College Library that there may be a breach of copyright or other restraint, it is the policy to withdraw or take down access to a thesis while the issue is being resolved.

Access Agreement

By using a Digitised Thesis from Trinity College Library you are bound by the following Terms & Conditions. Please read them carefully.

I have read and I understand the following statement: All material supplied via a Digitised Thesis from Trinity College Library is protected by copyright and other intellectual property rights, and duplication or sale of all or part of any of a thesis is not permitted, except that material may be duplicated by you for your research use or for educational purposes in electronic or print form providing the copyright owners are acknowledged using the normal conventions. You must obtain permission for any other use. Electronic or print copies may not be offered, whether for sale or otherwise to anyone. This copy has been supplied on the understanding that it is copyright material and that no quotation from the thesis may be published without proper acknowledgement.

A STUDY OF THE RELEASE OF THE AMPHOTERIC DRUG AMOXYCILLIN FROM BIODEGRADABLE POLYMERS

Being a thesis submitted for the degree of

Doctor of Philosophy

in

Pharmaceutics

at

University of Dublin

Trinity College

by

Ana Rosario Mollo, B.Sc. (Pharm.)

under the direction and supervision of

Owen I. Corrigan, B.Sc. (Pharm.) M.A. Ph.D. F.T.C.D.

October 1999

DECLARATION

This thesis is submitted by the undersigned to the University of Dublin for examination for the degree of Doctor of Philosophy. It has not been submitted as an exercise for a degree at any other university. I carried out all the practical work except where duly acknowledged. This manuscript was written by me with the aid of editorial advice from Prof. O.I. Corrigan.

Ana Rosario Mollo.

To my mother

SUMMARY

Poly-alpha-hydroxy-aliphatic esters constitute a group of biodegradable polymers which have been actively investigated over the past three decades for the sustained release of drug compounds. A literature review revealed that the mechanisms of drug release from these esters had not yet been established for amphoteric compounds.

Amoxycillin is a commonly used penicillin which was chosen as a model amphoteric drug, since sustained release antibiotics have potential commercial applications. Drug/polymer discs were compressed from either mechanical mixture of the raw powders (MM) or from films prepared through a solvent-evaporation procedure (SE). Four polymers of varying molecular weight and monomer composition were used in the investigation. Among the methods used to characterize the polymeric devices were differential scanning calorimetry (DSC), X-ray diffraction (XRD) and scanning electron microscopy (SEM). Drug release studies were carried out in phosphate buffer pH 5.9, with drug concentration measured by UV spectroscopy and high-performance liquid chromatography (HPLC). Polymer molecular weight and mass loss were evaluated during drug release, both in drug loaded and drug-free discs.

In general, drug release profiles were dependant on the type of polymer used, the preparative technique (i.e. MM or SE) and the drug loading. A range of physicochemical models were employed to fit the data and obtain model parameters for the prediction of the release profiles. These may have application in predicting the release of other amphoteric entities, such as peptides and proteins. For a given polymer system, at low drug loading at least two drug release phases were observed: an initial burst was followed by an induction period of negligible drug release and a final polymer-degradation-controlled phase. At higher drug loading, the release showed greater dependence with matrix diffusion.

A retardation of the polymer degradation in the presence of the amphoteric drug was identified by means of comparative studies performed on drug loaded and drug-free discs. The effect of the drug on the kinetics of polymer degradation contrasted with the previously reported effect of basic drugs whereby similar polymers degraded at a faster rate. Furthermore, an erosion mechanism consistent with the Hixson-Crowell

cube root model, and not commonly reported for poly-alpha-hydroxy-aliphatic esters, played a part at long dissolution times.

The chemical stability of the penicillin carried in the polymeric matrices was evaluated by means of extracting residual drug from discs subjected to partial release studies. A mathematical model was proposed for the estimation of *intact drug* dissolved, using parameters estimated from the profiles of *total drug* (degraded and non-degraded drug) and the degradation rate constant of pure drug in solution. The new model was subsequently modified by the inclusion of an additional parameter to account for the degradation of drug dissolved in the microenvironment of the eroding matrix. It was found that Amoxycillin's degradation rate was accelerated due to the acidification of the matrix microenvironment. The use of higher drug loadings, which promoted drug release via a non-polymer-degradation-dependant mechanism, reduced the overall proportion of drug released in a degraded form.

TABLE OF CONTENTS

Acknowledgements I

Publications and presentations associated with this thesis II

Abbreviations and symbols III

Chapter 1. Characteristics of Amoxycillin trihydrate

1.1. Physicochemical properties of Amoxycillin trihydrate 1

1.1.1. Amoxycillin trihydrate 1

1.1.2. Physical properties 3

1.1.3. Solubility 3

1.1.4. Stability 4

1.1.5. Solid state degradation 7

1.1.6. Effect of temperature on the degradation of aqueous solutions of Amoxycillin 8

1.1.7. Comparison of the physicochemical properties of Amoxycillin trihydrate and other α-amino penicillins 8

Chapter 2. Characteristics and Formulation Aspects of PLA and PLGA

2.1. Introduction 10

2.2. Synthesis of poly-alpha-hydroxy-aliphatic esters 11

2.2.1. Direct polycondensation of monomers 11

2.2.2. Ring opening polymerization of cyclic diesters 11

2.3. Morphology and Characterisation of poly-alpha-hydroxy-aliphatic esters 14

2.3.1. Parameters used to describe polymer systems 16

2.4. Degradation of poly-alpha-hydroxy-aliphatic esters 18

2.4.1. Surface Erosion and Bulk Erosion 18

2.4.2. Polymer composition and polymer molecular weight 19

2.4.3. The presence of drugs and polymer degradation products 21

2.4.4. The surrounding medium 22

2.4.5. Gamma-irradiation 24

2.4.6. Random chain scission and end-group scission 24

2.5. Formulation with poly-alpha-hydroxy-aliphatic esters 25

2.5.1. Implants 25

2.5.2. Microparticulate systems 27

2.5.3. Miscellaneous formulation techniques 28

2.6. Formulation variables affecting drug release from PLA/PLGA 29

2.7. Effects of storage on formulations prepared with PLA/PLGA 31

2.8. Behavior of poly-alpha-hydroxy-aliphatic esters *in vivo* 31

2.9. Biocompatibilitiy information and products licensed 32

Chapter 3. Mechanisms of Drug Release from PLA and PLGA Drug Delivery Systems

3.1. Introduction 34

3.2. Diffusion Mechanisms 35

3.2.1. Reservoir systems 35

3.2.2. Monolithic devices 36

3.2.3. Diffusion through the polymer matrix 37

3.2.4. Diffusion through solvent-filled pores 38

3.2.5. Percolation Theory 39

3.3. Polymer degradation controlled drug release 40

Chapter 4. Origin and Scope of the Thesis

4.1. Origin of the work 45

4.2. Objectives 46

Chapter 5. Materials and Experimental Methods

5.1. Drug, Polymers and Salts used 47

5.2. Solvents used 48

5.3. Instrumentation 49

5.4. Physicochemical characterization of powders 50

5.4.1. X-ray diffraction analysis (XRD) 50

5.4.2. Differential Scanning Calorimetry (DSC) and Thermogravimetric Analysis (TGA) 51

5.4.3. Particle Size Analysis 52

5.5. Studies performed on Amoxycillin trihydrate 52
5.5.1. Drug solubility studies 52
5.5.2. Degradation of drug in solution 53
5.5.3. Determination of water content 54
5.5.4. Effect of ambient Relative Humidity on the solid drug 54
5.5.5. Dehydration/re-hydration studies 55
5.5.6. Hot stage microscopy 56
5.5.7. Effect of the addition of D,L-lactic acid to Amoxycillin solutions on the pH of the dissolution media 56
5.6. Gel Permeation Chomatography (GPC) 56
5.7. Nuclear Magnetic Resonance (NMR) 57
5.8. Manufacture of polymer discs by mechanical mixture (MM) 57
5.8.1. Method 1: simple mechanical mixtures 57
5.8.2. Method 2: mechanical mixtures with particle size control 58
5.9 Manufacture of polymer discs by solvent evaporation (SE) 58
5.9.1. Preparation of drug loaded SE discs 58
5.9.2. Preparation of drug-free SE discs 59
5.10. Drug release experiments 59
5.11. Analysis of drug concentration 60
5.11.1 HPLC assay 60
5.11.2 UV assay 61
5.12. Drug stability inside PLA/PLGA matrices 62
5.13. Polymer mass loss studies during release experiments 62
5.13.1 Polymer mass loss from drug-free discs 62
5.13.2 Polymer mass loss from drug loaded discs 63
5.14. Swelling studies 63
5.15. Mathematical modelling of release profiles 64

Chapter 6. Characterization of Raw Materials and Preliminary Experiments

6.1. Amoxycillin trihydrate 66

6.1.1. X-ray Diffraction 66

6.1.2. Determination of water content 66

6.1.3. Thermal Analysis 67

6.1.4. Dehydration/re-hydration experiments 69

6.1.5. Constant Relative Humidity experiments 70

6.1.6. Particle size analysis 70

6.1.7. Hot stage microscopy 71

6.2. Analysis of Amoxycillin concentration

6.2.1. Examination of the HPLC method as a stability indicating assay 72

6.2.2. UV spectroscopy for the quantification of total drug 72

6.3. Drug solubility studies 74

6.4. Drug degradation studies 75

6.4.1. Effect of the pH of the media on the degradation rate 75

6.4.2. Degradation pattern (HPLC) 77

6.4. Characterization of polymers 79

6.4.1. X-ray Diffraction of polymers 80

6.4.2. Particle size analysis of polymers 80

6.4.3. Gel Permeation Chromatography 80

6.4.4. Thermal analysis of polymers 81

6.6. Filmcasting studies 83

6.6.1. Solvents tested for filmcasting 83

6.6.2. Drug distribution in polymer films 85

Chapter 7. RG 503 and RG 504 Systems

7.1. Introduction 86

7.2. RG 503 systems prepared by mechanical mixture (MM systems) 87

7.2.1. Physicochemical and morphological characteristics of RG 503 MM systems 88

7.2.2. Preliminary drug release studies with RG 503 MM discs prepared by Method 1 92

7.2.3. Long-term studies with RG 503 MM discs prepared by Method 1 104

7.2.4. Studies with RG 503 MM discs prepared by Method 2 109

7.3. RG 503 systems prepared by solvent evaporation (SE systems) 117

7.3.1. Physicochemical and morphological characteristics of RG 503 SE systems 117

7.3.2. Drug release studies with RG 503 SE discs 123

7.3.3. Polymer mass loss studies with RG 503 SE discs: drug-free and drug loaded discs 126

7.3.4. Preliminary stability tests on RG 503 formulations 129

7.3.5. RG 503 SE versus RG 503 MM 130

7.4. RG 504 systems prepared by solvent evaporation (SE systems) 131

7.4.1. Physicochemical and morphological characteristics of RG 504 SE systems 132

7.4.2. Drug release studies with RG 504 SE discs 133

7.4.3. Polymer mass loss studies with RG 504 SE discs: drug-free and drug loaded 136

7.5. RG 503 versus RG 504 systems 139

7.6. Conclusions 141

Chapter 8. RG 755 and R 203 Systems

8.1. Introduction 143

8.2. RG 755 systems prepared by mechanical mixture (MM systems) 143

8.2.1. Physicochemical and morphological characteristics of RG 755 MM systems 143

8.2.2. Drug release from RG 755 MM discs 145

8.2.3. RG 755 versus RG 503 MM discs 148

8.3. RG 755 systems prepared by solvent evaporation (SE systems) 150

8.3.1. Physicochemical and morphological characteristics of RG 755 SE discs 150

8.3.2. Drug release studies with RG 755 SE discs 155

8.3.3. RG 755 MM versus RG 755 SE discs 164

8.3.4. Polymer mass loss studies with RG 755 SE discs: drug-free and drug loaded discs 165

8.4. R 203 discs prepared by solvent evaporation (SE systems) 170

8.4.1. Physicochemical and morphological characteristics of R 203 SE discs 170

8.4.2. Drug release from R 203 SE discs 172

8.4.3. Polymer mass loss studies with R 203 SE discs: drug-free and drug loaded 175

8.5. Conclusions 177

Chapter 9. Stability aspects of PLA and PLGA formulations containing Amoxycillin

9.1. Introduction 178

9.2. Stability of Amoxycillin in PLA/PLGA formulations 178

9.2.1. Release profiles of intact AMOX-H from RG 503, RG 504, RG 755, R 203 SE discs containing 20% drug load 178

9.2.2. Quantification of the amount of intact Amoxycillin released from RG 503 SE systems containing between 10% and 30% drug loading 182

9.2.3. Quantification of the amount of intact Amoxycillin released from RG 755 SE systems containing between 10% and 30% drug loading 184

9.2.4. Comparison of intact drug release profiles of RG 503 and RG 755 SE discs containing between 10% to 30% Amoxycillin load 186

9.2.5. Quantification of the amount of intact Amoxcycillin released from RG 755 SE systems containing 40%, 50% and 60% drug loading 187

9.2.6. Quantification of the amount of intact Amoxycillin released from R 203 SE systems containing 40% drug loading 189

9.2.7. Drug stability inside poly-alpha-hydroxy-aliphatic esters during drug release studies 191

9.3. Degradation of PLA/PLGA matrices in the presence and absence of Amoxycillin 192

9.3.1. pH and colour changes during drug release studies 192

9.3.2. Effect of the addition of D,L-lactic acid to Amoxycillin solutions on the pH of the media 193

9.3.3. Gel Permeation Chromatography studies on polymer discs 195

9.4. Studies performed to explore the observed effect of the drug on the

degradation of the polymer 199
9.4.1. Nuclear Magnetic Resonance studies 199
9.4.2. Effect of the drug on the pH of the medium 201
9.4.3. Swelling studies 204
9.5. The erosion of PLA/PLGA discs prepared with Amoxycillin 207
9.6. Conclusions 211

Chapter 10. General Discussion

10.1. Introduction 213
10.2. Amoxycillin Release from poly-alpha-hydroxy-aliphatic esters 214
10.2.1. Effect of the polymer molecular weight 214
10.2.2. Effect of the lactide to glycolide ratio 215
10.2.3. Effect of processing conditions 216
10.2.4. Effect of the drug loading 217
10.3. Degradation of poly-alpha-hydroxy-aliphatic esters 218
10.3.1. Polymer degradation dependant drug release 218
10.3.2. The effect of the drug on the kinetics of polymer degradation 219
10.3.3. Surface Erosion of poly-alpha-hydroxy-aliphatic esters 222
10.4. Interaction between Amoxycillin and PLA/PLGA 225
10.4.1. pH dependent degradation 225
10.4.2. Possible reaction between Amoxycillin and poly-alpha-hydroxy-aliphatic esters 226
10.5. The degradation of Amoxycillin in the presence of poly-alpha-hydroxy-aliphatic esters 228
10.5.1. Changes occurring in the discs and in the dissolution medium 228

10.5.2. The prediction of intact drug released 233
10.6. Conclusion 238

References 241

Appendices 253

ACKNOWLEDGEMENTS

I would like to extend my thanks to the following people:

My Supervisor, Professor Owen I. Corrigan, for his patience, continuous guidance and much valued expertise.

Dr. Caitriona O'Driscoll for always supporting my work and for her friendship.

Bio Research Ireland who funded this project and provided a grant for myself. Special thanks to Dr. Margaret Woods for her commitment to Research.

The academic and technical staff of the School of Pharmacy, Dr. Majella Lane, Dr. John Walsh, Teresa Sweeny, Mary Reilly, Pat Quinlan, Brian Canning, Derek Bell. Special thanks to Dr. Anne-Marie Healy and Dr. John Gilmer for their friendship and advice.

Dr. John O'Brien from the Chemistry Department for his help with the NMR work. The staff in the Electron Microscopy unit, David John, Colin Reid and Adrienne, and Dr. David Doff from Geology, for his help with XRD.

The Postgrads, for making the best out of my years in Trinity. Thanks to the "oldies", still remembered: Rachel, Mark, Clare, Abina, Janet, Michelle, Idris, my lab partner Karen G.; and to those who shared my times of writing-up, for their encouragement: Colleen, Nicole, Denis, Brendan, Sally-Anne, Catriona, Stephen, Shane, Len, Tina, Sheila and the Chemistry crowd. Thanks to Louise for so many good times. Thanks to my lab partner Bronagh, for being great. Thanks to Karen O.C. for proof-reading most of the chapters in this work.

My friends in Buenos Aires for always keeping in touch: Celia, Claudia, Maria Julia, Ines and Carina. For so many adventures and 15 years of friendship.

Finally, I would like to thank my family:

My boyfriend Adrian, who is now my husband, for asking me to follow him to Ireland, and for contacting the School of Pharmacy. For his love and support, for the endless conversations on varied pharmaceutical subjects.

My brother, Fernando, for his support throughout my life. Thanks to his girlfriend, Rosana, for her friendship.

My granny, Ana, for always believing in what I do. For her many, many good wishes. Thanks to Osvaldo and Juan Carlos, for their love.

My mother, Beatriz, for her love and unconditional support, for always giving me great opportunities in my life.

PRESENTATIONS ASSOCIATED WITH THIS THESIS

"Release of Amoxycillin from Poly(D,L-lactide-co-glycolide) biodegradable matrices: I", in Proceedings of 21st Annual Joint Research Seminar, The Schools of Pharmacy, Queen's University of Belfast, March (1996), R. Mollo and O.I. Corrigan. **Poster Presentation.**

"An Investigation of the Release of Amoxycillin from PLGA Biodegradable Matrices", R. Mollo and O.I. Corrigan, in Proceedings of the 17th Pharmaceutical Technology Conference, Dublin, March (1998), vol. I, pp. 184-192. **Poster Presentation.**

"Release of Amoxycillin from Poly(D,L-lactide-co-glycolide) biodegradable matrices: II", 23rd Annual Joint Research Seminar, The Schools of Pharmacy, Queen's University of Belfast, March (1999), R.Mollo and O.I. Corrigan. **Oral Presentation.**

ABBREVIATIONS AND SYMBOLS

AMOX	Amoxycillin
AMOX-H	Amoxycillin trihydrate
cm	centimeters
cpm	counts per minute
C_o	intrinsic solubility of drug
C_s	saturated solubility of drug
DCM	dichloromethane
dH	enthalpy change
D_m	diffusion coefficient of drug in polymeric membrane
D_w	diffusion coefficient of drug in water
DSC	differential scanning calorimetry
GPC	gel permeation chromatography
G_1, G_2, G_3	shape factors
f_b	fraction of drug in solution arising from release by an exponential mechanism
f_P	fraction of drug in solution arising from release by polymer degradation
F_i	fraction of drug released by a non-degradation controlled mechanism
f_t	fraction of solute released at time t by surface erosion
Fb_∞	fraction of drug released in the burst phase at time infinity
Fd_∞	fraction of drug released by diffusion at time infinity
F_{tot}	fraction of total drug released at time t
$\frac{df_{TOTAL}}{dt}$	change of total intact drug concentration arising from the burst and the polymer degradation controlled release phases

ABBREVIATIONS AND SYMBOLS (continued)

GPC	gel permeation chromatography
h	hour
h_i	half of the initial disc height
k_b	first order release rate constant
k_r	Cobby release rate constant
k_{deg}	drug degradation rate constant
k_{degb}	degradation rate for drug arising in solution during the burst release phase
k_{degP}	degradation rate for drug arising in solution during the polymer controlled release phase
k	polymer degradation rate constant determined from drug release profiles
k_P	polymer degradation rate constant determined from polymer mass loss profiles
k_2	surface erosion rate constant
K_H	Higuchi rate constant
MM	mechanical mix
M_w	weight average molecular weight
M_n	number average molecular weight
M_v	viscosity average molecular weight
min	minutes
mm	millimetres
MSC	model selection criterion
n	number of arguments in a sample/experiment
η	intrinsic viscosity
n.a.	non applicable
NMR	nuclear magnetic resonance
P	polydispersity
PLA	poly-lactide
PLGA	poly-lactide-co-glycolide

ABBREVIATIONS AND SYMBOLS (continued)

r_i	initial radius
SD	standard deviation
SE	solvent evaporate
t	time
t_{lag}	lag-time prior to onset of surface erosion
t_{max}	time to 50% drug release via polymer degradation estimated from drug release data
t_{maxP}	time to 50% drug release via polymer degradation estimated from polymer mass loss
SD	standard deviation
$T_{50\%}$	time to 50% desorption of the total drug load
T_g	glass transition
µ or mcg	micrograms
µm	micrometres
V_i	initial volume
V_t	volume at time t
W_i	initial weight
W_d	dried weight
W_t	weight at time t
x	fraction of drug released via polymer degradation at time t
$xtot$	total fraction of drug released via polymer degradation
XRD	X-ray diffraction
$\cong$	approximately equal to

CHAPTER 1. CHARACTERISTICS OF AMOXYCILLIN TRIHYDRATE

1.1. PHYSICOCHEMICAL PROPERTIES OF AMOXYCILLIN TRIHYDRATE

1.1.1. Amoxycillin trihydrate

Penicillins and cephalosporins have become the most frequently prescribed antibacterial drugs during the past decades. Together with more recently developed analogues, e.g. penems and monobactams, the compounds are referred to as β-lactam antibiotics, due to the common β-lactam ring structure, which is essential for antibacterial activity. AMOX-H, similar to the other penicillins, contains a structure called 6-amino-penicillanic acid (6-APA). Figure 1.1 shows the general structure of penicillins (Van Krimpen et al., 1987).

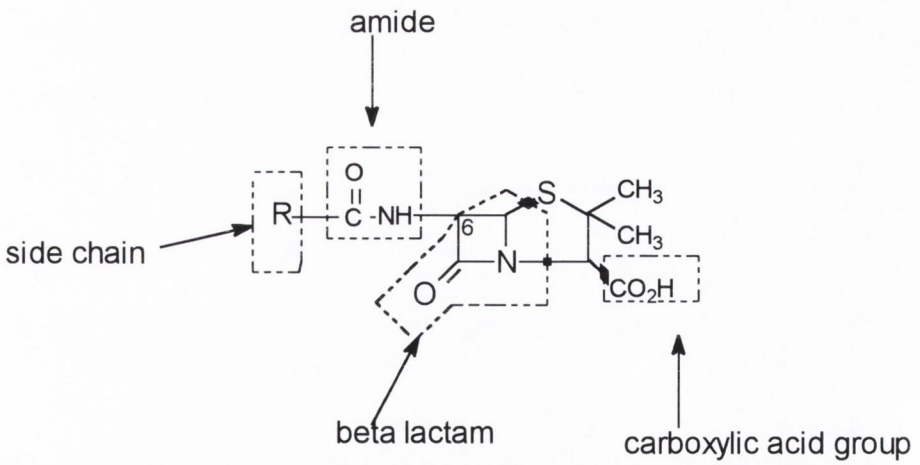

Figure 1.1. General structure of penicillins.

In addition, AMOX-H features a reactive α-amino group constituent of the acyl-amido side-chain at position 6. The amphoteric nature of AMOX-H is due to its constituent

acidic and basic moieties. The carboxylic group at position 3 is responsible for the acidic properties of the drug, with a pK_a of 2.67, (Tsuji et al.1978). The pK_a of the N-atom of the beta-lactam ring is 7.11 and that of the phenolic group in the side-chain is 9.55, Tsuji et al. (1978). Other amphoteric penicillins studied by Tsuji et al. include: Ampicillin anhydrate, Cyclacillin anhydrate and Epicillin anhydrate.

According to the Merck Index, 12th edition, various chemical names are used to describe Amoxycillin, also known as Amoxicillin (official name given by the British Pharmacopoeia 1999). Common names include 6-[D(-)-α-amino-p-hydroxyphenyl acetamido] penicillanic acid and p-hydroxyampicillin.

The drug is available in the anhydrous and the trihydrate forms. It is also available as the sodium salt. The trihydrate form and the sodium salt are currently used in the manufacture of pharmaceutical products. Figure 1.2 shows a representation of the two structures.

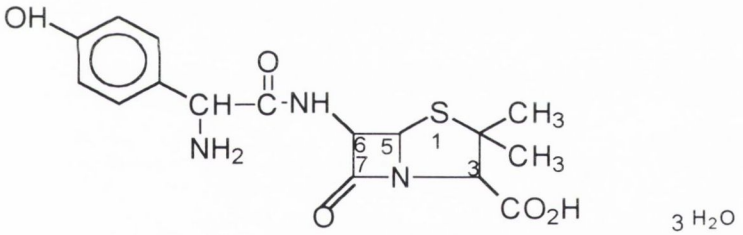

(a) Amoxycillin trihydrate $C_{16}H_{19}N_3O_5S.3H_2O$

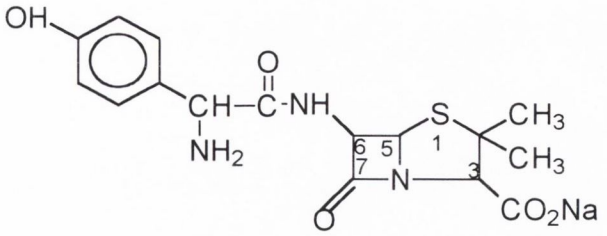

(b) Amoxycillin Sodium $C_{16}H_{19}N_3NaO_5S$

Figure 1.2. Structure of Amoxycillin trihydrate (a) and Amoxycillin sodium (b).

1.1.2. **Physical Properties**

AMOX-H is a white or almost white odourless powder constituted by crystals that present birefringence (British Pharmacopoeia). Van Krimpen et al. (1987) explained that the absorption at wavelengths longer than 230 nm is due to the structure of the side-chain. In ethanol, AMOX exhibits maximum absorption (λ_{max}) at 230 nm and at 274 nm, reported by Bhattacharyya and Cort (1978). The authors also recorded the infrared (IR) and the proton-nuclear magnetic resonance (^{1}H-NMR) spectra of the drug. The latter was obtained with a sample of the drug in D_2O.

X-ray diffraction was used in the characterization of the crystal structure of the trihydrate. Bhattacharyya and Cort (1978) reported that the main signals were observed at two theta values of 15.13°, 16.25°, 20.20°, 25.76°, 26.68° and 28.71°.

1.1.3. **Solubility**

AMOX-H exhibits lowest aqueous solubility in the pH range between 5 and 6 (Tsuji et al., 1978). AMOX-H sodium exhibits higher aqueous solubility than AMOX-H. The Merck Index, 12th Edition states that approximately 4 mg of the trihydrate form dissolve in 1 ml of water. Table 1.1 lists solubility values for AMOX-H in various organic solvents.

Table 1.1. Solubility of AMOX-H in various organic solvents (The Merck Index, 12th Edition).

Solvent	Solubility (mg/ml)
Methanol	7.5
Ethanol (absolute)	3.4
Acetone	1.3
Ethyl Acetate	INSOLUBLE
Hexane	INSOLUBLE
Acetonitrile	INSOLUBLE
Benzene	INSOLUBLE

1.1.4. **Stability**

The degradation of AMOX-H in aqueous solutions at a concentration of $5x10^{-3}$ M units was reported to follow first order kinetics (Tsuji et al., 1978). It is recognized that the introduction of the electron withdrawing α-amino group in the side-chain of AMOX-H reduces acid degradation (Tsuji et al., 1978, and Van Krimpen et al., 1987). In neutral to alkaline solution the α-amino group greatly increased the rate of hydrolysis.

The rate of degradation was reported to increase along with the buffer capacity increase (Tsuji et al., 1978), particularly at low pH values. The experiments were carried out using different citrate buffer strengths at various pHs. The maximum stability pH was approximately 6.

The degradation of penicillins in acid medium (Van Krimpen et al., 1987) leads to three primary degradation products. Figure 1.3 is a schematic representation of the primary degradation products all converted into benzylpenicilloic acid, when benzylpenicillin was used as a model compound. The degradation in neutral and alkaline medium (Van Krimpen et al., 1987) is represented in figure 1.4. β-lactam antibiotics containing an α-amino group in their side-chain can undergo self-aminolysis (Van Krimpen et al., 1987), as shown in figure 1.5. This is an intermolecular reaction resulting in the formation of an oligomer, which can follow simultaneously more than one reaction pathway.

The degree and rate of polymerization increases with increased initial concentration and higher pH values. The degree and rate of polymerization depend also upon the structure of the alpha-amino penicillin. The following is the rank order (from highest to lower polymerization) reported by Tsuji et al. (1978):

Amoxycillin > Epicillin > Ampicillin > Cyclacillin.

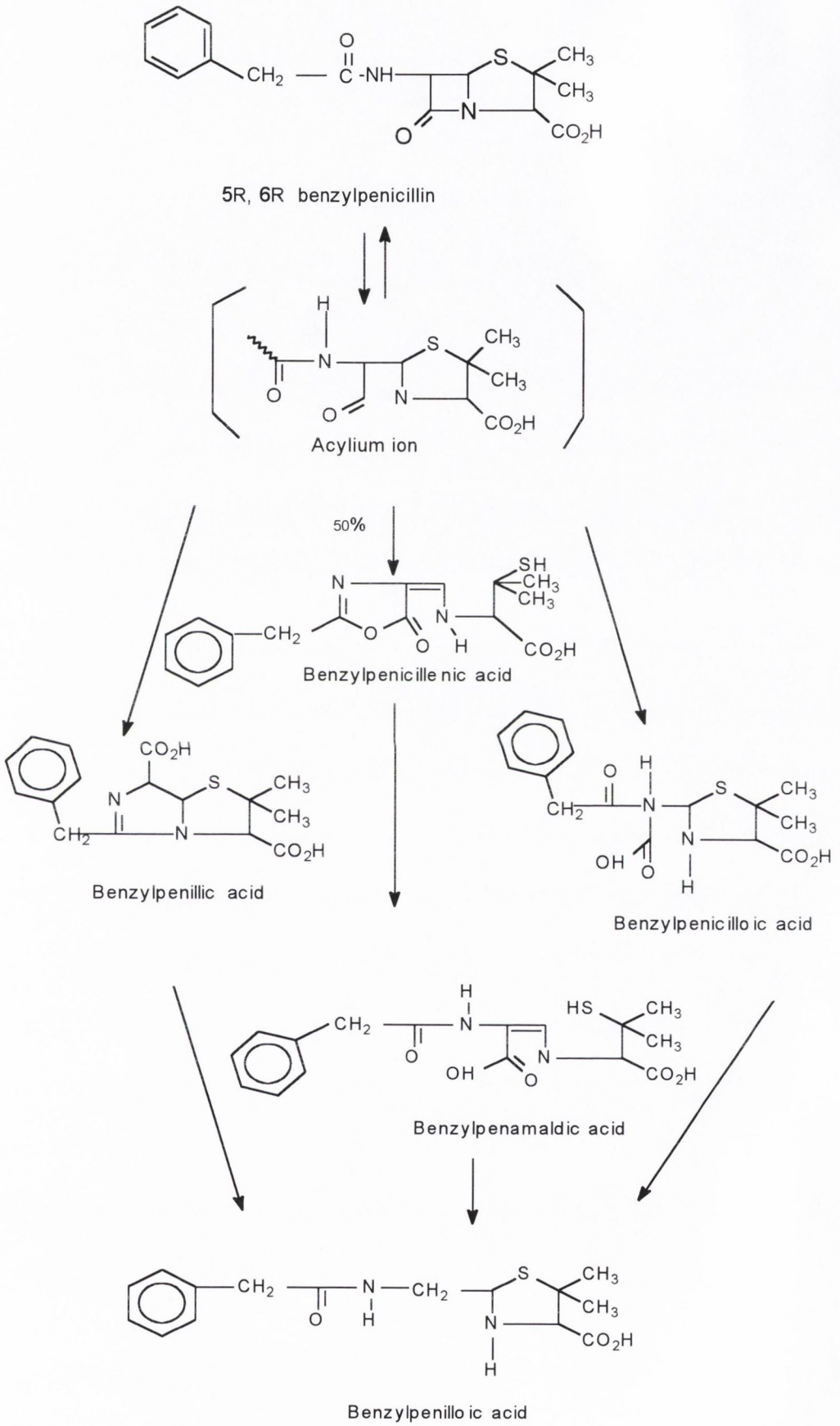

Figure 1.3. Degradation of penicillins in acid medium.

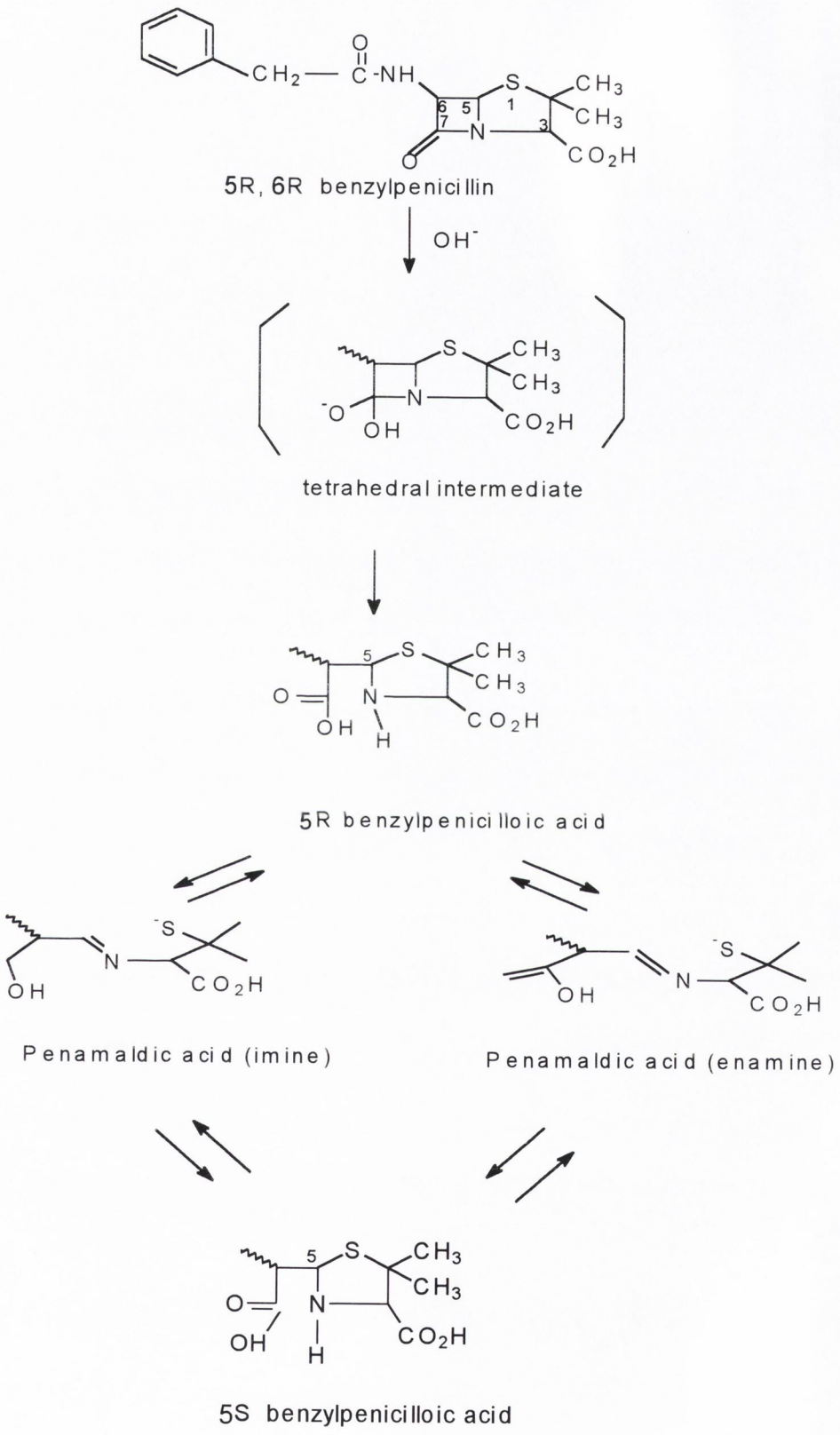

Figure 1.4. Degradation of penicillins in neutral and alkaline medium.

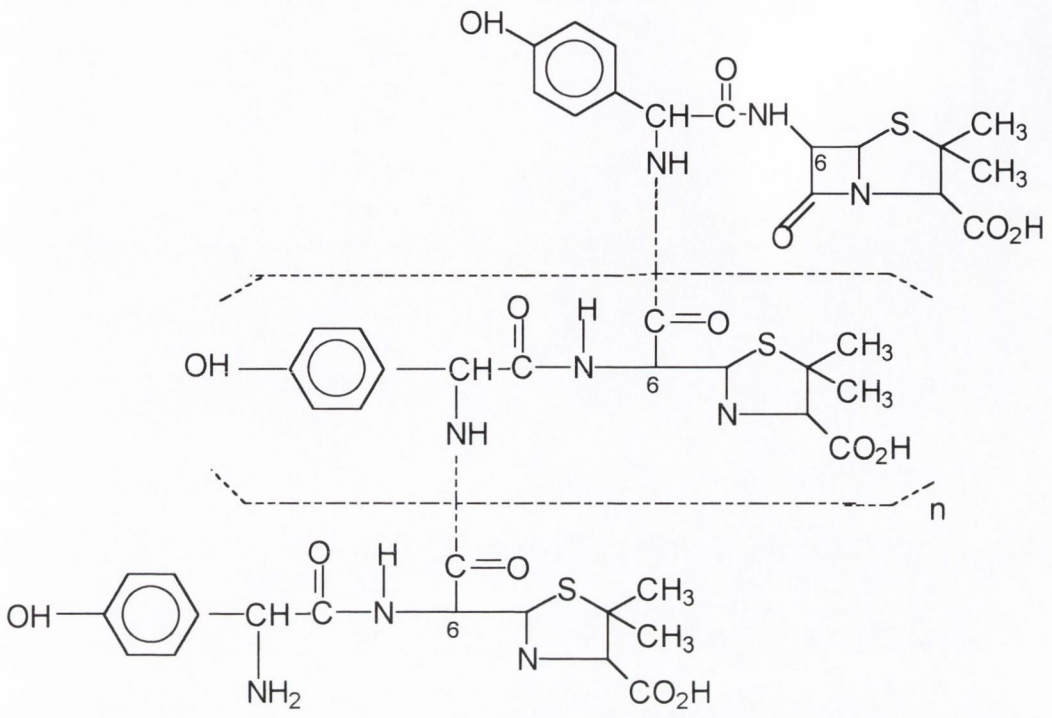

Figure 1.5. Structure of an oligomer of Amoxycillin, taken from the European Pharmacopeia, 1998.

1.1.5. **Solid state degradation**

Mendez et al. (1989) studied the degradation of AMOX-H in the solid state. They showed that the time for 10% of AMOX-H to degrade at 20°C was 3 years, while only 1.25 years for the sodium salt. The effect of temperature on the solid state degradation of AMOX-H was investigated for the range between 37°C and 110°C for up to 1400 hours. Semilogarithmic plots of residual drug (%) versus time were sigmoidal for temperatures higher than 50°C and followed the Prout-Tomkins model.

Some of the degradation products identified by Mendez et al. (1989) using HPLC were Amoxicilloic acid and piperazine-2,5-dione. They observed that the piperazine peak increased with time, while the Amoxicilloic acid decreased. When degradation of the sample was advanced, many small peaks appeared which possibly corresponded to

dimeroates, trimeroates, tetrameroates, trimers and tetramers. A mechanism of successive reactions in two steps was proposed to describe the solid state degradation of the drug, where the first product serves as substrate for the second product.

Thermodynamic data for AMOX was found in The Merck Index (12^{th} edition) for the hydrochloride form, which browns at 90°C, then dehydrates, and finally decomposes at 216-218°C.

1.1.6. **Effect of temperature on the degradation of aqueous solutions of Amoxycillin**

A study performed on the stability of the drug in normal saline and glucose (5%) determined that the maximum stability of the solutions examined was at 0°C in normal saline, with a shelf-life of 252 h, and at -26°C in glucose (5%) with a t_{90} value of 25.5 h (Mc Donald et al., 1989).

A study by Concannon, et al. (1986) recommended that aqueous solutions of Amoxycillin sodium should be stored below -30°C.

1.1.7. **Comparison of the physicochemical properties of Amoxycillin trihydrate and other α-amino penicillins**

AMOX-H constitutes a compound of interest due to its wide spectrum of antibacterial activity, often used for veterinary purposes (Van Krimpen et al., 1987). It has been reported (Tsuji et al., 1978) that the intrinsic solubility (C_0) (solubility of the electrically neutral form), dissolution rate and degradation rate of the trihydrate form are lower than those of Ampicillin trihydrate. Comparison with other amphoteric penicillins is shown in tables 1.2 and 1.3.

Table 1.2. Intrinsic solubility (C_0) of various alpha-amino penicillins at 37°C and ionic strength (μ) of 0.5 units (Tsuji et al., 1978).

Amino Penicillin	Solubility, $10^2 C_0$, M
Epicillin anhydrate	1.20
Amoxycillin trihydrate	1.30
Ampicillin anhydrate	3.97
Ampicillin trihydrate	2.23
Cyclacillin anhydrate	8.90

Table 1.3. Rate constants (k_H and k_{OH}) for the degradation of various alpha-amino penicillins at 35°C and ionic strength (μ) 0.5 units (Tsuji et al., 1978).

Penicillin	k_H, M^{-1} h^{-1}	10^{-3} k_{OH}, M^{-1} h^{-1}
Epicillin	1.35	1.23
Amoxycillin	1.68	1.16
Ampicillin	1.82	2.57
Cyclacillin	4.61	1.10

CHAPTER 2. CHARACTERISTICS AND FORMULATION ASPECTS OF PLA AND PLGA

2.1. INTRODUCTION

A variety of polymers are currently used as excipients for the sustained release of drugs. Heller (1993) classified non-degradable and degradable polymers according to their hydrophilic/hydrophobic properties, as shown in table 2.1. When implanted, non-degradable systems require surgical removal once delivery of the drug is complete. In applications where this is not important the use of non-degradable polymers, such as silicone elastomers, has been a useful means of achieving sustained delivery.

Table 2.1. Polymers currently investigated for controlled parenteral delivery of peptides and proteins.

	Non-degradable	Degradable
Hydrophilic	polyacrilamide hydrogels	crosslinked N-vinyl pyrrolidone; *crosslinked water soluble polyesters;
Hydrophobic	ethylene vinyl acetate co-polymer; silicone elastomers	lactide/glycolides; lactone co-polymers; poly(ortho esters); polyanhydrides

* The preparation of these systems from fumaric acid and poly(ethylene glycol) is described by Heller (1983).

The work of this thesis concentrates on lactide/glycolide polymers. Since approximately 1970 there has been considerable interest on these polymers as biodegradable materials in dental, orthopaedic and drug delivery (Gilding and Reed, 1979).

For the purpose of this work, the term 'poly-alpha-hydroxy-aliphatic esters' refers to poly-lactide (PLA), poly-glycolide (PGA) and poly-lactide-co-glycolide (PLGA).

2.2. SYNTHESIS OF POLY-ALPHA-HYDROXY-ALIPHATIC ESTERS

2.2.1. Direct polycondensation of monomers

The synthesis of homo-polymers by simple polycondensation of either lactic or glycolic acid using antimony trioxide, resulted in compounds of low molecular weight (Gilding and Reed, 1979). Fukuzaki et al. (1989) produced low molecular weight D,L-lactide by direct polycondensation in the absence of a catalyst at 200°C and in a N_2 atmosphere.

2.2.2. Ring opening polymerization of cyclic diesters

The preferred method for producing high molecular weight polymers is the ring opening polymerization of the cyclic diester (glycolide or lactide). The reaction takes place by heating with an acidic catalyst such as $SnCl_4$ (Heller, 1993). The synthesis is shown in figure 2.1.

Frazza and Schmitt (1971) proposed a mechanism for the production of polyglycolide (and polylactide) from the cyclic diesters, using tin catalysts and lauryl alcohol as a chain modifier, as shown in figure 2.1

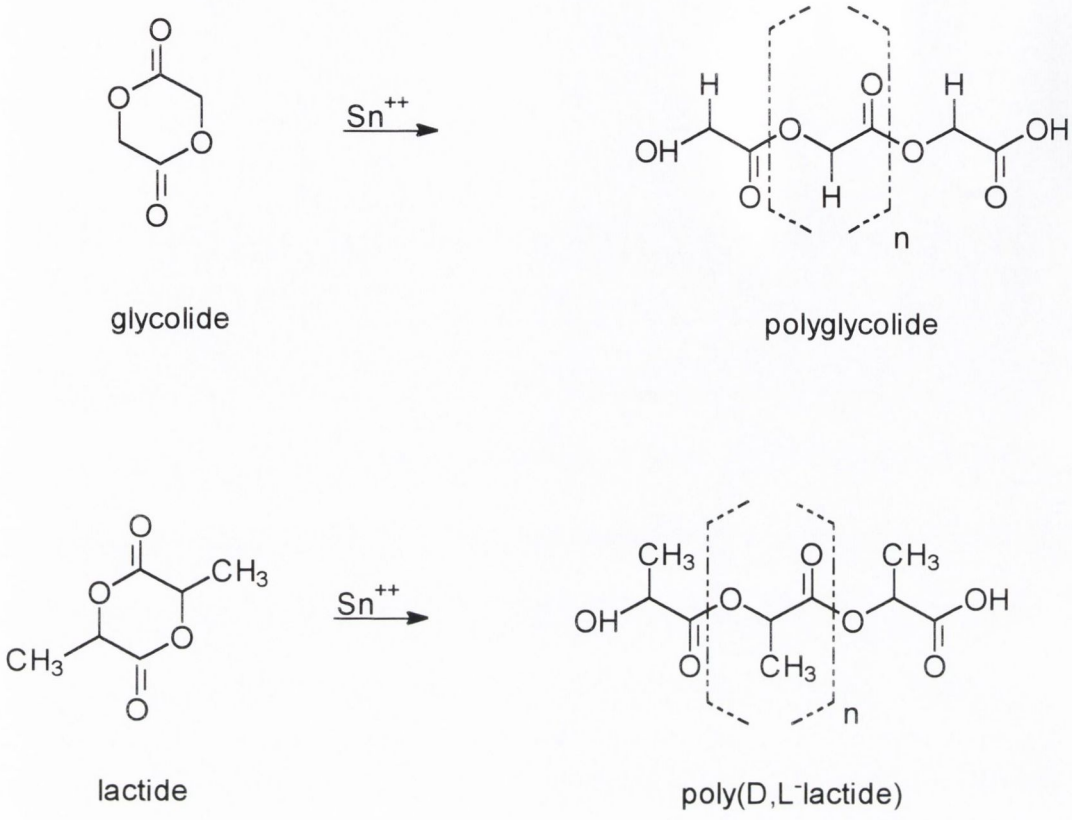

Figure 2.1. Ring opening polymerization of the cyclic diesters glycolide and lactide to form the corresponding homo-polymers, polyglycolide and poly(D,L-lactide).

A set of homopolymerizations of glycolide were carried out by Gilding and Reed (1979) to gain insight into the rate of conversion and changes in molecular weight distribution as a function of the reaction time. The results obtained for % conversion versus time indicated that 80% conversion takes place within the first 30 minutes. After 4 hours, 96% is the maximum polymerization that takes place. The molecular weight results of polymer fractions characterized by gel permeation chromatography indicated a range of propagation rates. They suggested that the broadening in molecular weight distribution at 94-96% conversion was indicative of transfer polymerization between chains, resulting in longer and shorter chains.

Copolymers of lactic and glycolic acids are prepared by polymerizing an appropriate mixture of lactide and glycolide in a similar reaction to that previously described for the homo-polymers. Gilding and Reed calculated the relative reactivity of each monomer in a series of copolymerizations. The % conversion and % composition of the copolymers were obtained by thermogravimetric analysis. The results showed that the copolymers initially obtained were considerably richer in glycolide compared to the starting monomer mix. It was concluded that glycolide was preferentially polymerized at low conversions, with lactide increasingly incorporated as the glycolide depleted. Further investigation was performed using various monomer ratios in the initial mixture, resulting in the synthesis of copolymers of broad compositional range.

The conditions of reaction have been found to affect the characteristics of the polymers obtained. Avgoustakis and Nixon (1991) reported that during preliminary experiments the recrystallization process was found to affect the polymerization. Significant variation was obtained in the inherent viscosity of polymers synthesized under similar conditions with different catalysts, whereby stannous octoate produced polymers of higher viscosity compared to antimony trifluoride. Moreover, the effect of catalyst concentration also determined the molecular weight of the product. Avgoustakis and Nixon also studied the effect of temperature on the polymerization reaction. It appeared that higher molecular weights were obtained with the lower temperature investigated (130°C). These workers reported that the inclusion of lauryl alcohol in the polymerization mixture caused both a lowering of the molecular weight and percentage yield. This was in disagreement with the earlier reports by Schmitt et al. (1969) that indicated an acceleration of the polymerization reaction in the presence of lauryl alcohol.

De Luca (1993) explained that often 'polyglycolic acid and polylactic acid' are used interchangeably with 'polyglycolide and polylactide'. The latter should only be used to describe polymers prepared from the cyclic dimers, in contrast to those obtained by direct polycondensation.

2.3. MORPHOLOGY AND CHARACTERIZATION OF POLY-ALPHA-HYDROXY-ALIPHATIC ESTERS

Gilding and Reed (1979) investigated the mechanism of polymerization of glycolide and lactide by means of characterization methods applied to the products obtained at different reaction times. Such methods also served the purpose of identifying optimum reaction conditions and admixtures that would produce copolymers with particular characteristics. For instance, gel permeation chromatography determinations showed increased molecular weights as the glycolide content increased. X-ray diffraction analysis showed a certain degree of crystallinity for PGA and PLA, while poly-D,L-lactide was completely amorphous. Copolymer composition determines the degree of crystallinity. Gilding and Reed examined polymers with different ratios of monomers. Glass transition temperatures (T_g) were exhibited by all the polymers investigated. Such transitions represent the temperature at which the polymer changes from the glassy state to a more flexible state. Differential scanning calorimetry (DSC) showed that PGA, PLA and PGLA (90:10) presented glass transition temperatures followed by a crystallization exotherm and a melting endotherm. In contrast, the (30:70), (50:50) and (70:30) glycolide/lactide copolymers presented by Gilding and Reed, were found to be amorphous, with DSC thermograms that exhibited glass transitions only. Examination of T_g, melting and crystallinity as a function of composition showed that the range of glycolide/L-lactide copolymers with compositions from 25-70 mol % glycolide are amorphous. The amorphous region extended from 0-70mol% glycolide when the D,L-lactide isomer was used.

Free volume, permeability and chain mobility are higher above the T_g. This means that formulations prepared with low molecular weight polymers displaying a T_g below 37°C, would present significant differences in their in vivo drug release rates compared to higher molecular weight systems.

The effect of copolymer composition on T_g can be estimated by the following equation (Pitt and Schindler, 1980):

$$\left(1/T_g\right)_{AB} = \left(W/T_g\right)_A + \left(W/T_g\right)_B \qquad \text{equation 2.1}$$

where W represents the weight fraction of each monomer A and B in the co-polymer. This equation was shown to be valid when examining the variation of T_g of co-polymers of caprolactone and D,L-lactide as a function of D,L-lactide.

Ford and Timmins (1989) have explained the effects of quenching and annealing on the thermal history of a sample and the importance of standardizing the thermal history of a polymer prior to its analysis. For instance, samples annealed at 45°C showed an endothermic peak at their T_g, but samples which had been rapidly quenched showed only an endothermic inflection. This was attributed to a stress relaxation phenomenon that occurred within the polymer when allowed to stabilize. Gilding and Reed (1979) reported that amorphous polymers partially crystallized over 24-72 hours when placed in water (or buffer). Crystalline compositions are necessary in cases where mechanical integrity needs to be sustained, such as sutures and orthopaedic or dental applications. However, as soon as hydrolysis begins to disrupt the grain boundaries, tensile strength decreases.

Avgoustakis and Nixon (1991) characterized their polymers by DSC. Because D,L-lactide was used, all copolymers produced were amorphous, showing only a glass transition temperature. Amorphous polymers are preferable in drug delivery since the active can be homogeneously dispersed in a monophasic matrix. The authors reported an increase in molecular weight with an increase in the T_g. An increase in the lactide content also increased the T_g. The increased number of methyl side groups in those polymers containing higher lactide content was thought to contribute to an increase in the difficulty of molecule rotation.

Schartel et al. (1997) suggested that not only the molecular weight but also the polydispersity of the polymer influences drug release from PLGA systems. Some properties, e.g. tensile and impact strength, are specifically governed by the short molecules. The authors explained that thermodynamic properties can be described by an equation of the type

$$Z = Z_0 - A/M_n \qquad \text{equation 2.2}$$

where Z is the value of a specific property, Z_0 is the asymptotic value at a very high molecular weight, A is a constant and M_n is the number average molecular weight. Based on equation 2.2 the authors postulated that by means of a reduction in the number of short molecules, changes in physical properties could improve the release of hydrophilic and low molecular weight drugs. The removal of short molecules by ultrafiltration of the polymers resulted in reduced hydrophilicity of the polymers and less water uptake during drug release studies. Employing dielectric measurements, it was found that the glass transition shifts to a higher temperature value as the low molecular weight fraction in the polymer is reduced. The dielectric investigations allowed a quantitative interpretation of molecular motions taking place in the polymer carrier within the temperature range of its application. Dynamic mechanical thermal analysis (DTMA) was applied to the investigation of dynamic-mechanical properties of two PLGA polymers supplied by Boehringer Ingelheim (RG 503 M_w 39,500; RG 505 M_w 69,000) treated by ultrafiltration in dichloromethane to remove the short chains. The ultrafiltration procedures resulted in copolymers of higher molecular weight, higher molecular number and lower polydispersity. A more rapid mass loss was observed for those polymers of lower polydispersity. At the glass transition temperatures the rigidities of RG 503 (treated by ultrafiltration and untreated) declined rapidly and as the temperature increased, the polymers appeared 'in a rubbery flow', or even liquid state, corresponding to another transition of amorphous polymers. At temperatures below the T_g, only vibrations of atomic groups exist in the glassy polymer, independently of the chain length, i.e. molecular weight and polydispersity. Above the T_g, the amorphous polymer is in the rubbery state, and the chain entanglement becomes important. The positions of two transitions (glassy to rubbery and rubbery to liquid) and the length of the region between these two transitions are dependent on the molecular weight and polydispersity of the polymer.

2.3.1. **Parameters used to describe polymer systems**

Several important parameters are used to describe polymer systems. The most common of these are the number-average molecular weight (M_n) and the weight-

average molecular weight (M_w), represented by equations 2.3 and 2.4, respectively, as defined by Painter and Coleman (1994):

$$M_n = \frac{\sum N_i M_i}{\sum N_i} = \sum X_i M_i \qquad \text{equation 2.3}$$

$$M_w = \frac{\sum N_i M_i^2}{\sum N_i M_i} = \frac{\sum W_i M_i}{\sum W_i} \qquad \text{equation 2.4}$$

where M_i is the molecular weight or molar mass of a molecule corresponding to a degree of polymerization i (consisting of i monomer units of a given molecular weight M_o) and N_i and W_i are the total number and weight of molecules of length i, respectively. X_i is the number fraction or mole fraction, defined as $N_i/\Sigma N_i$.

The number average M_n is obtained by "sharing" the total weight of all the species equally amongst each of the species. The weight average, in contrast, takes into account the weight of each species. Therefore, M_w is always greater than M_n, except for the uncommon case of a monodispersed polymer (composed entirely of one molecular weight). The polydispersity P of a polymer can be calculated by equation 2.5:

$$P = M_w / M_n \geq 1 \qquad \text{equation 2.5}$$

Polymer molecular weight can also be estimated through intrinsic viscosity (η) determinations. The viscosity average molecular weight M_v of a polymer is obtained using the Mark-Houwink equation:

$$\eta = KM_v^a \qquad \text{equation 2.6}$$

where K and a are constants that vary with the nature of the polymer, the solvent and the temperature. The values of molecular weight obtained through this method are not absolute.

Gallagher and Corrigan (1998) determined the η ($\cong$ 0.5 dl/g) of RG 504 and used equation 2.6 to calculate the M_v which was reported as 13,070.

2.4. DEGRADATION OF POLY-ALPHA-HYDROXY-ALIPHATIC ESTERS

Polymer degradation has been defined as "the chain scission process that breaks polymer chains down to oligomers and finally into monomers" (Göpferich, 1996). Degradation is part of the erosion process, which is the loss of material from the polymer bulk. The erosion process also involves water uptake and mass transfer. Passive hydrolysis is the main mechanism of degradation for synthetic polymers. The rate of hydrolysis is largely dependent on the chemical structure of the polymer, the type of neighboring groups to the polymer bonds and the pH. Hydrolysis can be catalyzed by either acidic or basic components.

Amorphous polymer regions are more susceptible to degradation and erosion than the crystalline ones (Li et al., 1990). Amongst other factors, crystallinity changes during erosion can occur due to the crystallization of degradation products (Li et al., 1992).

2.4.1. Surface erosion and bulk erosion

Polymer erosion has been classified as surface (or heterogeneous) erosion and bulk (or homogeneous) erosion (Langer and Peppas, 1983). If the diffusion of water into the polymer is faster than the degradation of the polymer bonds, the polymer may swell

prior to erosion (bulk erosion). If polymer degradation is faster than water ingress, polymer swelling may be of minor importance (surface erosion). During erosion, the surface eroding polymer shrinks in its dimensions. In contrast, the matrix geometry of bulk eroding polymer does not change for a substantial length of time. De Luca et al. (1993) explained that heterogeneous degradation occurs at the surface of the device where it is interfaced with the physiologic environment. The degradation rate is constant and the undegraded carrier retains its chemical integrity during the process. Homogenous degradation involves a random cleavage throughout the bulk of the matrix. While the molecular weight of the polymer steadily decreases, the carrier can retain its mass until the polymer has undergone significant degradation, i.e. as much as 90%, and reaches a critical molecular weight, at which time solubilization and mass loss commences. Examples of typically bulk eroding polymers are PLA and PLGA. Mass loss studies performed on pellets prepared with PLGA 50:50 resulted in sigmoidal curves typical of polymers undergoing bulk hydrolysis (Schmitt et al., 1993).

In a study of the effect of temperature on mechanisms of drug release and matrix degradation of PLA microspheres, Aso et al. (1994) showed that at temperatures above the T_g matrix degradation was a bulk process and drug release was a diffusion controlled process. On the other hand, below the T_g, degradation was restricted to the surface of the matrix and drug release was caused by matrix surface erosion.

2.4.2. **Polymer composition and polymer molecular weight**

Copolymer composition can affect degradation. The increase in lactic acid content decreases the degradation rate by reducing the access of water, which is restricted by the bulky methyl groups (Miller et al., 1977).

Studies of the *in vitro* degradation of poly-D,L-lactide-co-glycolide in buffer pH 7.4 at 37°C were carried out by Hutchinson and Furr (1990) using polymer films or slabs of known thickness and weight. They found an induction period prior to weight loss for the high molecular weight polymers and that water uptake occurred to a lower degree (and with more extended time scales) in those polymers with higher content of lactide. The profiles of weight loss and change in molecular weight were consistent with

hydrolysis mechanisms. High molecular weight polymers degraded to lower molecular weight polymers and yet retained their water insolubility. Only after an extended time of degradation, weight loss started to take place, in contrast to that of low molecular weight polymers which can degrade with weight loss immediately. The results were consistent with bulk hydrolysis under *in vitro* conditions, and correlated with degradation of the polymers *in vivo*, suggesting that even in subcutaneous tissue, enzymatic degradation is less important than simple hydrolysis.

Hutchinson and Furr (1990) explained that there is a linear relationship between the logarithm of M_n versus time until water uptake commences. Thereafter a discontinuity arises in the linear relationship. Water uptake takes place by two processes. The first stage is the ingress of water by diffusion, which occurs to a level depending on the equilibrium swelling of the material. Secondly, or even during the initial diffusional phase, more ingress of water is aided by the increase in the number of hydrophilic groups arising from the degradation of the polymer. This is why profiles for high molecular weight polymers show two water uptake phases, with hardly any water ingress in between. For low molecular weight polymers, the profiles show continuous water uptake. In conclusion, hydrolytic degradation is characterized by reduction in molecular weight, enhanced water uptake and, finally weight loss of polymer. Assuming a normal initial polydispersity and hydrolysis of the polymer as a random process, equations were used to characterize the degradation, based on water uptake and the appearance of carboxylic end groups. The water uptake is described by equation 2.7,

$$[Water]_t = a\left[1 + \frac{b}{aPM_n^0 e^{-akt} - b\left(1 - e^{-akt}\right)}\right] \qquad \text{equation 2.7}$$

Equation 2.8 describes the appearance of the carboxylic groups expressed as a function of the number average molecular weight:

$$M_n^t = M_n^0 e^{-akt} - b\frac{(1-e^{-akt})}{aP} \qquad \text{equation 2.8}$$

where M_n^t is the number average molecular weight at time t, M_n^0 is the initial number average molecular weight, a and b are constants related to polymer composition, $k = K$ [ester] derived from the normal kinetic equation for ester hydrolysis, and P is the polydispersity.

The effect of H^+ liberated from hydrolytic cleavage of poly-alpha-hydroxy-aliphatic esters on the permeability and degradability of the polymers was evaluated by Sah and Chien, 1995. The concentration of hydrogen ions released into the bulk medium was calculated from the change in buffer pH. The rate of release of H^+ was found to be dependent upon the polymer composition since blending high molecular weight copolymers with lower molecular weight fractions drastically enhanced the hydrolytic rates of the modified samples.

2.4.3. **The presence of drugs and polymer degradation products**

Drugs added to the polymer may play a part in its degradation kinetics. Basic drugs, for example, have been reported to affect degradation through pH changes (Cha and Pitt, 1989) when a series of four amines were incorporated in poly-alpha-hydroxy-aliphatic esters.

Dependence of the release profiles on the chemical state of the drug was shown with gentamycin base and gentamycin sulfate/poly(D,L-lactic acid) oligomeric systems (Mauduit et al., 1993). For both types of mixtures biphasic release profiles were observed, the first phase corresponding to a fast release where the proportion of antibiotic released was greater for the sulfate form of the drug. Differences in the release profiles were attributed to acid-base interactions between the carboxylic-acid end-groups of the polymer and the cationic antibiotic, whereby the free base reacted with the polymer during the preparation of the blends with the formation of ionic

clusters known to crosslink the chains. An acid-base reaction, however, was not permitted with the sulfate form of the drug due to its lower solubility in the manufacturing solvent employed (acetone). The reaction between gentamycin sulfate and the oligomer end-groups was postulated to occur at a later stage, upon contact with water.

Polymer degradation products can also affect degradation rates. For most degradable polymers, its monomers are protolytes with an acid functionality. These compounds can then cause a marked deviation of the pH inside eroding polymers from the pH value of the surrounding buffer medium. The effect has been investigated for polymers such as poly(lactic acid) and poly(lactic-co-glycolic acid). The pH inside eroding poly(lactic acid) and poly(lactic-co-glycolic acid) rods can be as low as 2 even when exposed to a buffer of pH 7.4, as determined by Herrlinger (1994). Such pH changes during erosion produce a feedback effect on the degradation rate of the polymers (autocatalysis). The shorter the half-life of the polymer bonds, the faster monomers are created upon degradation causing a rapid decrease of the pH. The higher solubility and lower pKa of α-hydroxy acids compared to unsubstituted aliphatic carboxylic acids (like sebacic acid) explained the lower pH values during degradation inside eroding poly(α-hydroxy esters) matrices compared to poly(anhydride) matrices, for example (Göpferich, 1996).

'Inversely' moving erosion fronts have been observed in PLA and PLGA rods and discs (Herrlinger, 1994), for which there is increased polymer degradation inside the matrices due to the activity of created monomers.

2.4.4. **The surrounding medium**

Makino et al. (1985) have found that the rate of hydrolytic degradation of PLA microcapsules prepared by using D,L-PLA or L-PLA was extremely pH dependent, lowest at around pH 5.0, higher in both strongly acidic and strongly alkaline solutions. Later (1986) the same authors reported that at pH 5.4 the molecular weight of PLA increased in the time range between 50 and 70 days. The explanation they gave was that the molecular weight has a greater dependency on the weight of fractions with

higher molecular weights and much less on the weight of fractions with low molecular weights. The degradation of those fractions of lower molecular weight should be followed by the removal of the degraded fractions into solution. Molecular weight can increase if such removal is slower than the degradation of the higher molecular weight fractions.

From the investigation of oligomers from poly(lactic acid), the hydrolysis rates were found to be inversely proportional to the pH in the degradation medium (Herrlinger, 1994). Göpferich, (1996) estimated that a decrease of the pH from 7.4 to 2 would increase the values for the first order rate constant of such oligomers from 10^{-8} to 10^{-3} s^{-1}, closer to the value of the rate constants for surface eroding polymers.

Park et al. (1995) investigated the effect of both pH and low molecular weight oligomers on the degradation of PLGA microspheres. The microspheres were either incubated in closed containers or in a dialysis bag. The latter allowed the removal of acidic degradation products of molecular weight lower than 3,500. After a period of 40 days, the pH of the closed container samples decreased from 7.4 to 3. During this period, the pH in the dialysis bag remained unchanged. A slower degradation of polymer was obtained by maintaining a constant pH due to removal of degradation products.

Makino et al. (1987) studied the effects of plasma proteins on the degradation of intermediate molecular weight PLA microcapsules. The degradation rate in aqueous medium was accelerated by the addition of albumin, γ-globulins and fibrinogen. For all proteins, as their concentration increased, the released amount of lactic acid increased at any time period.

Composition and ionic strength of the in vitro release medium affected the release behavior of octreotide from branched poly(DL-lactide-co-glycolide-D-glucose) microspheres (Bodmer et al., 1992). At a constant peptide loading of 6% the fractional release decreased with increasing ionic strength of the medium. Independent of the ionic strength of the medium complete release was achieved after four weeks in acetate buffer and after five weeks in saline.

2.4.5. **Gamma-irradiation**

Sanders et al. (1984) carried out a study on the effect of gamma-irradiation on the intrinsic viscosity of a 69:31 copolymer and the performance *in vivo* of microspheres made from that polymer loaded with LH-RH-analogue. There was a decrease of the intrinsic viscosity of the polymer with increase in radiation dose and a concomitant decrease in the time of onset of the final phase, as shown in profiles of estrus suppression in rats.

Hausberger et al. (1995) investigated the effects of gamma-irradiation on molecular weight and *in vitro* degradation of PLGA microparticles. A reduction in the initial molecular weight distributions was observed. The onset times for mass loss decreased with increasing irradiation dose, but no effect was observed on rate of mass loss.

2.4.6. **Random chain scission and end-group scission**

Gilding and Reed (1979), in a study of the effect of γ-irradiation on the tensile strength of Dexon® sutures found an unexpected more rapid fall of the M_n than the M_w of the sutures. This suggested that random chain scission was not the primary mechanism of degradation, and that large quantities of low M_w fractions were formed by unzipping (chain-end scission). Shih et al. (1995) reported that the hydrolysis of chain-ends was approximately 10 times faster than the hydrolysis of internal PLA bonds.

In examining the effect of γ-irradiation on the degradation of sutures, Chu and Campbell (1982) proposed that chain scission (which was considered to initially take place through ester bonds) gradually exposed increasing number of CH_2 moieties, promoting secondary crosslinking reactions through free radicals resulting in the formation of a C-C bond.

2.5. FORMULATION WITH POLY-ALPHA HYDROXY ALIPHATIC ESTERS

There are several techniques under evaluation for the production of controlled release systems with PLA and PLGA. Microspheres and nanospheres are certainly amongst the most broadly investigated drug delivery systems at present. Routes of administration are multiple for such systems (oral, intramuscular, subcutaneous and inhalations) and many approaches have been made to their manufacture. Principal techniques include emulsification and solvent evaporation, as well as some contributions of spray drying.

The preparation of cylindrical implantable discs is amongst the simplest manufacturing techniques. Therefore these systems will be reviewed in the first place.

2.5.1. Implants

Implants can be manufactured with large drug loading efficiency and acceptable uniformity. Of course, there are some disadvantages too, such as the often necessity of surgery or special equipment for their implantation, and safety concerns when they carry large amounts of drug. The treatment of prostate cancer has been aided by a PLA implantable market-product containing LHRH agonists (Zoladex®, ICI Pharmaceuticals, UK) which releases the drug continuously over at least 28 days (Furr and Hutchinson, 1992).

The various poly-alpha-hydroxy aliphatic esters are thermoplastics whose properties can be adjusted depending on the intended use. As thermoplastics, they can be processed at temperatures above their melting and glass transition point. In general, low glass transitions, good solubility in common organic solvents and free flow of the polymer powder have been reported (Boehringer Ingelheim Catalogue). Taking advantage of these properties, many techniques such as direct compression, compression moulding, solvent casting and extrusion have been developed for the preparation of implants.

A procedure combining solvent casting and extrusion was reported by Phillips and Gresser (1984). Disulfiram composites were prepared from a cosolution of the drug and PLGA in dichloromethane and cast as a thin film on a glass surface. The thickness of the film was adjusted to 0.06 cm with a film spreader, air dried and then vacuum dried at 45°C. Rods were extruded through a 0.3175 cm die at a temperature of 70-80°C and pressure up to 140 psi.

A melt-press technique was used by Fitzgerald and Corrigan (1993, 1996) to produce discs from PLGA drug loaded films. Preparation of drug/copolymer solution was followed by solvent evaporation over a hot plate to form a film, which was dried under vacuum for 24 hours. Films were then cut into segments and heated in a 13-mm die for 15 minutes. The die was allowed to cool after which discs were compressed under 8000 kg/cm3 at room temperature for one minute. Direct compression of mechanical mixtures of the drug and copolymer were also prepared. The powders were previously mixed in a mortar and pestle.

A solvent-evaporation method employing a solution of dichloromethazone was recently mentioned by Min et al. (1995). They mixed anhydrous ampicillin and PLA in the solvent and homogenized for 24 hours (details not given), after which the mixture was placed on a Teflon® cast with solvent removal at high temperature. Semitransparent films were obtained.

In an attempt to provide a system with higher acceptance by patients, a liquid that may be injected and solidified in situ was evaluated as a novel implant system (Shively et al., 1995). The rationale for the investigation of such systems was that upon injection into an aqueous environment, the biocompatible solvent diffuses out of the polymer while water diffuses into the polymer matrix causing its precipitation. The study compared formulations with PLA/PLGA concentrations above and below the precipitation threshold, previously calculated by phase diagrams. In a similar work, Chandrashekar and Udupa (1996) prepared in situ-gel forming diclofenac sodium systems. A solution of (50:50) PLGA was prepared by stirring the polymer in triacetin at 50°C and cooled to room temperature. Diclofenac sodium was incorporated into the PLGA solution as a fine dispersion using sonication.

Phase inversion dynamics of PLGA solutions related to drug delivery were recently studied by Graham et al. (1999) when they prepared a gelled implant, which is a liquid that solidifies upon injection to the body. Solutions of the polymer and biocompatible solvents were prepared by mixing in a glass vial at room temperature, allowing several hours for complete dissolution to occur. These workers studied the gelation rate, which is the rate at which the solution is transformed into a semi-solid porous implant. This determines the properties of the diffusional path that the drug molecules take as they leave the implant and, consequently, the characteristics of drug release.

2.5.2. **Microparticulate systems**

In 1984 Sanders et al. prepared PLGA microspheres loaded with a LH-RH analogue by a phase separation technique. An aqueous solution of the compound and a solution of the copolymer in dichloromethane were emulsified to form a water-in-oil emulsion. A nonsolvent for the copolymer was then added to precipitate out the polymer around the aqueous droplets. The suspension of semi-formed microspheres was added to a large volume of nonsolvent to cause them to harden and to complete the extraction of dichloromethane. The microspheres were then sieved, washed and dried. The final compound loading was approximately 1% w/w.

Jalil and Nixon (1990a) explained that microencapsulation of PLA can be prepared using both O/W or W/O emulsion systems. In the O/W emulsion technique, also known as emulsion-solvent evaporation, the polymer is dissolved in a solvent such as methylene chloride. The core is either solubilized or suspended in this solution, which is then emulsified with water containing a suitable emulsifier. Phase separation of the polymer and core to produce a microcapsule occurs upon removal of the solvent, by heat, vacuum or both. Iwata and McGinity (1992) prepared "multi-phase" microspheres of PLA and PLGA by a multiple emulsion solvent-evaporation technique. The first step was the preparation of a conventional W/O emulsion (aqueous solution of drug in soybean oil). Then, a W/O-in-acetonitrile (W/O/'W') emulsion was prepared by dispersing the W/O emulsion in a polymer-acetonitrile solution. Compared to conventional microspheres, multi-phase microspheres demonstrated a greater drug

loading efficiency for water soluble drugs. Drug release profiles were different when conventional microspheres were compared with multi-phase preparations (Iwata and McGinity,1993). A lag-phase of 10-16 days was observed for conventional microspheres. Multi-phase microspheres were characterized by an initial uniform release for the first 20 days followed by a more rapid phase of drug release.

A modification of the emulsion-solvent evaporation method is the emulsion solvent extraction, reviewed by Conti et al. (1992). The technique consists in preparing an O/W emulsion and subsequently pouring it into a diluent phase miscible with the polymer solvent, but not miscible with the polymer. As a consequence the solvent migrates from polymer microdroplets into the diluent phase. The system is continuously agitated until extraction of solvent from the polymer droplets is completed. Solid microspheres are usually recovered by filtration, washed and dried under vacuum. One of the advantages of the method is that it is possible to obtain extraction of the solvent at low temperatures, without having to approach the solvent boiling point. Kim et al. (1997) presented a modification of the solvent-extraction method for the preparation of drug loaded PLA microspheres by which the loading content increased. These workers used 2% v/v ethyl acetate as the diluent solvent.

Paul et al. (1997) described the preparation of pentamidine loaded poly(D,L-lactide) nanoparticles by a nanoprecipitation method. The free base of the drug, phospholipids and PLA were dissolved in acetone. This solution was mixed with an alkaline aqueous solution (to improve the fixation yield) containing Poloxamer 188. After 15 min. of stirring, the acetone and part of the water were evaporated in a rotor evaporator under reduced pressure. The highest drug loading percentage ($\cong$ 75%) was obtained with a concentration of the phospholipid mixture of 1.25%. Under these conditions, 379 μg of the drug were loaded per ml of suspension. Exponential dependence of the amount of drug released on time was evidenced.

2.5.3. **Miscellaneous formulation techniques**

PLA hollow fibres for the controlled release of hormones (H-levonorgestrel) were prepared using a dry-wet phase inversion spinning process (Eenink et al., 1987). A

viscous spinning solution (polymer and solvent) was pumped through a heated tube into the spinneret. The applied spinneret was a tube-in-orifice device with an orifice diameter of 1.0 mm an injection tube outside diameter of 0.6 mm and an inside diameter of 0.4 mm. The contents of the spinneret were not heated, except for particular cases. A coagulation bath was placed at a specified distance from the spinneret. From the coagulation bath the hollow fibre was transferred to a self-advancing godet, the speed of which determined the withdrawal rate of the yarn from the spinneret. The bundles of hollow fibre were air dried. Hollow fibres were filled with a 25% dispersion of micronized hormone in castor oil. The hollow fibre levonorgestrel release rates were found to be dependent on the membrane structure of the hollow fibre wall. For the different hollow fibres, zero-order levonorgestrel release rates were found with possible applications as a long-acting contraceptive delivery system.

"Matrix formation" of PGA by annealing was reported by Ries and Moll (1994) in the preparation of theophylline tablets. Annealing of the tablets after compression influenced the physicochemical and mechanical properties of the tablets. This in turn had an effect on the disintegration and in vitro release behavior of the devices, with prolongation of the drug release profiles. The temperatures applied ranged between 40°C and 120°C for not less than 20 minutes. The values of the release rate constants decreased for increasing temperature and duration of the treatment applied.

2.6. FORMULATION VARIABLES AFFECTING DRUG RELEASE FROM PLA/PLGA

The influence of the polymer composition and molecular weight on drug release has been studied by many workers. Increasing the proportion of lactide content in polymer implants showed an increasing duration of drug release and lag time before onset of degradation controlled release (Sanders et al., 1986a). Jalil and Nixon (1990b) reported the influence of the molecular weight on the drug release kinetics. They found higher rates for phenobarbitone released from microcapsules prepared with

polymers of lower molecular weight; a linear correlation, however, was not found. Sah and Chien (1995) showed that the adjustment of the hydrolytic rates of microcapsules by blending polymers of different molecular weight was found to be critical in achieving a controlled release of entrapped protein. The incorportation of lower molecular weight polymer fractions drastically enhanced hydrolytic rates of microcapsules.

The type of drug and the drug loading has a significant effect on the mechanism of release from PLA/PLGA. Wakiyama et al. (1981) reported the release of an anaesthetic changed from being diffusion controlled to degradation controlled, at higher and lower drug loadings respectively. Incorporation of a tertiary amine, caffeine base, into high molecular weight PLA showed an increase in the degradation rate of the polymer at low drug contents ($\leq$ 2%) (Li et al., 1996). The increase of polymer degradation rate was not proportional to the caffeine content; this was due to the combined effects of base/carboxyl end-group interaction, crystallization and matrix-controlled diffusion of the drug.

Sato et al. (1988) assessed drug release for methylene blue and prednisolone acetate PGA microspheres. Complete release of the highly water soluble methylene blue occurred within 72 hours, while the less soluble prednisolone was released much more slowly. The authors reported that release from these systems appeared to be governed principally by the solubility of the drug. Suzuki and Price (1985) reported that the rate of chlorpromazine release decreased as the PLA microcapsule size increased.

Fitzgerald and Corrigan (1993) reported the effect of processing conditions on the release of diltiazem from PLA/PLGA matrices. Mechanical mixes of drug and polymer resulted in diffusion based drug release. In contrast, systems prepared by solvent-evaporation released the drug by a polymer degradation mediated mechanism. Redmon et al. (1989) reported that differences in the release characteristics of prednisolone loaded PGA microspheres prepared by solvent-extraction precipitation and freeze drying were likely to be attributable to surface area differences of the two products. The product with the greater surface area (solvent-extraction precipitation method) released more drug initially whereas that with the lower surface area (freeze dried product) exhibited sustained release of a greater amount of drug. They

concluded that a major influence upon drug release was the porosity, as reflected in the specific surface area.

2.7. EFFECTS OF STORAGE ON FORMULATIONS PREPARED WITH PLA/PLGA

Aso et al. (1993) studied the changes in the physicochemical properties of PLA microspheres that occurred during storage. Progesterone-loaded microspheres were stored at 50°C and 30°C under dessicated and moist atmospheres. The surface morphology did not change significantly under storage in any of the conditions studied. The drug release rate of stored microspheres was faster than that of microspheres before storage. The polymer crystallized when stored above the T_g under moist conditions. The T_g of the systems stored at high relative humidity decreased considerably, which may be attributable to the plasticizing effect of water absorption. The drug release of these systems was faster compared to the systems stored under dessicated conditions.

2.8. BEHAVIOR OF POLY-ALPHA-HYDROXY ALIPHATIC ESTERS *IN VIVO*

Comparison of the *in vitro* and *in vivo* degradation of poly-alpha-hydroxy aliphatic esters suggested similar polymer behavior in the two conditions (Gilding and Reed, 1981). Using white rabbits, Pitt et al. (1981) studied the *in vivo* degradation of drug-free PLA implantable films and capsules. They reported that the rate of chain scission increased after the commencement of weight loss. Linear relationships between the ln $[\eta]$ or $[M_n]$ and time *in vivo* were observed for substantial time periods. Sanders et al. (1984) studied the *in vivo* performance of nafarelin microcapsules prepared with high molecular weight (50:50) or (69:31) PLGA. The data were consistent with the release

of a compound by homogenous polymer erosion, with clear triphasic compound release. Fukuzaki et al., (1991) obtained a typical S-degradation for the *in vivo* degradation of pure PLGA, which characterizes a rapid degradation occurring some time after an initial lag period during which the weight of the polymer remains unchanged.

Le Ray et al. (1991) studied the distribution of radiolabelled PLGA nanospheres which showed an obvious tropism for the liver (83% after 4 hours) and a lower but significant affinity in the lungs and the spleen. Radioactivity was also confirmed in urine and feces.

2.9. **BIOCOMPATIBILITY INFORMATION AND PRODUCTS LICENSED**

Long experience with homo- and co-polymers of lactic and glycolic acids has shown that these materials are inert and biocompatible in the physiological environment and degrade to toxicologically acceptable products (Hutchinson and Furr, 1990). In a study comparing the effects of systemic antibiotic and local therapy, PLA-ampicillin films were placed in the maxillary sinus of rabbits with experimentally induced sinusitis. Examination against the two control groups (group 1 without ampicillin and group 2 with ampicillin given intramuscularly) showed that the histopathological findings were less severe in those animals receiving the ampicillin film (Min et al., 1995). Calhoun and Mader (1997) have recently reported studies on animals using poly-alpha-hydroxy-aliphatic esters for osteomyelitis infections. Although not primarily intended to evaluate toxicological aspects of the formulations prepared, the results of the studies indicated clinical improvement in the cases treated with the formulations when compared to the control groups (untreated with PLA/PLGA or treated with placebo PLA/PLGA).

Products currently licensed for commercialization include luteinizing hormone releasing hormone analogues such as the implant Zoladex® (ICI) and the microsphere formulations Prostap SR® (Lederle) and Enantone® (Takeda Pharma GmbH Aachen,

Germany). Parlodel LAR® (Sandoz) is a microsphere formulation for the once monthly delivery of bromocriptine.

CHAPTER 3. MECHANISMS OF DRUG RELEASE FROM PLA AND PLGA DRUG DELIVERY SYSTEMS

3.1. INTRODUCTION

The mechanisms governing drug release from poly-alpha-hydroxy aliphatic esters are dependent on both polymer and drug characteristics. For a given polymer system, drug release appears to be highly dependant on loading and molecular size of the compound carried. In general, macromolecules such as polypeptides are considered to be released by polymer degradation control (Maulding, 1987). For the release of smaller compounds, however, various mechanisms have been reported, ranging from purely diffusion mechanisms to degradation controlled release. Release profiles of many basic drugs appear to be dependent on the degradation of the polymeric matrix, particularly at low loadings, for example, diltiazem co-evaporates (Fitzgerald and Corrigan, 1993), fluphenazine hydrochloride (Ramtoola et al., 1992), doxepin hydrochloride (Gido et al., 1994) and levamisole base microspheres (Fitzgerald and Corrigan, 1996). Neutral compounds appear to have a matrix-controlled release. The dissolution of dehydro-isoandrosterone from drug-polymer compressed discs of constant surface area was found to be proportional to the square root of time (Ramtoola et al., 1991). Drug release for acidic compounds such as phenobarbitone microcapsules (Jalil and Nixon, 1990c) can be fitted to Higuchi's spherical matrix model.

Existing equations proposed for the release of various drugs from PLA and PLGA matrices are listed below. It is the combination of two main processes, diffusional mechanisms and polymer degradation control, that is involved in the release of drug from most systems.

3.2. **DIFFUSION MECHANISMS**

Diffusion is defined as a process of mass transfer of individual molecules of a substance, brought about by random molecular motion and associated with a concentration gradient. The passage of matter through a barrier may occur by simple molecular permeation, by dissolution of the permeating molecules in the bulk membrane, or by movement through solvent-filled pores and channels (Martin, 1993).

Diffusional release of a dissolved or dispersed solute from a polymeric matrix is often governed by complex release kinetics due to the presence of a moving diffusional front separating the undissolved core and the partially extracted region. For an erodible polymer matrix, the release kinetics are also determined by the presence of a second moving boundary, the eroding polymer front, in addition to the diffusion front (Lee, 1980).

The more simple cases, for drug release occurring from a non-erodible matrix, will be discussed in the next sections.

3.2.1. **Reservoir systems**

Reservoir systems are typically the case of a compound encapsulated within a polymer membrane. If the case of a macroporous membrane impermeable to the drug is assumed, then transport occurs exclusively through water-filled pores. The membrane of area A and thickness l separates the drug reservoir (saturated solution with concentration C_{is}) from a perfect sink. The concentration of drug within the pores at position d along the membrane is $C_{iw}(d)$. The steady-state flux J_{ss} of drug out of the pores is then given by Fick's first law:

$$J_{ss} = -D_{eff}\frac{\partial C_{iw}}{\partial d} \qquad \text{equation 3.1}$$

The steady-state flow rate Q_{ss} can be described by (Siegel, 1989):

$$Q_{ss} = A\varepsilon \cdot D_{eff} \cdot \frac{C_{is}}{l} \qquad \text{equation 3.2}$$

where ε is the porosity of the membrane and D_{eff} is the effective diffusion coefficient of the drug in water. Here $D_{eff} = F.\ D_{iw}$ where F is the formation factor and D_{iw} is the aqueous diffusion coefficient of the drug. The formation factor reflects the amount by which the porous structure affects the time scale of drug release through a specific mechanism of drug transport retardation. The development of equation 3.2 assumes the absence of boundary layer effects. If the membrane does not provide a great resistance to drug flow, that is if F is close to 1, then stagnant layers near the membrane may contribute to the resistance to drug flow and boundary layer terms should be added. In equation 3.2 it is clear that Q_{ss} is independent of time, i.e., the kinetics is of zero order. Such situation was described by a simple general equation proposed by Ritger and Peppas (1987a):

$$\frac{M_t}{M_\infty} = k't \qquad \text{equation 3.3}$$

Here M_t/M_∞ is the fraction of drug released, k' is the zero order rate constant and t is time.

PLA hollow fibers loaded with levonorgestrel hormone (described in section 2.5.3) showed zero-order release profiles. This was shown by the linear cumulative-amount-released versus time plots obtained, and by the constant daily amounts delivered that were observed when the rate was plotted versus time. The release rates were found to be dependent on the membrane structure of the hollow fiber wall.

3.2.2. **Monolithic devices**

Release of drug from matrix or monolithic systems may occur by diffusion through the polymer membrane or through solvent-filled pores. Fick's second law can be used to

describe the change in concentration of diffusant with time $\frac{\partial C}{\partial t}$ from a thin polymer slab, with one-dimensional diffusion in the direction d (Ritger and Peppas, 1987a):

$$\frac{\partial C}{\partial t} = D \frac{\partial^2 C}{\partial d^2} \qquad \text{equation 3.4}$$

where sink conditions apply and D is the diffusion coefficient of the diffusant.

3.2.3. **Diffusion through the polymer matrix**

Assuming a constant drug diffusion coefficient D_m and sink conditions, the trigonometric solution to Fick's law for the one-dimensional fraction of drug released at any given time from a thin polymer slab of thickness l can be approximated as:

$$\frac{M_t}{M_\infty} = 4\left[\frac{D_m t}{\pi . l^2}\right]^{0.5} \qquad \text{for } 0 \leq \frac{M_t}{M_\infty} \leq 0.6 \qquad \text{equation 3.5}$$

As indicated in equation 3.5, Fickian diffusional release from a thin slab is characterized by an initial $t^{0.5}$ dependence of the drug released. Release at later time periods is given by a more complex equation.

Higuchi (1961) proposed an equation for the release from planar matrix systems containing suspended drug particles, where Q is the amount of drug released at time t per unit area of exposure:

$$Q = \sqrt{D_m t (2A - C_s) C_s} \qquad \text{equation 3.6}$$

Where A (the total concentration of drug) is larger than the C_s the saturated solubility of the drug in the membrane. The equation was derived for a system in which the suspended drug is in fine state and sink conditions are maintained. For the common case of $C_s << A$, the relationship is simplified to the expression $Q = \sqrt{2AD_m C_s t}$.

3.2.4. **Diffusion through solvent-filled pores**

Square root of time kinetics for the release of drug from a planar surface where the rate determining process is diffusion was described by an equation proposed by Higuchi (1963),

$$Q = \sqrt{\frac{D\varepsilon}{\tau}\left(2A - \varepsilon \cdot C_s\right)C_s t} \qquad \text{equation 3.7}$$

where Q is the amount of drug released, D is the diffusion coefficient of the drug in the permeating fluid, ε is the porosity of the matrix, τ is the tortuosity of the matrix, C_s is the solubility of the drug in the solvent, A is the concentration of the dispersed drug in the matrix and t is the elapsed time. The equation is valid for the first 60% of the total released drug.

A reduced form of equation 3.7 may be written as follows:

$$X = K_H t^{0.5} \qquad \text{equation 3.8}$$

where X is the fraction of drug released at time t and K_H is the Higuchi rate constant.

Diffusion controlled drug release from matrices having either spherical, biconvex or cylindrical shape was described by Cobby et al. (1974),

$$X = G_1.k_r.t^{1/2} - G_2.(k_r.t^{1/2})^2 + G_3.(k_r.t^{1/2})^3 \qquad \text{equation 3.9}$$

where X has the same meaning as in equation 3.8, k_r is the rate constant, G_1, G_2, G_3 are parameters that depend on the shape of the device and t is the elapsed time. In the case of a cylinder the equation becomes

$$X = (q+2).k_r.t^{1/2} - (2.q+1).(k_r.t^{1/2})^2 + q.(k_r.t^{1/2})^3 \qquad \text{equation 3.10}$$

with q as the shape parameter. The rate constant k_r relates to the Higuchi rate constant K_H by $k_r = 2\ K_H\ /q$. The shape parameter q is equal to the initial disc radius (r_i) divided by half the initial disc height (h_i). Appendix I shows the Scientist software model file corresponding to equation 3.10, where X is always ≤ 1. Ramtoola et al. (1992), used equation 3.9 to fit the release kinetics of fluphenazine from PLA and

PLGA matrices. Diffusion or matrix controlled drug release has been fitted to the general equation proposed by Ritger and Peppas (1987a) for the profiles obtained with PLA microspheres containing dihydro-iso-androsterone (Ramtoola et al., 1991) and pentamidine loaded PLA nanoparticles (Paul et al., 1997),

$$X = B.\ t^n \qquad \text{equation 3.11}$$

where X was defined in equation 3.8, B and n are constants and t is the elapsed time. The diffusional exponent, n, specifies the mechanism of release. Originally introduced for the description of solute release from non-swellable matrices, the use of equation 3.11 was later extended to drug release from swellable devices (Ritger and Peppas, 1987b).

3.2.5. **Percolation theory**

The topology or arrangement of pores plays a part in the mechanisms of drug release from a solid system. At a critical loading the porosity of the matrix reaches the critical percolation threshold porosity ε_c. Below this value, all pore clusters are finite while above it there exists a cluster of infinite extent. In this context, a cluster of pores includes all those pores that are interconnected and $P(\varepsilon)$ is the probability that a pore belongs to an infinite pore cluster and that is therefore ultimately connected to the surface of the matrix system. By definition of ε_c, $P(\varepsilon)$ must be zero for $\varepsilon < \varepsilon_c$.

Another important parameter of percolation theory is the coordination number z. This number is the maximum number of bonds that may emanate from each site or pore. For three dimensional simulations (3-D lattice), the simple cubic lattice is the easiest to work with, having a coordination number $z = 6$. The Voronoi representation of the porous medium is more "random" than the regular lattice representation and appears to be more realistic. The regular lattice models imply a degree of order that does not exist in a porous polymer. A remarkable property of percolation is that the behavior of $P(\varepsilon)$ near the percolation threshold ε_c is virtually independent of the lattice structure.

When considering the fraction of releasable drug F_∞ from a finite slab, it must be considered that the drug contained in finite pore clusters connected to the surface also contributes to F_∞. Mathematically this means that at a given porosity, $F_\infty(\varepsilon) \geq P(\varepsilon)$. Furthermore, in a slab of finite depth there is a finite probability that a pore (or hence a drug particle) will reside on the surface of a slab, so that F_∞ is nonzero for all values of ε.

The topological contribution $\alpha(\varepsilon)$ to the formation factor F in the case of steady-state diffusive flow is given by

$$\alpha(\varepsilon) \approx (\varepsilon - \varepsilon_c)^{\mu} \qquad \text{equation 3.12}$$

where μ is approximately 2.0 for a 3-D lattice.

At low porosities not all the drug is released and the kinetics become "droopier" than $t_{1/2}$. Thus, for the topologically random systems, it appears that the diffusion equation with a formation factor that is uniform throughout the membrane, does not adequately describe transport processes. There are two possible explanations for the topology-induced retardation and droopiness of the kinetic curves. First, the overall tortuosity (tortuosity defined in Siegel's terms as a specific mechanism of lengthening of the diffusion path) does increase as ε decreases. Second, dead-end pores exist. The likelihood of encountering a dead-end pore increases as one goes into the membrane.

3.3. **POLYMER DEGRADATION CONTROLLED DRUG RELEASE**

Drug release dependent on polymer degradation and dissolution, may be described by the Prout-Tomkins model (Fitzgerald and Corrigan, 1993):

$$\ln\frac{c}{1-c} = k \cdot t + m \qquad \text{equation 3.13}$$

This model assumes that oligomer/drug dissolution occurs only as a function of polymer decomposition, where $m = -k \cdot t_{max}$, c is the drug released, t is time, k is the acceleratory coefficient and t_{max} is the time when the extent of drug release is equal to 50% of the final drug concentration. Ramtoola et al. (1992) and Fitzgerald and Corrigan (1993; 1996) have fitted the profiles of fluphenazine and levamisole hydrochloride, respectively, to equation 3.13.

More recently (Corrigan et al., 1997), a model was proposed to account for the initial burst of drug in a polymer degradation related release process. The release of levamisole was fitted to equation 3.14:

$$Ftot = Fb_{\infty}\left(1 - e^{-k_b t}\right) + (1-Fb_{\infty})\left(\frac{e^{kt - kt_{max}}}{1 + e^{kt - kt_{max}}}\right)$$

equation 3.14

which was based on equations 3.13 and 3.15, the latter shown below:

$$F_b = Fb_{\infty} \cdot \left(1 - e^{-k_b t}\right)$$ equation 3.15

where k_b is the burst rate constant, F_b is the fraction of drug released by burst effect at time t and Fb_{∞} is the total burst fraction at time infinity.

Equation 3.15 describes a first order process as earlier presented by Wagner (1969). If F is the fraction of drug released by degradation at time infinity then,

$$Fb_{\infty} + F = 1$$ equation 3.16

The fraction of drug released by degradation at time t (F_{deg}) is related to c (equation 3.13) by

$$F_{deg} = F\,c$$ equation 3.17

The total fraction of drug released at time t (F_{tot}) is given by

$$F_{tot} = F_{deg} + F_b$$ equation 3.18

A model combining square root of time diffusive kinetics and polymer degradation-dependent drug release was recently presented by Gallagher and Corrigan (1998) applied to the release of drug from PLA and PLGA matrices. The model is described by equation 3.19,

$$F_{tot} = Fd_\infty \left(G_1 k_r t^{0.5} - G_2\left(k_r t^{0.5}\right)^2 + G_3\left(k_r t^{0.5}\right)^3\right) + (1 - Fd_\infty)\left(\frac{e^{kt-kt_{max}}}{1+e^{kt-kt_{max}}}\right)$$

equation 3.19

where Fd_∞ is the fraction of drug released by a diffusion mechanism at time infinity and G_1, G_2, G_3 are parameters that depend on the shape of the device. In addition to equations 3.14 and 3.19, a model comprising exponential burst, diffusion and degradation dependent drug release was presented by the same authors (1998), described by equation 3.20:

$$F_{tot} = Fb_\infty \left(1 - e^{-k_b t}\right) + Fd_\infty \left(G_1 k_r t^{0.5} - G_2\left(k_r t^{0.5}\right)^2 + G_3\left(k_r t^{0.5}\right)^3\right)$$

$$+ (1 - (Fb_\infty + Fd_\infty))\left(\frac{e^{kt-kt_{max}}}{1+e^{kt-kt_{max}}}\right)$$ equation 3.20

For the case in which polymer-degradation-dependent drug released is followed by degradation of the drug in the dissolution medium, an equation that takes into account the formation of degradation products may be useful in estimating the release profile. Gallagher and Corrigan (1998) introduced an equation for the rate of change of the concentration of drug in the dissolution medium over time $\frac{df_P}{dt}$ when drug release

occurs by a bulk process (similar to the Prout-Tomkins model) and drug degradation occurs by a first-order decay process:

$$\frac{df_P}{dt} = k.x\left(1-\frac{x}{x_{tot}}\right) - k_{\deg}.f_P \qquad \text{equation 3.21}$$

where k is the rate of drug released by a polymer degradation dependent mechanism, x is the fraction of drug released via polymer degradation at time t, x_{tot} is the total fraction of drug released via polymer degradation, f_P is the concentration or fraction of drug in solution, $k_{\deg}$ is the first-order degradation rate constant of the drug in the dissolution media.

A theoretical model of bulk-erosion and macromolecular drug release from biodegrading spherical microspheres was proposed by Batycky et al. (1997). The principles of random chain scission and unzipping are both combined in the model proposed. The analysis carried out in the derivation of the model assumed that the microspheres radius remains fixed although the porosity changes with time. It was also assumed that water and monomers are able to diffuse through the matrix (i.e. through micropores), yet the macromolecular drug, by virtue of its size, is not able to diffuse through the polymer matrix. For a polymer composed of monomers j, which appear in the ratio $j_1 : j_2 : .... : j_J$, where J is the number of different monomers, the equation proposed for the prediction of drug release was expressed as

$$\frac{m_d(t)}{m_d(0)} = 1-\phi_d^{\,burst}\left(1-e^{-k_d t}\right) - (1-\phi_d^{burst})\left(1-\frac{6}{\pi^2}\sum_{j=1}^{\infty}\frac{e^{-j^2\pi^2 D_d(t-t^d)/r_0^2}}{j^2}\right)$$

equation 3.22

where $m_d(0)$ and $m_d(t)$ are the mass of drug present in the microspheres at time zero and t respectively, $\phi_d^{\,burst}$ is the mass fraction of drug involved in the initial burst, k_d is the drug desorption rate constant, D_d is the effective drug diffusivity, t^d is the induction time before the final drug release phase and r_0 is the initial microparticle radius.

An initial burst originates from drug contained on the surface of the sphere. This is followed by an induction time sufficient to allow for coalescence of micropores and permit the passage of the macromolecular drug; i.e. drug release from the occlusions is precluded until the mean pore radius exceeds the characteristic molecular radius of the drug. The paradigm was applied to the case of (50:50) PLGA microspheres encapsulating a glycoprotein with potential use as an AIDS vaccine. Interaction between monomers (or oligomers) and pore walls have not been accounted for, nor have the effects of variable pH accompanying the solubilization of acidic monomers from a bulk-eroding polymer like PLGA.

As earlier introduced in Chapter 2, degradation controlled drug release has been referred to as homogeneous bulk erosion and heterogeneous surface erosion (Göpferich, 1996). Hixson and Crowell (1931) recognizing that the surface area of a regular particle is proportional to the two-thirds power of its volume, derived their classic "cube root law", which may be written as:

$$\left(\frac{W_d}{W_i}\right)^{1/3} = 1 - k_2 t \qquad \text{equation 3.23}$$

where W_i is the initial weight of the disc, W_d is the dry weight of the disc after exposure to a dissolution process for time t, k_2 is a rate constant having the dimensions of the cube root of mass per unit time. This relationship applies to tablets where dissolution takes place normal to the exposed surface area, and if the tablet dimensions decrease in proportion to one another, the exact initial geometric shape of the tablet is maintained at all times, such as for surface eroding systems.

CHAPTER 4. ORIGIN AND SCOPE OF THE THESIS

4.1. **Origin**

Drug release from poly-alpha-hydroxy-aliphatic esters has been extensively investigated for many basic drugs (Ramtoola et al., 1992; Fitzgerald and Corrigan, 1993; Gido et al., 1993; Fitzgerald and Corrigan, 1996). The release profiles of neutral compounds, such as dehydro-isoandrosterone (Ramtoola et al., 1991), and acidic compounds, such as phenobarbitone microcapsules (Jalil and Nixon, 1990), have also been investigated. Physicochemical models were employed to describe the release of basic (Fitzgerald and Corrigan, 1993), acidic (Jalil and Nixon, 1990) and neutral (Ramtoola et al., 1991) drugs. The preparation of amphoteric compounds in a polylactide matrix was presented by Hutchinson and Furr (1990) as a product called Zoladex®. These authors investigated the rates of polymer degradation and water uptake; drug release was not fitted to physicochemical models. A more recent publication on poly-alpha-hydroxy-aliphatic esters includes the amphoteric drug ampicillin (Min et al., 1995), however the mechanisms of drug release from this compound was not the primary focus of the report.

Many biological compounds have a complex chemical structure containing both basic and acidic groups (amphoteric compounds or ampholytes). Therefore, the use of mathematical models that aid the formulator to predict the release of biological compounds from PLA/PLGA systems constitutes a field for research. Amoxycillin is a possible model drug for such purpose due to its amphoteric nature. Delivery of biological compounds from PLGA matrices has been investigated for tetanus toxoid and synthetic malaria antigen using a mouse model (Thomasin et al., 1996). PLGA microparticles for a controlled release HIV-1 vaccine (Singh et al., 1997) constitute another example of biologicals delivered by a polymer system.

The antibacterial spectrum of Amoxycillin is very broad. Due to its short residence time in the body, current single-dose antibiotic therapy requires frequent administration. This gives another reason for the development of a controlled release

system for Amoxycillin, with potential applicability in various human and veterinarian areas. PLA-ampicillin films for maxillary sinusitis (Min et al., 1995) and gentamicin/PDLLA cylinders for osteomyelitis associated infections (Zhang et al., 1994) are presently being investigated for administration to humans.

A single dose of a sustained release formulation has the potential to discharge in the body an amount of drug equivalent to an overdose, should the device fail to comply with its specifications. Drugs that posses high therapeutic indexes constitute safer candidates for the formulation of sustained release dosage forms, such is the case of Amoxycillin.

4.2. **Objectives**

From the above mentioned potential applications of an Amoxycillin-PLA/PLGA system the following were the objectives of the present work:

I) to investigate the mechanisms involved in the release of Amoxycillin from poly-alpha-hydroxy aliphatic esters.

II) to identify suitable physicochemical models represented by mathematical equations to describe the release of Amoxycillin from within PLA/PLGA systems and predict the release of larger amphoteric molecules, such as biologicals.

III) to assess the suitability of PLA/PLGA as carriers for Amoxycillin. For example, to develop a system that releases intact Amoxycillin beyond 7 days.

CHAPTER 5. MATERIALS AND EXPERIMENTAL METHODS

5.1. DRUG, POLYMERS AND SALTS USED

Material	Supplier/Manufacturer
Amoxycillin trihydrate (BN 84H0450)	Sigma Chemical Co., Switzerland
Disodium hydrogen phosphate-12-hydrate	Riedel-de-Haën, Germany
D,L-Lactic Acid approx. 98%	Sigma-Aldrich Co., U.K.
Magnesium chloride hexahydrate	Sigma-Aldrich Co., U.K.
Potassium dihydrogen orthophosphate	BDH, U.K.
Potassium hydroxide	Sigma-Aldrich Co., U.K.
Polystyrene molecular weight standards	Aldrich, U.K. and Tosoh, Japan
Resomer® RG 503 (BN 34033)	Boehringer Ingelheim, Germany
Resomer® RG 504 (BN 34012)	Boehringer Ingelheim, Germany
Resomer® RG 755 (BN 15047)	Boehringer Ingelheim, Germany
Resomer® R 203 (BN 15004)	Boehringer Ingelheim, Germany
Sodium chloride	Riedel-de-Haën, Germany
Sodium dihydrogen phosphate-2-hydrate	Riedel-de-Haën, Germany

The manufacturer's specifications for Amoxycillin trihydrate were 99% purity (anhydrous basis) and 12.9% water content. For convenience, Amoxycillin trihydrate will be referred to as AMOX-H. The term Amoxycillin will be abbreviated to AMOX.

The manufacturer's specifications for the polymers used in the present work are listed in table 5.1.

Table 5.1. Characteristics of the polymers used in the present thesis according to the manufacturer's specifications (Boehringer Ingelheim).

Polymer	Composition	Inherent viscosity (η)
RG 503	Poly(D,L-lactide-co-glycolide) 50 : 50	0.4
RG 504	Poly(D,L-lactide-co-glycolide) 50 : 50	0.5
RG 755	Poly(D,L-lactide-co-glycolide) 75 : 25	0.6
R 203	Poly-D,L-lactide	0.3

5.2. **SOLVENTS USED**

Solvent	Supplier/Manufacturer
Acetone reagent grade	BDH, U.K.
Acetonitrile HPLC grade	Rathburn Chemical Ltd., Scotland
Cyclohexane	Riedel-de-Haën, Germany
Chloroform	Riedel-de-Haën, Germany
Dichloromethane (DCM) reagent grade	BDH, U.K.
Dimethylformamide	Riedel-de-Haën, Germany
Karl Fischer Hydranal®-Composite 5	Riedel-de-Haën, Germany
Karl Fischer Hydranal®- Standard 5.00	Riedel-de-Haën, Germany
Methanol HPLC grade	Rathburn Chemical Ltd., Scotland
Tetrahydrofuran (THF) HPLC grade	Sigma-Aldrich Co., Germany

5.3. **INSTRUMENTATION**

Equipment/Instrumentation	Supplier/Manufacturer
Bransonic 200 sonic bath	AGB
EDX (Energy Dispersive X-ray analysis)	PGT, U.S.A.
Gallenkamp oven	AGB
Heidolph stirrer RZR 1	AGB
Hamilton microliter syringes	Hamilton Bonaduz, Switzerland
Hettich Universal Centrifuge	AGB
HP 845 2A diode array spectrophotometer	Hewlett Packard, U.S.A.
Hot stage mounted on a Meopta microscope	Meopta, Czechoslovakia
IKA Ultra-Turrax T 25 Disperser	IKA-Labortechnik, Germany
Leica Stereoscan 440 electron microscope	Leica, Germany
Leica Stereoscan 360 electron microscope	Leica, Germany
Malvern series 2600C, particle sizer	Malvern, U.K.
Marvac mechanical high vacuum pump	Marvac Scientific, U.S.A.
Methrom Karl-Fischer	Methrom, Germany
Mettler AE 240 Analytical Balance	Mettler, Switzerland
Mettler MT/UMT microbalance	Mettler, Switzerland
Mettler Toledo DSC 821	Mettler, Switzerland
Mettler Toledo TC 15/TG 50	Mettler, Switzerland
Mettler Toledo STAR^e Software version 5.1 for Thermal Analysis Evaluations	Mettler, Switzerland
Millex-HV Hydrophilic PVDF filters, 0.45 μm	Millipore
NMR dpx400	Bruker, Germany
Nylaflo® membrane filters 47 mm, 0.2 μm	Gelman Sciences, U.S.A.

Equipment/Instrumentation (continued)	Supplier/Manufacturer
Omnifix 5 ml Luer syringes	Braun, Germany
Orion Model 520A pH meter	Orion, U.S.A.
Perkin Elmer 13-mm hydraulic press	Graseby Specac, U.S.A.
Plunger-operated pipetter Transferpette, 0,5-5 ml	Brand, Germany
Polystyrene standards	Aldrich Chemical Co., U.S.A.
Reciprocal shaking bath model 25	Precision Scientific, U.S.A.
Retsch Ultra Centrifugal Mill ZM 100	Retsch, Germany
Supor® membrane filters 47 mm, 0.2 μm	Gelman Sciences, U.S.A.
Test sieve shaker (50 cycles) and laboratory test sieves (brass frame, s/steel mesh)	Endecotts Ltd., UK.
Waters Styragel HPLC Column	Waters
Waters Novapack C18 HPLC Column	Waters
Waters LC Module I for HPLC	Waters
Waters Refractive Index Detector 410	Waters
Waters Millenium Chromatography Manager	Waters
X-Ray Diffractor, Siemens Diffraktometer, Germany	Siemens, Germany

5.4. **PHYSICOCHEMICAL CHARACTERIZATION OF POWDERS**

5.4.1. **X-ray Diffraction Analysis (XRD)**

Samples in the form of 13-mm compressed discs were analyzed by XRD in the range of 5-35 2θ. Nickel filtered copper kα radiation was used, with a 1.00° dispersion slit,

a 1.00° scatter slit and a 0.15° receiving slit. The X-ray tube was maintained at 40 kV and 40 mA.

The relationship between the % drug load and the X-ray diffraction of a given AMOX-H system was investigated, since the intensities of the individual patterns from a mixture of components are known to be proportional to the concentrations of the phases present. A linear relationship between the intensity of a diffraction line and the weight fraction of a component, however, often may not exist. This may be due to preferred orientation effects arising when the distribution of crystal orientations in a sample is non-random, which result in the enhancement of some diffraction lines and the reduction of others (Doff et al., 1986). By measuring multiple diffraction lines and averaging the results, the influence of preferred orientation effects can be reduced (Ellis and Corrigan, 1994). For Amoxycillin trihydrate, the average relative intensity was calculated from the intensity values of two given diffraction lines. The reading from each diffraction line was firstly corrected for background reading. Intensity averaging was earlier applied in the XRD quantitative analysis of ibuprofen loaded PLA and PLGA microparticles by Ellis and Corrigan (1994).

5.4.2. **Differential Scanning Calorimetry (DSC) and Thermogravimetric Analysis (TGA)**

AMOX-H and polymer powders were characterized by DSC in the temperature range 0°C to 180°C at a rate of 10°C per minute. The amount of sample used varied from 5 mg to 15 mg depending on the type of material analyzed. DSC analyses were performed in 40 µl aluminium crucibles that were sealed and pierced at the top, under N_2 atmosphere. The heating and cooling cycle was repeated twice in all samples. Glass transition temperatures estimated from the first and second heating curves were found to be different in all the samples investigated. However, the T_g values estimated from the second and third heating curves were similar.

The glass transition temperature of a polymer can either be estimated from the first heating curve (Park et al., 1995) or the second heating curve (Gallagher and Corrigan, 1998). In the present work, glass transition temperatures are quoted on the basis of

the second heating scans. Appendix II shows a scheme illustrating the mode of T_g determination using the STAR^e Software (Mettler Toledo).

Enthalpy changes attributable to the drug were estimated by integration of the corresponding endothermic events using STAR^e Software.

TGA was performed in the temperature range between 30°C and 250°C at 10°C per min. These scans were performed under N_2 atmosphere using open crucibles. Similar sample sizes were used in the various runs.

5.4.3. **Particle Size Analysis**

Particle size analysis of AMOX-H was performed by laser diffraction with the use of a Malvern particle sizer. The 63-mm lens, which covers a particle size range between 1.2 and 118 microns was employed. The drug powder was dispersed in cyclohexane. The mean particle size was calculated for three independent samples.

Particle size analysis of the polymers was performed by sieving approximately 1g of powder through a set of laboratory sieves (mesh apertures: 1.00 mm; 500 μm; 355 μm; 250 μm; 125 μm) on an Endecotts laboratory sieve shaker for 5 minutes. The resulting fractions were plotted as cumulative (%) undersize together with a histogram of the distribution.

SEM imaging performed on gold-coated samples was used to examine the appearance of the individual materials, drug and polymer powders, and that of mechanical mixtures of the two.

5.5. **STUDIES PERFORMED ON AMOXYCILLIN TRIHYDRATE**

5.5.1. **Drug solubility studies**

Solubility studies were performed at 37°C in a jacketed-water vessel containing 50 ml of buffer medium with three times the amount of drug expected to dissolve. The vessel was linked to a temperature controlled (Heto) water bath. The buffers employed (Pharmaceutical Handbook, 1980) were phosphate buffer pH 5.9 and phosphate buffer

pH 7.4. Agitation involved the use of overhead stirrers (Heildolph). Each experiment was performed in duplicate and materials employed for sampling purposes were maintained at 37°C at all times.

Samples of 2 ml were taken every 10 minutes, immediately filtered through membranes of pore size 0.2 μm, and appropriately diluted in the relevant buffer for UV absorbance determination at 230 nm. The solubility of the drug was determined by reference to the calibration curve obtained with the relevant buffer. Sampling was continued for approximately 2 hours by which time a constant solubility value was obtained; the pH of the media was then recorded.

5.5.2. **Degradation of drug in solution**

Studies of the degradation of the drug in aqueous solutions were undertaken using a reciprocal shaking water bath set at 37° C and 95 rpm. AMOX-H powder (30 mg) was added to 100 ml of buffered media (table 5.2) contained in 100 ml conical flasks. Drug degradation was monitored by means of the HPLC assay described in section 5.11.1.

Table 5.2. Composition of buffered media employed in AMOX-H degradation studies (Pharmaceutical Handbook, 1980).

Buffer Medium	Composition (g/l)
citrate buffer pH 5.0	Disodium hydrogen phosphate-12-hydrate 36.9; Citric acid 10.2
citrate buffer pH 5.9	Disodium hydrogen phosphate-12-hydrate 43.3; Citric acid 8.3
normal saline	Sodium chloride 9
phosphate buffer 5.9	Sodium chloride 5.2 ; Disodium hydrogen phosphate-12-hydrate 2.4; Sodium dihydrogen phosphate-2-hydrate 9.4
phosphate buffer 7.4	Sodium chloride 4.4 ; Disodium hydrogen phosphate-12-hydrate 19.1; Sodium dihydrogen phosphate-2-hydrate 2.1

5.5.3. **Determination of water content**

Determination of water content in AMOX-H powder was performed using a Methrom Karl-Fischer instrument. The working medium was methanol and the Karl Fischer reagent was Hydranal®-Composite 5 (titre: 5 mg H_2O/ml), which contains imidazole, sulfur dioxide and iodine dissolved in diethylene glycol monomethyl ether. The titre of the Karl Fischer reagent was determined anew with Hydranal®-Standard 5.00. This is a mixture of solvents of a defined partial pressure of water which, under normal atmospheric conditions, neither absorbs nor desorbs moisture (Riedel-de-Haën Hydranal Manual, 1988).

The working medium was titrated to dryness with Hydranal®-Composite 5, following which the drug was added and titrated using the same reagent. Determinations were performed in duplicate.

5.5.4. **Effect of ambient Relative Humidity on the solid drug**

To examine the possibility of solid-state phase conversions of the drug under atmospheric conditions, constant Relative Humidity (R.H.) environments were generated in closed containers. The conditions of these environments were 9, 33, 76 and 95% moisture at room temperature (Pharmaceutical Handbook, 1980). To generate these humidity conditions, 200 ml saturated solutions of various salts (table 5.3) were placed in plastic containers and sealed. A platform placed inside each container supported a pan containing the drug sample (5 grams) which was then monitored for weight changes over a period of 3 months. HPLC, TGA and XRD analysis were performed on the samples at the end of the experiment to be compared with the standard drug.

Table 5.3. Saturated salt solutions used to generate constant humidity environments (Pharmaceutical Handbook, 1980).

R.H. %	Salt used
9	Potassium hydroxide
33	Magnesium chloride hexahydrate
76	Sodium chloride
95	Disodium hydrogen phosphate-12-hydrate

5.5.5. **Dehydration/re-hydration studies**

Phase conversions upon dissolution of the drug in an organic solvent was investigated using methanol, a good solvent for AMOX-H. A solution of the drug in methanol was prepared in a wide-mouth container suitable for evaporation of the solvent at ambient temperature. The container with the solution was placed overnight in a vacuum dessicator. TGA, DSC and XRD were performed on the drug after evaporation of the solvent.

Subsequently the powder was re-dissolved, using water this time, and allowed to dry under vacuum until constant weight. XRD and TGA were performed on the dried powder.

5.5.6. **Hot stage microscopy**

Hot stage microscopy was performed using a Reichert hot stage mounted on a Meopta microscope. Samples were mounted in air and were examined with and without crossed polarising filters.

5.5.7. **Effect of the addition of D,L-lactic acid to Amoxycillin solutions on the pH of the dissolution media**

The following aqueous solutions were prepared in order to monitor their pH changes and to examine the effect of the addition of D,L-lactic acid on Amoxycillin solutions:

A) 100 ml saturated solutions of AMOX-H in phosphate buffer pH 5.9 were prepared in duplicate. (Appearance: white powder in clear liquid)

B) 100 ml saturated solutions of AMOX-H in water were prepared in duplicate. (Appearance: white powder in clear liquid)

C) 100 ml saturated solutions of AMOX-H in phosphate buffer pH 5.9 containing 1 g of D,L-lactic acid (Sigma) were prepared in duplicate. (Appearance: white powder in clear liquid)

D) 100 ml solutions of D,L-lactic acid in phosphate buffer pH 5.9 (1 g in 100 ml buffer) were prepared in duplicate. (Appearance: clear liquid)

Solutions were placed in a shaking water bath at 95 cpm/37°C and monitored over 480 hours. The pH of freshly prepared phosphate buffer (blank sample) was determined at 25°C and 37°C, presenting similar values at both temperatures.

5.6. **GEL PERMEATION CHROMATOGRAPHY (GPC)**

This technique was employed in the characterization of polymer powders and discs. In the case of discs exposed to drug release studies, GPC analysis was undertaken on samples obtained from dried discs.

Approximately 5 mg samples were weighed in a 10 ml volumetric flask subsequently filled with THF and allowed to stand overnight. The system employed was similar to that described by Gilding and Reed (1981). It consisted of a Waters Styragel column

with THF as the mobile phase, set at a flow rate of 1ml/min with a Waters 510 pump, and a Refractive Index Detector RI 410 from Waters. The internal and external temperatures were 30°C and 25°C respectively. Millenium Chromatography software version 2.0 was employed to integrate the peaks and calculate the results. Samples were evaluated against a series of polystyrene standards of M_w 2,500, 13,000, 90,000 (Aldrich) and 5,970, 37,900 (Tosoh, Japan). Samples were injected at least in duplicate.

5.7. NUCLEAR MAGNETIC RESONANCE (NMR)

The sample preparation for these studies involved the dissolution of approximately 5 mg polymer samples in 2 ml $CDCl_3$, aided by sonication when required. The ^{13}C-NMR acquisitions were performed under the following parameter settings: SW 316.4919 ppm, TD 32,768 and TE 300.0 K. The data was processed at 100.6127690 MHz. In the case of the ^{1}H-NMR acquisitions, the parameters employed were: SW 20.5524 ppm, TD 32,768 and TE 300.0 K. Processing was carried out at 400.1300090 MHz.

5.8. MANUFACTURE OF POLYMER DISCS BY MECHANICAL MIXTURE (MM)

5.8.1. Method 1: simple mechanical mixtures

Known amounts of drug and polymer were ground and mixed in a mortar and pestle for 5 minutes. 120 mg portions of the powder mixture were then transferred to a 13-mm hot (45°C) press (pre-heated in an oven). Discs were compressed at 10,000 kg/cm^3 for 10 minutes under vacuum.

The rationale for the use of temperature during compression was based on the method employed by Ries and Moll (1994) for matrix formation of polyglycolic acid tablets by

annealing. Smoothening of the surface structure was observed for tablets that had been thermally treated after compression; the data could be fitted well to the square root of time-law. The temperature range used in the compression of AMOX-H discs (45°C) was chosen taking into account the reported solid-state thermal stability of the drug (Mendez et al., 1989). Temperatures above 50°C were reported to affect the chemical stability of the drug.

5.8.2. **Method 2: mechanical mixtures with particle size control**

The technique involved the use of a Retsch ultra centrifugal mill ZM 100 for particle size reduction and sieving of the powders. The pin-rotor attachment was employed to grind the larger polymer particles at 18,000 rpm for 10 seconds. Finer polymer and drug powders were ground and sieved using the 24-tooth rotor and the 200 μm mesh ring-sieve. A known quantity of polymer and drug passed through the 200 μm mesh were mechanically mixed for 1 minute and 120 mg portions were compressed under the conditions stated for method 1.

Drug loadings are quoted as the nominal % w/w, unless otherwise stated.

5.9. **MANUFACTURE OF POLYMER DISCS BY SOLVENT EVAPORATION (SE)**

5.9.1. **Preparation of drug loaded SE discs**

Drug loaded solvent evaporation systems were prepared by the following procedure:

A known amount of polymer was dissolved in DCM using sonication and an Ultra Turrax T 25 mixer at 8,000 rpm for 5 minutes. AMOX-H was dispersed in a mixture of DCM and Acetone (50:50) in a separate container using sonication. The polymer solution was then added to the drug suspension and homogenised with the mixer (Ultra Turrax T 25) for a further 5 minutes. The homogeneous suspension was cast on a Teflon plate. Evaporation of the solvent took place at room temperature and the film

was subsequently dried in a vacuum dessicator for not less than 2 days. The dried film was then cut into smaller segments and transferred to a 13-mm hot press (45°C) to be compressed at 10,000 kg/cm^3 for 10 minutes under vacuum.

The assayed drug content of SE discs was not less than 90% w/w of the nominal loading.

Drug loadings are quoted as the nominal % w/w, unless otherwise stated.

5.9.2. **Preparation of drug-free SE discs**

Drug-free solvent evaporation systems were prepared by dissolving the polymer in the solvent system (DCM and Acetone) of section 5.9.1. This was aided by sonication followed by mixing with an Ultra Turrax T25 homogenizer at 8,000 rpm for 10 minutes. The resulting solution was poured onto a Teflon plate. Evaporation of the solvent and compression of the film took place as described in section 5.9.1.

5.10. **DRUG RELEASE EXPERIMENTS**

Release experiments were performed in a shaking water bath set at 95 cpm and 37°C using 25 ml conical flasks containing 25 ml of phosphate buffer pH 5.9 (table 5.2). 2 ml samples were withdrawn and replaced with an equivalent amount of buffer at regular intervals. In the first day discs were transferred into fresh buffer in order to ensure sink conditions, unless otherwise stated. For subsequent time points, buffer replacements took place every 5 to 10 days to eliminate degradation products generated in the release media.

The duration of experiments varied between 10 days and 7 months, depending on the type of polymer used and drug loading.

Drug release experiments were performed at least in duplicate. Completion of drug release was determined by comparison of the cumulative release with the initial nominal load or by extraction for residual drug.

Unless otherwise stated: The mean fraction of total drug released was calculated relative to the amount of total drug recovered upon completion of release. The mean fraction of intact drug released was calculated relative to the amount of intact drug recovered upon completion of release.

Variations in the release profiles were calculated using standard deviations (SD), as described in section 5.15, when the number of replicates was at least 3. The range of the data was used otherwise.

5.11. **ANALYSIS OF DRUG CONCENTRATION**

HPLC analysis was employed to determine the concentration of *intact* AMOX. When degradation was apparent, quantification of *total* drug (intact AMOX and degradation products) was performed by UV analysis.

Drug release profiles presented in this thesis should be understood to correspond to *total* drug unless the wording '*intact* drug' was specifically stated.

5.11.1. **HPLC assay**

The method employed was based on that described in USP XXIII. The composition of the mobile phase was adjusted, as indicated in the official monograph, to enhance resolution of the Amoxycillin peak.

The chromatographic system consisted of a reversed phase Novapack C18 column and a Microbondapack C18 guard-column, through which the mobile phase was pumped at a flow rate of 0.9 ml/min. The composition of the mobile phase changed exponentially over the first 10 minutes of elution time from 100% buffer A to 90% of buffer A and 10% of acetonitrile. Buffer A was prepared by dissolving 6.8 g potassium dihydrogen orthophosphate in 1000 ml of water and adjusting to a pH of 5.0 ± 0.1.

Samples and standards were injected (60 µl) alternately. The run time per sample was 18 minutes, plus 7 minutes for compositional recovery between injections.

Chromatography was performed at room temperature with the detector wavelength set at 230 nm.

Calibration curves were obtained from at least five solutions of AMOX-H in phosphate buffer pH 5.9 (as per table 5.2). Dilutions of the samples, when required, were performed with phosphate buffer pH 5.9. The limit of quantification was set to 2 μg/ml, based on the signal-to-noise ratios obtained. Relative standard deviations were examined on five replicate injections as outlined in the USP XXIII. The HPLC method proved to be consistent between days.

Amoxicillin trihydrate samples contain Amoxicilloate as the main impurity (De Pourcq et al., 1985). The preparation of Amoxicilloate followed the method reported by these authors. The compound was formed in solution by dissolving 100.0 mg of AMOX-H in 20 ml of 0.1 N potassium hydroxide. After standing overnight, the solution was neutralized to pH 7.0 with 0.2 M potassium dihydrogen phosphate and diluted to 50.0 ml with water.

5.11.2. **UV assay**

Samples obtained from the release experiments were assayed at λ=230 nm in a Hewlett Packard UV/visible spectrophotometer. Calibration curves were obtained from five solutions of AMOX-H in buffer pH 5.9, ranging between 5.0 and 40.0 μg/ml. Drug release samples required dilution to fall within the linear range of concentration. Dilutions were done with phosphate buffer pH 5.9.

The UV method was examined as an assay for the quantification of total drug (Amoxycillin and degradation products). Solutions of AMOX-H in phosphate buffer pH 5.9 were allowed to degrade in a shaking water bath maintained at 37°C for a period of two weeks. The experiments were carried out in duplicate and at two concentration levels, as will be shown in Chapter 6. Samples were analyzed by UV spectroscopy and HPLC (5.11.1). Absorbance values obtained by UV spectroscopy as a function of time were compared to the absorbance at time zero (intact Amoxycillin). The variation in the readings, expressed as the coefficient of variation, was less than 3.2%.

In order to investigate the absorption levels of polymer sub-units, the dissolution media obtained from eroding drug-free systems was analyzed at 230 nm. Samples were diluted with phosphate buffer in similar manner as for drug release studies. The absorbance values obtained were below the detection level of the drug, indicating that there was no significant interference from polymer components at 230 nm in diluted samples.

5.12. **DRUG STABILITY INSIDE PLA/PLGA MATRICES**

Solid-state stability studies of formulated AMOX-H involved the extraction of drug from polymer discs and subsequent assay of the extracted drug.

Polymer discs were dissolved in 5.0 ml DCM using sonication. 5.0 ml of an aqueous phase were subsequently added to the flask containing the dissolved polymer and the suspended drug. The mixture was then centrifuged at 4000 rpm for a fixed time and the drug was extracted from the upper phase. A second extraction was performed to the organic phase. Quantification of the extractions was proceeded by HPLC analysis following appropriate dilution of the samples to fall within the linear range of concentration. The relevant calibration curves were obtained with a set of drug standards treated in similar manner to the samples.

The technique was tested with freshly prepared samples of known concentration and the average drug recovery, based on the results of three samples, was 98.3%.

5.13. **POLYMER MASS LOSS STUDIES**

5.13.1. **Polymer mass loss from drug-free discs**

Mass loss was monitored for a series of drug-free discs placed in phosphate buffer pH 5.9 using a shaking water bath (37°C and 95 cpm). The buffer was periodically

changed, as described for drug release experiments (5.10). A disc was removed at intervals and was then dried in a dessicator until constant weight was achieved. Comparison of the initial weight (W_i) and the final dried weight (W_d) was used to calculate the fraction of residual mass (F_{RM}) by means of the following equation:

$$F_{RM} = \frac{W_d}{W_i} \qquad \text{equation 5.1}$$

5.13.2. **Polymer mass loss from drug loaded discs**

These studies were performed as described in section 5.13.1. The mass loss of drug loaded discs was corrected for the loss of drug determined as described in section 5.11. Equation 5.2 was used to obtain the fraction residual polymer mass (F_{RPM}):

$$F_{RPM} = \frac{W_i - (W_d + M_d)}{W_i - D_i} \qquad \text{equation 5.2}$$

where W_i and W_d have the meaning given in equation 5.1, M_d is the mass of drug released until removal of the disc from the dissolution media and D_i is the initial drug loading expressed in % w/w.

5.14. **SWELLING STUDIES**

Swelling studies were performed on drug-free and drug loaded discs. Each sample was placed in a glass vial containing 2 ml DCM, stoppered and observed for a given period of time. The appearance of the samples was recorded, such as colour changes and integrity. Apparent changes in the dimensions of the discs were measured using a vernier callipers. Photographs were taken in some cases.

5.15. MATHEMATICAL MODELLING OF RELEASE PROFILES

Drug release and polymer mass loss profiles were fitted by non-linear regression to various mathematical models. Micromath Scientist software version 1.05 was employed to fit the data to a particular model at 95% confidence level. Estimated parameters and standard deviations (SD) were generated by the software. The goodness of fit was judged by the values of the coefficient of determination (r^2) and the model selection criterion (MSC) obtained, where higher values indicated a better fit. Relevant equations are defined below (Scientist User Handbook, 1995):

$$SD = \sqrt{\frac{n\Sigma x^2 - (\Sigma x)^2}{n(n-1)}} \qquad \text{equation 5.3}$$

where n is the number of arguments in the study.

$$r^2 = \frac{\sum_{i=1}^{n} w_i \left(Y_i - \bar{Y}\right)^2 - \sum_{i=1}^{n} w_i \left(Y_i - \hat{Y}_i\right)^2}{\sum_{i=1}^{n} w_i \left(Y_i - \bar{Y}\right)^2} \qquad \text{equation 5.4}$$

where n is the number of arguments or data points in the study, w_i are the weights applied to each argument, Y_i, $\hat{Y}_i$, $\bar{Y}$ are the observed data points, the model-predicted data points and the weighed mean of the observed data respectively.

$$MSC = \ln\left(\frac{\sum_{i=1}^{n} w_i \left(Y_i - \bar{Y}\right)^2}{\sum_{i=1}^{n} w_i \left(Y_i - \hat{Y}\right)^2}\right) - \frac{2p_p}{n} \qquad \text{equation 5.5}$$

where p_p is the number of parameters estimated and the rest of the symbols have the same meaning as in equation 5.4.

The coefficient of determination is a fraction of the total variance accounted for by the model. It is a more appropriate measure of the goodness of fit than correlation (Scientist User Handbook, 1995). The MSC is a normalized modification of the Akaike Information Criterion (AIC) and gives the same rankings between models but is independent of the scaling of the data points. The MSC attempts to represent the "information content" of a given set of parameter estimates by relating the coefficient of determination to the number of parameters (or degrees of freedom). When comparing two models with different number of parameters, the MSC places a burden on the model with the more parameters so that the system has to return a better coefficient of determination. This takes into account how much better the fit should be for the model with the higher number of parameters to be deemed more appropriate.

Equal weights were used for all the data.

CHAPTER 6. CHARACTERIZATION OF RAW MATERIALS AND PRELIMINARY EXPERIMENTS

6.1. AMOXYCILLIN TRIHYDRATE

6.1.1. X-ray Diffraction (XRD)

The diffractogram obtained for the drug powder is shown in figure 6.1. The profile displayed diffraction peaks associated with the scattering of X-rays from crystal faces (Young and Lovell, 1991).

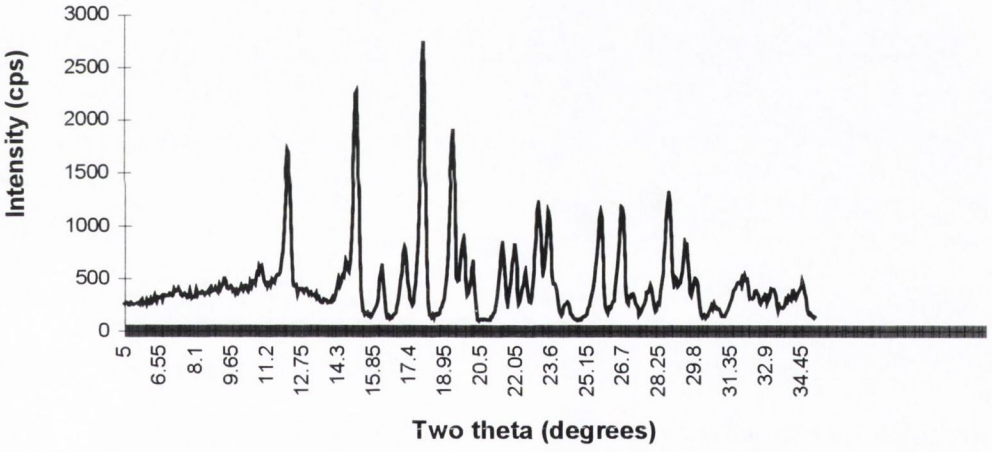

Figure 6.1. X-ray diffractogram of AMOX-H powder.

6.1.2. Determination of water content

Determination of water content in AMOX-H powder was performed by Karl Fischer analysis as described in section 5.5.3. The mean water content was determined as 13.7% w/w. This is within the limits for water specified for the drug (11.5-14.5% w/w) in the British Pharmacopoeia (1993). Based on the molecular formula of Amoxycillin trihydrate three moles of water account for 12.9% w/w, which indicates

that the current batch of drug (Sigma) contained circa 0.8% w/w of water in excess to that required to form the trihydrate.

6.1.3. **Thermal Analysis**

Results obtained by DSC (a) and TGA (b) of AMOX-H powder are shown in figure 6.2. An endothermic peak (143.3°C) with onset at approximately 70°C is observed in the DSC trace. Such transition has a corresponding event in the TGA scan, where 12.0 % w/w of mass was lost up to 100°C. The Karl-Fischer results obtained in the previous section support the concept that the mentioned thermal transitions correspond to the loss of three moles of water. After 180°C, further weight loss was observed in the TGA scan, probably due to decomposition of the drug at higher temperatures.

AMOX-H 13-mm discs, prepared with drug only, were analyzed by DSC and TGA for use as a yardstick in thermal analysis of drug-polymer discs. Figure 6.3 compares the DSC traces of AMOX-H powder (a) and 100% AMOX-H discs (b). The dehydration event appears to be 'continuous' in the case of the powder and 'discontinuous' in the case of the compressed system.

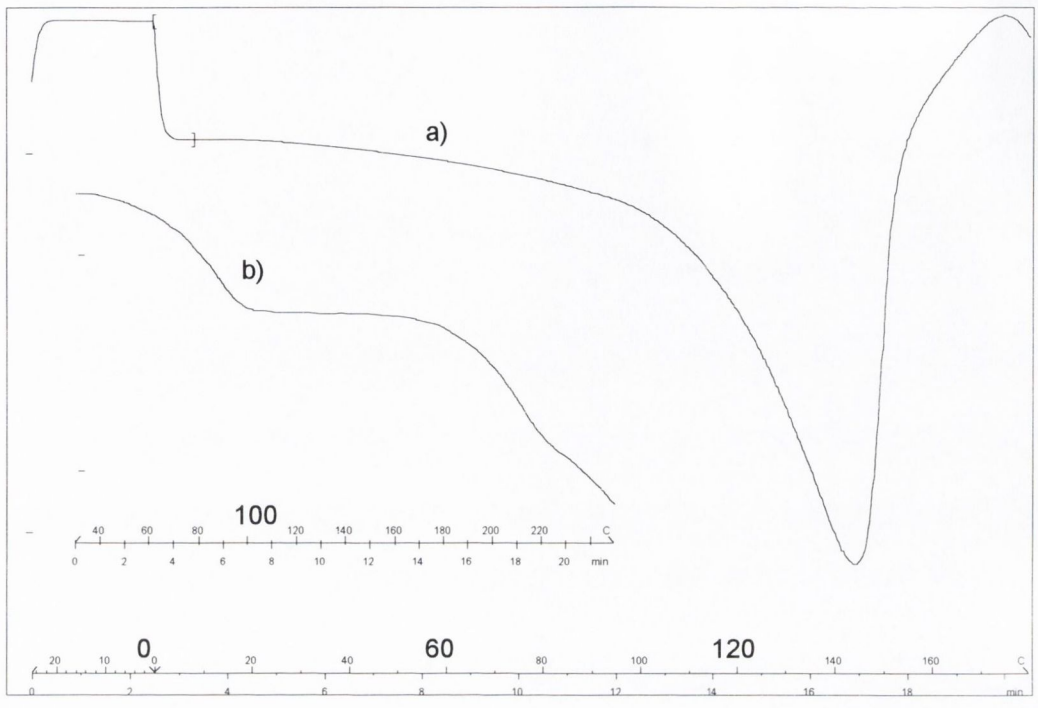

Figure 6.2. DSC (a) and TGA (b) of AMOX-H powder.

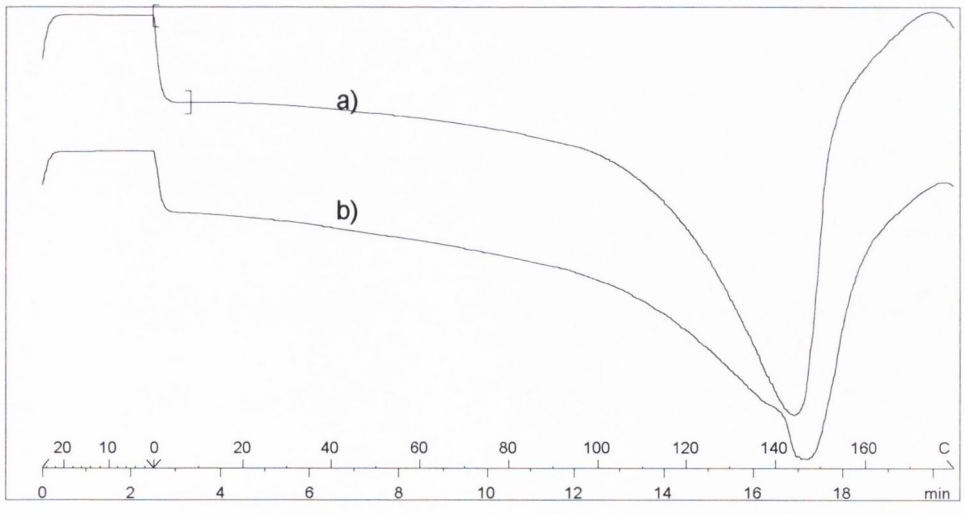

Figure 6.3. DSC of AMOX-H powder (a) and 100% AMOX-H discs (b).

Figure 6.4 illustrates the results obtained by TGA of AMOX-H powder (a) and 100% AMOX-H discs (b). Mass loss was consistent with the initial dehydration of AMOX-H followed by decomposition at higher temperatures. When the drug was compressed (b) dehydration took place beyond 100°C whereas for the powder dehydration appeared to be complete by 100°C (a). This is in accordance with the DSC results previously shown in figure 6.3 where a 'discontinuous' trace had been obtained for the compressed sample, possibly due to a different dehydration profile in the centre and the surface of the disc.

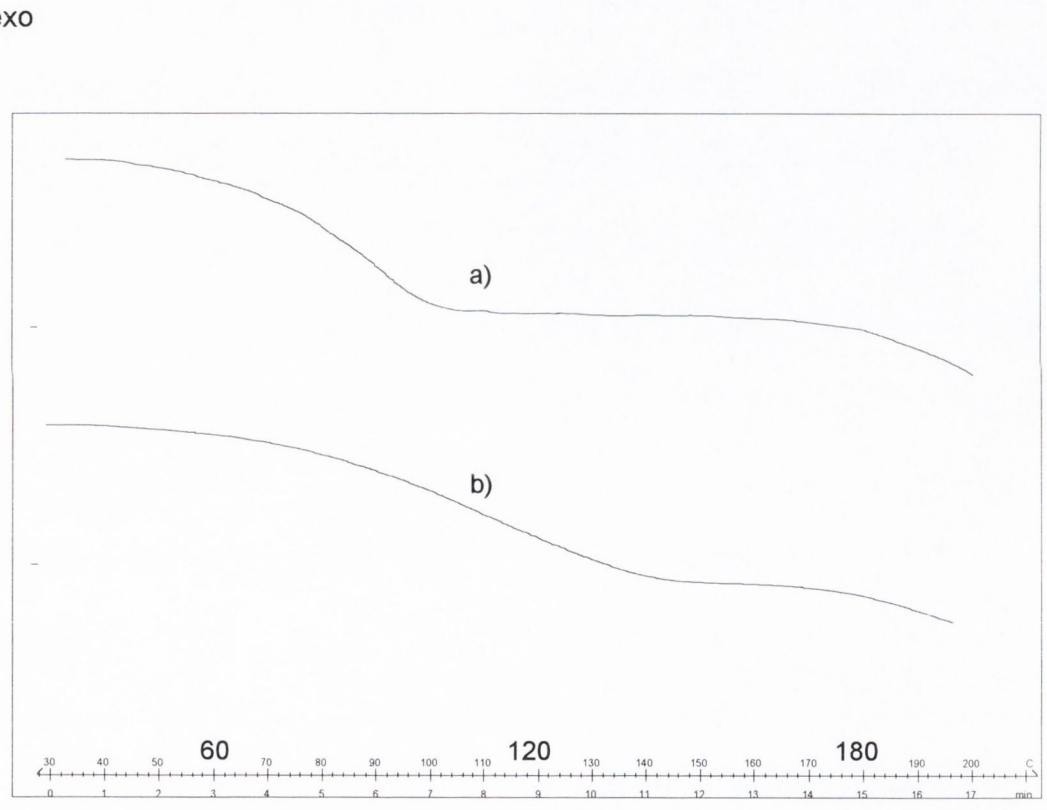

Figure 6.4. TGA of AMOX-H powder (a) and 100% AMOX-H discs (b).

6.1.4. **Dehydration/re-hydration experiments**

Dissolution of AMOX-H in methanol and subsequent drying at ambient temperature under vacuum showed absence of the dehydration transition, associated with the

trihydrate form, when the treated material was analysed by DSC. XRD analysis of the treated material resulted in a scan with absence of peaks, indicating that the drug treated with the organic solvent was amorphous. Appendix II shows the relevant XRD scan.

The amorphous material was then dissolved in water and dried in a dessicator until constant weight. TGA of the re-hydrated material showed results consistent with the loss of three molecules of water and DSC analysis exhibited the dehydration transition attributable to the trihydrate. XRD analysis showed a pattern matching that of crystalline AMOX-H (previously shown in figure 6.1).

6.1.5. **Constant Relative Humidity experiments**

Constant Relative Humidity environments (9, 33, 76, 95%) were generated for exposure of AMOX-H to different ambient conditions, as described in section 5.5.4. Weight changes were only evident at the 95% environment, where a slight weight increase (approximately 3%) in the powder sample occurred upon storage over 3 months.

None of the samples exhibited changes in their physicochemical properties when examined after the three month period. HPLC analysis did not show degradation products. XRD analysis confirmed that the drug was in the same crystalline form as the starting material. In all cases, including the 95% R.H. sample, TGA showed a dehydration event corresponding to the loss of three molecules of water. It appears that the weight increase that was observed in the sample at 95% R.H. corresponded to water in excess to that necessary to form the trihydrate, no longer present when the TGA analysis was carried out.

6.1.6. **Particle size analysis**

Particle size analysis of AMOX-H performed on a Malvern 2600 instrument resulted in an average size of 10 microns with 90% of the particles below 30 microns. Appendix II shows the overall profile of the particle size distribution.

Figure 6.5 shows photographs obtained by scanning electron microscopy of the drug powder magnified 235 (a) and 1K times (b) respectively. AMOX-H is composed of small, rod-shaped particles, the majority of which appears to be less than 30 μm in length, in agreement with the (Malvern 2600) particle size analysis results.

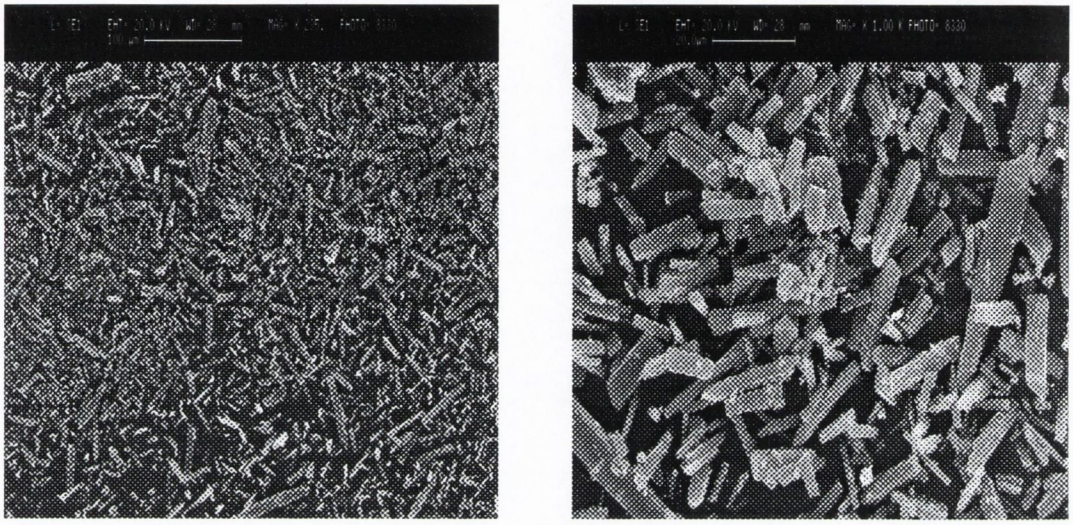

a) b)

Figure 6.5. Scanning electron microscopy of AMOX-H powder magnified 235 times (a) and 1K times (b).

6.1.7. **Hot stage microscopy**

AMOX-H observed under the microscope appeared as a white powder composed of irregular and rod-shaped particles. Birefringence (interference colors) was observed under polarized light, in compliance with the crystallinity requirement stated in the official monograph (USP Pharmacopeia, XXIII).

Structural changes of the particles were not apparent upon heating in the hot stage. Browning of the material commenced at approximately 120°C. Further coloration was observed at 180°C concomitantly with a strong decomposition smell. Alterations in the shape or size of the particles were still not evident past 230°C.

6.2. ANALYSIS OF AMOXYCILLIN CONCENTRATION

6.2.1. Examination of the HPLC method as a stability indicating assay

Amoxycillin solutions were spiked with a) aqueous solutions of decomposed Amoxycillin, b) commercially available related substances (6-APA) and c) the degradation product Amoxicilloate, prepared as described in section 5.11.1. The chromatograms obtained showed that Amoxycillin eluted at approximately 7.5 minutes; 6-APA and Amoxicilloate eluted at 4.5 and 5.5 minutes, respectively. Drug samples previously decomposed in aqueous media mainly contained degradation products that eluted after the Amoxycillin peak, i.e. after 8 minutes. These peaks were not identified but possibly corresponded to oligomers of the drug originated from self-aminolysis reactions (Van Krimpen et al., 1987). An example of a chromatogram from a degraded Amoxycillin sample is shown in section 6.4.2, figure 6.11 (d).

6.2.2. UV spectroscopy for the quantification of total drug

The UV method was examined as an assay for the quantification of total drug (Amoxycillin and degradation products). As explained in section 5.11.2, absorbance values at 230 nm obtained for degraded Amoxycillin solutions were compared with the readings from non-degraded samples (absorbance at time zero). Figure 6.6 shows the resulting plots obtained for two concentration levels of the drug (20 and 230 μg/ml). The results show that, for the period investigated, the total absorbance values (drug and degradation products) are randomly distributed around the unity. The coefficient of variation obtained at each concentration level was less than 3.2%.

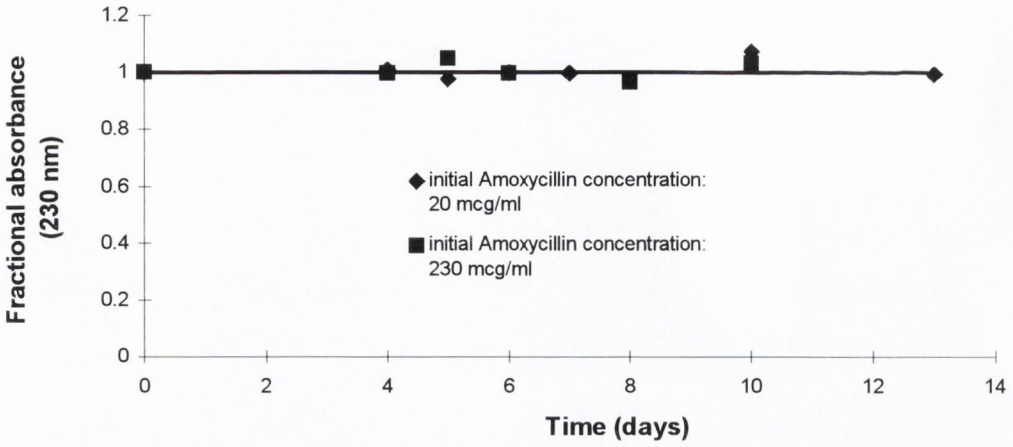

Figure 6.6. Fractional absorbance (230 nm) obtained for pure Amoxycillin degraded in phosphate buffer pH 5.9. The absorbance value at each time point was normalized by the absorbance at time zero.

The sum of HPLC peak areas in a degraded sample was compared to the corresponding UV absorbance values. Figure 6.7 shows the resulting plot obtained for samples of initial concentration levels ranging between 2 and 230 μg/ml conserved between 5 to 10 days in phosphate buffer. A linear relationship was found. The coefficient of determination was 0.9956.

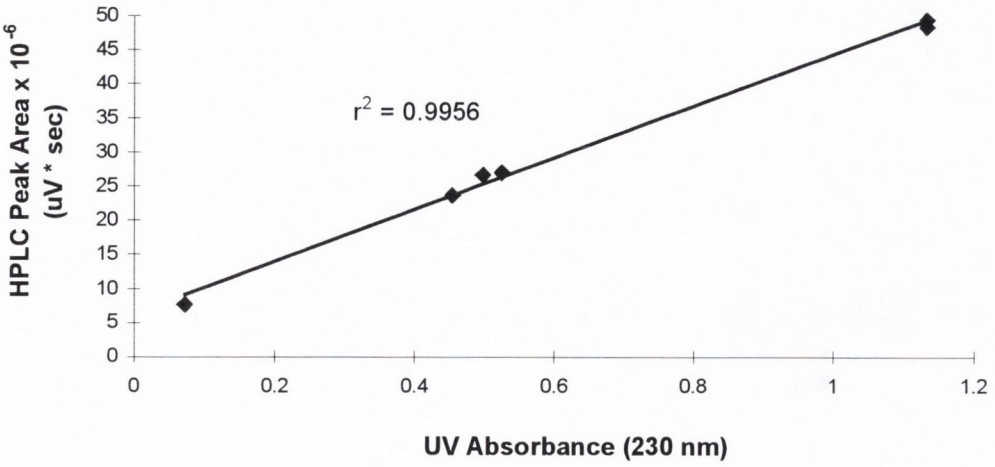

Figure 6.7. The sum of HPLC peak areas (sum of degradation components) versus UV absorbance values for Amoxycillin solutions (2 to 230 μg/ml) which degraded in phosphate buffer for a period of 5 to 10 days.

6.3. DRUG SOLUBILITY STUDIES

Solubility studies of AMOX-H were performed in phosphate buffers of pH 5.9 and 7.4 as described in section 5.5.1. The average results are shown in figure 6.8. A higher solubility was obtained in the media of higher pH, as expected from the results of Tsuji et al. (1978). The pH values measured at the last sampling points were 5.8 and 7.3 for the lower and higher pH buffers, respectively.

Equilibrium solubility measurements should be taken when all solid phase conversions are complete (Ledwidge and Corrigan, 1997). In the case of AMOX-H, dehydration/re-hydration experiments (section 6.1.4) have shown that AMOX stoichiometrically binds to water to ultimately form a trihydrate, which is the form supplied by the manufacturer. Therefore, solubility studies with AMOX-H did not require the kinetics of solid phase conversion to be taken into account.

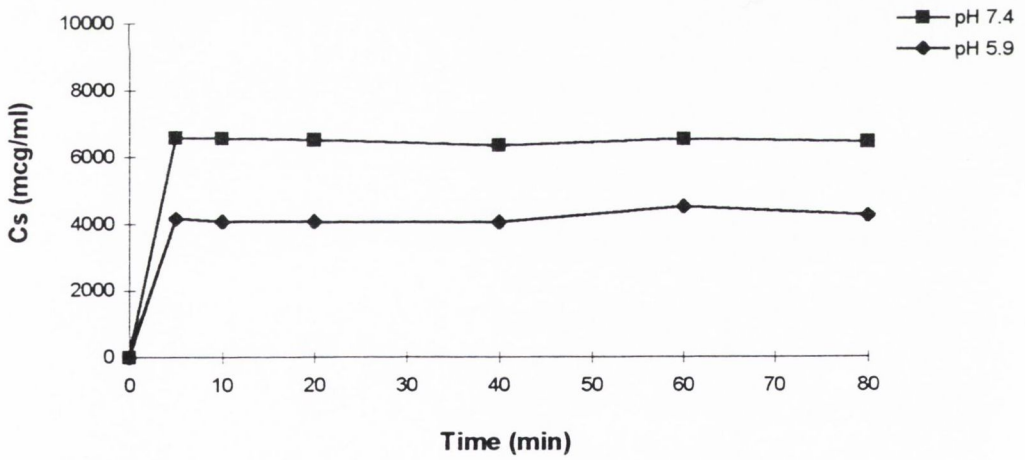

Figure 6.8. Solubility of AMOX-H at pH 5.9 and pH 7.4.

Tsuji et al. (1978) reported that the intrinsic solubility (C_o) of AMOX-H, measured at 37°C and ionic strength 0.5 units, was 0.013 M (5.45 mg/ml). This value was determined from the solubility of the electrically neutral zwitterion, which exists at a pH of approximately 5.5, and is the minimum solubility of the drug. In the present work, however, the solubility at pH 5.9 was 4.2 mg/ml (figure 6.8). Differences in the

solubility results may be due to variations in the ionic strength of the dissolution media employed, as reported by Hou and Poole (1969) for the parent drug ampicillin. These authors observed both a 'salting in' and a 'salting out' effect, at low and high concentrations respectively. Tsuji et al. (1978) also investigated the effect of the ionic strength on the solubility of penicillins. They reported for Amoxycillin trihydrate that the solubility of the drug was not affected by the concentration of potassium chloride in the media. However, such studies did not cover solutions of lower ionic strength (i.e., below 0.4 units), unlike Hou and Poole (1969).

6.4. **DRUG DEGRADATION STUDIES**

6.4.1. **Effect of the pH of the media on the degradation rate**

The degradation of the drug was studied in various aqueous solutions with the aim to select a suitable media for subsequent use in drug release studies. Figure 6.9 shows the plots of residual Amoxycillin (log μg/ml) versus time, determined as described in section 5.5.2. The results indicate pseudo-first order degradation profiles. Table 6.1 lists the estimates obtained for the degradation rate constants (k_{deg}). These values were dependent on the pH of the media. Normal saline and distilled water (pH determined as 6.05 and 5.90, respectively) showed the slowest degradation rates. Amongst the buffered media, phosphate buffer pH 5.9 showed the slowest degradation rate. Tsuji et al. (1978) reported the slowest degradation rate for citrate buffer pH 5.5, at 35°C and ionic strength equal to 0.5 units. These authors did not investigate the effect of the phosphate buffers. They experimented with other citrate buffers (pH 2.80; 3.13; 3.80; 4.23 and 6.80) for which the rates of degradation obtained, expressed as the pseudo-first order rate constants, were higher than the rate at pH 5.5.

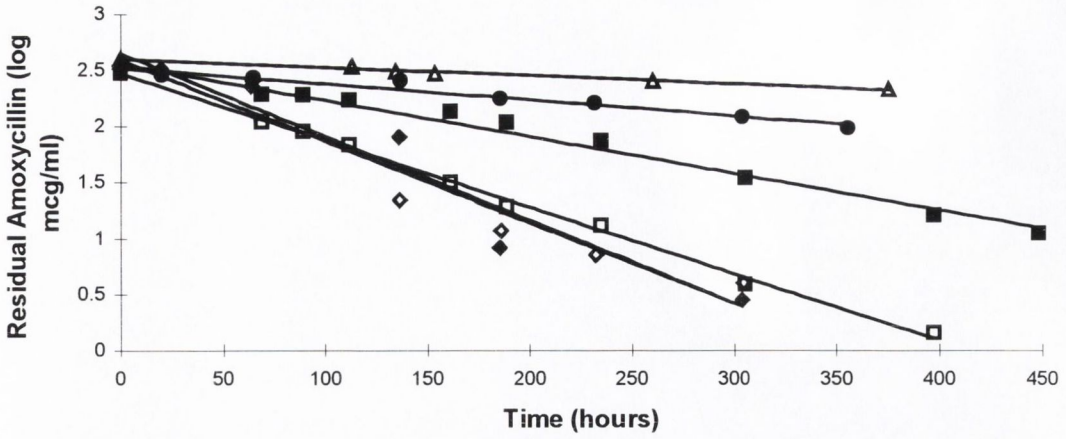

Figure 6.9. Pseudo first-order plots of residual Amoxycillin (log μg/ml) in various aqueous media as a function of time, determined by HPLC analysis. The dissolution media used were △ normal saline, ● distilled water, ■ phosphate buffer pH 5.9, □ phosphate buffer pH 7.4, ◆ citrate buffer pH 5.4, ◇ citrate buffer pH 5.0.

Table 6.1. Estimates of the pseudo first-order degradation rate constants for the degradation of Amoxycillin in aqueous media.

Medium	k_{deg} (h^{-1})	r^2	MSC
water (pH 5.90)	$6.08 \times 10^{-4} \pm 4.8 \times 10^{-5}$	0.9653	2.86
normal saline (pH 6.05)	$3.04 \times 10^{-4} \pm 2.6 \times 10^{-5}$	0.9806	3.28
phosphate buffer pH 5.9	$1.43 \times 10^{-3} \pm 7.4 \times 10^{-5}$	0.9781	3.42
phosphate buffer pH 7.4	$2.57 \times 10^{-3} \pm 5.2 \times 10^{-5}$	0.9970	5.35
citrate buffer pH 5.0	$3.22 \times 10^{-3} \pm 4.3 \times 10^{-4}$	0.9353	2.07
citrate buffer pH 5.4	$3.13 \times 10^{-3} \pm 3.4 \times 10^{-4}$	0.9456	2.34

A plot of the pseudo-first order rate constants versus pH is shown in figure 6.10. The data appears to be distributed along a U-shaped curve consistent with the results obtained by Tsuji et al. (1978) which are shown in Appendix II.

Based on the results of figures 6.9 and 6.10, phosphate buffer pH 5.9 was selected as the media to be used in drug release experiments. It is expected that a buffered media will control the pH as dissolution of the polymeric matrix and concurrent generation of free lactic acid proceed.

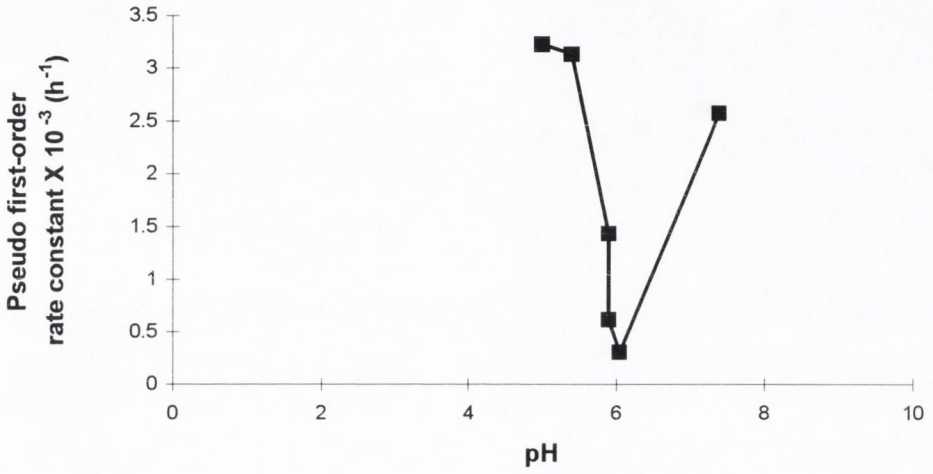

Figure 6.10. Pseudo first-order degradation rate constants for Amoxycillin trihydrate as a function of the pH.

6.4.2. **Degradation pattern (HPLC)**

Figure 6.11 shows a degradation sequence determined by HPLC for Amoxycillin aqueous solutions after 24 (a), 120 (b), 290 (c) and 500 (d) hours at 37°C and 95 cpm. Degradation increased with time, this was evidenced by the increasing number of peaks observed in the chromatograms.

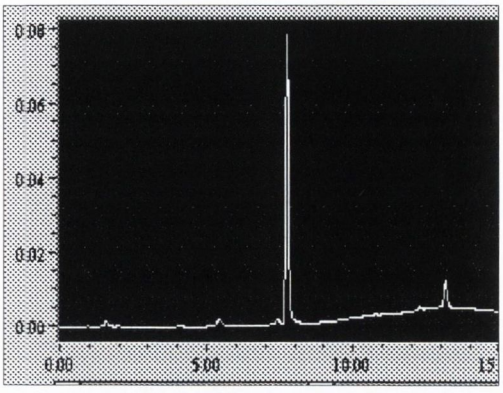

a) 24 hours

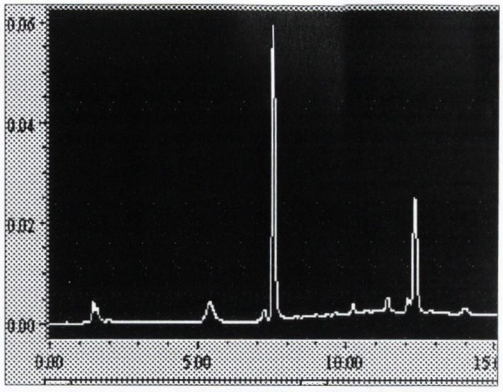

b) 120 hours

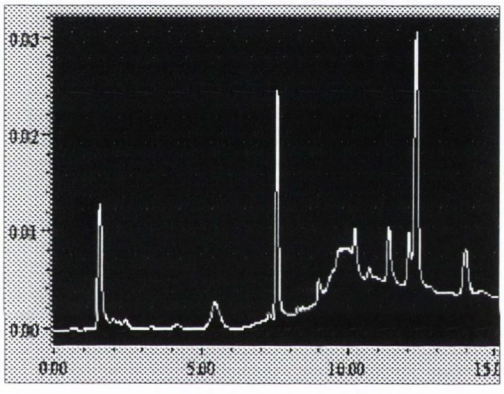

c) 290 hours

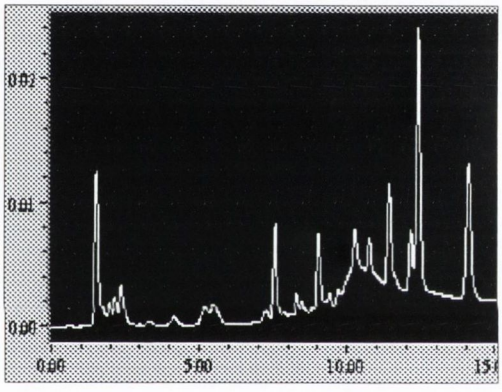

d) 500 hours

Figure 6.11. HPLC traces corresponding to the degradation of Amoxycillin (7.5 minutes) in phosphate buffer pH 5.9 at 37°C and 95 cpm after 24 (a), 120 (b), 290 (c) and 500 (d) hours.

As previously described, two peaks were matched with well recognized degradation products: Amoxicilloate, prepared as described in section 5.11.1, and 6-amino-penicillanic acid (6-APA) (Sigma Chemical Co.). Degradation components that eluted after the drug's elution time were unidentified. Depending on the progress of the degradation process, which is dependant upon the initial concentration of drug (Van Krimpen et al., 1997), some samples showed a main peak at approximately 8.5 minutes, others showed two main peaks eluting between 12 and 15 minutes. The development of some peaks appeared to occur at the expense of others. One of the late

eluting components may possibly correspond to the piperazine-2,5-dione reported by Mendez et al. (1989).

Analysis of samples exposed to degradation for more than one month showed that all the components appear to convert to a product eluting at approximately 11 minutes. Scheme 2.3 showed that when benzylpenicillin was used as a model penicillin the degradation in acidic media finally leads to benzylpenicilloic acid.

6.5. CHARACTERIZATION OF POLYMERS

6.5.1. X-ray Diffraction of polymers

X-ray diffractograms of RG 503, RG 504, RG 755, R 203 polymer powders showed complete absence of defined peaks (figure 6.12). This confirmed the amorphous nature of these polymers.

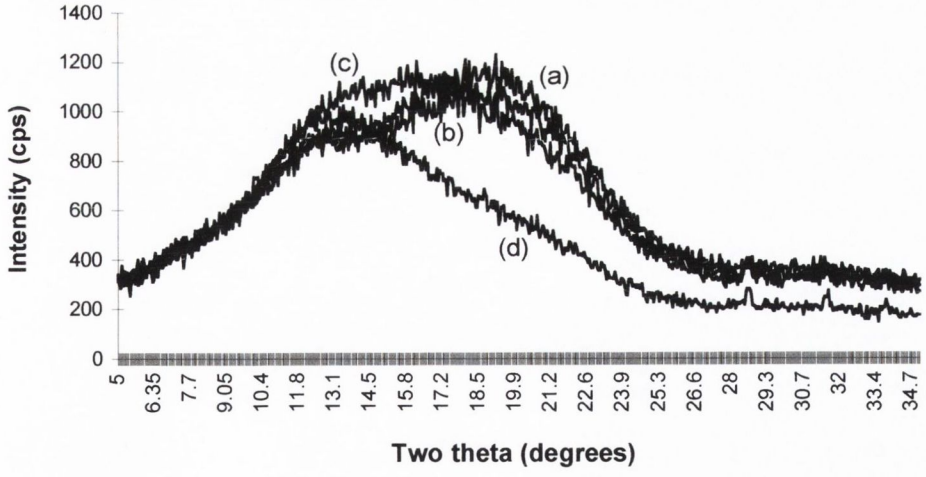

Figure 6.12. X-ray diffractogram of RG 503 (a), RG 504 (b), RG 755 (c) and R 203 (d) powders.

6.5.2. **Particle size analysis of polymers**

As described in section 5.4, a study of the size distribution of the polymer particles was carried out by means of sieving a sample of the raw materials supplied by Boehringer Ingelheim. Figure 6.13 shows the cumulative undersize (%) plot corresponding to RG 503, RG 504, RG 755 and R 203 polymer powders. Approximately 15% of RG 504 particles were larger than 500 μm. This fraction increased for R 203 and RG 503 where approximately 60% of the particles showed a size between 500-1000 μm. RG 755 displayed the highest fraction of particles in the large particle size range, with 80% of the material aggregated as particles greater than 500 μm. This polymer could not be size reduced in a mortar and pestle. Appendix II shows SEM of the polymer powders.

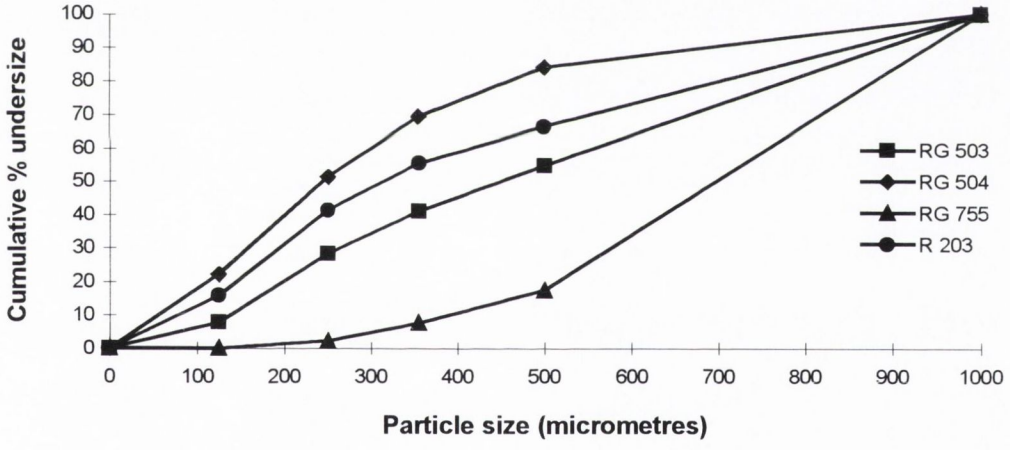

Figure 6.13. Cumulative % undersize versus particle size (micrometres) plot obtained for the sieving results of RG 503, RG 504, RG 755 and R 203 polymer powders.

6.5.3. **Gel Permeation Chromatography**

RG 503, RG 504, RG 755 and R 203 powders were characterized by GPC. Table 6.2 shows the M_w, M_n and polydispersity (P) values obtained for each polymer. The results obtained for M_w differed from the estimated molecular weight values declared

by the manufacturer (Boeringher Ingelheim Catalogue). However, the methodology employed by the manufacturer in the determination of molecular weight was not specified. Viscosity average molecular weight (M_v) determinations performed by Gallagher and Corrigan (1998) resulted in values (M_v 13,070 and 10,064 for RG 504 and R 203, respectively) consistent with the molecular weight values declared by the manufacturer (table 6.2).

Table 6.2. M_w, M_n and P values determined by GPC for RG 503, RG 504, RG 755, R 203.

Polymer	M_w (daltons)	M_n (daltons)	P	Molecular weight (manufacturer)
RG 503	34,896	21,235	1.66	9,000
RG 504	54,123	33,878	1.60	12,000
RG 755	73,854	35,902	2.06	18,000
R 203	26,613	16,211	1.64	16,000

Schartel et al. (1997) reported the molecular weight of RG 503 supplied by Boehringer Ingelheim as 39,500. Values reported by Gallagher and Corrigan (1998) for RG 504 (50,343 M_w; 33,292 M_n) and R 203 (24,173 M_w; 15,015 M_n) are consistent with the M_w and M_n results obtained in the present work (table 6.2), for the same batches of product. Thomasin et al. (1996) reported average weight molecular weight values determined by GPC for Boeringher Ingelheim polymers RG 503, RG 755 and R 203 as 35,100; 68,600 and 23,300 respectively. These values are consistent with the results obtained in the present work.

6.5.4. **Thermal analysis of polymers**

It has been reported Fitzgerald and Corrigan (1993) that TGA of RG 504 showed decomposition after 230°C. This is in line with the results obtained in the current work

where TGA of RG 503 powder did not exhibit any significant mass loss in the temperature range between 30 and 250°C.

Traces obtained by DSC of RG 503 powder are shown in figure 6.14. The first scan gave a glass transition temperature of 51.2°C (a). The sample was then quenched and immediately re-scanned. The results of the second scan showed a decrease in the value of the T_g (b). Subsequently, the same sample was allowed to stand overnight at room temperature and scanned the following day (c), then quenched and immediately re-scanned (d). The T_g values obtained for traces (b), (c) and (d) were similar. This indicated that once the thermal history of the polymer has been standardized the glass transition for RG 503 occurs at 45.0 ± 1.8°C.

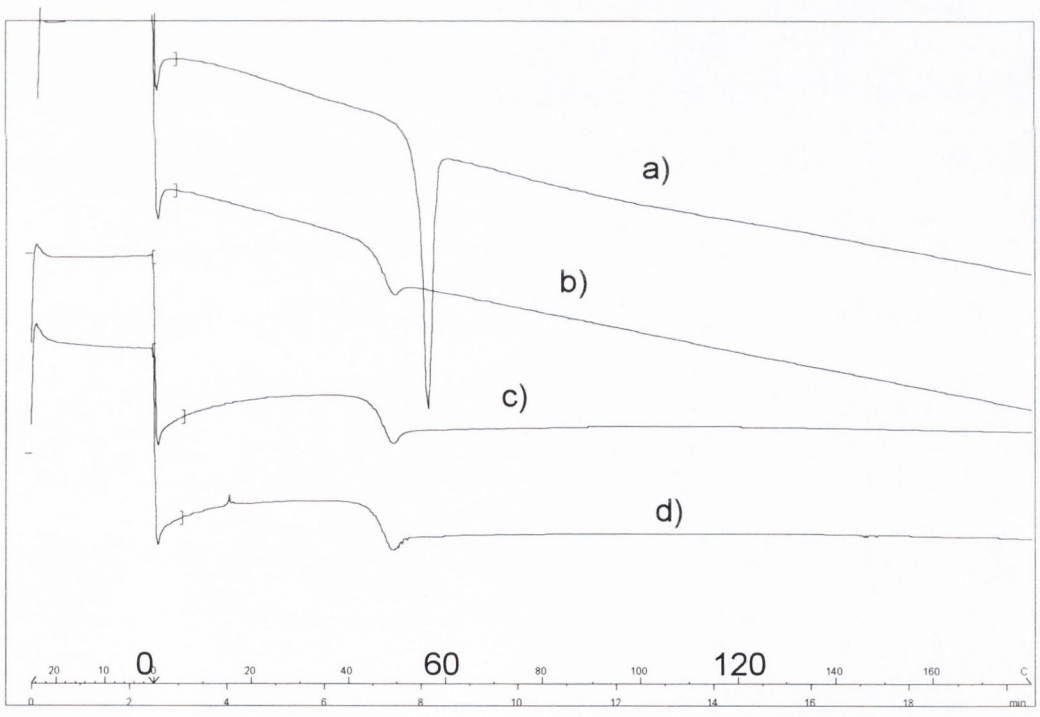

Figure 6.14. DSC of first (a), second (b), third (c) and fourth (d) scan of RG 503 untreated powder.

Table 6.3 below compares the T_g values obtained for the reruns of RG 503, RG 504, RG 755 and R 203 polymers. Appendix II shows DSC traces obtained for the first and second heating scans of RG 504.

Table 6.3. Glass transitions obtained for DSC reruns of RG 503, RG 504, RG 755 and R 203 polymer powders.

System	T_g (°C) from first scan	T_g (°C) from second scan
RG 503	51.2	45.0
RG 504	52.7	46.8
RG 755	58.2	49.7
R 203	53.0	46.6

6.6. **FILMCASTING STUDIES**

6.6.1. **Solvents tested for filmcasting**

Various solvents were tested with the purpose of obtaining a homogeneous solution of the drug and polymer utilizing a minimum amount of fluid. The rationale for the combination of solvents tested was the reported solubility of each compound (Boehringer Ingelheim catalogue for the polymers and Bhattacharyya and Cort (1978) for the drug).

PLGA and drug films prepared with Chloroform were smooth and showed a homogeneous dispersion of the drug. However since this solvent has been banned by the FDA for use in foods, drugs and cosmetics (The Merck Index, 12th Edition) it was not employed in any further tests.

Both AMOX-H and PLGA dissolved in DMF upon sonication. Evaporation of the solvent at ambient pressure, however, required the use of heat. Solutions obtained

with DMF and subsequently poured onto a Teflon plate showed browning of the film upon heating at 70°C for 30 minutes.

As shown in table 6.4, 20 mg of drug were added to a range of solvents of constant quantity (5 ml). PLGA (100 mg) was dissolved in a separate container using DCM.

The results obtained when the polymer solution (DCM) was added to the drug solution/suspension are listed in table 6.4. Systems 1 and 4, prepared with Methanol, which is also a toxic solvent, and Ethyl acetate respectively, resulted in the formation of a precipitate. In contrast, systems number 2 and 3 resulted in homogeneous suspensions. Consequently, Amoxycillin-polymer films were prepared with DCM and Acetone, as previously described in section 5.9. Since Acetone has a higher boiling point than DCM (56.5°C versus 39.75°C) the amount of Acetone used to disperse the drug was kept to a minimum, to prevent the entrapment of residual filmcasting solvent.

Table 6.4. Solvent systems tested for use in the preparation of Amoxycillin/PLGA films.

System	AMOX-H (20 mg)	RG 503 (100 mg)	Resulting mixture
1	Methanol	DCM	precipitates out as white flakes
2	Acetone	DCM	homogeneous suspension
3	Acetone/Methanol	DCM	homogeneous suspension
4	Ethylacetate	DCM	precipitates out

DCM and Acetone mixtures have been previously used to prepare PLGA films such as in the case of diltiazem and levamisole systems, prepared by Fitzgerald and Corrigan (1993). DCM has been used to date in innumerable applications with polylactic polymers in the pharmaceutical field (Schlicher et al, 1997; Calhoun and Mader, 1997).

6.6.2. **Drug distribution in polymer films**

The uniformity of drug distribution in the films was examined. This firstly involved the extraction of drug from three different sections of a single film. Quantification of the drug extracted was then carried out by HPLC analysis, with resulting chromatograms showing the absence of degradation products in the films.

Table 6.5 lists the results obtained for PLGA films at 20% drug loading. The standard deviation between sections was 1.34.

Table 6.5. Distribution of Amoxycillin in a 20% drug loaded PLGA film manufactured by solvent evaporation.

Weight of film section (mg)	drug present (%)	average(%) and S.D.
25.07	19.97	
28.76	18.18	19.65 $\pm$ 1.34
29.36	20.82	

CHAPTER 7. RG 503 AND RG 504 SYSTEMS

7.1. INTRODUCTION

Previous work carried out by Fitzgerald and Corrigan (1993) indicated that the t_{max} for polymer mass loss of drug-free RG 504 discs was approximately 25 days. This is longer than the release period of seven days set as an objective of the present work and previously introduced in Chapter 4. On this basis, it was expected that a lower molecular weight copolymer of similar composition, such as RG 503 (MW 34,896), would bring the value of t_{max} closer to seven days.

RG 503 is a copolymer constituted by equal amounts of lactide and glycolide. Discs were prepared by mechanical mixture with AMOX-H (MM discs) and by a solvent evaporation technique (SE discs). In the second part of this chapter results obtained with RG 504 (MW 54,123) will be discussed.

7.2. RG 503 SYSTEMS PREPARED BY MECHANICAL MIXTURE (MM SYSTEMS)

7.2.1. Physicochemical and morphological characteristics of RG 503 MM discs

RG 503 MM discs were prepared from mechanical mixtures of the drug and the copolymer powders. Characterization of MM discs manufactured by methods 1 and 2 (section 5.8) resulted in similar DSC, TGA and X-ray diffraction scans. HPLC analysis of drug extracted from the discs resulted in chromatograms having a single peak, indicating the absence of degradation products.

X-ray diffraction patterns obtained for RG 503 powder (a), RG 503 MM discs at 10% (b), 20% (c), 35% (d) drug loading and AMOX-H powder (e) are shown in figure 7.1. The scan obtained for the pure copolymer powder (a) was typical of amorphous materials. No differences were found in the location of the peaks between the diffractograms of the pure drug (e) and those corresponding to the preparations of

drug and copolymer (b, c, d). These results indicated the presence of crystalline drug in RG 503 MM discs.

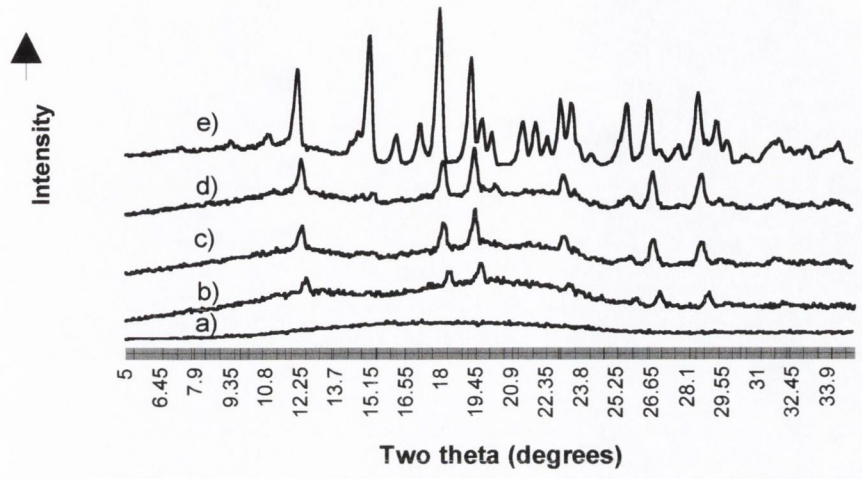

Figure 7.1. X-ray diffractogram of RG 503 powder (a), RG 503 MM discs at 10% (b), 20% (c), 35% (d) drug loading and Amoxycillin trihydrate powder (e).

From the results of figure 7.1 it appears that the diffraction intensity increased in rank order with the drug load. Therefore, the average intensity of two main peaks corrected for background counts (section 5.4.1) was plotted versus % drug load as shown in figure 7.2. A linear trend through the origin (r^2=0.9897; MSC=4.07) suggests that the intensity is directly proportional to the drug load.

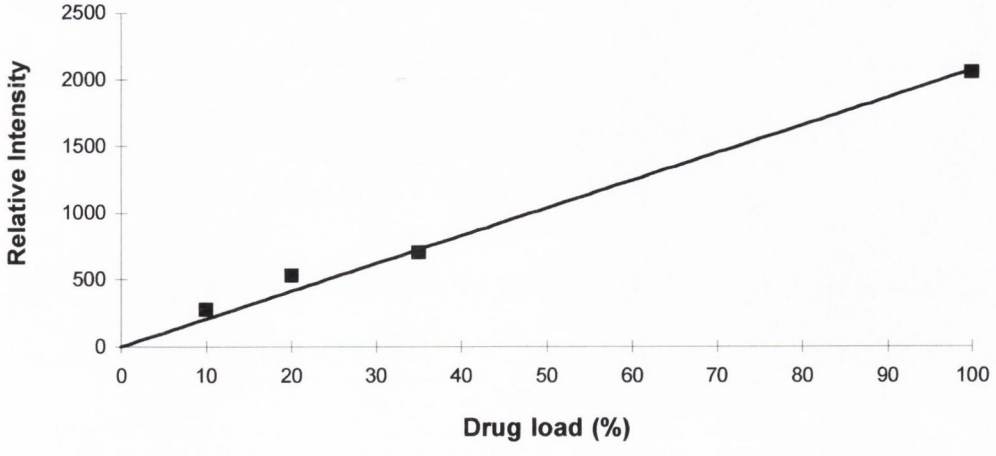

Figure 7.2. Relationship between drug load (%) and X-ray diffraction intensity for RG 503 MM discs.

Figure 7.3 shows the traces obtained by DSC on first heating RG 503 powder (a), AMOX-H powder (b), RG 503 MM discs at 20% (c), 35% (d) drug loading. Traces (c) and (d) showed endotherms characteristic of the copolymer and the drug. The magnitude of the endothermic events corresponding to the drug were in rank order with the drug load of the systems. The transition corresponding to the polymer occurred at lower temperatures in the discs compared to the polymer powder (44.2°C (c) and 44.3°C (d) versus 51.4°C (a)).

Ford and Timmins (1989) explained the importance of standardizing the thermal history of a polymer when performing comparative studies. These authors also mentioned that a reduction in the polymer T_g could be due to a plasticising effect of the drug. To examine this possibility, a thermal treatment simulating the manufacturing conditions was then applied to RG 503 powder.

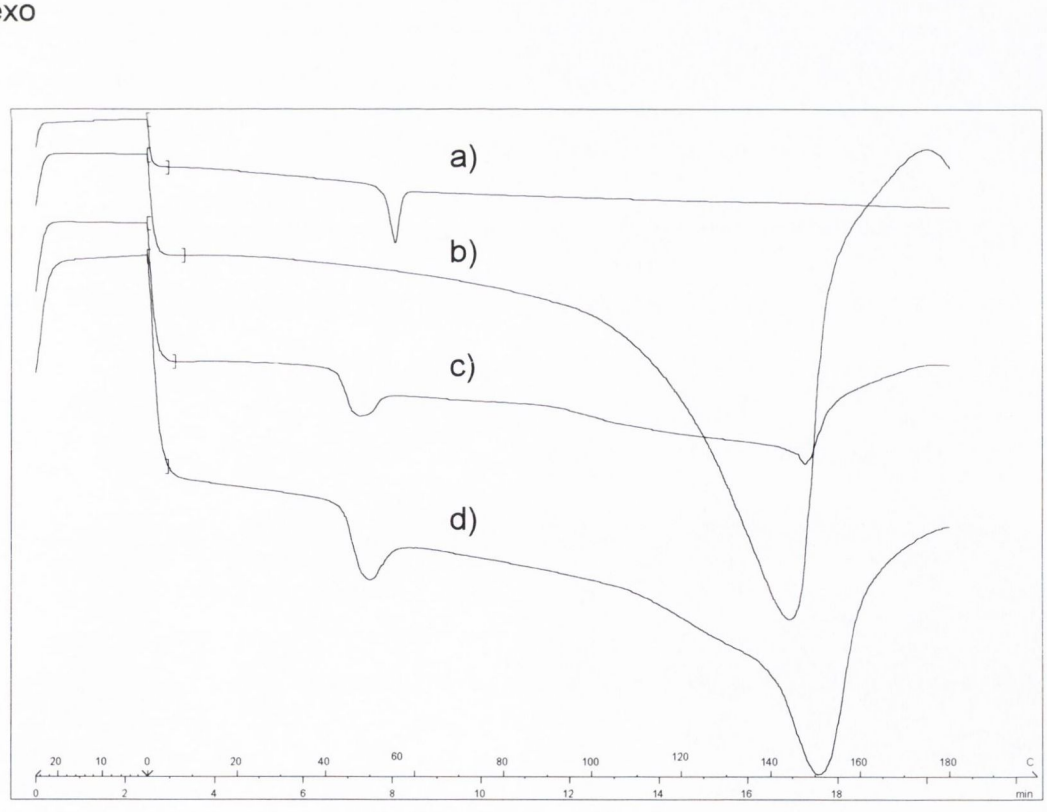

Figure 7.3. First DSC heating scans of pure RG 503 powder (a), pure AMOX-H powder (b), and RG 503 MM discs containing 20% (c) and 35% (d) drug loading.

Figure 7.4 shows the DSC traces obtained for the thermally treated copolymer powder (heated to 45°C for 15 minutes and then rescanned) versus the scan obtained for untreated RG 503. The results showed that the thermal treatment decreased the value of T_g by approximately 4°C.

^exo

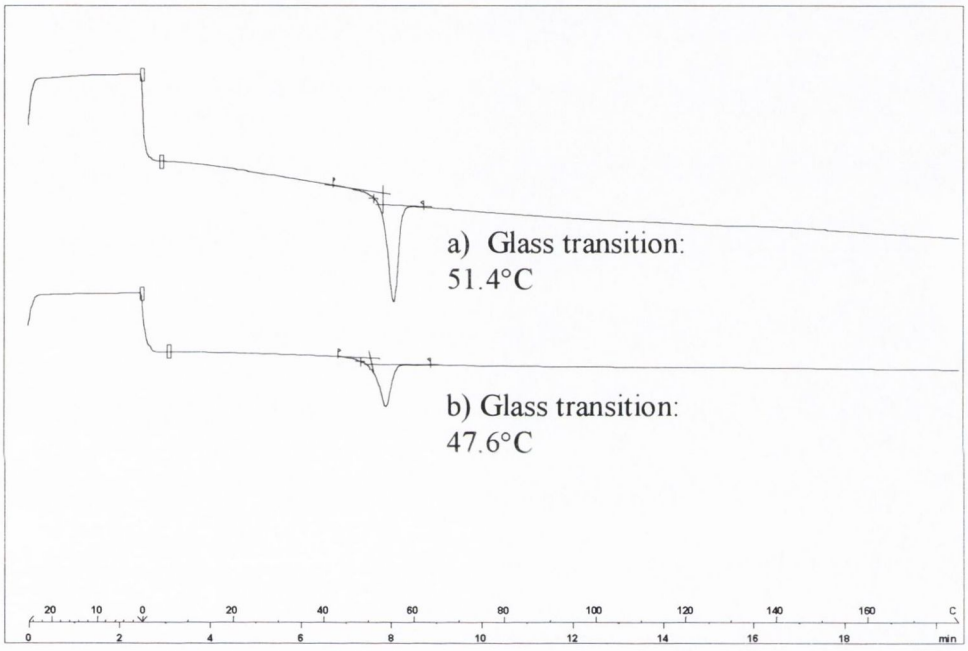

Figure 7.4. DSC of untreated (a) and thermally treated (45°C for 15 min) (b) RG 503 powder.

Figure 7.5 compares the TGA scans of RG 503 MM discs at 20% (a) and 30% (b) drug loading with the scan of AMOX-H powder (c). Mass loss was observed in all the samples, with traces corresponding to drug loaded polymer discs mirroring that of the drug powder. As explained in section 6.5.4, TGA results from RG 503 powder did not show any significant mass loss in the temperature range between 30°C to 250°C. The loss of volatile components in figure 7.5 is therefore attributable to the drug.

Karl Fischer results for the drug powder (Chapter 6) confirmed that the first horizontal step displayed in trace (c) corresponds to the loss of three molecules of water from the

trihydrate. The second horizontal step possibly relates to decomposition of the pencillin at higher temperatures.

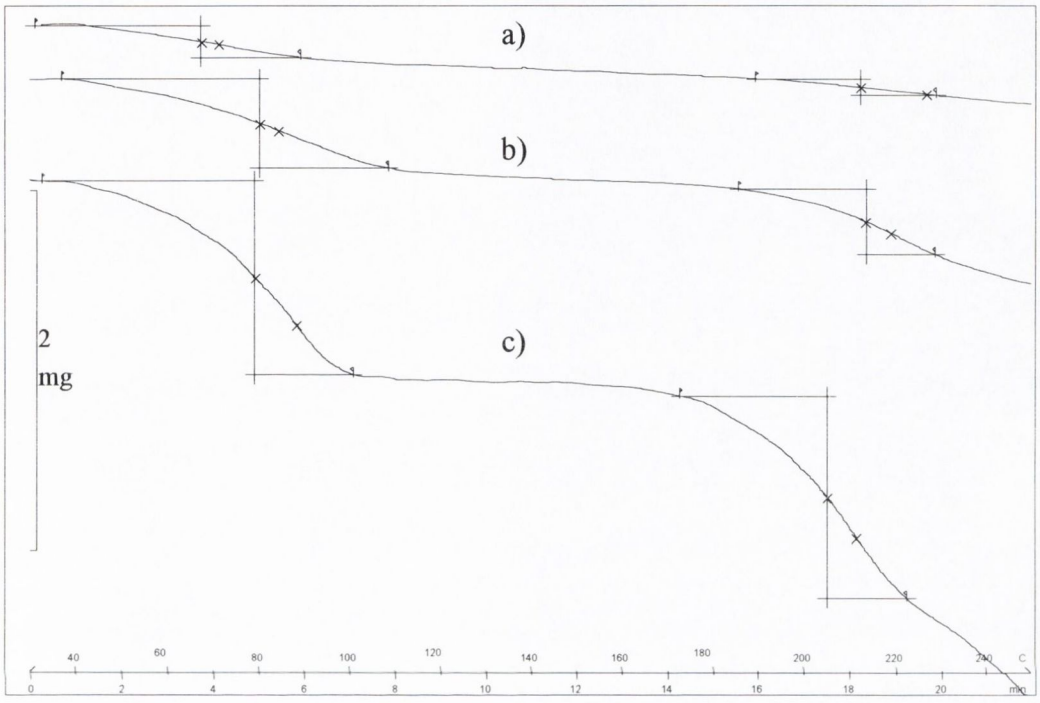

Figure 7.5. TGA traces for RG 503 MM discs at 20% (a), 30% (b) drug loading and AMOX-H powder (c).

Figure 7.6 shows a plot of percentage mass loss per unit weight of sample, obtained from the first horizontal steps of the previous figure, versus the percentage drug load. A linear trendline fitted the data with a coefficient of determination equal to 0.9963, indicating that the mass loss is in reasonable agreement with the drug load.

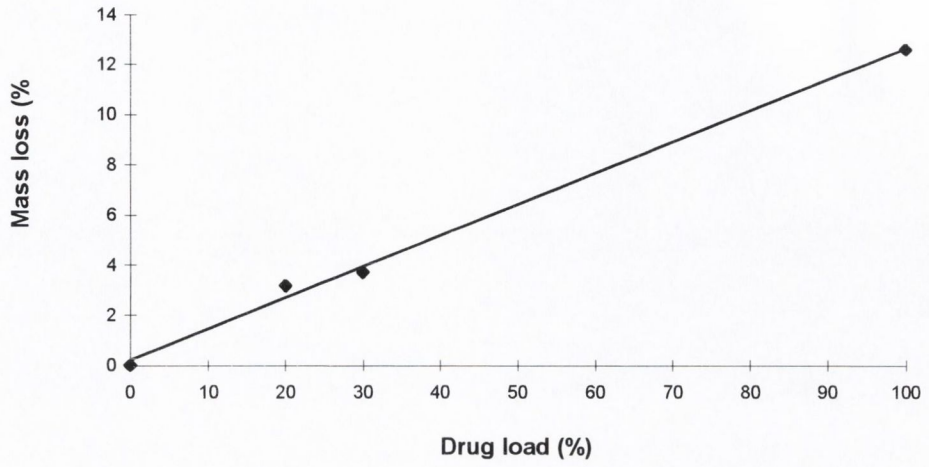

Figure 7.6. Percentage mass loss per unit weight sample (determined by TGA) versus drug load for RG 503 MM discs and AMOX-H powder.

SEM was used to examine the particle characteristics of mixtures of drug and copolymer. An example is given in figure 7.7, corresponding to 20% AMOX-H and 80% RG 503 powders, mixed as described in method 1.

Previously in Chapter 6, SEM images of the individual materials showed that the drug particles are rod-shaped and have a length of approximately 20 μm. In contrast, the copolymer is composed of larger, irregular particles (SEM images in Appendix II). This suggests that, in the mixture of figure 7.7, small rod-shaped drug particles adhered to the copolymer particles giving a 'flaky' appearance to the surface of RG 503.

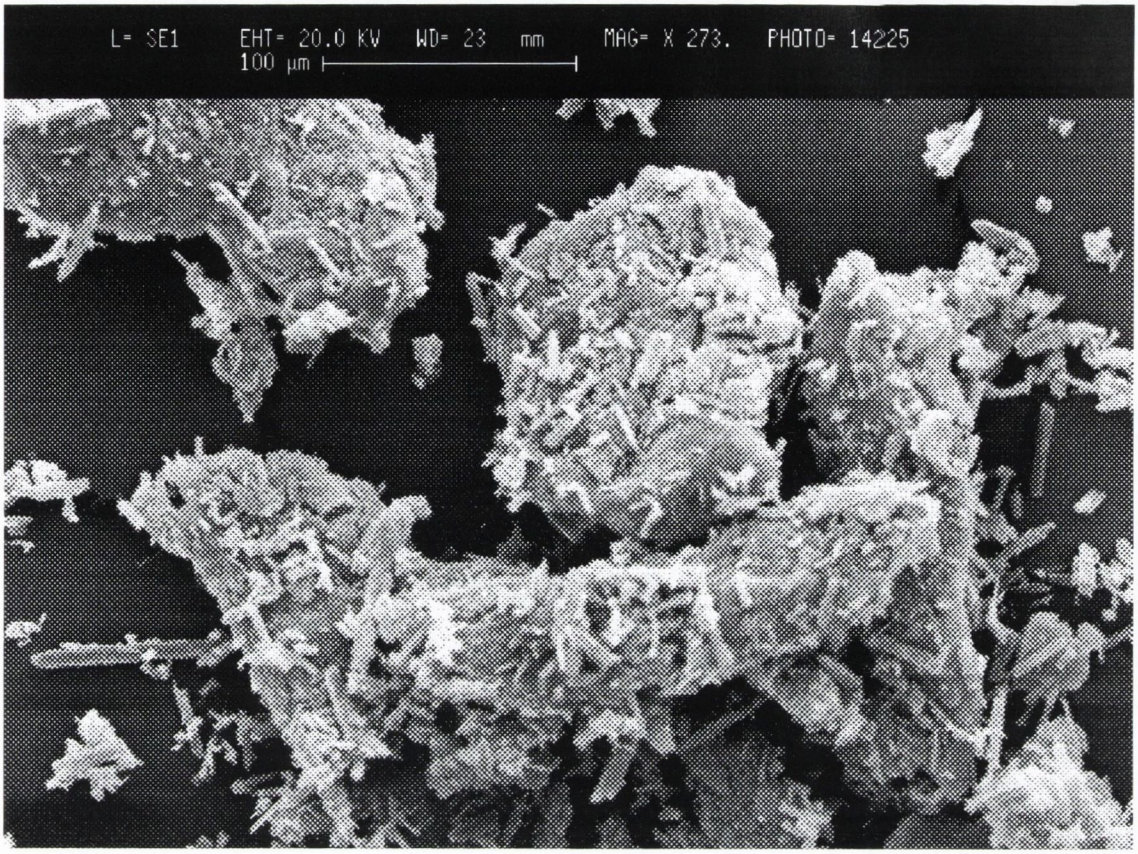

Figure 7.7. SEM of a 20% AMOX-H and RG 503 mixture obtained by manufacturing method 1.

7.2.2. **Preliminary drug release studies with RG 503 MM discs prepared by Method 1**

Preliminary release studies were performed with MM discs containing between 10% and 35% of AMOX-H prepared by Method 1 (section 5.8.1) over an eight-day period.

Initially, aliquots of 2 ml were withdrawn at regular intervals for the first 48 hours, at which time the buffer was sampled and discarded and the discs placed into fresh medium. Drug release was determined by HPLC which enabled evaluation of chemical stability.

Figure 7.8 shows the drug release profiles of systems containing 10%, 20% and 35% AMOX-H, expressed as amount of intact drug released (I) and fraction of intact drug released (relative to the initial loading) (II). There is an initial phase of rapid drug release which slows after the first two days. The amount of drug released at a given time increased with the drug load (I), with greater fractions of drug being released at the higher loads (II).

Figure 7.9 shows a conventional drug release versus square root of time plot. A linear trend was observed for the data of the first 24 hours although the line appeared to deviate from the origin. Therefore, a constant was added to the model to account for the initial burst in the release resulting in an equation of the form $Q = B \cdot t^{0.5} + c$, where Q is the amount of drug released at time t and B and c are constants. At the 10% drug loading the goodness of fit was poor (table 7.1). Higher r^2 and MSC values were obtained for the higher drug loads which suggests significant matrix type release in those systems containing between 20% and 35% AMOX-H. The parameters obtained are also listed in table 7.1.

This release model was obeyed in the first day only, the fit being very poor when the data points thereafter were included.

(I)

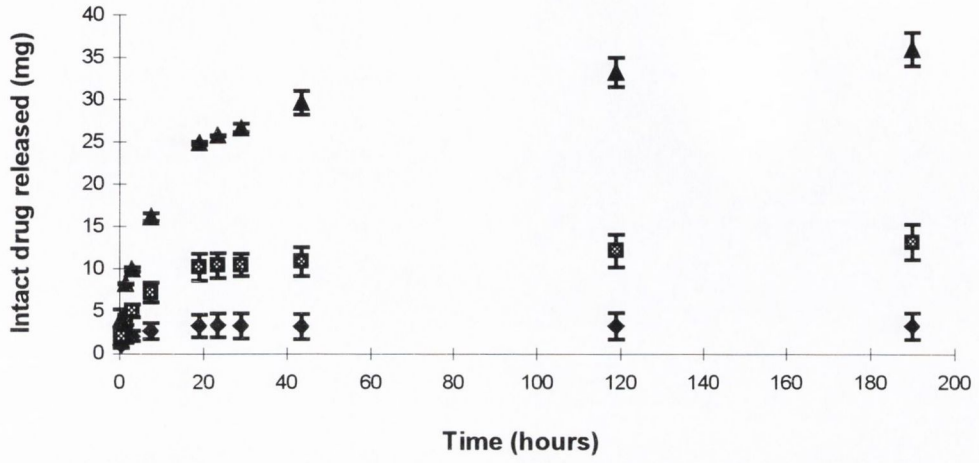

(II)

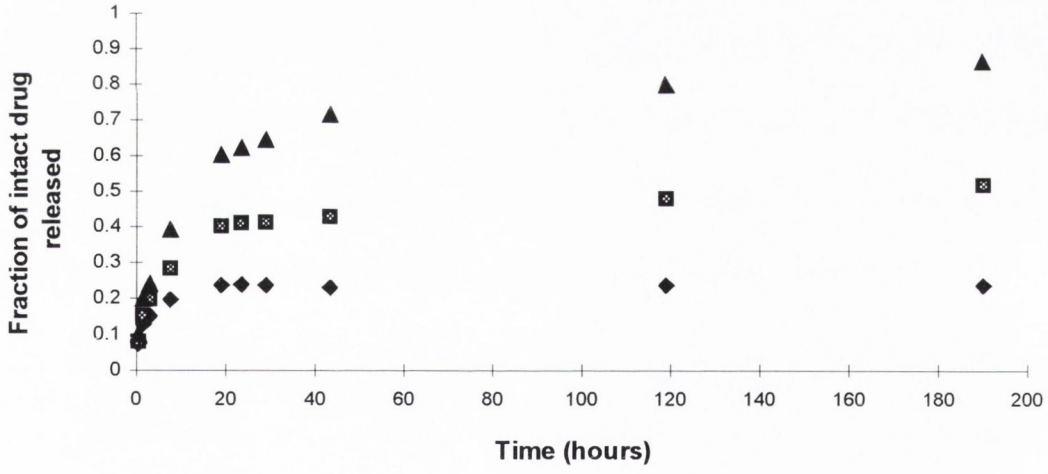

Figure 7.8. Effect of the initial load on the release profiles of RG 503 MM discs prepared by Method 1 at 10% (◆), 20% (▩), 35% (▲) AMOX-H loading, expressed as amount of intact drug released (mg) (I) and fraction of intact drug released (II) versus time. Error bars indicate the range of the data.

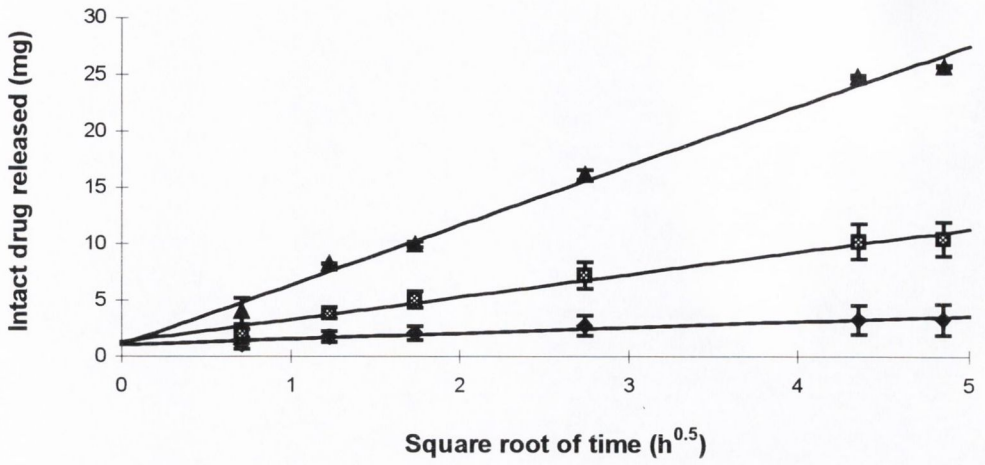

Figure 7.9. Release of intact Amoxycillin from RG 503 MM discs prepared by Method 1 at 10% (◆), 20% (▩), 35% (▲) loading, plotted against the square root of time for day one.

Table 7.1. Parameters and statistics obtained for the first day of Amoxycillin release from RG 503 MM discs prepared by Method 1 at 10%, 20%, 35% drug load plotted versus the square root of time.

	10% AMOX-H	20% AMOX-H	35% AMOX-H
slope B ($mg.h^{-0.5}$) $\pm$ SD	0.515 $\pm$ 0.071	1.995 $\pm$ 0.138	5.290 $\pm$ 0.226
intercept c (mg) $\pm$ SD	1.006 $\pm$ 0.215	1.264 $\pm$ 0.417	1.030 $\pm$ 0.685
r^2	0.9290	0.9813	0.9927
MSC	1.98	3.31	4.26

Fractional drug release profiles were fitted to equation 3.8, as shown in figure 7.10. The fit obtained for the 10% system was very poor, with higher coefficients of determination and MSC obtained at the higher drug loads. Table 7.2 lists the corresponding statistics.

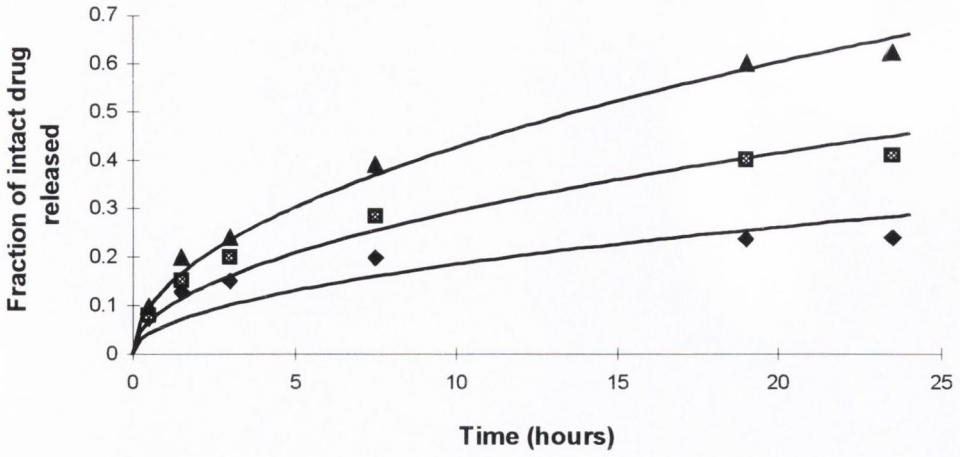

Figure 7.10. Release of intact Amoxycillin from RG 503 MM discs prepared by Method 1 at 10% (◆), 20% (▩), 35% (▲) drug loading, fitted to equation 3.8 which describes drug release by matrix control.

An alternative approach in the investigation of the mechanistic aspects of drug release is to consider that the initial release is due to a "burst effect" which could be described by an exponential equation (Gallagher and Corrigan, 1998). Therefore, the data was fitted to equation 3.15 describing drug release for the case in which sink conditions are maintained and the surface area available for dissolution decreases exponentially with time. Figure 7.11 shows the results obtained for the three systems. The fit was poor, as indicated by r^2 values below 0.96 and MSC below 2.6. Very little improvement was shown when only the first four points (8 hours) were used. Table 7.3 lists the statistics obtained using equation 3.15. The goodness of fit increased with increasing drug load, both for the exponential and the previously described square root of time model. At the lower drug loading, the results obtained with both equations were poor.

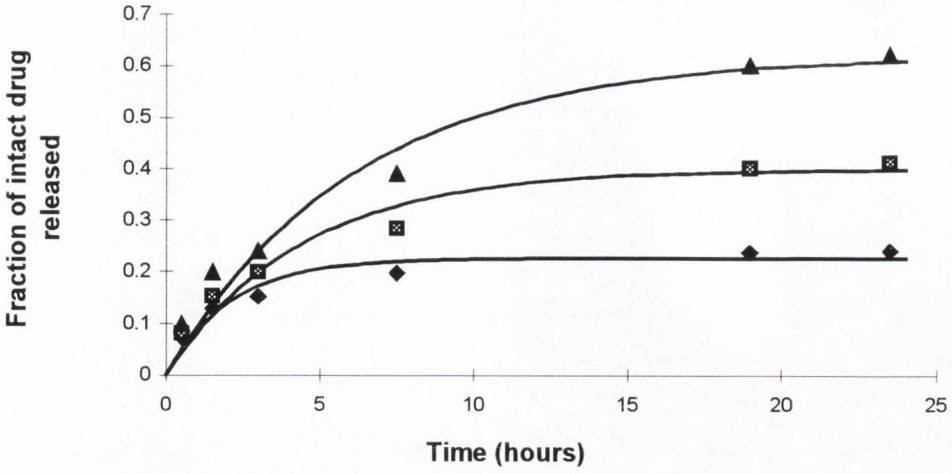

Figure 7.11. Release of intact Amoxycillin from RG 503 MM discs prepared by Method 1 at 10% (◆), 20% (■), 35% (▲) drug load, fitted to equation 3.15 describing a first-order dissolution process.

Table 7.2. Statistics obtained for the first day of intact Amoxycillin release from RG 503 MM discs prepared by Method 1 at 10%, 20% and 35% drug load fitted to equation 3.8.

RG 503 MM System	r^2	MSC
10% AMOX-H	0.5266	0.41
20% AMOX-H	0.9385	2.45
35% AMOX-H	0.9885	4.13

Table 7.3. Statistics obtained for the first day of intact Amoxycillin release from RG 503 MM discs prepared by Method 1 at 10%, 20% and 35% drug load fitted to equation 3.15.

RG 503 MM System	r^2	MSC
10% AMOX-H	0.9031	1.66
20% AMOX-H	0.9463	2.26
35% AMOX-H	0.9618	2.60

In order to distinguish between first-order dissolution kinetics and matrix controlled kinetics, Schwartz et al. (1968) proposed a test based on predicted rate equations derived from each of the models. First-order kinetics would be operative when the rate (dQ/dt) plotted as a function of the amount released (Q) yields a straight line. In contrast, a straight line obtained when the rate was plotted versus the *reciprocal* of the amount released would be indicative of matrix diffusion. This treatment was applied to the fraction drug release data from 35% AMOX-H discs, previously shown in figure 7.8. Figure 7.12 illustrates the plot obtained for rate versus drug released, where a linear relationship was not obtained. In contrast, figure 7.13 shows that the analogous plot of *reciprocal* fraction of drug released obeyed a linear trend (r^2=0.9731), supporting a release mechanism consistent with square root of time kinetics.

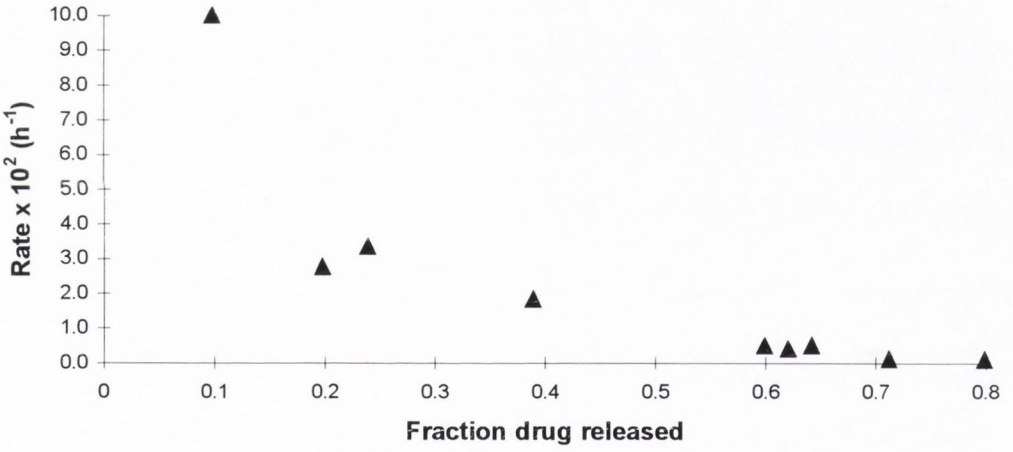

Figure 7.12. Rate versus fraction intact drug released for RG 503 MM discs containing 35% AMOX-H.

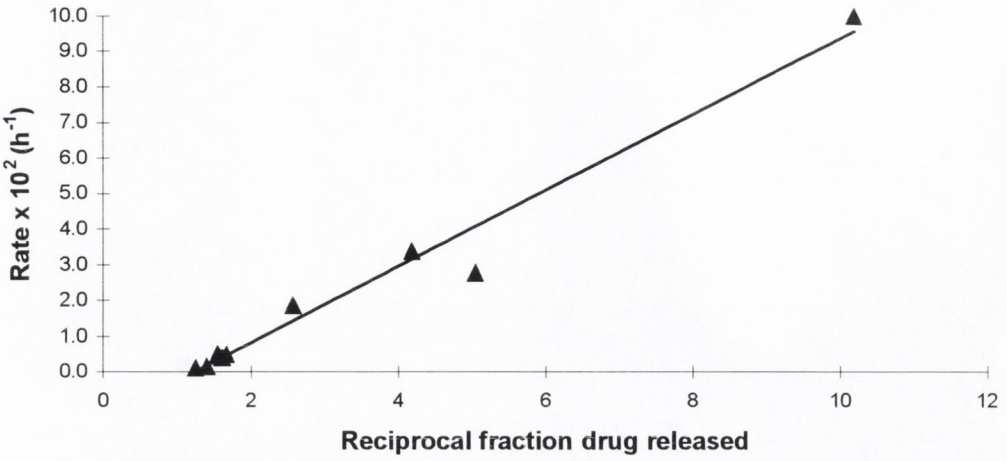

Figure 7.13. Rate versus reciprocal fraction of intact drug released from RG 503 MM discs containing 35% AMOX-H.

Since matrix-type mechanisms appear to predominate in determining drug release from RG 503 MM discs containing above 10% AMOX-H, an additional square root of time model was then assessed (equation 3.10). This model takes into account dimensional changes of the surface area from which release is occurring. Figure 7.14 shows the plots obtained with equation 3.10 when a shape parameter (q) of 16.25 was used, calculated with r_i (initial radius) equal to 6.5 mm and h_i (half the initial height) equal to 0.4.

Comparison of the results obtained with equation 3.10 with those previously shown in figure 7.10 indicates that the inclusion of the shape factor in the square root of time model improved the goodness of fit for 10%, 20% and 35% drug loaded systems (table 7.4).

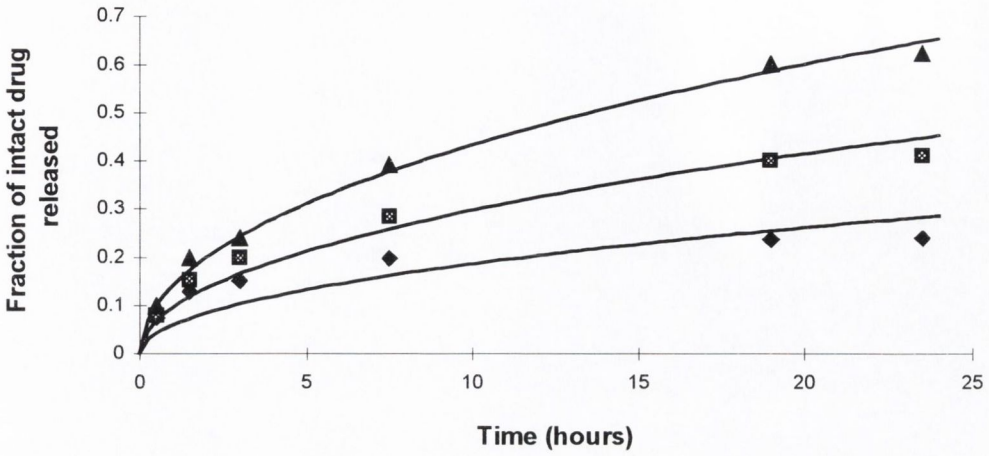

Figure 7.14. Plot of intact fraction drug released versus time for RG 503 MM discs prepared by Method 1 at 10% (◆), 20% (■), 35% (▲) loading fitted to equation 3.10.

Table 7.4. Statistics obtained for the first day of intact Amoxycillin release from RG 503 MM discs prepared by Method 1 at 10%, 20% and 35% drug load fitted to equation 3.10.

RG 503 MM System	Equation 3.8		Equation 3.10	
	r^2	MSC	r^2	MSC
10% AMOX-H	0.5266	0.41	0.5528	0.47
20% AMOX-H	0.9385	2.45	0.9497	2.66
35% AMOX-H	0.9885	4.13	0.9929	4.62

After the first two days, release appeared to have ceased in the 10% drug loaded discs. Referring back to the plot of these systems in figure 7.8, there was a downward trend in the profile between 30 to 80 hours which may have been the result of drug degradation in the surrounding medium. This was consistent with the presence of degradation peaks in the relevant HPLC traces, not evidenced at the higher drug loadings where drug continued to be released.

By approximately 200 hours of release studies, drug release from discs at 10%, 20% and 35% AMOX-H was minimal. Discs were then removed from the medium for HPLC analysis of drug potentially entrapped in the matrices.

The significant amounts of residual intact drug found in the discs indicated that longer-term experiments were required and that further drug release should be expected after a lag time. Analysis of the drug extracted from the discs suggested that the degradation of Amoxycillin, over the short-term release study, was mainly occurring outside the matrix, in the surrounding medium. This was in agreement with the well known instability of penicillins in aqueous media (previously discussed in Chapter 1). Mass loss and drug release data (quantified by HPLC analysis) resulted in a difference of less than 4%, indicating that polymer loss was negligible over the period studied.

Amoxycillin released during the first 24 hours of the studies resulted in approximately 20% saturation of the surrounding medium. A short experiment was then undertaken to assess the effect of these concentration levels on the release profiles. Figure 7.15 shows the results obtained when the buffer was replaced during the first 24 hours, in order achieve more effective sink conditions.

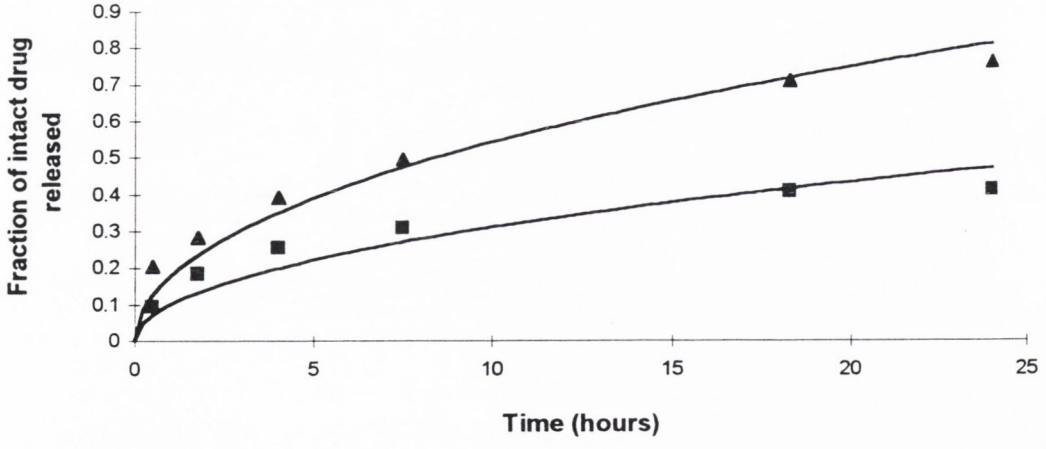

Figure 7.15. Intact drug release profiles, obtained under sink conditions, for RG 503 MM discs at 10% (■), 20% (▲) loading prepared by Method 1. The data was fitted to equation 3.10.

The fraction of drug released (relative to the initial load), determined by HPLC analysis, significantly increased for the 20% MM discs during day one (figure 7.14 versus 7.15). To a lesser extent, enhanced release was also observed for the 10% systems. The fitted lines in figure 7.15 were obtained with equation 3.10. The values of r^2 and MSC are listed in table 7.5.

Table 7.5. Statistics obtained for intact Amoxycillin release profiles of RG 503 MM systems prepared by Method 1 at 10% and 20% loading, fitted to equation 3.10. Sink conditions were maintained.

RG 503 MM System	r^2	MSC
10%	0.8571	1.61
20%	0.9501	2.66

The square root of time plots of these systems (figure 7.16) gave the best results at the higher drug loading, as indicated by r^2 and MSC. A positive intercept on the *y* axis may be due to the release of drug located at the surface. Initial rapid release appeared to predominate in the first 2 to 4 hours, which would explain the poorer fit previously obtained with equation 3.10. Table 7.6 lists the statistics obtained for the square root of time plots together with the corresponding results from the experiment in figure 7.9 obtained under less effective sink conditions. In both cases, agreement with square root of time kinetics improved at the higher drug load. The fit to this model was poorer at the lower drug load.

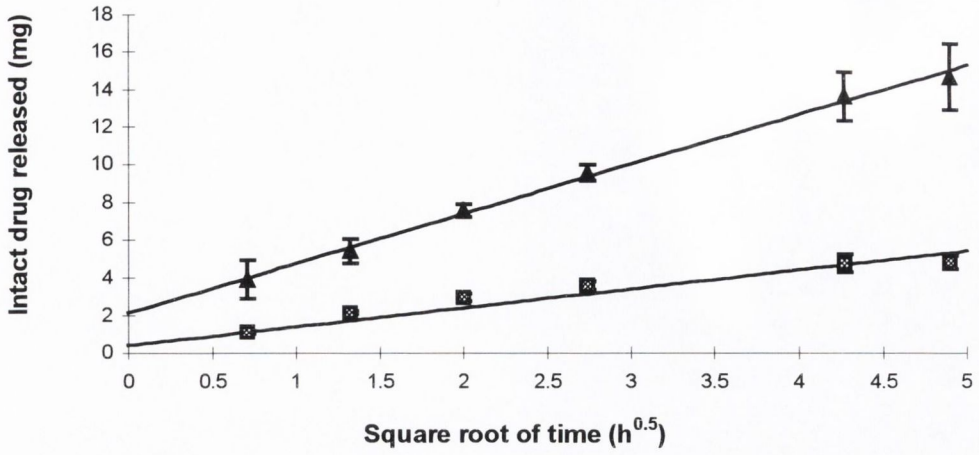

Figure 7.16. Profiles of intact Amoxycillin released under sink conditions from RG 503 MM discs prepared by Method 1 containing 10% (■) and 20% (▲) drug loading plotted in square root of time fashion. Error bars indicate the range of the data.

Table 7.6. Statistics obtained for the square root of time plot of drug release profiles from RG 503 MM discs under 20% saturated media versus a perfect sink.

RG 503 MM System	20% saturated media		sink conditions	
	r^2	MSC	r^2	MSC
10% AMOX-H	0.9290	1.98	0.8751	1.41
20% AMOX-H	0.9813	3.31	0.9967	5.05

The first-order plots for the 10% and 20% systems obtained under more effective sink conditions are shown in figure 7.17. At the lower drug load the fit was described by an r^2 equal to 0.9395 and a MSC equal to 2.14, which were higher than the values previously obtained for the square root of time model. At the 20% load, the fit to the exponential model was poor.

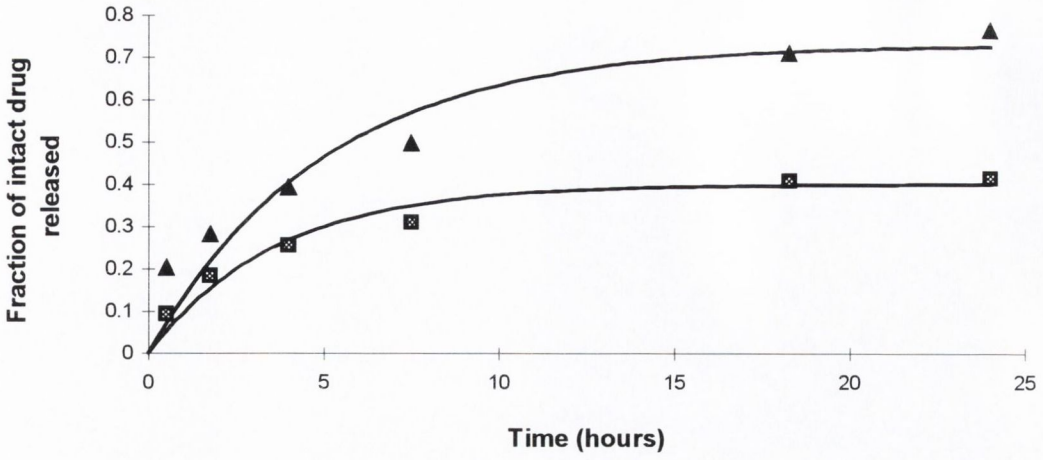

Figure 7.17. First-order plot (equation 3.15) for the release of intact Amoxycillin from RG 503 MM discs at 10% (▩) and 20% (▲) load.

The preliminary studies discussed above showed that drug release was slowed down in partly saturated media. In order to better approximate sink conditions, the dissolution medium should be replaced during the first day of drug release. This was therefore incorporated into subsequent release studies, as per section 5.10.

A square root of time mechanism appeared to determine drug release in RG 503 MM systems, particularly at the higher drug loads. Initial fast release of drug directly in contact with the surface may be the reason for the positive intercepts with the y axis. At the lower loading (10%), the goodness of fit was better for the first-order plots.

7.2.3. **Long-term studies with RG 503 MM discs prepared by Method 1**

As discussed in the previous section, extraction of drug from discs removed after 200 hours of dissolution (figure 7.8) showed that release profiles obtained over this period were incomplete. Therefore, release studies were undertaken beyond 200 hours.

Total drug released was measured simultaneously with mass loss, by means of removing discs at various time intervals (figure 7.18).

Fractional drug release profiles were calculated relative to the drug recovered, as outlined in section 5.10. Approximately 70% of the drug was released in the first two

days while polymer loss was apparent only after 600 hours, at which time further drug release occurred. Drug release in the final phase appeared to parallel polymer mass loss, suggesting a release mechanism mediated by polymer degradation. Only 30% of the polymer had been lost when drug release was completed.

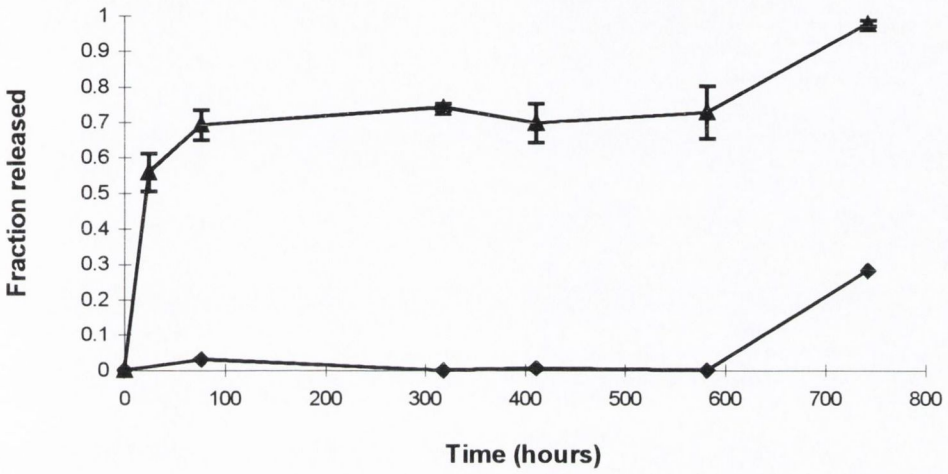

Figure 7.18. Relationship between fraction of drug released (▲), fraction of polymer mass loss (n=2) (◆) and time for RG 503 MM discs at 20% drug load, prepared by Method 1. Error bars indicate the range of the drug release data.

Figure 7.19 shows a photograph of discs removed from the release medium at successive time intervals. There is an evident colour change from off-white to dark yellow as the experiment proceeded, particularly after 400 hours of experimental time. These colour changes of the discs resembled those observed in the medium during degradation studies of AMOX-H solutions, introduced in Chapter 6.

A time-dependent decrease in the diameter of the discs is also evident and suggested that surface erosion (Göpferich, 1996) could be contributing to the degradation process. However, differences between the surface and the core of the discs were not evidenced, with similar colour changes evident throughout.

The same discs were photographed on a light box (Hancocks, U.K.) to provide a translucent image of the matrices (figure 7.20). To the eye, however, the colour of the discs was that of the previous photograph, shown in figure 7.19.

The images obtained with the light box suggested that during the initial phase of drug release a "ghost" area was formed, such as the process described by Cobby et. al (1974). This may relate to the boundary retreat distance of the dissolution front mentioned by these workers.

At 743 and 936 hours the "ghost" portion was not apparent, supporting the view that at this stage drug release was entirely determined by the degradation of the polymer.

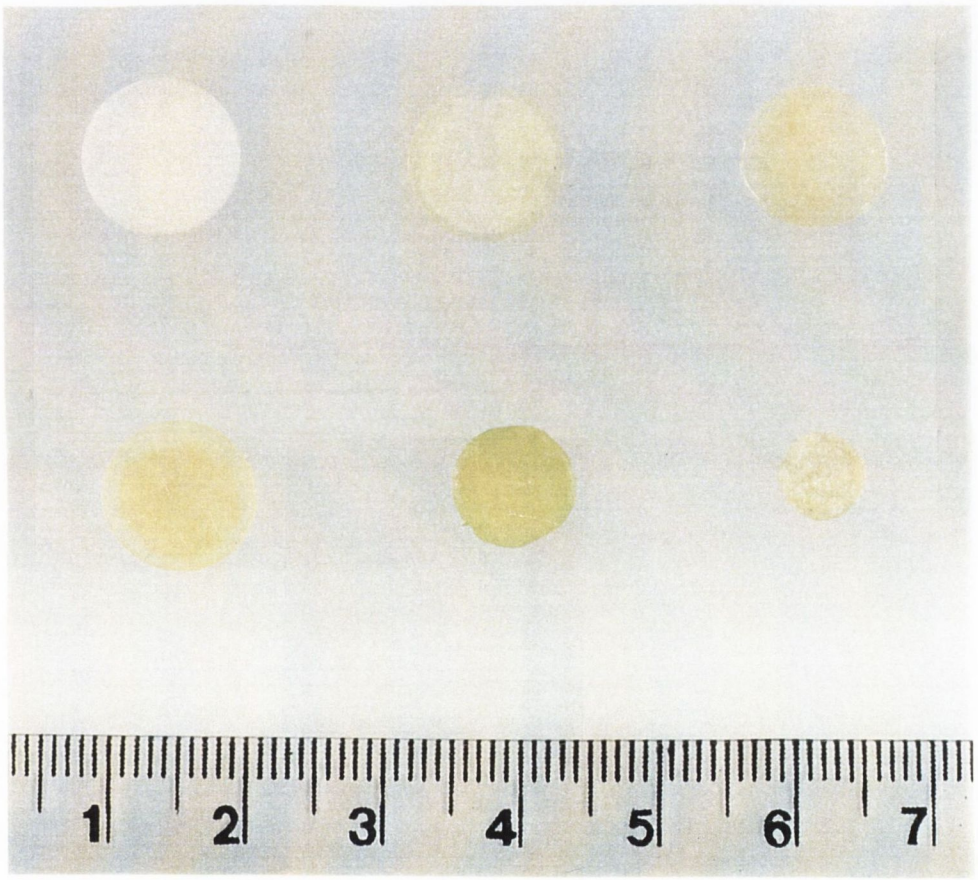

Figure 7.19. Photograph of 20% drug loaded RG 503 MM discs after 76, 318, 411, 582, 743 and 936 hours of drug release studies (top to bottom). Scale in cm.

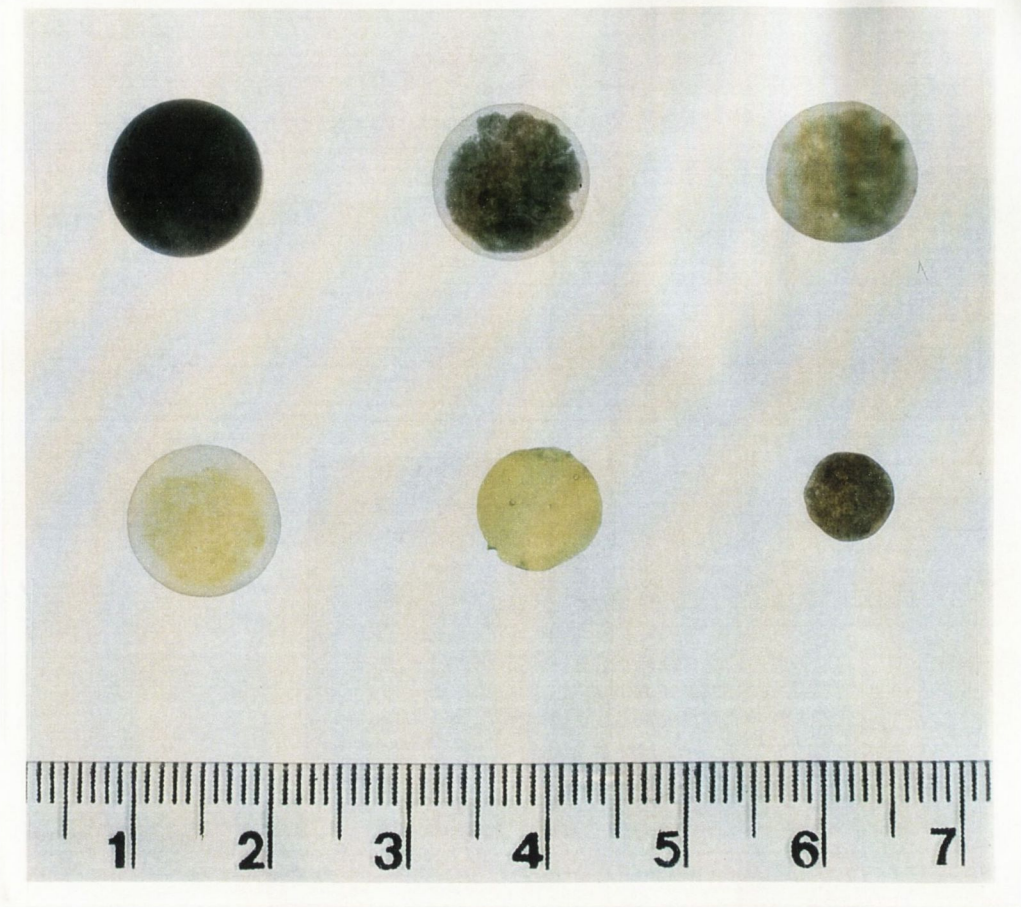

Figure 7.20. Photograph of 20% drug loaded RG 503 MM discs after 76, 318, 411, 582, 743, 936 hours of dissolution studies (top to bottom). A (Hancocks, U.K.) lightbox with 15W tubes was used to provide transparency to the discs. Scale in cm.

Scanning electron microscopy was performed on discs upon removal from the dissolution medium. Figure 7.21 illustrates the results obtained at successive time points, as indicated beside each image. The magnification was fixed at X 235 for comparative purposes.

Initially, the surface of the discs was relatively smooth (a). Brighter regions attributable to higher atomic contrast (i.e. sulphur containing) possibly reflected the presence of drug at the surface. After 76 hours of a release study (b) increased porosity was observed, consistent with the dissolution of drug at the surface. Large interconnecting pores were observed after 582 hours of dissolution (c). This was in agreement with the commencement of polymer mass loss and the onset of the final drug release phase, both of which occurred around this time.

The last image (d) corresponds to a disc exposed to 936 hours of dissolution, showing a hollow inside. The surface of the disc (bottom right-hand area of the photo) appeared to be relatively intact compared to the center of the matrix. This may be related to the findings of Park and Crotts (1995). The authors reported a heterogeneous bulk degradation mechanism for drug-free PLGA microspheres, with center/surface differential degradation rates. Enhanced autocatalytic reaction occurs in the central region of the matrix while the surface region in contact with bulk medium degrades at a slower rate. The autocatalytic reaction is caused by protonated carboxylic acid end groups generated by cleavage of the ester bonds.

Similar hollow carcasses have been recently reported by Gallagher and Corrigan (1998) for drug-free PLA discs, observed during polymer mass loss studies.

By 936 hours of dissolution the discs were apparently depleted of drug. Therefore, it is conceivable that the mechanism reported by Park and Crotts (1995) for drug-free PLGA was operative in the final degradation stages of the RG 503 MM discs described in the current section.

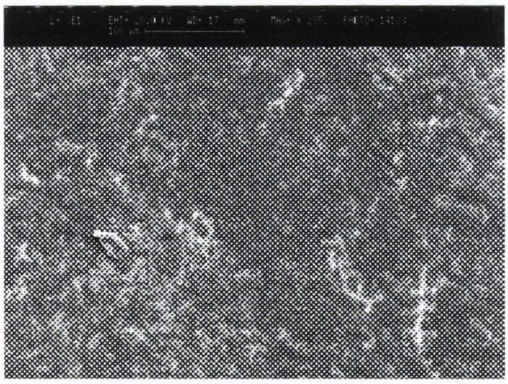

a) 0 hours

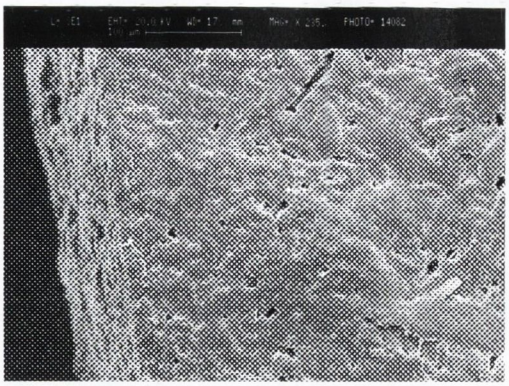

b) 76 hours

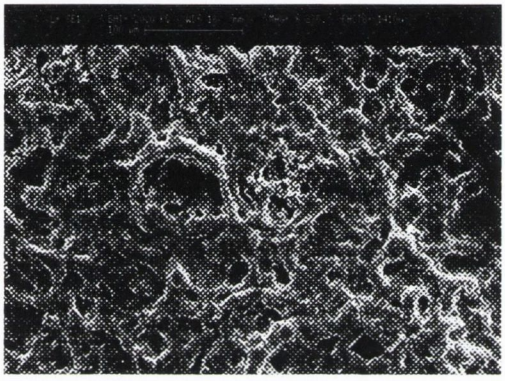

c) 582 hours

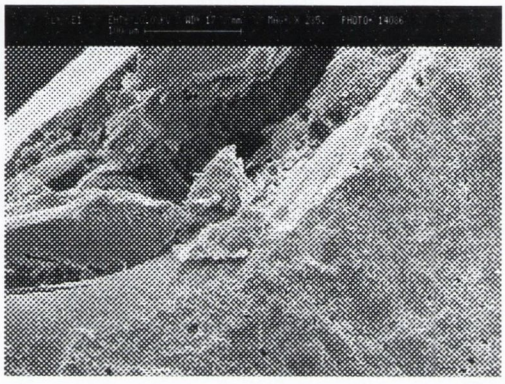

d) 936 hours

Figure 7.21. SEM (X 235) of Amoxycillin loaded RG 503 MM discs after 0 (a), 76 (b), 582 (c) and 936 (d) hours of drug release studies.

7.2.4. **Studies with RG 503 MM discs prepared by Method 2**

To control the particle size of the drug and the polymer, Method 2 (section 5.8.2) was employed in the preparation of further MM discs. A recent model proposed by Gallagher and Corrigan (1998) shows that the fraction of drug available for direct surface release is dependent upon the particle size of the drug.

Figure 7.22 illustrates long-term profiles of *total* drug release for RG 503 MM discs at 20% and 30% AMOX-H loading. Between 70% and 80% of the drug load was released during the first 48 hours. This was followed by an induction period of approximately 600 hours (25 days) after which time the remaining drug was released.

The study was continued until 1600 hours, to find that small solid pieces of material were still present in the dissolution media. Recovery of the pieces by filtration and subsequent analysis by extraction failed to reveal the presence of drug.

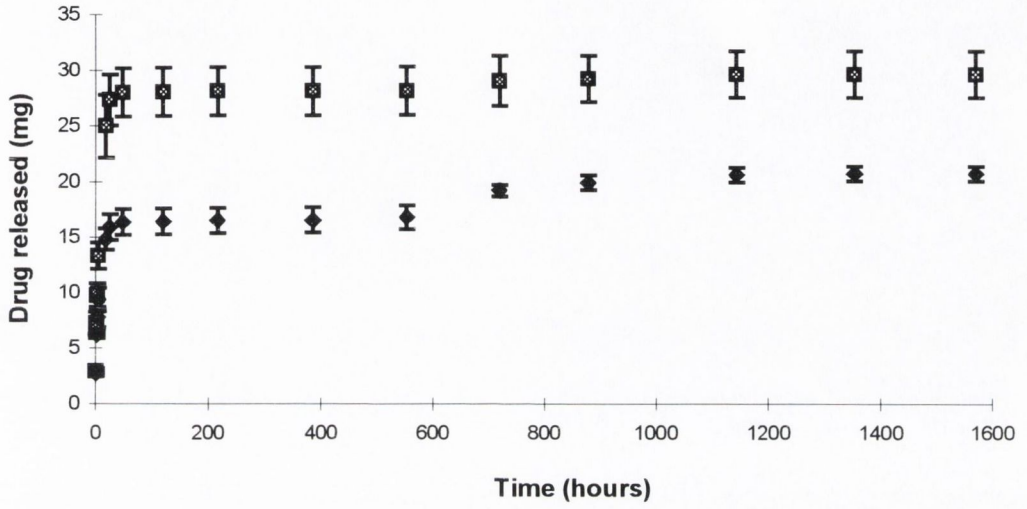

Figure 7.22. Drug released (mg) from RG 503 MM discs at 20% (◆) and 30% (▩) AMOX-H load, prepared by Method 2. Error bars indicate the range of the data.

Figure 7.23 shows the plot obtained for fractional drug release over the first 24 hours fitted to equation 3.10, a square root of time model that accounts for shape changes. Table 7.7 lists the corresponding statistics.

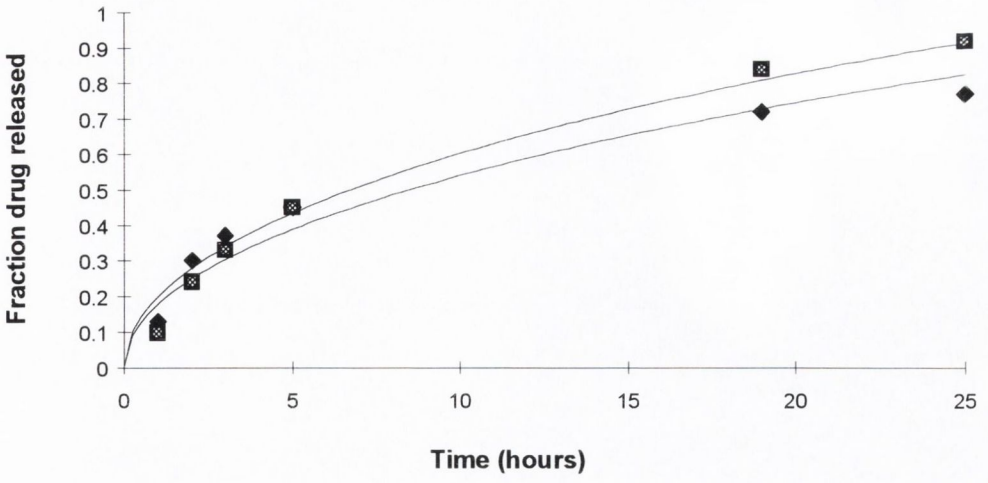

Figure 7.23. First day of drug release from RG 503 MM discs prepared by Method 2 at 20% (◆) and 30% (▩) loading fitted to equation 3.10.

Table 7.7. Estimates of the rate constant and statistics obtained for the first day of release from RG 503 MM discs prepared by Method 2 fitted to equation 3.10.

Drug loading (%)	k_r ($h^{0.5}$) $\pm$ SD	r^2	MSC
20	0.0099 $\pm$ 0.00049	0.9561	2.79
30	0.0111 $\pm$ 0.00045	0.9713	3.21

The effect of grinding and sieving procedures on the initial drug release profiles was investigated by comparison of the systems containing similar drug loading prepared by manufacturing Methods 1 and 2.

Table 7.8 lists the parameters and statistics obtained when the individual and the average data of 20% systems (data from figures 7.15 and 7.23) was fitted to equation 3.10. It is apparent that the two manufacturing methods are equivalent in terms of the resulting drug release profiles although Method 1 was possibly more variable.

Table 7.8. Estimated release rate constant and statistics obtained for the fit to equation 3.10 of first day release profiles from RG 503 MM discs, 20% loading, prepared by Methods 1 and 2.

RG 503 MM 20% System	k_r ($h^{0.5}$) ± SD	r^2	MSC
METHOD 1			
disc 1	0.0114 ± 0.0005	0.9404	2.49
disc 2	0.0085 ± 0.00041	0.9407	2.49
average data	0.0099 ± 0.00099	0.9500	2.66
METHOD 2			
disc 1	0.0094 ± 0.0004	0.9538	2.74
disc 2	0.0104 ± 0.0006	0.9308	2.34
average data	0.0099 ± 0.00049	0.9561	2.79

In order to describe the total drug release, a more complex model, which accounts for not just the initial square root of time diffusion phase but also the degradation-dependant drug release, is described by equation 3.19. Figure 7.24 shows the complete drug release profiles obtained for 20% and 30% RG 503 MM discs fitted to this equation. The initial phase accounts for most of the drug release, with only a small proportion of drug being available for degradation control at approximately 700-800 hours.

Table 7.9 lists the parameters and statistics obtained with equation 3.19. Agreement with this release model was good, as indicated by the values of r^2 and MSC. The estimate of Fd_∞ was greater for the 30% system. No differences were apparent in the values of the square root of time rate constants k_r, as these values overlap when the standard deviations are taken into account. The degradation parameters predict similar kinetics for 20% and 30% loading, with t_{max} occurring at approximately 700 hours. The large variation in these parameters, particularly at the higher drug loading, was possibly

related to the relatively low slopes of the profiles in the second phase, at around 600 hours.

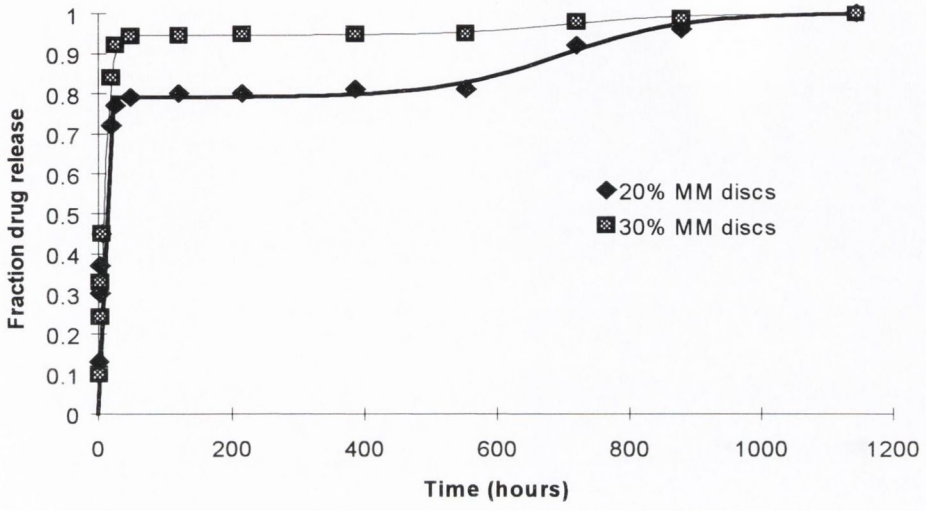

Figure 7.24. Drug release from RG 503 MM discs prepared by Method 2 at 20% (◆) and 30% (■) loading fitted to equation 3.19, describing initial diffusion followed by degradation-dependant drug release.

Table 7.9. Parameters and statistics obtained for release profiles of RG 503 MM discs, 20% and 30% drug load, fitted to equation 3.19.

Drug loading (%)	20	30
k_r ($h^{-0.5}$) ± SD	0.0135 ± 0.0006	0.0118 ± 0.0004
Fd_∞ ± SD	0.79 ± 0.02	0.95 ± 0.02
k (h^{-1}) ± SD	0.0116 ± 0.0058	0.0110 ± 0.0252
t_{max} (h) ± SD	685 ± 49	713 ± 224
r^2	0.9884	0.9901
MSC	3.89	4.05

The drug release data of the 20% and 30% systems was then fitted to the two-term release model describing an exponential phase followed by a polymer degradation phase (equation 3.14). These results are shown in figure 7.25.

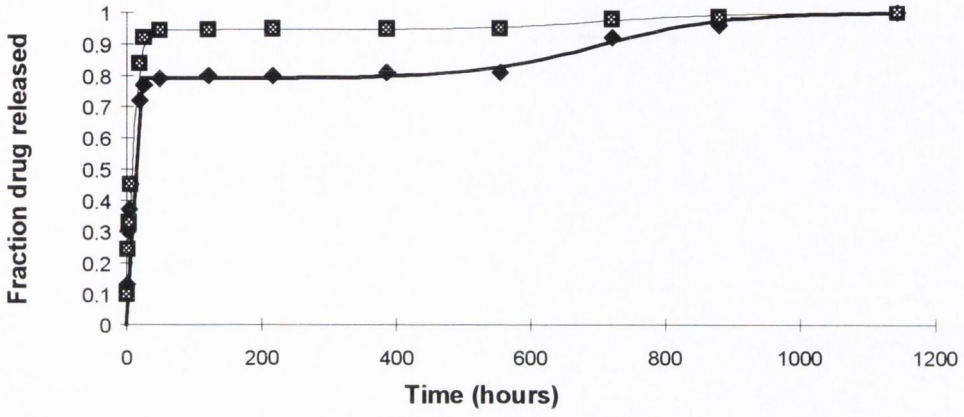

Figure 7.25. Drug release profiles of RG 503 MM discs, ◆ 20% and ▩ 30% load, fitted to equation 3.14.

The parameters estimated with this model (table 7.10) were similar to the estimates previously obtained with the square root of time-polymer degradation model, however the fit improved. Estimates of Fd_∞ and Fb_∞ were of similar order. The degradation parameters, t_{max} and k, obtained with equations 3.14 and 3.19 were comparable.

The preliminary results presented in section 7.2.2 had suggested that the initial release profiles (i.e. the first 24 hours), particularly at the higher drug loadings, were better approximated by a square root of time related mechanism, with the final phase of release determined by polymer degradation. In the current section, comparison of the results obtained with equations 3.14 and 3.19 indicates that the *overall* release profile prior to polymer degradation is better approximated by an exponential than by a square root of time mechanism.

Table 7.10. Parameters and statistics obtained for drug release data from RG 503 MM discs fitted to equation 3.14.

Drug loading (%)	20	30
k_b (h^{-1}) ± SD	0.1952 ± 0.0120	0.1330 ± 0.0050
Fb_∞	0.78 ± 0.01	0.94 ± 0.008
k (h^{-1}) ± SD	0.0103 ± 0.0037	0.0088 ± 0.0073
t_{max} (h) ± SD	677 ± 39	696 ± 102
r^2	0.9923	0.9982
MSC	4.39	5.77

Equation 3.20 is a three-term equation which describes a pseudo first-order dissolution process followed by square root of time diffusion and a final release phase controlled by polymer degradation. Figure 7.26 shows the data fitted to equation 3.20 and table 7.11 lists the parameters and statistics obtained.

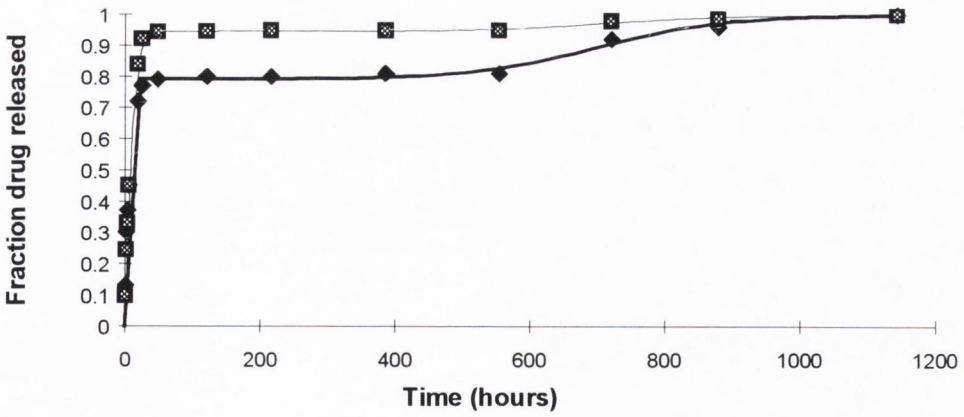

Figure 7.26. Drug release from RG 503 MM discs, ◆ 20% and ■ 30% loadings, fitted to equation 3.20.

Table 7.11. Parameters and statistics obtained for drug release from RG 503 MM discs fitted to a three-term model (equation 3.20).

Drug loading (%)	20	30
Fb_∞	0.47 ± 0.15	0.81 ± 0.13
k_b (h^{-1})	0.240 ± 0.034	0.1340 ± 0.0083
Fd_∞	0.32 ± 0.15	0.134 ± 0.127
k_r ($h^{-0..5}$)	0.0111 ± 0.0011	0.0111 ± 0.0022
t_{max} (h)	690 ± 31	711 ± 101
k (h^{-1})	0.0124 ± 0.0042	0.0103 ± 0.0099
r^2	0.9964	0.9985
MSC	4.76	5.65

The degradation parameters estimated with the three-term equation paralleled those obtained with the corresponding two-term models previously described. The fraction of drug released by a non-degradation mechanism was determined by both first-order and square root of time kinetics, given by Fb_∞ and Fd_∞. At low drug loading the release profiles of the phase prior to onset of polymer degradation appeared to obey an exponential mechanism. At the higher drug loadings, square root of time kinetics also played a part in the release mechanism.

7.3. RG 503 SYSTEMS PREPARED BY SOLVENT EVAPORATION (SE SYSTEMS)

7.3.1. Physicochemical and morphological characteristics of RG 503 SE discs

X-ray diffractograms obtained for RG 503 SE systems at 10%, 20%, 30% drug load are shown in figure 7.27 compared to the scans of pure RG 503 and pure AMOX-H.

Crystalline samples produce diffraction line patterns that are highly specific. In contrast, broad patterns, lacking in intense, defined peaks, are typically associated with amorphous samples. The results indicate the presence of crystalline AMOX-H in the discs. Since the drug is barely soluble in the filmcasting solvent employed, it was expected that most of the particles dispersed remained in the polymorphic form and crystal size of the starting material (Ford and Timmins, 1989).

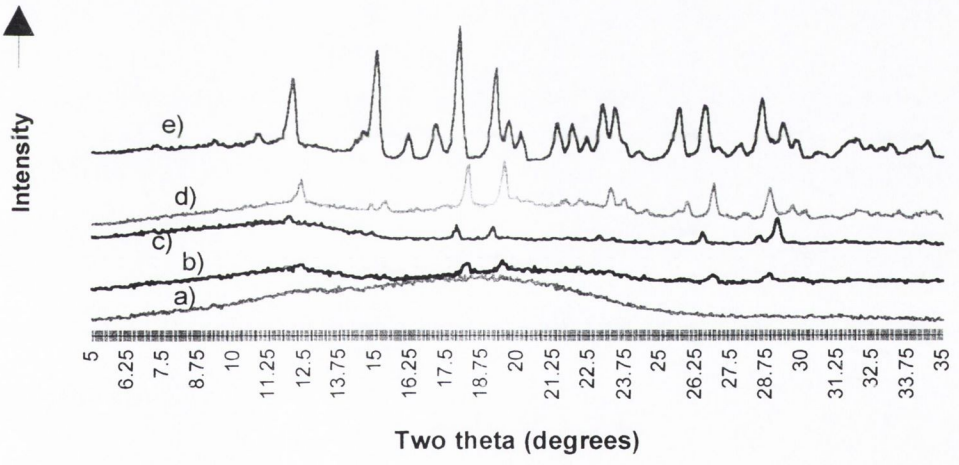

Figure 7.27. X-ray diffractograms of RG 503 powder (a), RG 503 SE discs at 10% (b), 20% (c), 30% (d) drug load and pure AMOX-H powder (e).

A plot of the diffraction intensity versus drug load (%) is shown in figure 7.28 for SE discs (r^2=0.9616 and MSC=2.76). The corresponding trendline previously obtained for MM discs (r^2=0.9897 and MSC=4.07) was superimposed on the graph, whereby the fitted lines overlap. Despite the poorer fit obtained for SE systems the trend was still the same and deviation from the origin was not significant. From the limited data

available, there appears to be a direct proportionality between the % drug load in SE discs and the XRD intensity.

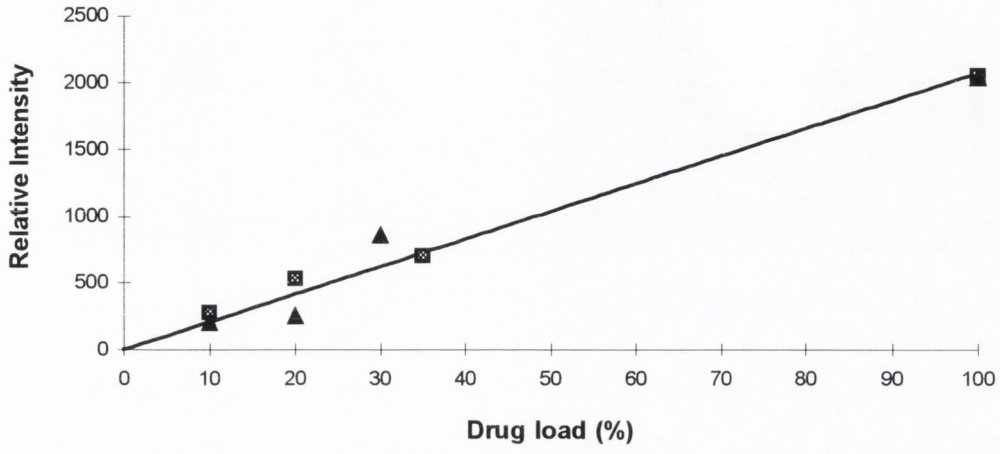

Figure 7.28. Relationship between average X-ray diffraction intensity and percentage drug load for (■) RG 503 MM and (▲) RG 503 SE discs. (Fitted lines overlap).

As outlined in section 5.4.2, two consecutive DSC determinations were performed on the same disc sample following the methodology proposed by Ford and Timmins (1989) to provide a constant thermal history to the polymer. The glass transition temperature of drug-free SE systems was reduced from 51.1°C to 31°C and further reduced to 20-25 °C when the drug was added. However, the rerun samples displayed T_g values in agreement with that of the untreated copolymer powder, suggesting that the lowered T_g values observed with the first heating cycles reflected the presence of residual filmcasting solvent in the samples. Table 7.12 shows the T_g results, quoted for the second heating scan, together with those obtained for MM discs (previously discussed in section 7.2.1).

DSC scans of drug loaded RG 503 discs displayed endothermic events attributable to the drug, as previously discussed in section 7.2.1. Reruns of the same samples did not display transitions attributable to the drug, which is consistent with dehydration of AMOX-H in the first heating cycle.

Table 7.12. Glass transition temperatures of RG 503 MM systems versus SE systems determined by DSC.

RG 503 System	T_g (°C)
copolymer powder	45.0
10% AMOX-H MM	45.4
20% AMOX-H MM	46.8
30% AMOX-H MM	45.8
35% AMOX-H MM	46.9
drug-free SE	44.2
10% AMOX-H SE	43.6
20% AMOX-H SE	45.5
30% AMOX-H SE	46.4

Figure 7.29 shows the plots of enthalpy change (J/g) due to dehydration of the drug as a function of the drug load (%), in RG 503 MM and SE systems. Linear least square regression analysis fitted the data well, as measured by r^2=0.9862, MSC=3.62 for MM systems and r^2=0.9951, MSC=4.32 for SE systems.

The intercept on the ordinate axis was higher in the processed systems (SE). By least square regression analysis it was determined that this intercept occurred at 3.13 $\pm$ 2.5 % w/w, expressed in unit weight of drug per unit weight of disc. The formation of a molecular dispersion of the drug in the polymer (Corrigan and Holohan, 1984; Benoit et al., 1986) may account for the positive intercept. The effect of organic solvents on the crystalline structure of Amoxycillin was previously discussed in section 6.1.4. Based on these findings, it is conceivable that some of the water of crystallization was removed during the solvent-evaporation procedure of the filmcasting technique resulting in a small proportion of amorphous drug. However, the presence of amorphous Amoxycillin was not evidenced in the XRD analysis and, given the value of

the relative standard deviation of the DSC estimate, it is possible that in the statistical sense there were no significant differences between MM and SE discs.

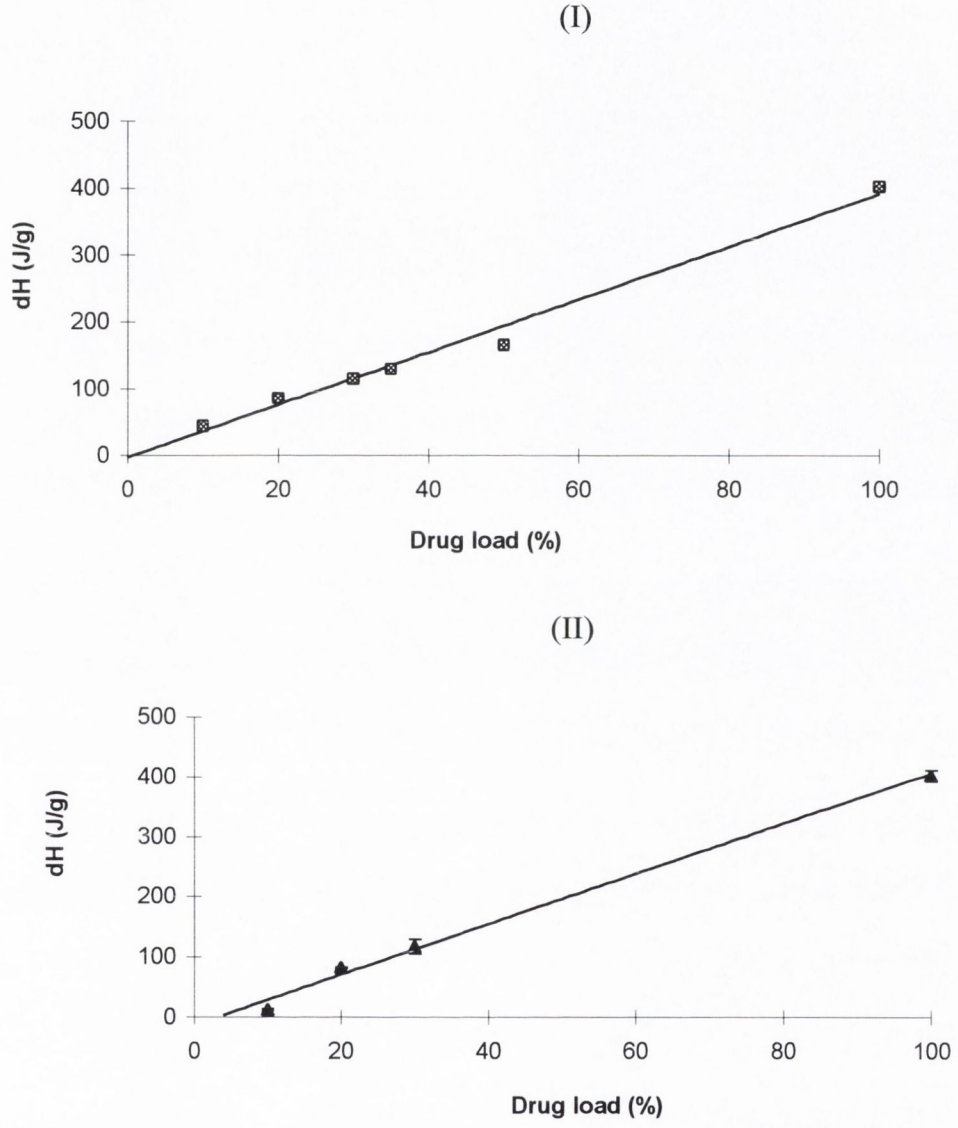

Figure 7.29. Plot of change of enthalpy (J/g) determined by DSC versus drug load (%) for RG 503 MM (I) and SE (II) discs. Error bars indicate the range of the data.

Figure 7.30 illustrates TGA results for RG 503 SE systems at 0% (a), 20% (b) and 30% (c) AMOX-H. All three scans showed loss of volatile components from the samples. The loss of mass before 100°C was consistent with the dehydration of the drug (sections 6.1.2 and 6.1.3) and the evaporation of residual filmcasting solvent. A

second event, possibly due to decomposition of Amoxycillin, was observed after approximately 200°C in traces (b) and (c).

Estimation of the percentage of residual filmcasting solvent in the samples was calculated by comparison of the (%) mass loss of drug loaded discs (as marked in figure 7.30) and pure drug (section 6.1.2) attributable to dehydration. Table 7.13 shows the actual values determined by TGA and the values predicted on the basis of 12.59% water loss from pure drug samples. By difference, the maximum value predicted for residual filmcasting solvent in these systems is approximately 0.6% w/w. This is in the order of the mass loss (1.4%) determined for drug-free SE discs, as marked on trace (a) in figure 7.30.

In the past, Benoit et al. (1986) estimated the proportion of dichloromethane entrapped in P-dlLA microspheres loaded with 23% progesterone using TGA. The values reported by these workers were between 1.8 and 4.7%. More recently, Gallagher and Corrigan (1998) showed that the drug release characteristics of RG 504 discs were not altered by the presence of residual filmcasting solvents in the systems compared to discs incubated in a vacuum oven at 40°C for 96 hours.

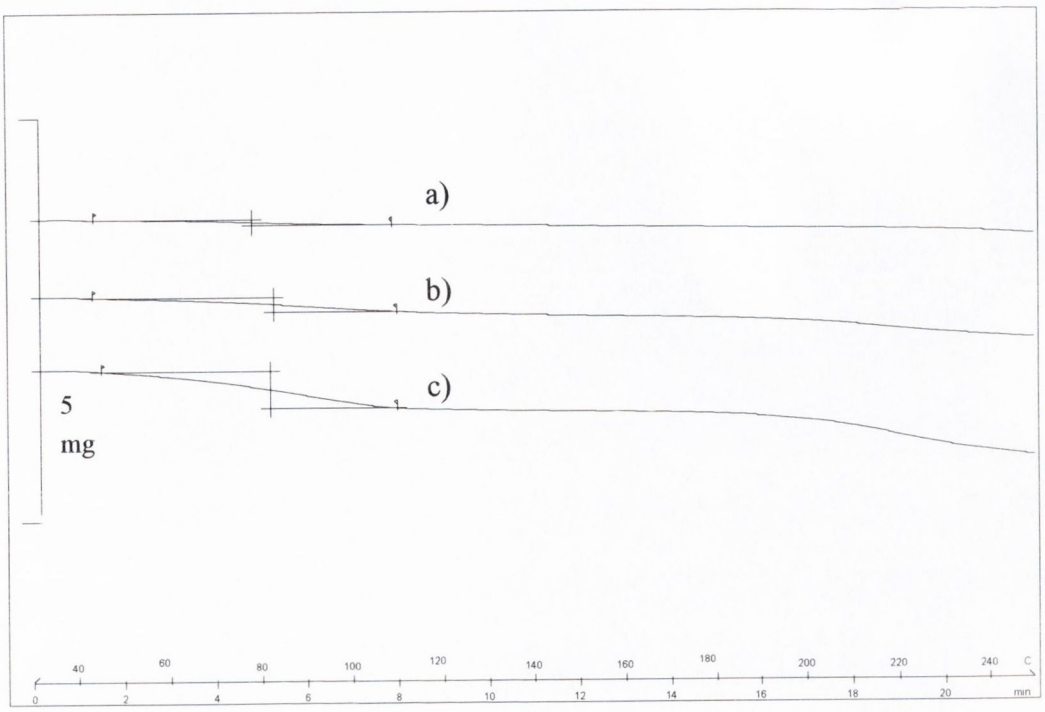

Figure 7.30. TGA scans of RG 503 SE systems containing 0% (a), 20% (b), 30% (c) AMOX-H.

Table 7.13. (%) Mass loss obtained by TGA for RG 503 SE systems containing 20%, 30% AMOX-H and predicted residual solvent (%) based on 12.59% dehydration of the pure drug.

	Drug loading (%)	
	20	30
Mass loss determined by TGA (%)	3.16	3.69
Predicted residual solvent (%)	~ 0.6	0

7.3.2. **Drug release studies with RG 503 SE discs**

The *total* amount of drug released from RG 503 SE discs as a function of time is plotted in figure 7.31 for systems containing 10%, 20% and 30% drug loading. Two separately manufactured batches of 20% drug loaded SE discs are superimposed (■, ◆).

The release profiles at 10%, 20% and 30% loading showed an initial fast release in the first day which was followed by an induction period of approximately 400 hours and a final drug release phase lasting until 700 to 900 hours. In contrast to MM discs, the greater proportion of the drug load was delivered in the final phase.

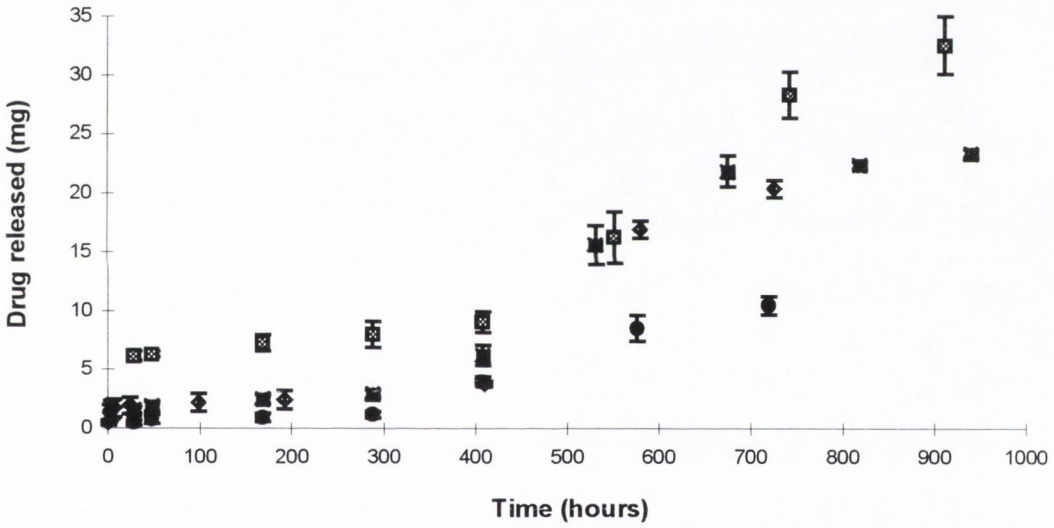

Figure 7.31. Drug released (mg) versus time plot for RG 503 SE discs containing 10% (●), 20% (■, ◆) and 30% (▩) AMOX-H.

To investigate possible mechanisms determining drug release from these systems the mathematical models introduced for MM systems were evaluated. The release profile obtained over the first 24 hours for the 20% drug loaded discs is expanded in figure 7.32, which shows a plot of fractional drug release versus time. The data was fitted to a first-order release model (equation 3.15) and gave a k_b value of 0.58 ± 0.074 h^{-1} (r^2= 0.9829; MSC=3.3).

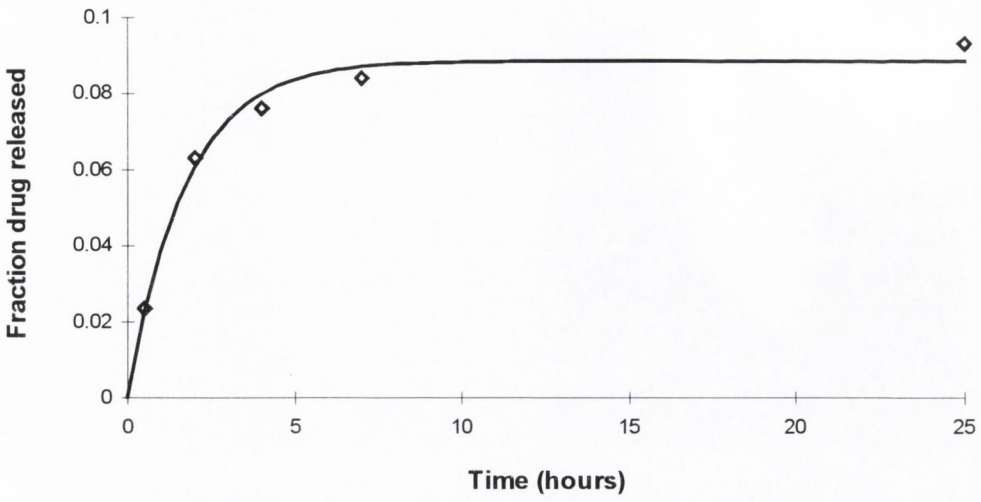

Figure 7.32. First day of drug release from RG 503 SE discs loaded with 20% AMOX-H, fitted to an exponential model (equation 3.15).

The first day data was also fitted to an equation describing square root of time kinetics (equation 3.10). In contrast to the results previously obtained with MM discs, SE discs showed very poor agreement with the square root of time model.

Figure 7.33 shows the plot of fraction drug released versus time for the overall profiles of 10%, 20%, 30% systems fitted to equation 3.14 describing first-order kinetics followed by degradation control. The data of the 20% system results from amalgamating the two experiments of figure 7.31 (Appendix III shows the fits to equation 3.14 obtained for the individual experiments).

The initial release was lower than in the corresponding MM systems, leaving a larger proportion of drug to be released in the second phase. The estimated parameters and the goodness of fit are listed in table 7.14. There was a trend towards a higher agreement with the model at the higher drug loading, indicated by (r^2) and the (MSC) obtained.

Greater proportion of drug was released in the rapid initial phase at the higher drug loads. The burst fractions (Fb_∞) estimated by the two-term equation conformed with these observations. The estimates obtained for the first-order rate constants k_b showed large standard deviation. This was dependent on the number of experimental points

available in the exponential phase, as shown in Appendix III for the 20% drug loaded systems.

Approximately 80-90% of the release profile is concentrated on the second phase, i.e. determined by polymer degradation. The onset of degradation control occurred earlier in the lower drug loads, indicated by the values of t_{max}. This may be due to the lower relative proportion of drug available for release by degradation control at the higher drug loading. Estimates obtained for the degradation controlled release parameter k were of similar order of magnitude at all the drug loads.

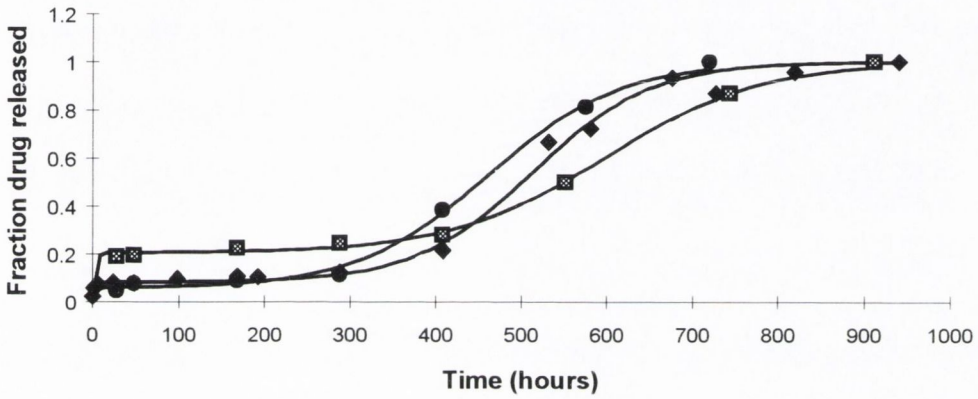

Figure 7.33. Drug released (fraction) versus time for RG 503 SE discs containing 10% (●), 20% (◆) and 30% (■) AMOX-H fitted to equation 3.14.

Table 7.14. Estimated drug release parameters for profiles obtained with RG 503 SE discs at 10%, 20% and 30% AMOX-H fitted to equation 3.14.

Drug loading (%)	10%	20%	30%
k_b (h^{-1})	0.26 ± 33	0.49 ± 0.51	0.30 ± 17
Fb_∞	0.056 ± 0.023	0.081 ± 0.015	0.203 ± 0.012
k (h^{-1})	0.0130 ± 0.0014	0.0146 ± 0.0014	0.0110 ± 0.0009
t_{max} (h)	462 ± 10	514 ± 8	598 ± 9
r^2	0.9970	0.9920	0.9979
MSC	4.66	4.42	5.20

Figure 7.34 shows the profiles of RG 503 MM discs versus RG 503 SE discs at equivalent drug loads. Lower fractions of drug were released in the initial phase of SE systems compared to MM systems. The onset of degradation occurred in a shorter time with SE systems, possibly reflecting an effect of processing on the polymer decomposition kinetics.

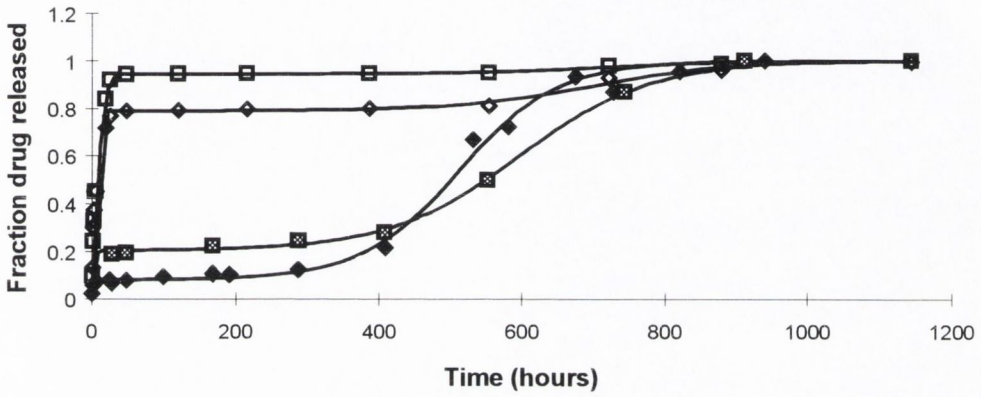

Figure 7.34. Release profiles of RG 503 MM versus SE systems at 20% (◇), 30% (□) loading in MM discs and 20% (◆), 30% (▩) loading in SE discs.

7.3.3. **Polymer mass loss studies with RG 503 SE discs: drug-free and drug loaded**

Since the degradation process of poly-alpha-hydroxy-aliphatic esters may be affected by the physicochemical properties of the drug formulated with these polymers, the mass loss profile of both drug-loaded and drug-free discs was investigated.

Figure 7.35 shows polymer mass loss versus drug release for RG 503 SE discs at 20% load. The mass loss profile presents an initial lag time of 400 hours with negligible oligomer dissolution. At 400 hours, an increase in the rate of drug release was accompanied by a considerably slower increase in the rate of polymer loss. It was only when 80% of the drug was released that the kinetics of polymer degradation were dramatically accelerated. In the corresponding MM systems (figure 7.18) the polymer degradation rate increased when 70% of the drug load had been released.

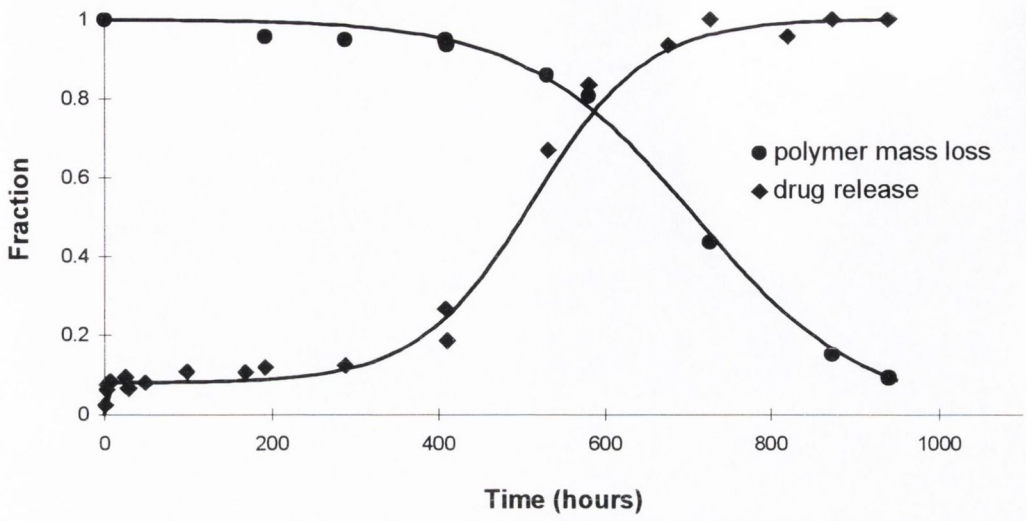

Figure 7.35. The relationship between fraction of drug released (◆) and fraction of polymer remaining (●) during drug release from RG 503 SE discs containing 20% AMOX-H.

Equation 3.13 was used to fit the polymer loss data of the 20% drug loaded discs. To distinguish between the t_{max} estimated from drug release profiles and that obtained from polymer mass loss data, the latter will be referred to as t_{maxP}. Degradation rate constants estimated from polymer mass loss data will be referred to as k_P. The resulting estimated t_{maxP} was 707 hours and the rate constant k_P was 0.0098 h^{-1}, r^2=0.9935.

In figure 7.36 the profile of polymer mass loss from the 20% drug loaded systems is compared with a polymer mass loss profile generated using drug release parameters t_{max}= 514 h and k=0.0146 h^{-1}). It appears that the second phase of drug release begins around the same time as polymer mass loss but occurs at a faster rate. Once significant polymer mass loss occurs, trapped drug has access to the dissolution media thereby allowing further release.

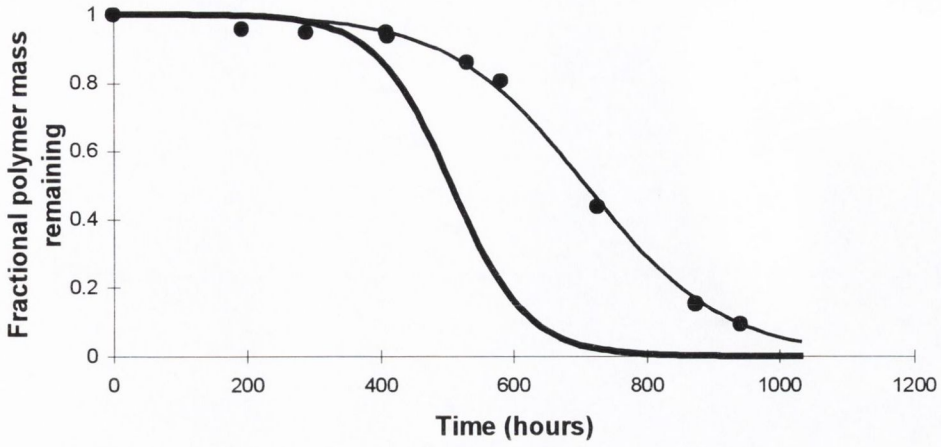

Figure 7.36. Polymer mass loss profile (●) of RG 503 20% drug loaded SE discs fitted to equation 3.13 and predicted polymer loss profile (heavier line) simulated with parameters from drug release data from the same systems.

To explore the possibility of an interaction between the drug and the polymer species, the mass loss profile of SE drug-free discs was also investigated (figure 7.37).

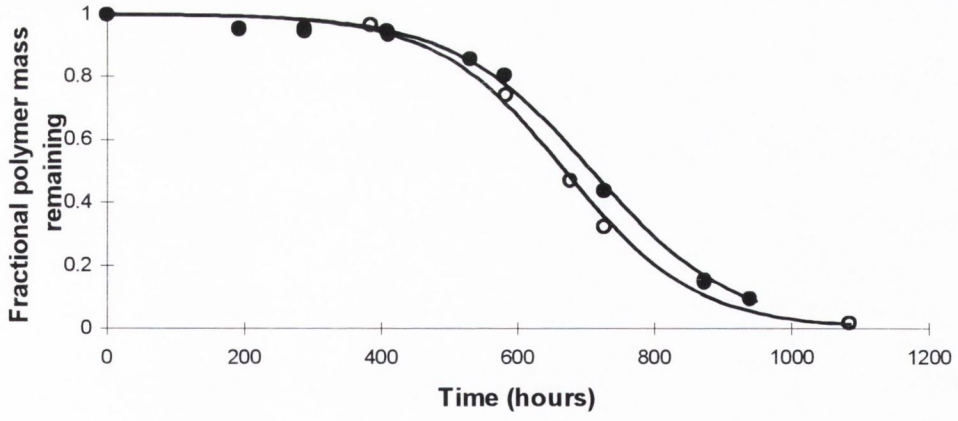

Figure 7.37. Fractional polymer mass remaining in drug-free (O) and 20% drug loaded RG 503 SE discs (●) fitted to equation 3.13.

The profile obtained for the drug-free systems was qualitatively similar to that of the 20% drug-loaded discs. After 400 hours, however, the degradation rate of drug-free discs appeared to be the highest, with estimates for t_{maxP} and k_P equivalent to 669 hours and 0.011 h^{-1} respectively, r^2=0.9951. These results compared to those of the 20%

drug loaded systems suggest that the degradation of the polymer was slowed down by the presence of AMOX.

7.3.4. **Preliminary stability tests on RG 503 formulations**

The previous release studies with RG 503 SE discs monitored *total* drug release. In order to establish the extent of drug degradation, the dissolution media of drug release experiments performed was sampled at regular time intervals for HPLC analysis.

The drug in the formulation appeared to be chemically stable during the first 400 hours of the release study. This was apparent from the chromatography traces obtained over this period which were qualitatively similar to that previously shown in figure 6.11 (a), corresponding to a solution of the pure drug prepared within 24 hours of analysis. In contrast, by 530 hours of release study the chromatograms obtained for the dissolution media of the 20% drug loaded discs showed presence of degradation products, such as illustrated in figure 7.38. This degradation, however, appears to be less than for the unformulated drug after a similar period of time (figure 7.38 versus 6.11 (d)), indicated by the relative areas of intact drug to degradation peaks.

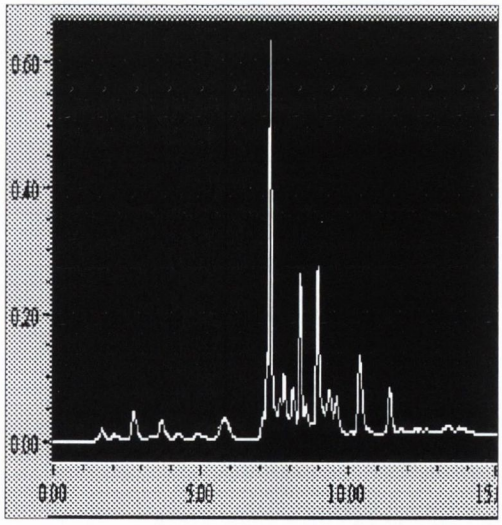

Figure 7.38. HPLC trace corresponding to a sample of the dissolution media obtained after 530 hours of drug release studies with 20% AMOX-H loaded RG 503 SE discs.

In the previous section, the t_{maxP} of RG 503 in the presence of 20% AMOX-H was estimated as approximately 707 hours. This value represents the time at which the initial polymer mass is reduced to 50%. Applying calculations for first-order kinetics, the onset of degradation may be estimated by subtracting 4 half-lives from t_{maxP}. This gives a value of 424 hours, corresponding to 6.25% polymer decomposition, which supports the view that the commencement of AMOX-H degradation (shortly after 400 hours) is triggered by the onset of polymer degradation and indicates a decrease in the local pH.

7.3.5. **RG 503 SE versus RG 503 MM**

The release profiles of systems prepared with RG 503 were characterized, both for MM and SE discs, by an initial burst of drug release followed by an induction period lasting between 400 to 600 hours and a final phase of drug release controlled by the degradation of the polymer. The proportion of the drug released in each phase was dependant upon the processing method.

Drug release during the final phase does not parallel polymer degradation but is faster. The practical consequence of such release/polymer degradation kinetics is that the drug is protected in the non-degraded matrix. However, upon degradation of the polymer the drug does degrade.

Pulse delivery of Amoxycillin is conceivable combining the properties of MM and SE discs into one final dosage form.

7.4. RG 504 SYSTEMS PREPARED BY SOLVENT EVAPORATION (SE SYSTEMS)

In this section, the release of drug from SE systems prepared with RG 504 will be reported. RG 504 is a copolymer of similar composition and higher molecular weight than RG 503 (M_w 54,123 versus 34,896 respectively).

7.4.1. Physicochemical and morphological characteristics of RG 504 SE discs

Dispersion of 20% AMOX-H in the polymeric solution resulted in smooth, flexible films subsequently compressed into discs, as described in section 5.9.

XRD scans of RG 504 systems are shown in figure 7.39. The results show that the polymer powder was amorphous. A 20% loading disc showed a pattern of peaks matching that of the pure drug.

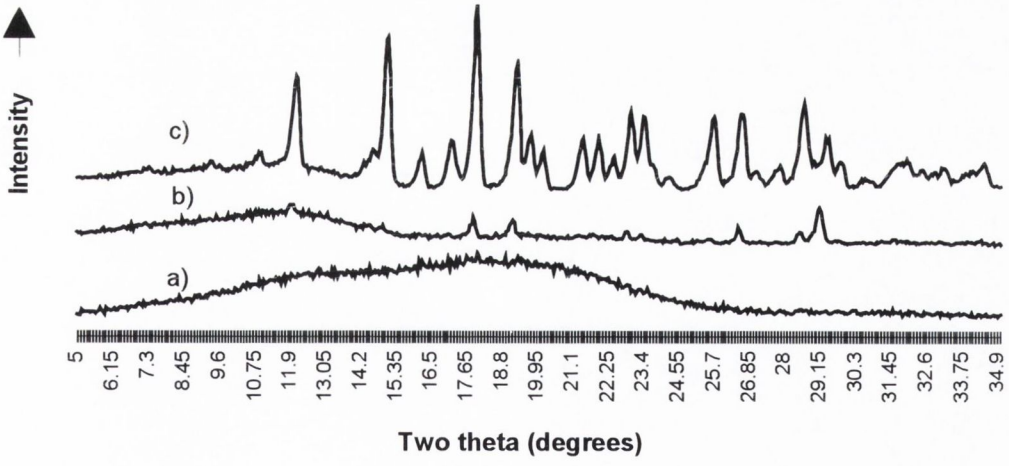

Figure 7.39. X-ray diffraction scans obtained with RG 504 powder (a), RG 504 SE disc at 20% drug load (b) and AMOX-H powder (c).

Figure 7.40 shows DSC scans obtained for the first heating cycle of RG 504 systems. Thermograms for 0% (a) and 20% (b) SE systems presented glass transition temperatures at approximately 25°C. This represents a significant decrease in the T_g of

the polymer, compared to that of the untreated powder (52.7°C). Subsequent reruns of SE samples resulted in new and constant T_g values, as previously found with RG 503. Table 7.15 lists the T_g values corresponding to the second heating scans. These results when compared to those previously shown for the lower molecular weight copolymer (table 7.12) indicate that the physicochemical properties of SE discs prepared with RG 503 and RG 504 are similar.

AMOX-H formulated with RG 504 (b) presented an endothermic event possibly corresponding to water loss, parallelling that observed for AMOX-H powder (section 6.1.3).

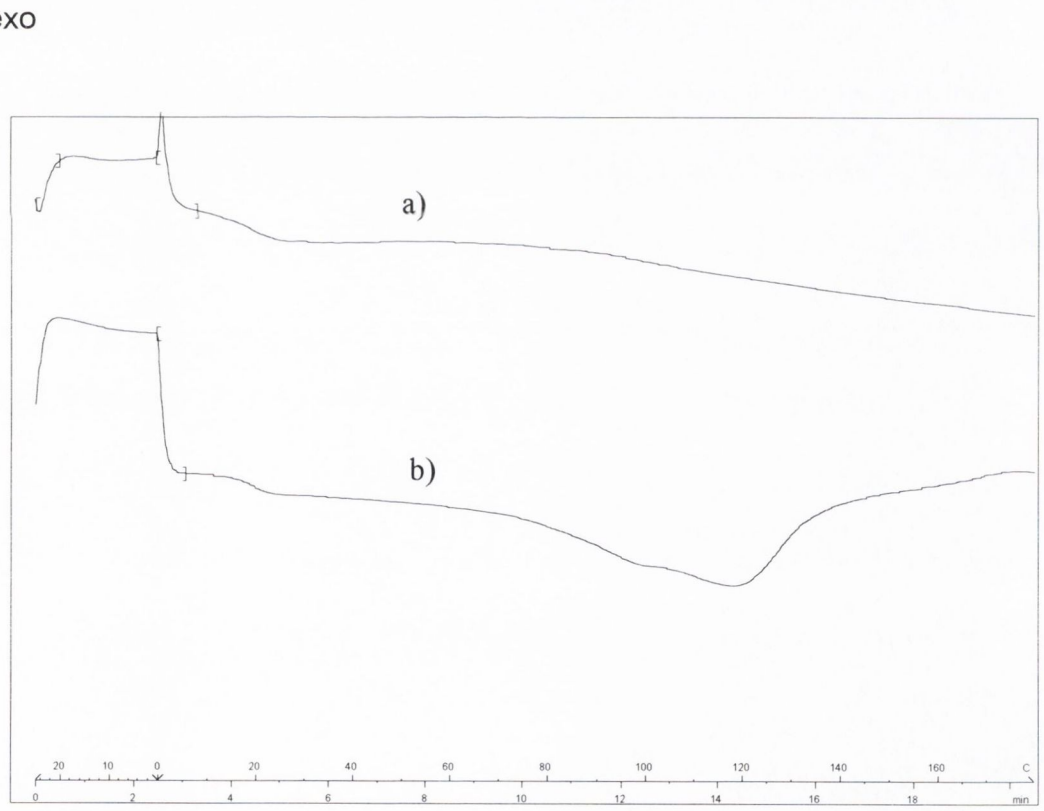

Figure 7.40. First heating scan obtained by DSC of drug-free (a) and 20% drug loaded (b) RG 504 SE systems.

Table 7.15. Glass transition temperatures determined by DSC for the second heating cycle of RG 504 systems.

RG 504 System	T_g (°C)
copolymer powder	46.8
20% AMOX-H MM	47.6
drug-free SE	43.7
20% AMOX-H SE	46.4

7.4.2. **Drug release from RG 504 SE discs**

Figure 7.41 illustrates the *total* drug release profile of RG 504 SE 20% AMOX-H discs. An initial rapid release is followed by a gradual release of drug up to 600 hours, at which time there is an apparent increase in the rate of release possibly related to polymer degradation.

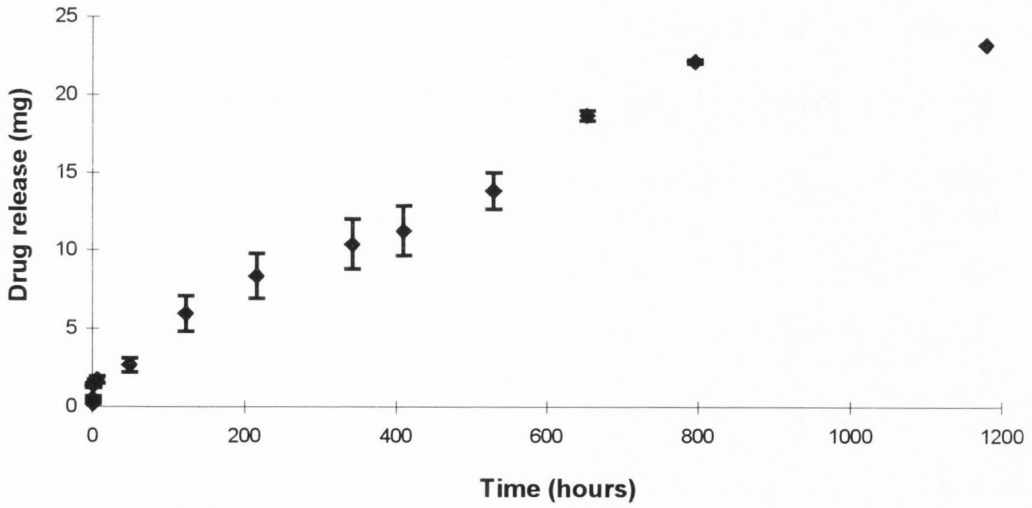

Figure 7.41. Drug release (mg) from RG 504 SE discs (120 mg) containing 20% AMOX-H. Error bars indicate the range of the data.

Figure 7.42 shows the data of the first 500 hours fitted to equation 3.10 (square root of time model). Agreement with square root of time was good, indicated by r^2=0.9939 and MSC=4.91. The first-order equation displayed a poorer fit.

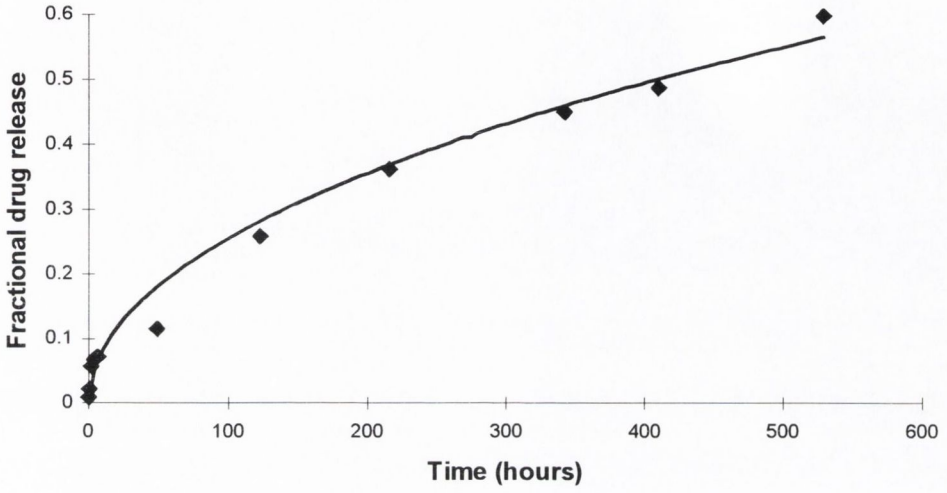

Figure 7.42. Drug release from RG 504 SE 20% AMOX-H (◆) fitted to a square root of time model, r^2= 0.9949.

Figure 7.43 shows the fractional drug release data of the 20% loading fitted to equation 3.19, the two-term release model combining square root of time followed by polymer degradation control. The fit to this equation was substantially better than that obtained with equation 3.14 (first-order followed by polymer degradation), confirming that the initial release phase obeys square root of time kinetics. The three-term equation (equation 3.20) comprising first-order, square root of time and degradation release phases gave a poorer MSC than equation 3.19. The results obtained for the various models are given in table 7.16.

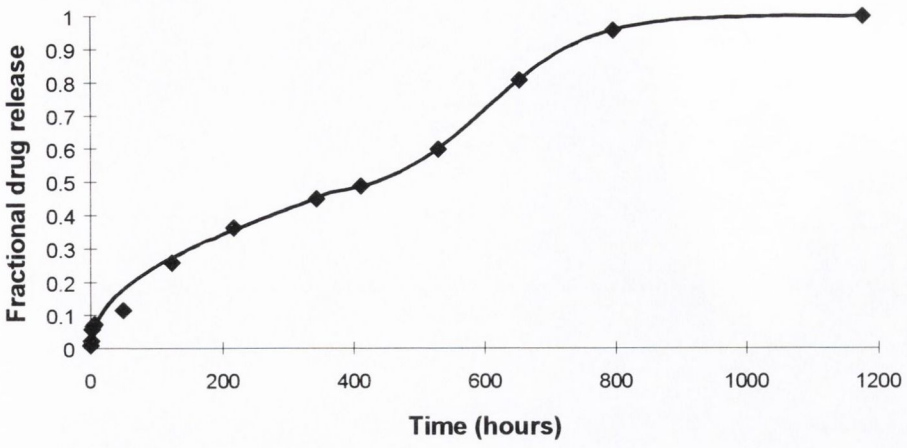

Figure 7.43. Fractional drug release from RG 504 SE discs at 20% AMOX-H loading fitted to equation 3.19.

Table 7.16. Parameters estimated for drug release profiles of 20% drug loaded RG 504 SE discs loaded fitted to equations 3.14, 3.19 and 3.20. (n.a. = "non applicable")

	Equation 3.14	Equation 3.19	Equation 3.20
k_b (h^{-1})	0.0423 ± 0.0184	n.a.	0.692 ± 2.64
Fb_∞	0.265 ± 0.364	n.a.	0.0079 ± 0.0124
k_r ($h^{-0.5}$)	n.a.	0.0032 ± 0.0001	0.0039 ± 0.0004
Fd_∞	n.a.	0.44 ± 0.02	0.56 ± 0.044
k (h^{-1})	0.0076 ± 0.0010	0.0127 ± 0.0011	0.0138 ± 0.0014
t_{max} (h)	523 ± 22	604 ± 9	637 ± 15
r^2	0.9949	0.9994	0.9993
MSC	4.66	6.75	6.46

SEM images of the surface of RG 504 SE discs before dissolution studies and during the initial drug release phase, magnified 235 times, are shown in figure 7.44. Initially,

the surface of the discs is relatively smooth, i.e. without pores. After 12 hours of drug release extensive pore formation is already observed, which increases by 20 hours of dissolution.

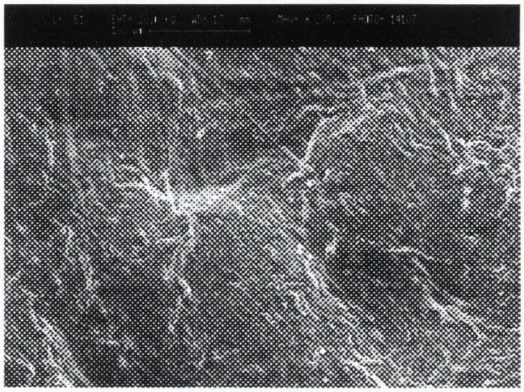

a) 0 hours

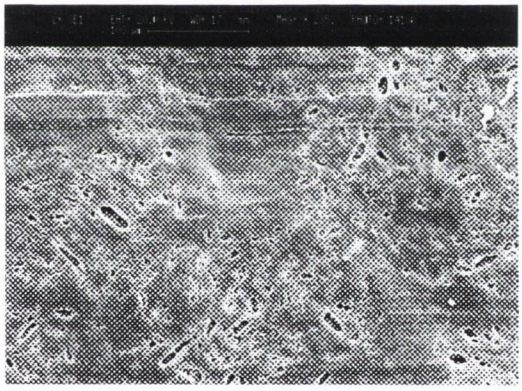

b) 12 hours

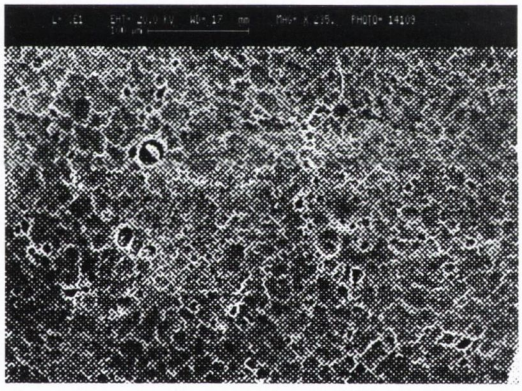

c) 20 hours

Figure 7.44. SEM images of RG 504 SE discs at 20% drug load before dissolution studies (a) and by 12 hours (b) and 20 hours (c) of the same studies, magnified 235 times.

7.4.3. **Polymer mass loss studies with RG 504 SE discs: drug-free and drug loaded**

Figure 7.45 compares drug release and polymer mass loss versus time for 20% drug loaded systems prepared by the solvent-cast method. Two batches of discs, prepared and assayed 12 months apart, are compared. Similar profiles were obtained for the

two batches. Less than 4% of polymer mass loss was observed for the period up to 400 hours, at which time circa 50% of the drug was already released. After this period, there is an increase in both the polymer loss and the release of drug suggesting that the degradation of the polymer contributes to the final phase of drug release.

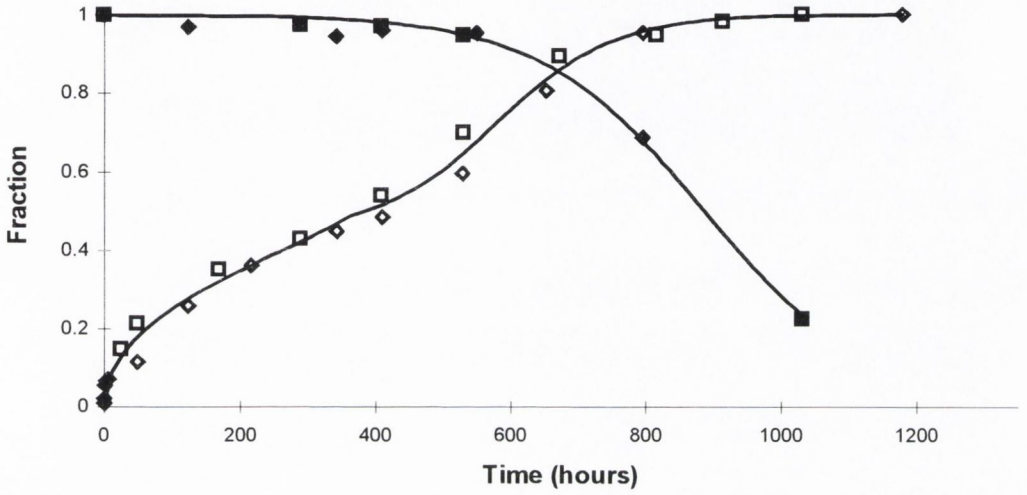

Figure 7.45. Fractional drug release (◇, □) and fractional polymer mass remaining (◆, ■) for RG 504 SE discs loaded with 20% AMOX-H. Two separately manufactured batches of discs are compared.

Figure 7.46 shows the plot of polymer mass loss from drug-free versus 20% drug loaded discs. From the graph, it is suggested that the inclusion of the drug has an effect on the polymer degradation kinetics, retarding its degradation rate. This effect was also observed with RG 503. Table 7.17 lists the estimated parameters and statistics obtained for the polymer loss from 20% drug loaded and drug-free RG 504 systems fitted to equation 3.13, showing that the presence of drug increased the value of t_{maxP} and decreased the degradation rate constant k_P. In the terminology of the current report, the t_{maxP} for drug-free discs reported by Gallagher and Corrigan (1998) was 655 h and the k_P was 0.00647 h^{-1}. Differences with the k_P values obtained in the present work may originate from variability inherent to the raw materials employed (different batches).

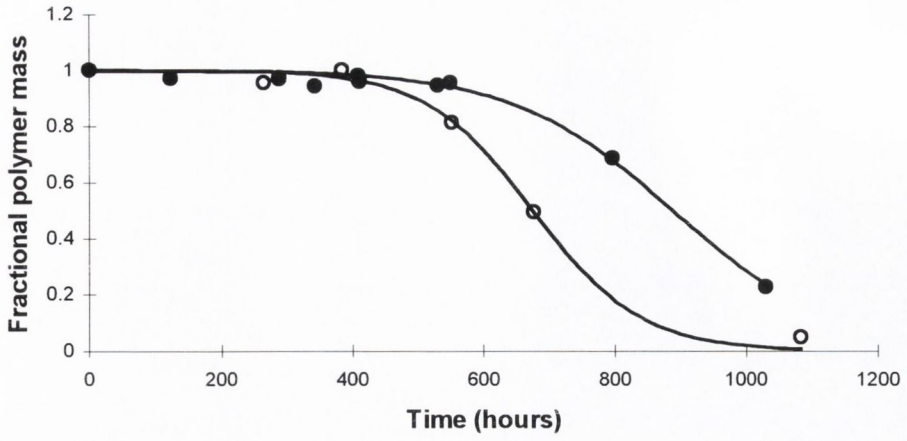

Figure 7.46. Fractional polymer mass versus time plot for drug-free (O) and 20% drug loaded (●) RG 504 SE discs fitted to equation 3.13.

Table 7.17. Parameters estimated for the polymer mass loss of drug-free and 20% drug loaded RG 504 SE systems fitted to equation 3.13.

	drug-free discs	20% drug loaded
t_{maxP} (h)	674 ± 9	886 ± 10
k_P (h^{-1})	0.01227 ± 0.00143	0.00818 ± 0.00052
r^2	0.9941	0.9922
MSC	4.64	4.45

At 20% loading, t_{max} obtained for drug release was lower than the estimate for polymer mass loss (t_{maxP}), i.e. 604 hours versus 886 hours. A similar situation was previously observed with RG 503 SE discs (section 7.3.3). These results possibly indicate that at least some of the drug released by a degradation mechanism is not "bound" to the polymer. Drug bound to the polymer would not be released prior to dissolution and mass loss of the matrix. However, drug entrapped but unbound may be released upon onset of degradation which is normally preceeded by ingress of water.

7.5. **RG 503 VERSUS RG 504 SYSTEMS**

Release from RG 504 SE discs compared to RG 503 SE discs of similar AMOX-H content, differed in the mechanism determining the pre-degradation phase of the profile. Figure 7.47 compares the drug release and polymer mass loss profiles of SE discs prepared with RG 503 (□, ■) and RG 504 (◇, ◆) at 20% drug loading. An initial rapid release of surface drug was observed for both systems during the first day of the study. Subsequently, RG 503 discs showed a lag-time for a period of approximately 400 hours until the onset of degradation control. In contrast, RG 504 discs did not present a lag-time, showing continuous drug release, with possible square root of time kinetics, up until onset of the final phase at approximately 600 hours. The formulation with lower molecular weight copolymer showed greater proportion of drug released by degradation control than the equivalent higher molecular weight copolymer. Time for completion of drug release was similar for both formulations.

Polymer loss from RG 503 was apparent after 400 hours, when only 20% of the initial drug loading had been released. Higher proportion of drug (50% of the initial loading) was released from RG 504 before onset of polymer loss in this system. Approximately 80% of the drug was released from both systems when only 20% of the polymer was lost, as indicated in the figure by the intersections of the profiles within each system.

Onset of degradation control occurred in the order expected for these polymers (Göpferich, 1996), earlier for the lower molecular weight compound, RG 503. Since both copolymers have similar composition of constituent sub-units, the differences found in their drug release behavior may be attributed solely to the effect of the molecular weight differences, and hence the time to reach the molecular weight of soluble oligomers.

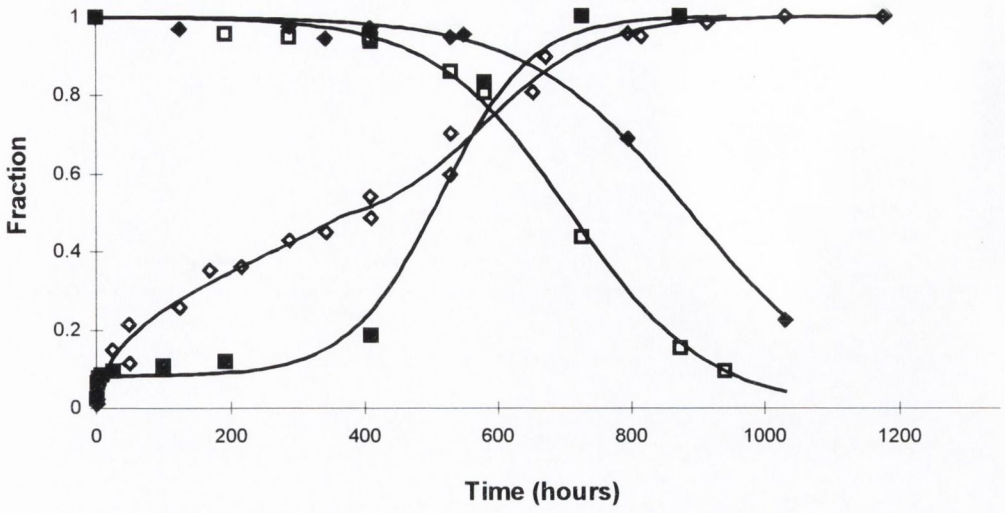

Figure 7.47. Comparison of fractional drug release (■) and fractional polymer mass remaining (□) in RG 503 SE discs containing 20% drug loading with the equivalent RG 504 drug release (◇) and polymer mass (◆) profiles.

Figure 7.48 shows a photograph of five discs from each formulation. The samples were removed from the release experiment at comparable times, indicated by the labels. There is a time-dependant change in the colour of the discs, particularly noticeable in RG 503 systems (polymer 1). The period of yellow coloration of RG 503 discs coincides with the degradation phase of the drug release profile. In addition, degradation of the drug during this period is supported by HPLC chromatograms containing multiple peaks (see Chapter 9 and Appendix V) suggesting that AMOX-H has degraded into yellow compounds. Around the onset time of polymer degradation, RG 504 discs (polymer 2) also presented a yellow coloration (364 h). However, this coloration was not evident at further time points (550 and 1179 hours).

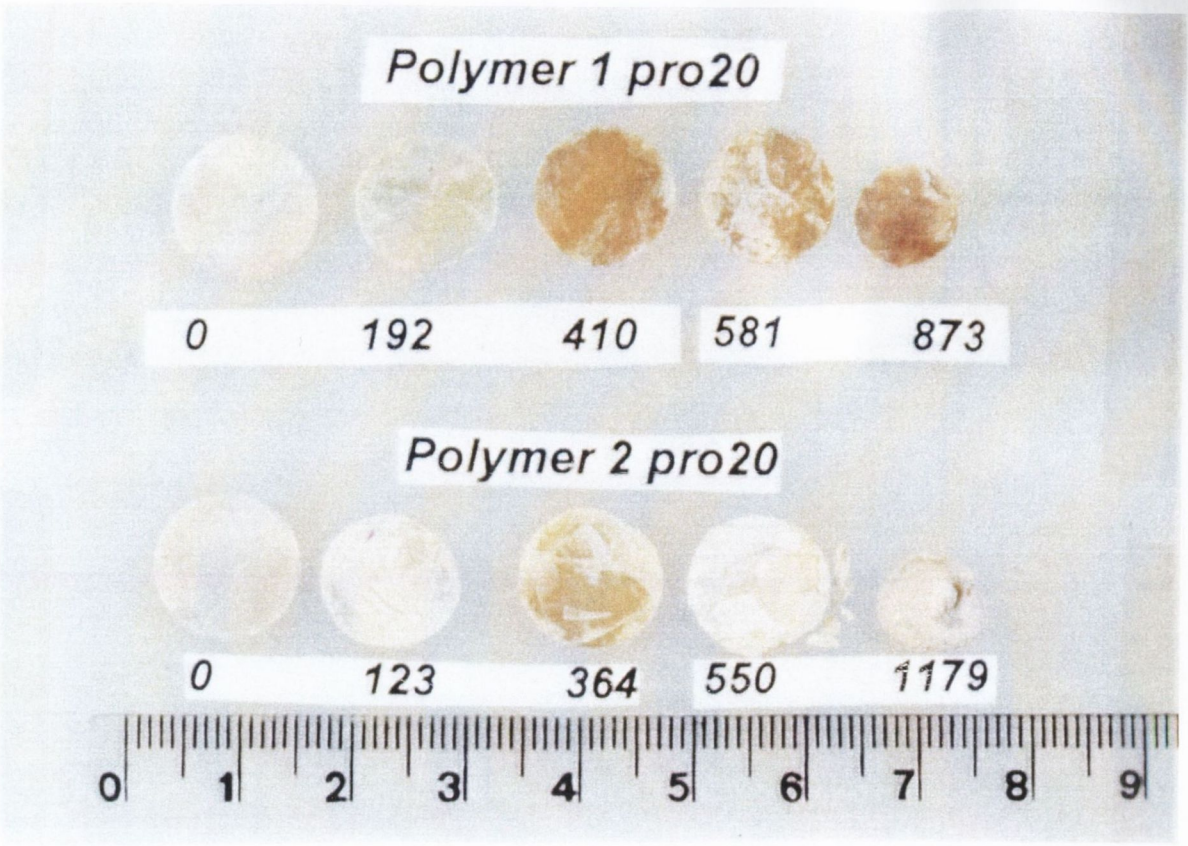

Figure 7.48. Photograph of RG 503 (polymer 1) and RG 504 (polymer 2) SE discs containing 20% AMOX-H during similar stages of drug release experiments, as per the indicated times (hours). Scale in cm.

7.6. CONCLUSIONS

Profiles obtained from RG 503 MM discs showed greater proportion of drug released prior to onset of polymer degradation than the corresponding SE discs. Equation fitting to these profiles resulted in longer t_{max} values than those obtained for SE discs. Hence, the manufacturing method plays a major role in defining drug release characteristics.

Drug release profiles for RG 503 and RG 504 SE discs showed an initial phase of drug release governed by dissolution-diffusion mechanisms followed by a polymer degradation controlled phase. For RG 503, the initial phase was rapid and relatively small compared to the higher molecular weight system, RG 504. The latter, showed

continuous drug release up to the commencement of polymer mass loss. Both systems exhibited a final phase of drug release governed by degradation of the polymer.

Release profiles for poly-alpha-hydroxy-aliphatic esters of similar polymer composition but different molecular weight are both bimodal, with an earlier degradation controlled phase for the lower molecular weight copolymer (RG 503) and larger proportion of drug released prior to polymer degradation found in the higher molecular weight copolymer (RG 504). The initial release phase appears to be governed by dissolution kinetics of two kinds: more contribution from a first-order mechanism for RG 503 systems while square root of time kinetics appear to determine drug release from RG 504 systems.

Polymer mass loss profiles of RG 503 and RG 504 discs showed that there is a retardation of the onset of polymer degradation due to the presence of AMOX-H in the discs compared to the equivalent drug-free systems.

Drug release from preparations with RG 503 and RG 504 continues for approximately 30 days, with chemical breakdown of the drug (shown in the HPLC traces of RG 503 discs) commencing concurrently with polymer degradation. The formulation of systems with PLGA of slower degradation rate resulted in higher proportion of drug released prior to onset of polymer mass loss (RG 503 versus RG 504 systems). With the aim to increase the proportion of intact AMOX-H delivered from within poly-alpha-hydroxy-aliphatic esters a combination of high loadings and polymers of slower degradation rates is investigated in Chapter 8.

CHAPTER 8. RG 755 AND R 203 SYSTEMS

8.1. INTRODUCTION

The present chapter explores both MM and SE systems prepared with RG 755 (M_W 73,854). The work with SE systems was later extended to R 203 (M_W 26,613), a polymer solely composed of lactide units. This expands the compositional range of poly-alpha-hydroxy-aliphatic esters covered in this thesis to between 50% and 100% of poly(D,L-lactide).

8.2. RG 755 SYSTEMS PREPARED BY MECHANICAL MIXTURE (MM SYSTEMS)

8.2.1. Physicochemical and morphological characteristics of RG 755 MM discs

The manufacture of RG 755 MM systems was performed by Method 2 as described in section 5.8.2. X-ray diffraction, DSC and TGA were used in the characterization of these systems. The results obtained are discussed below.

X-ray diffraction scans of RG 755 powder (a), RG 755 MM discs at 20% (b) and 30% (c) load and AMOX-H powder (d) are shown in figure 8.1. The diffractogram corresponding to the polymer powder was typical of amorphous materials, indicated by the absence of defined peaks. In contrast, AMOX-H powder and the 20% and 30% systems displayed diffractograms containing defined peaks, typical of crystalline materials.

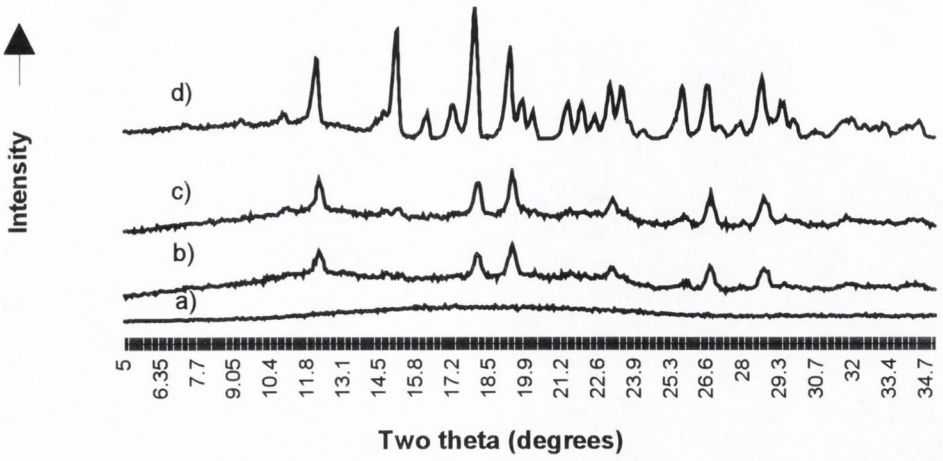

Figure 8.1. X-ray diffractograms of RG 755 powder (a), RG 755 MM discs at 20% (b) and 30% (c) drug load and AMOX-H powder (d).

As outlined in section 5.4.2, to provide a constant thermal history of the polymer (Ford and Timmins, 1989) samples were evaluated after two consecutive heating cycles. Table 8.1 summarizes the T_g results obtained for the reruns of RG 755 systems. Comparable glass transition temperatures were obtained for the copolymer powder and the polymeric discs.

As previously described in Chapter 6, powder AMOX-H displays an endothermic inflexion due to the loss of water of crystallization. Similar inflexions were displayed by drug loaded RG 755 MM discs, consistent with the presence of crystalline drug.

Table 8.1. Glass transition temperatures determined by DSC for the second heating cycle of RG 755 systems.

RG 755 System	T_g (°C)
copolymer powder	49.5
20% AMOX-H MM	50.7
30% AMOX-H MM	49.7
50% AMOX-H MM	49.8

8.2.2. **Drug release from RG 755 MM systems**

Total drug release profiles obtained with 20%, 30% and 50% MM systems are shown in figure 8.2. These systems released most of the drug during the first 100 hours of the study; drug release was in rank order with the % initial load. At the lower drug loads, drug was still entrapped after 1000 hours of dissolution, the remaining release occurring thereafter over 800-1000 hours. Thus, there would appear that there is an induction period at 20-30% loading. At the 50% loading, drug release after 1000 hours of dissolution was not apparent.

By 2000 hours, solid discs of smaller dimensions were still present. The discs were then removed from the dissolution medium, dried in a dessicator to a constant weight and treated as described in section 5.12 to extract any residual drug. HPLC analysis of the extractives confirmed that at 2000 hours the discs were depleted of drug.

During the initial phase, up to 100 hours, the formulations showed no evidence of AMOX-H degradation in the HPLC traces. In contrast, after 1000 hours, the HPLC chromatograms of samples from the dissolution media resembled those obtained with degraded drug during the preliminary stability studies described in Chapter 6.

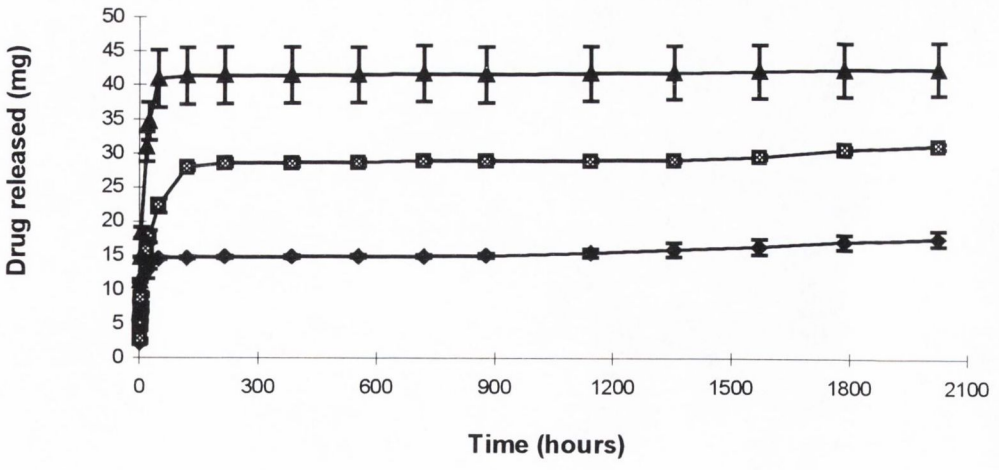

Figure 8.2. Drug release (mg) versus time for RG 755 MM discs at (◆) 20%, (▩) 30%, (▲) 50% drug load.

The data of the first day obeyed square root of time kinetics, as shown in figure 8.3. The statistical output was better for the 50% (r^2=0.9772; MSC=3.45) and 30% (r^2=0.9881; MSC=4.10) systems than for the 20% system (r^2=0.9534; MSC=2.73).

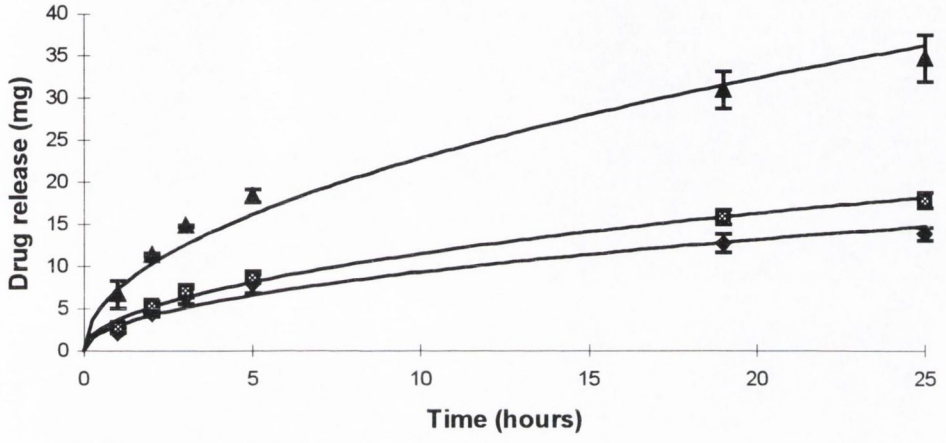

Figure 8.3. First day of drug release (mg) from RG 755 MM systems at 20% (◆), 30% (▩) and 50% (▲) drug loading fitted to equation 3.8. Error bars indicate the range of the data.

The criteria for distinguishing between matrix diffusion and first order release outlined by Schwartz (section 7.2.2) was applied to the 50% release data and suggested a matrix controlled process. Linearity was obtained when the rate of drug release was plotted against the reciprocal of fraction drug released (r^2=0.9832), consistent with square root of time kinetics. First-order plots assessed for RG 755 MM systems at 20%, 30% and 50% loading resulted in poorer fits.

Since both the 20% and 30% loaded discs showed the presence of an induction period in advance of the final drug release phase (figure 8.2), the overall release data from these systems was fitted to equation 3.19 which takes into account both a matrix and a degradation controlled phase (figure 8.4). The initial phase had a duration of approximately two days, after which time there was a lag period characterized by leaching of small proportions of drug until onset of the final phase after 1000 hours. The final phase was of larger proportion at the lower drug loading. This was in agreement with the relative amounts of drug available for release in the last phase.

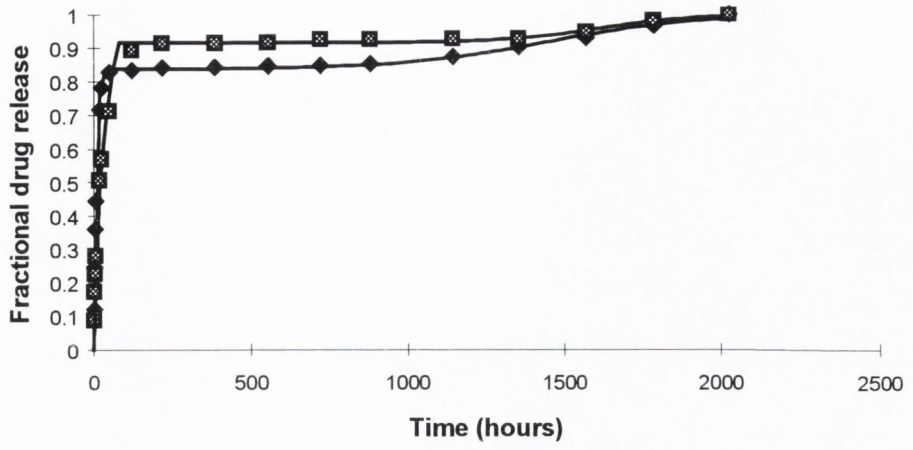

Figure 8.4. Fractional drug release profiles of RG 755 MM systems at 20% (◆), 30% (▩) drug loads fitted to equation 3.19.

Table 8.2 shows the parameters and statistics obtained. The values of Fd_∞ and k_r increased with the drug loading. The values of the degradation parameters, t_{max} and k, increased with increasing proportion of drug, however the differences may be statistically non-significant.

Table 8.2. Estimated parameters for drug release profiles of RG 755 MM systems at 20%, 30% loading fitted to equation 3.19.

Drug loading (%)	20	30
Fd_∞	0.84 ± 0.02	0.92 ± 0.0074
k_r ($h^{-0.5}$)	0.0012 ± 0.0007	0.0071 ± 0.0002
t_{max} (h)	1460 ± 187	1621 ± 104
k (h^{-1})	0.0042 ± 0.0020	0.0066 ± 0.0040
r^2	0.9748	0.9972
MSC	3.24	5.45

At the 50% loading drug release appeared to be entirely controlled by dissolution of the drug from the polymeric matrix, occurring during the first 100 hours of dissolution (figure 8.2). Therefore, the drug release profile of this system was fitted to equation 3.10 describing square root of time kinetics (table 8.3).

Table 8.3. Parameters estimated for drug release data of RG 755 MM discs at 50% loading, fitted to equation 3.10 describing square root of time kinetics.

k_r ($h^{-0.5}$)	0.0098 ± 0.00023
r^2	0.9916
MSC	4.66

8.2.3. **RG 755 versus RG 503 MM discs**

Figure 8.5 compares RG 755 with RG 503 MM systems. The graph suggests that, at a given drug load, the two copolymers release a similar proportion of drug in the first day. RG 503 systems showed greater agreement with initial exponential release than with square root of time (sections 7.2.4).

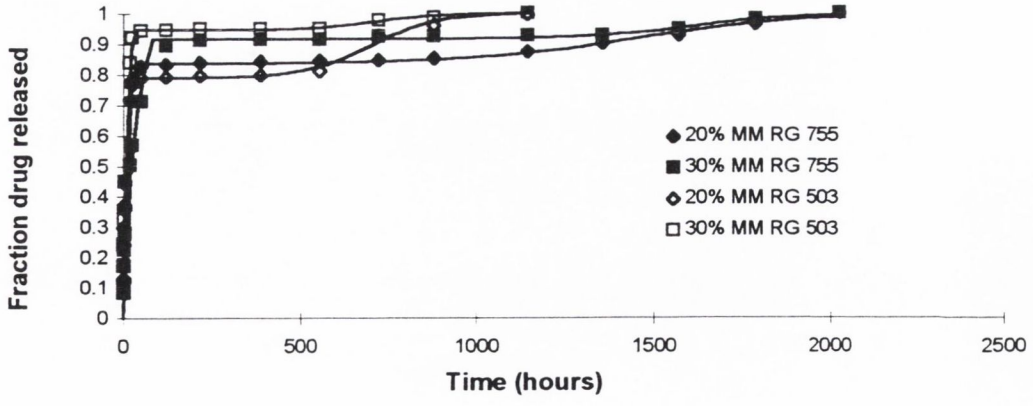

Figure 8.5. Comparison of drug release from RG 503 and RG 755 MM discs at 20% and 30% loading.

However, these systems were still well described by the square root of time models, therefore being valid to compare the parameters estimated by equation 3.19 for RG 503 and RG 755. The comparison is shown in tables 8.4 and 8.5 for the 20% and 30% drug loadings, respectively.

Table 8.4. Comparison of the parameters estimated for drug release from 20% drug loaded MM discs prepared with RG 503 and RG 755, fitted to equation 3.19.

	RG 503	RG 755
k_r ($h^{-0.5}$)	0.0135 ± 0.0006	0.0012 ± 0.0007
Fd_∞	0.79 ± 0.02	0.84 ± 0.02
k (h^{-1})	0.0116 ± 0.0058	0.0042 ± 0.0020
t_{max} (h)	685 ± 49	1460 ± 187
r^2	0.9884	0.9748
MSC	3.89	3.24

Table 8.5. Comparison of the parameters estimated for drug release from 30% drug loaded MM discs prepared with RG 503 and RG 755, fitted to equation 3.19.

	RG 503	RG 755
k_r ($h^{-0.5}$)	0.0118 ± 0.0004	0.0071 ± 0.0002
Fd_∞	0.95 ± 0.02	0.92 ± 0.0074
k (h^{-1})	0.0110 ± 0.0252	0.0066 ± 0.0040
t_{max} (h)	713 ± 224	1621 ± 104
r^2	0.9901	0.9972
MSC	4.05	5.45

It appears that for those systems containing between 20% and 30% AMOX-H the proportion of drug released in the initial phase is not determined by the type of polymer but it reflects dissolution/release of drug from interconnected surface particles which leaves pores upon release, facilitating the ingress of water and the rapid dissolution of more drug.

The induction period observed with RG 755 is longer than that reported in section 7.2.4 for RG 503, as expected from the differences in polymer composition. The rate constants, k_r and k, were lower for the higher molecular weight copolymer. This is consistent with the findings of Jalil and Nixon (1990b), where higher rates of phenobarbitone release was reported with polymers of lower molecular weight.

8.3. RG 755 SYSTEMS PREPARED BY SOLVENT EVAPORATION (SE SYSTEMS)

8.3.1. Physicochemical and morphological characteristics of RG 755 SE discs

RG 755 SE discs were manufactured by the solvent evaporation technique described in section 5.9. Figure 8.6 shows the X-ray diffraction scans of RG 755 copolymer powder (a), RG 755 SE discs at 10% (b), 20% (c), 30% (d), 50% (e) and AMOX-H powder (f). The patterns obtained for the discs contained defined peaks consistent with the presence of crystalline AMOX-H in the discs. The intensities obtained appeared to be in rank order with the drug load. Figure 8.7 shows the relevant plot, where data points corresponding to MM discs have been superimposed.

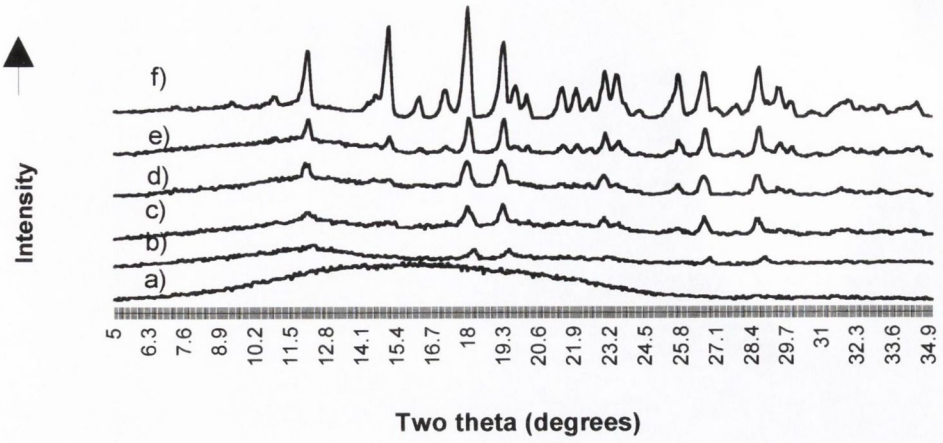

Figure 8.6. X-ray diffractograms of RG 755 powder (a), RG 755 SE discs at 10% (b), 20% (c), 30% (d), 50% (e) loading and AMOX-H powder (f).

For SE discs, a linear relationship between the diffraction intensity and the drug load was observed (r^2=0.9696 and MSC=2.69) in figure 8.7. The intercept on the ordinate axis was estimated as 3.38 $\pm$ 5.11%. On the basis of the range of the 95% confidence interval obtained for the intercept value (-12.89 to 19.66), there was no evidence that the line obtained deviated in the statistical sense from the origin. This is similar to the results previously obtained for RG 503 SE systems in Chapter 7. However, in RG 755 systems the superimposed MM data points (figure 8.7) showed higher intensity values than the corresponding SE data points. A Student t-test (Statistics, An Introduction, 1998) was subsequently performed on the limited data of figure 8.7 to evaluate the significance of the differences observed between MM and SE intensities.

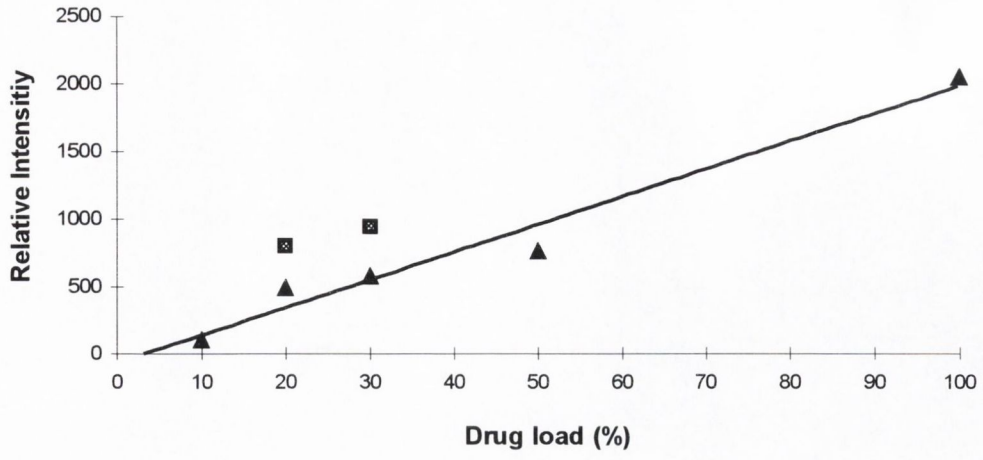

Figure 8.7. Relationship between X-ray intensity and % drug load for RG 755 SE systems (▲), where data points obtained for MM discs (▩) have been included .

The paired-test performed on the data is shown below:

The Null Hypothesis (H_0) was that there were no differences between the XRD intensity values obtained for MM and SE systems: $H_0 \quad \bar{d} = 0$

and the Alternate Hypothesis (H_1) was that there were differences between the two systems: $H_1 \quad \bar{d} \neq 0$

under H_0 equation 8.1 holds,

$$t = \frac{\bar{d} - 0}{\sqrt{\frac{s^2}{n}}} \approx t_v \qquad \text{equation 8.1}$$

where t is the test statistic, $\bar{d}$ is the mean difference between the paired observations (MM and SE), s is the standard deviation of the differences between the paired observations, n is the number of paired observations or arguments and v is the degrees of freedom, which is equal to (n-1).

A summary of the data used for the test is shown in Appendix III. On application of equation 8.1, the computed *t*-value (10.81) was compared to the *critical value* (12.71) for 1 degree of freedom at 95% confidence level in the *t*-distribution table.

The result of the test indicated that the average long run difference between the XRD intensities, at 95% confidence level, for MM and SE RG 755 systems was statistically non significant. The *p*-value (probability value) computed using Excell (Microsoft) was 0.059, which is consistent with the decision of not to reject the null hypothesis of no differences.

Therefore, from the data of figure 8.7 there was no evidence to support the existence of a phase transformation of the drug during processing with RG 755.

The T_g values obtained with the second heating scans of SE systems are listed in table 8.6.

Table 8.6. T_g values obtained by DSC for the second heating scans of RG 755 powder and SE systems at 0%, 10%, 20%, 30%, 40%, 50%, 60% AMOX-H loading.

RG 755 system	T_g (°C)
copolymer powder	49.5
SE drug-free	47.1
SE 10% AMOX-H	49.3
SE 20% AMOX-H	49.9
SE 30% AMOX-H	49.7
SE 40% AMOX-H	49.5
SE 50% AMOX-H	50.2
SE 60% AMOX-H	49.5

Similar T_g values were displayed by the drug-copolymer systems and the pure copolymer. Benoit et al. (1986) proposed that when the glass transition of a polymer is not lowered by the presence of the drug this is indicative of little mutual miscibility of the materials. All the drug loaded systems investigated displayed dehydration endotherms similar to the events observed in RG 503 discs, consistent with the presence of crystalline drug.

Enthalpy changes corresponding to the drug, calculated as described in section 5.4.2, increased in rank order with the drug load. Figure 8.8 shows the plots of enthalpy change (J/g) versus nominal drug load (%) obtained for RG 755 SE and MM discs for loadings in the range 10% to 60%. Linear least squares regression analysis fitted the data as indicated by r^2=0.9829, MSC=3.07 for MM systems and r^2=0.9973, MSC=5.25 for SE systems. The intercept on the ordinate of SE systems showed a value of 5.17 $\pm$ 0.89 %w/w which was significant in the statistical sense, as indicated by the 95% confidence range limits (1.84 and 8.5). This was in contrast to the results previously obtained for RG 503 SE systems, where the data of SE and MM systems was not significantly different.

As already discussed, it is conceivable that during the filmcasting procedure a molecular dispersion of Amoxycillin was formed, and may be the reason for the positive intercepts observed in the DSC results of RG 755 systems. However, these results were not supported by the XRD results previously shown for the polymer.

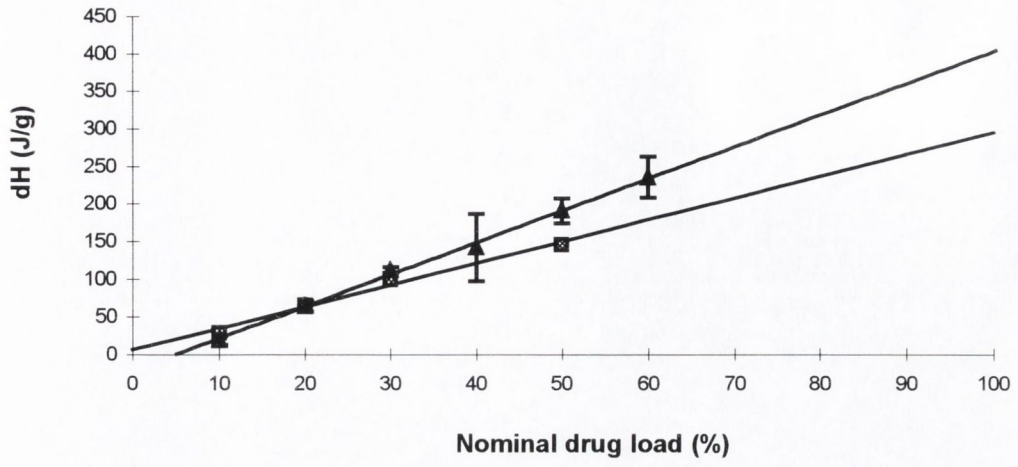

Figure 8.8. Plot of enthalpy change (J/g) determined by DSC versus nominal drug load (%) for RG 755 MM (■) and SE (▲) discs. Error bars indicate the standard deviation of the data.

TGA was performed on RG 755 SE discs loaded with 10%, 30% and 50% of drug. There was an initial loss of volatile components occurring prior to 110°C and no further mass loss until after 190°C. These results were qualitatively similar to those previously shown for the lower molecular weight copolymer RG 503, i.e. the dehydration and decomposition events paralleled those of the pure drug.

8.3.2. **Drug release studies with RG 755 SE discs**

Drug release profiles obtained with RG 755 SE discs are shown in figure 8.9, for systems at 10%, 20%, 30%, 40%, 50% and 60% loading.

The amount released was in rank order with the drug load. There is a trend towards increasing the time for completion of drug release as the drug load decreases. Release was completed in less than 600 hours for those systems containing 40% drug load or greater.

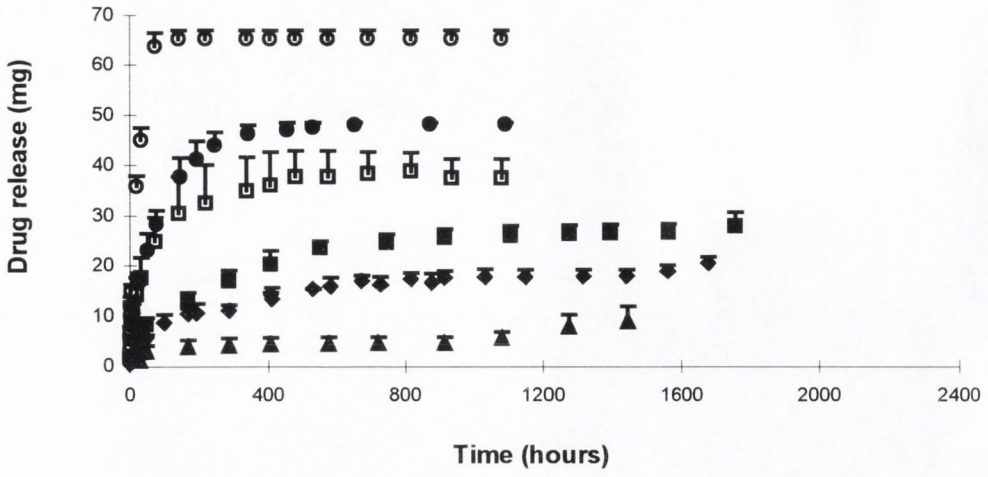

Figure 8.9. Drug release profiles of RG 755 SE discs containing 10% (▲), 20% (◆), 30% (■), 40% (□), 50% (●) and 60% (○) AMOX-H. Error bars indicate the standard deviation of the data, with the exception of the 50% system for which the error bars show the range of the data.

For further evaluation the profiles were divided into two groups. The 10%, 20%, 30% systems being investigated in the first place.

To explore the contribution from matrix control, the drug release data was plotted versus the square root of time. The fit was very poor for the 10% drug loaded system but improved at the higher drug loadings. The 20% and 30% systems showed a linear trend up to approximately 600 hours. Deviation from linearity occurred when the data points of the final profile (after 600 hours) were included. Least squares regression resulted in higher r^2 and MSC values for the 30% system than the 20% system (table 8.7). Both 20% and 30% systems showed a positive intercept with the *y* axis suggesting that there is an initial release of drug obeying different kinetics, possibly due to drug being released directly from the surface of the discs.

Table 8.7. Parameters estimated by linear least square regression for the square root of time plot of drug release data from RG 755 SE discs at 10%, 20%, 30% load.

	10%	20%	30%
slope ($mg.h^{-0.5}$)	1915 ± 695	0.63 ± 0.021	0.95 ± 0.029
intercept (mg)	-478 ± 274	1.05 ± 0.31	0.9356 ± 0.46
r^2	0.6554	0.9852	0.9962
MSC	0.3988	3.95	4.91

Equation 3.19 describing square root of time kinetics and degradation dependant drug release was then used to fit the full profiles of the 10%, 20%, 30% systems (figure 8.10). At the lower load, approximately one third of the drug was released in the first two days. There was an induction period of approximately 750 hours observed with all three loadings. The final release phase, consistent with polymer degradation control, accounted for approximately 60% of the overall profile. At 20% and 30% loading, square root of time diffusion accounted for circa 80% of the release profile, with approximately 10% of the initial load being released in the first day. An induction period commenced at 600 hours until onset of the final phase at 1500 hours. The final phase had very little contribution to the overall release profile.

At the end of the release study (1400-1700 hours depending on the loading), polymer discs were still formed. The weight and diameter of the discs was considerably smaller compared to the initial dimensions.

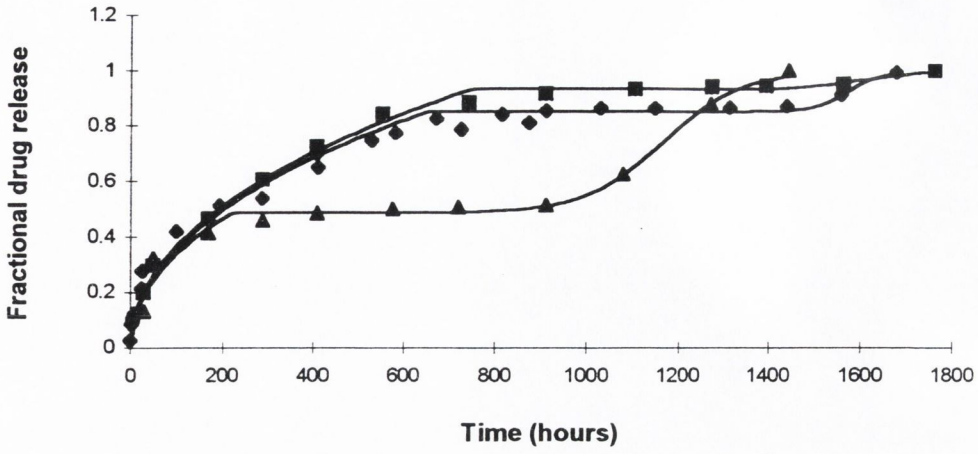

Figure 8.10. Drug release profiles of RG 755 SE at 10% (▲), 20% (◆), 30% (■) drug load fitted to equation 3.19.

The statistics and parameters obtained with equation 3.19 are listed in table 8.8. Fd_∞ increased with increasing drug load while k_r decreased from 10% to 30% load. There was an increase in the value of t_{max} with increasing load, probably due to the relative amount of residual drug available in each system for release in the final phase. The values of the degradation rate constant, k, were in the same order of magnitude for all the systems although showed large standard deviation values at the higher loads.

On the basis of the results obtained with RG 503 SE systems, which indicated better agreement with first-order than square root of time kinetics, the drug release data was then fitted to the two-term release model described by equation 3.14. The fit obtained for the 10% system is shown in figure 8.11, with estimated parameters that better describe the release profile (table 8.9). This is in agreement with the results obtained for the first-order plot of day one of the release, where the 10% system showed higher agreement (r^2=0.9234; MSC=1.91) than with the square root of time equation.

For the 20% and 30% systems the fit was better with the model comprising square root of time followed by polymer degradation.

Table 8.8. Parameters and statistics obtained for drug release profiles of RG 755 SE systems at 10%, 20%, 30% load fitted to equation 3.19.

	10% load	20% load	30% load
k_r ($h^{-0.5}$) x 10^5	410 ± 39	241 ± 0.57	225 ± 0.50
Fd_∞	0.48 ± 0.020	0.85 ± 0.0096	0.93 ± 0.0134
k (h^{-1})	0.0117± 0.0028	0.0269 ± 0.0248	0.0158 ± 0.0266
t_{max} (h)	1167 ± 27	1572 ± 26	1597 ± 104
r^2	0.9804	0.9958	0.9938
MSC	3.21	5.1	4.48

Comparison of the parameters and statistics listed in tables 8.7 and 8.8 indicates that drug release at the 10% load is better described by first-order than by square root of time kinetics.

The predominance of a particular mechanism determining the initial release of AMOX-H from RG 755 SE discs is possibly related to the extent to which the drug particles are interconnected in the matrix. At the lower loading, it is expected that the particles are isolated, the initial release primarily being determined by rapid dissolution of surface drug. With increasing drug content, the particles are closer to each or may be interconnected. Dissolution of interconnected particles favors the ingress of water to the inner layers of the matrix promoting further drug release. In the terminology of Bonny and Leuenberger (1991) this is referred to as percolation. When the drug load is at or above a *critical* loading, the dissolution kinetics are in agreement with the square root of time law, such as for the 20% and 30% systems.

The three-term model, equation 3.20, was also examined. However, the results did not improve compared to the two-term equations.

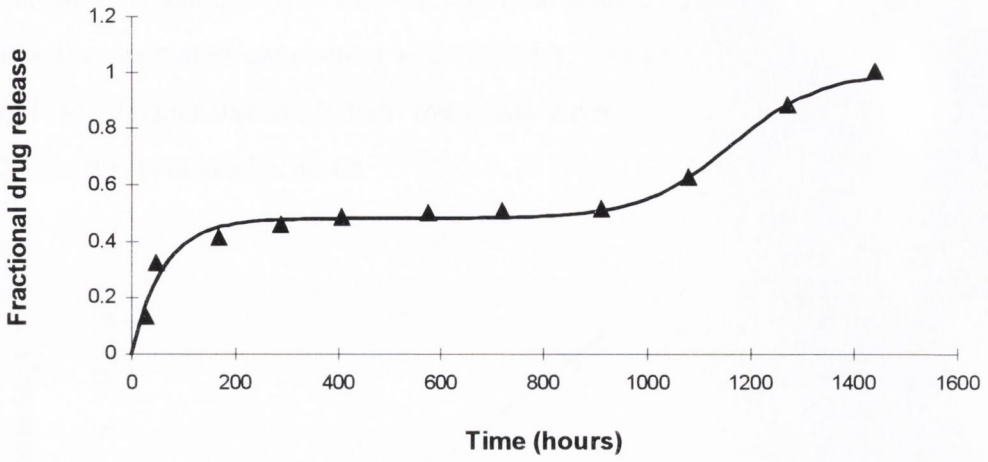

Figure 8.11. Drug release profile of RG 755 SE discs at 10% loading fitted to equation 3.14, which describes first-order kinetics followed by degradation control.

Table 8.9. Parameters and statistics obtained for RG 755 SE systems at 10% loading fitted to equation 3.14.

Fb_∞	0.48 ± 0.017
k_b (h^{-1})	0.016 ± 0.0027
k (h^{-1})	0.0115 ± 0.0024
t_{max}(h)	1165 ± 23
r^2	0.9850
MSC	3.48

Degradation of the drug contained in highly loaded systems (40% to 60%) was relatively low. This was apparent during observation of the HPLC chromatograms obtained with samples from the release medium, which were therefore not analysed by UV spectroscopy. The drug release profiles that will be discussed in the rest of the current section correspond to *intact* Amoxycillin.

RG 755 SE discs containing 40%, 50% and 60% drug load appeared to release all the drug prior to commencement of polymer mass loss. The square root of time plots of 40%, 50% and 60% systems are shown in figure 8.12. Agreement with the model was

good, linear trendlines were obtained by least square regression analysis. Table 8.10 shows the estimated parameters and statistics. The slope increased with increasing drug load. Higher intercepts with the y axis were obtained compared to the 20% and 30% systems previously shown.

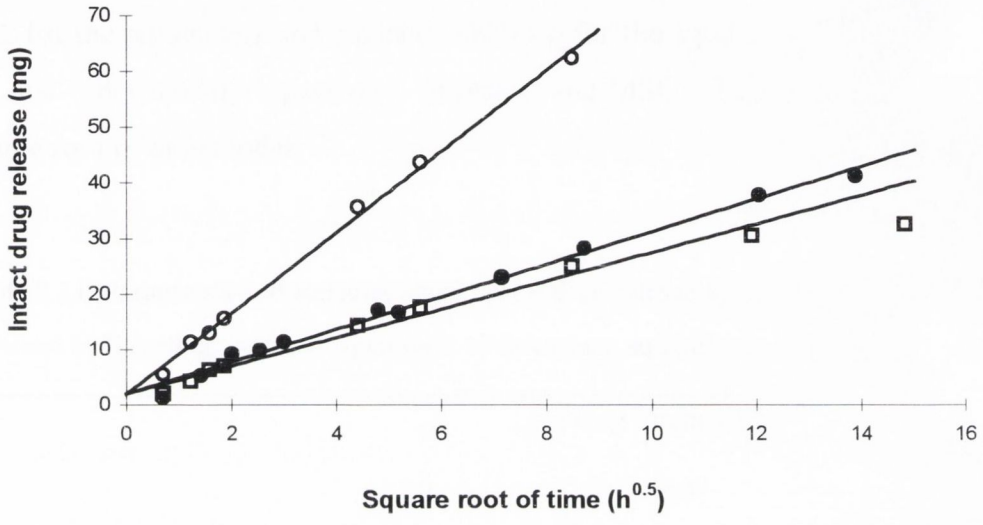

Figure 8.12. Intact drug release versus square root of time plot for RG 755 SE discs at 40% (□), 50% (●) and 60% (○) drug load. Fitted lines were obtained by linear least squares regression.

Table 8.10. Parameters and statistics obtained by linear least square regression analysis for the square root of time plot of drug release data from RG 755 SE discs at 40%, 50%, 60% load.

	Drug loading (%)		
	40	50	60
slope ($mg.h^{-0.5}$)	2.55 ± 0.136	2.94 ± 0.093	7.28 ± 0.18
intercept (mg)	1.88 ± 0.79	1.83 ± 0.65	1.81 ± 0.78
r^2	0.9831	0.9909	0.9969
MSC	3.58	4.35	5.21

The fractional drug release data of 40%, 50% and 60% systems was then fitted to equation 3.10, describing square root of time kinetics with the inclusion of a shape factor. The exponential model, equation 3.15, was also examined. Figure 8.13 shows the results obtained with both models for these systems. All the drug was released within 150-500 hours, depending on the drug load. As expected from the square root of time plots, the data was in better agreement with equation 3.10. Tables 8.11 and 8.12 list the parameters and statistics obtained for the square root of time model and the first-order model, respectively. Higher r^2 and MSC values were obtained with the square root of time model.

Table 8.11. Parameters and statistics obtained for drug release from RG 755 SE discs at 40%, 50% and 60% loading, fitted to equation 3.10 describing square root of time kinetics.

	Drug loading (%)		
	40	50	60
k_r ($h^{-0.5}$) x 10^4	39 ± 2	38 ± 0.7	71 ± 0.6
r^2	0.9743	0.9935	0.9991
MSC	3.53	4.92	6.78

Table 8.12. Parameters and statistics obtained for drug release from RG 755 SE discs at 40%, 50% and 60% loading, fitted to equation 3.15 describing first-order kinetics.

	Drug loading (%)		
	40	50	60
F_b	0.93 ± 0.028	0.96 ± 0.032	0.98 ± 0.067
k_b (h^{-1})	0.016 ± 0.003	0.015 ± 0.002	0.045 ± 0.0096
r^2	0.9612	0.9623	0.9560
MSC	2.98	3.03	2.63

(I)

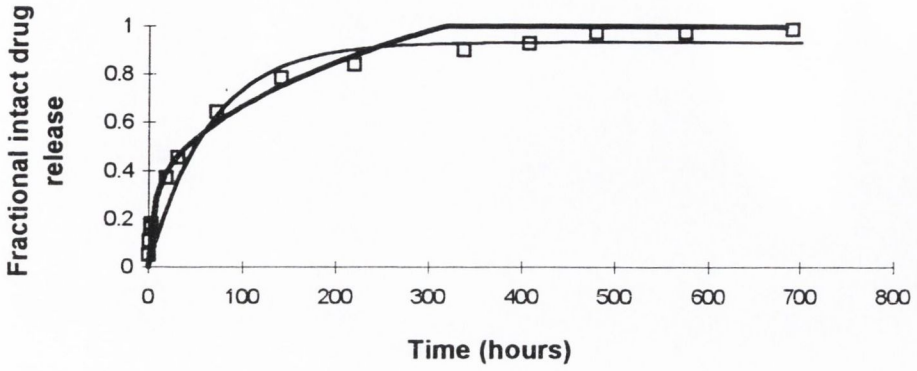

(II)

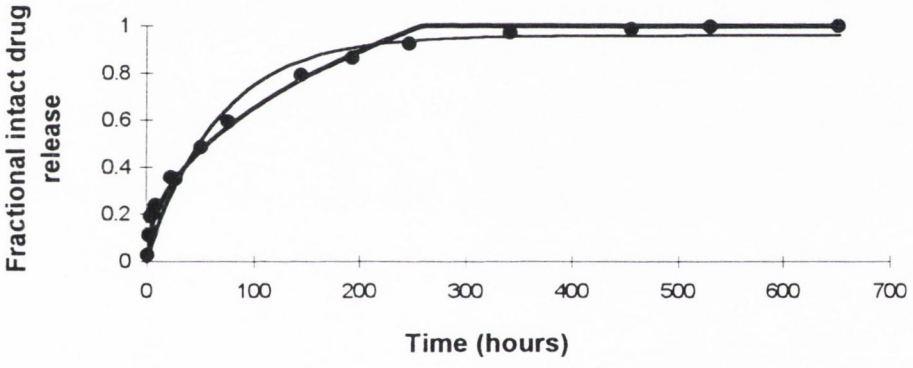

(III)

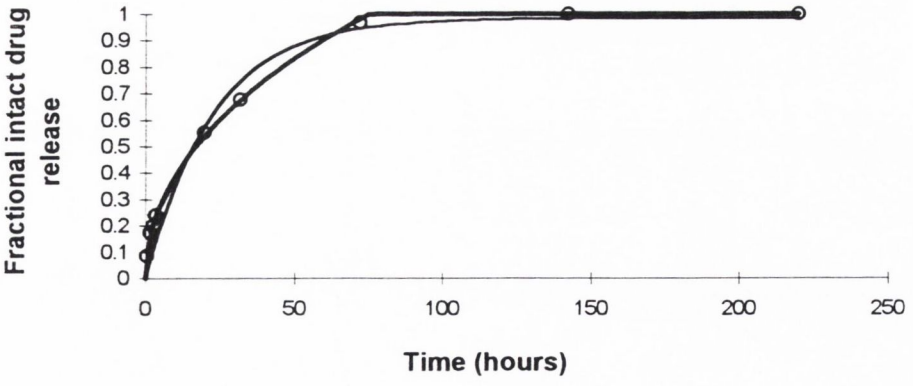

Figure 8.13. Fractional intact drug release profiles of RG 755 SE discs at 40% (I), 50% (II) and 60% (III) load fitted to equations 3.10 (heavier line) and 3.14.

By 1000 hours of release studies, 40% drug loaded discs had a yellowish colour. This suggested that drug was still entrapped. Therefore, one disc from each the 40% and the 60% systems was monitored in the release buffer to 4000 hours (5.5 months). The dissolution medium continued to be analyzed and replaced at regular intervals. At approximately 2000 hours, a small peak matching that of AMOX-H was detected by HPLC analysis, at both the 40% and 60% loads. When the discs were examined at 2400 hours the 40% drug loaded system no longer showed a yellow coloration and further drug release was not detected; both discs were very thin and appeared to be fragil. Subsequently, both discs broke into pieces while replacing the buffer at the next time point (2550 hours). The pieces continued to be monitored until 4000 hours, at which time some irrecoverable pieces from the original discs were still left.

8.3.3. **RG 755 MM versus RG 755 SE discs**

A comparison of the drug release profiles obtained with RG 755 MM and RG 755 SE at 20% and 30% drug load is shown in figure 8.14. For clarity, the simulated profiles are used. There is very little contribution from a degradation phase in any of these systems. The initial release was faster in MM systems, the proportion of drug released in this phase increasing in rank order with the load, for both preparative methods. Comparable t_{max} estimates were obtained for MM and SE discs, the degradation rate constant, k, being greater for the processed systems.

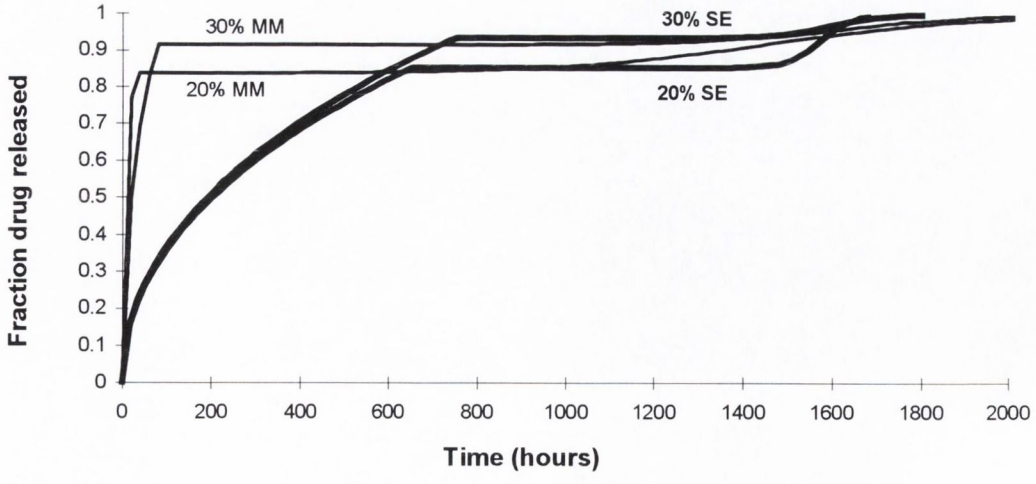

Figure 8.14. Comparison of simulated drug release profiles from RG 755 SE systems (heavier line) at 20% and 30% drug loading versus RG 755 MM systems of equivalent load.

8.3.4. **RG 503 SE versus RG 755 SE**

Drug release profiles of 10%, 20% 30% systems are compared in figure 8.15 to the corresponding profiles previously obtained with RG 503. The overall release time is approximately 50% shorter for RG 503 than for RG 755 SE discs. A greater proportion of drug released by polymer degradation control was observed with RG 503, as expected from the compositional and molecular weight differences between these two copolymers. Within each system, onset of the degradation phase appears to be prolonged at the higher drug loadings.

In the initial phase, first-order kinetics appear to prevail in RG 503 compared to RG 755. The latter showed better agreement with square root of time kinetics, particularly with increased drug loading.

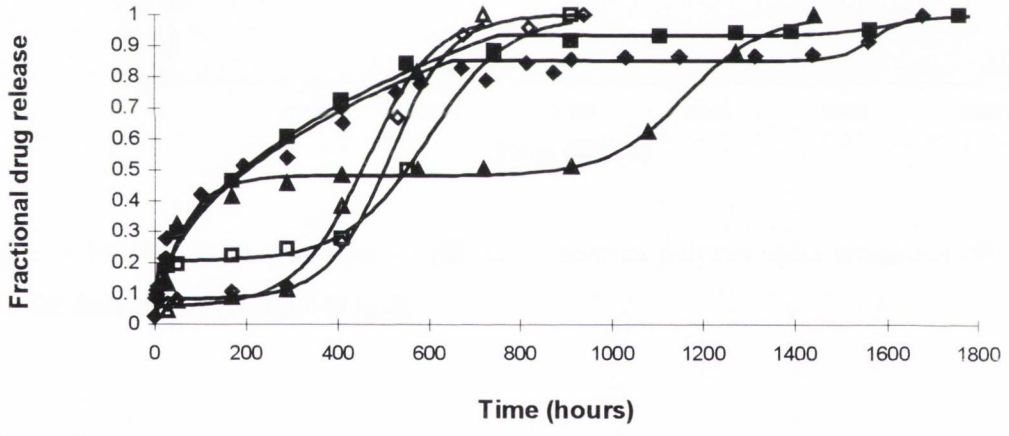

Figure 8.15. Drug release profiles of RG 503 SE discs at 10% (△), 20% (◇) and 30% (□) drug load versus equivalent profiles of RG 755 SE discs at 10% (▲), 20% (◆) and 30% (■) drug load.

8.3.5. **Polymer mass loss studies with RG 755 SE discs: drug-free and drug loaded**

Figure 8.16 illustrates the polymer loss profiles and the drug release profiles obtained for RG 755 SE discs at 20% loading. The intersection of the two curves occurred at the 0.9 fraction indicating that most of the drug was released when only 10% of the

polymer was dissolved. In addition, this appeared to indicate that the small final phase of drug release mirrored the polymer mass loss profile.

As will be shown in Chapter 9, GPC performed on 20% drug loaded discs after 1050 hours of release studies showed considerable reduction of the polymer M_w. Polymer degradation dependent drug release, however, was not evidenced until circa 1500 hours.

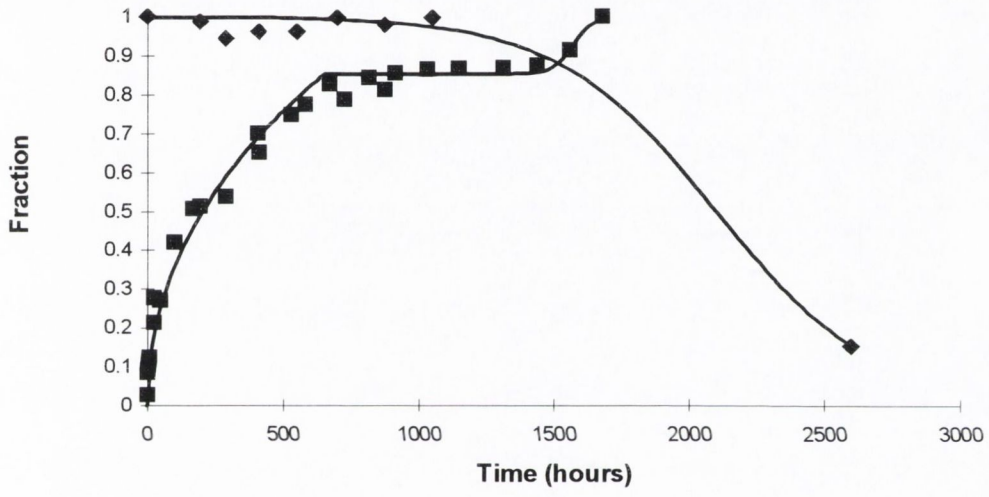

Figure 8.16. Fractional drug released (■) and fractional polymer mass remaining (◆) in RG 755 SE discs at 20% AMOX-H load.

Figure 8.17 compares polymer mass loss for drug-free and 20% drug loaded SE discs fitted to equation 3.13. Mass loss from drug-free discs showed a lag phase of approximately 800 hours, t_{maxP} occurring at approximately 1050 hours. Related time points were chosen for 20% drug loaded discs. Interestingly, the effect of the drug on the polymer degradation kinetics was greater than that expected from the results with RG 503 and RG 504. By 1100 hours, time taken for a 75% mass loss for drug-free discs, no apparent polymer degradation was evident in the drug loaded systems. It was then decided to continue observation of the remaining discs until complete dissolution occurred. The discs were monitored for more than 2000 hours. Complete dissolution did not occur during the time of the study.

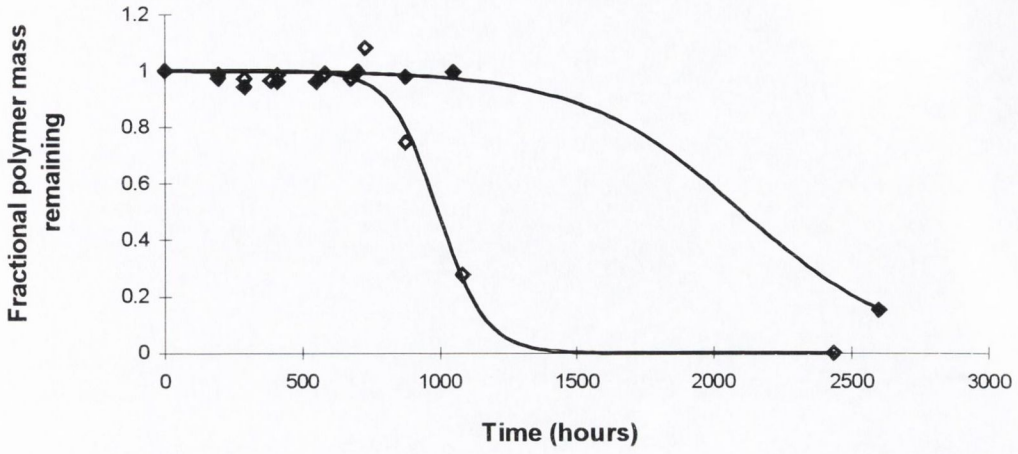

Figure 8.17. Polymer mass remaining versus time for 20% drug loaded (◆) and drug-free RG 755 SE discs (◇).

Table 8.13 lists the parameters and statistics obtained for the mass loss profiles of RG 755 SE drug-free and 20% drug loaded discs fitted to equation 3.13. The estimated value of the degradation constant k_P is lower for the drug-loaded discs, with greater t_{maxP} values for these discs. In the previous section it was found that discs maintained in the dissolution medium for a prolonged period of time, 40% and 60% systems, released a small amount of drug at approximately 2300 hours. This time is in the same order of the t_{maxP} estimated for the 20% systems.

Table 8.13. Parameters and statistics estimated for RG 755 SE drug-free and 20% drug loaded discs fitted to equation 3.13.

	drug-free discs	20% drug loaded discs
k_P (h^{-1})	0.0116 ± 0.0017	0.0034 ± 0.00057
t_{max} (h)	993 ± 16	2099 ± 94
r^2	0.9824	0.9899
MSC	3.68	4.15

It would be expected that after all the drug was apparently released from a system (1650 hours for 20% AMOX-H discs), the kinetics of polymer degradation should be restored to those of the native polymer (drug-free discs). Interestingly, the simulated profile (figure 8.17) suggests that the degradation rate of drug loaded discs continued to be slower even after all the drug was apparently released from the discs.

Figure 8.18 is a photograph of the 20% systems, showing the appearance of the discs before drug release studies and after 727 and 874 hours of the studies. Size changes were not apparent in the photograph.

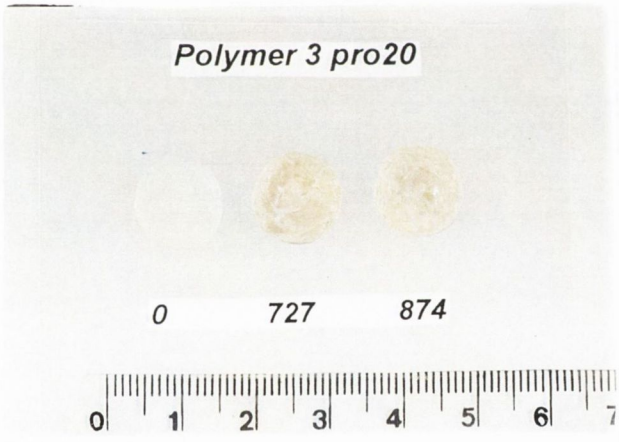

Figure 8.18. Photograph of 20% drug-loaded RG 755 SE discs before release studies (time zero) and after 727 and 874 hours of drug release studies.

Figure 8.19 shows the polymer loss in drug-free discs compared to that obtained with 40% and 60% AMOX-H loaded discs. Completion of drug release took place in approximately 600 and 150 hours at 40% and 60% loading respectively, as shown in the previous section. According to the degradation kinetics of drug-free discs (◆) 80% of the initial polymer mass should be dissolved by circa 1100 hours. Notwithstanding this solid discs were still present at this time, both at 40% and 60% loading, while the diameter of the discs was approximately 10 mm (measured at 1411 hours). The appearance of drug-free discs after 900 hours of the study, was that of a semi-solid system which stuck onto paper upon removal from the dissolution buffer. Table 8.14 lists the diameters and heights recorded for 40% and 60% drug loaded systems. There was a decrease in the diameter of the discs with increasing dissolution time. At 1723 hours, it appears that the height of the discs has slightly increased.

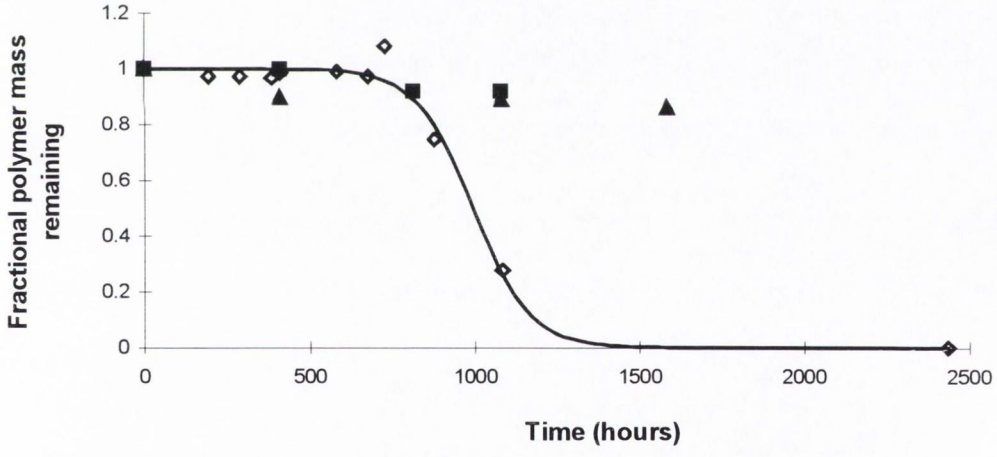

Figure 8.19. Fractional polymer remaining in RG 755 SE drug-free (◆) and 40% (■), 60% (▲) drug loaded discs.

Table 8.14. Diameters and heights of RG 755 SE discs at 40% and 60% drug load measured during drug release studies. (n.r. = not recorded)

Time (hours)	40%		60%	
	diameter (mm)	height (mm)	diameter (mm)	height (mm)
0	13.0	0.75	13.0	0.80
1411	10.3	n.r.	9.3-9.5	n.r.
1723	9.4	1.4	8.6	1.0

The results from 20% AMOX-H RG 755 SE discs indicated that some of the drug was physically trapped in the polymeric matrix and was not released until bulk mass loss occurs. At the higher drug loading, however, a distinct degradation controlled release phase was not observed since completion of drug release occurred prior to onset of mass loss.

8.4. R 203 SYSTEMS PREPARED BY SOLVENT EVAPORATION (SE SYSTEMS)

As pointed out previously, R 203 is not a copolymer but is a homopolymer composed of D,L-lactic acid units. The investigation of R 203 systems concentrated on solvent-cast discs.

8.4.1. Physicochemical and morphological characteristics of R 203 SE discs

R 203 discs were prepared by the solvent-cast technique described in Chapter 5. The characterization of these systems was undertaken by XRD and DSC methodologies.

HPLC analysis of AMOX-H was performed on freshly prepared discs, the results indicating that the drug was chemically intact upon filmcasting.

Figure 8.20 shows the X-ray diffractograms of R 203 powder (a), R 203 MM discs at 20% load (b), R 203 SE discs at 20% load (c) and 40% load (d) and AMOX-H powder (e). The scans obtained indicate that crystalline AMOX-H is present in SE discs prepared with R 203.

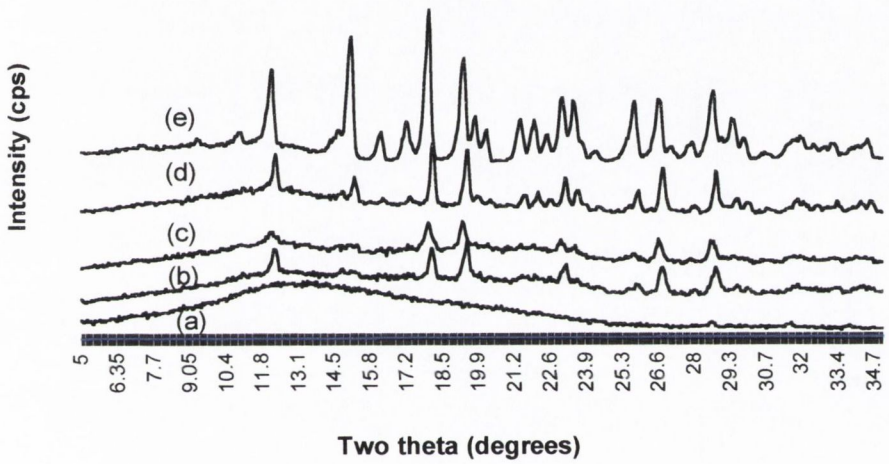

Figure 8.20. X-ray diffractogram of R 203 powder (a), R 203 MM discs at 20% loading (b), R 203 SE discs at 20% (c), 40% (d) loading and AMOX-H powder (e).

As occurred with the previous polymers, the T_g values obtained for the first DSC heating scans of R 203 discs were variable and below the glass transition of the polymer powder. Table 8.15 lists the values of T_g obtained for the second heating scans of R 203 systems, where the discs displayed glass transition temperatures comparable to that of the raw material, both in the presence and absence of the drug, as previously described for RG 503, RG 504 and RG 755 systems.

Table 8.15. Glass transition temperatures determined by DSC for the second heating scan of R 203 systems.

R 203 System	T_g (°C)
polymer powder	46.6
drug-free SE	47.0
20% AMOX-H SE	45.4
40% AMOX-H SE	46.6

8.4.2. **Drug release from R 203 SE discs**

In a recent work, Gallagher and Corrigan (1998) showed that R 203 SE discs loaded with 20% levamisole exhibited t_{max} at 320 hours. In contrast, R 203 SE discs containing an equivalent load of AMOX-H continued to release drug far beyond this time. Figure 8.21 shows the drug release profiles of 20% and 40% drug loaded discs. There is an initial fast release in the first two days followed by a period in which drug release appears to have ceased. HPLC analysis of a 20% loaded disc withdrawn from the experiment at 1100 hours showed the presence of entrapped drug. A 20% loaded disc left in the release experiment displayed an increase in the rate of drug release after 2000 hours. It was not until after 3000 hours that an increase in the rate of drug release was observed at the higher drug loading (40% AMOX-H load).

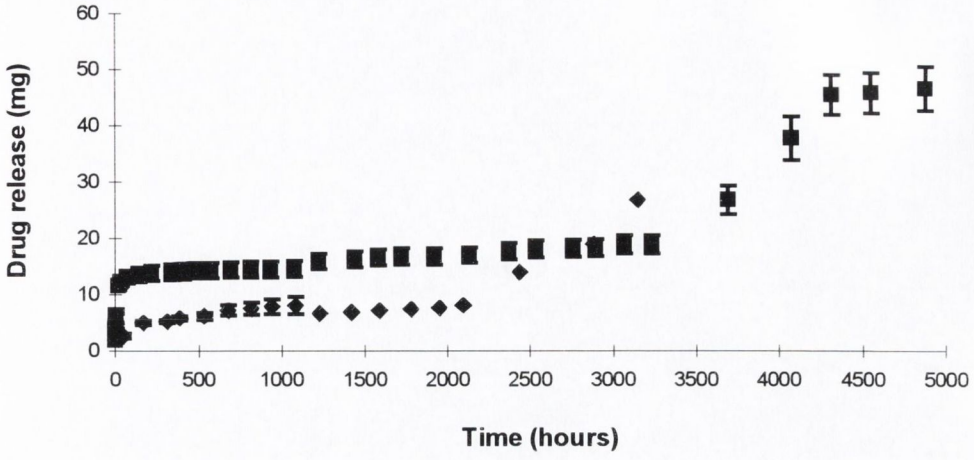

Figure 8.21. Drug release profiles from R 203 SE discs containing 20% (◆) and 40% (■) AMOX-H; error bars, where applicable, indicate the range of the data.

Figure 8.22 shows the fractional drug release profiles obtained for R 203 SE systems. The profiles are bi-phasic, consistent with polymer degradation dependent drug release. Onset of degradation control appears to depend upon the initial drug load, with increased duration of drug release at the higher loading. The fraction of drug released in the first two days increased with the initial loading.

At the higher drug load a better fit was obtained with equation 3.19 than 3.14, with parameters and statistics listed in table 8.16.

It was the three-term equation (equation 3.20) which resulted in the best fit, at 20% and 40% load. The fitting to this model is shown in table 8.17. The goodness of fit was greater at the higher drug load. The values of Fb_∞ and k_b were also greater for this system, consistent with a higher initial burst upon increase of the drug load. Fd_∞ and k_r were similar for both loadings. The value of the degradation parameter t_{max} was greater at the higher load as was the value of the rate constant k. The latter, however, was of a similar order of magnitude for both loadings.

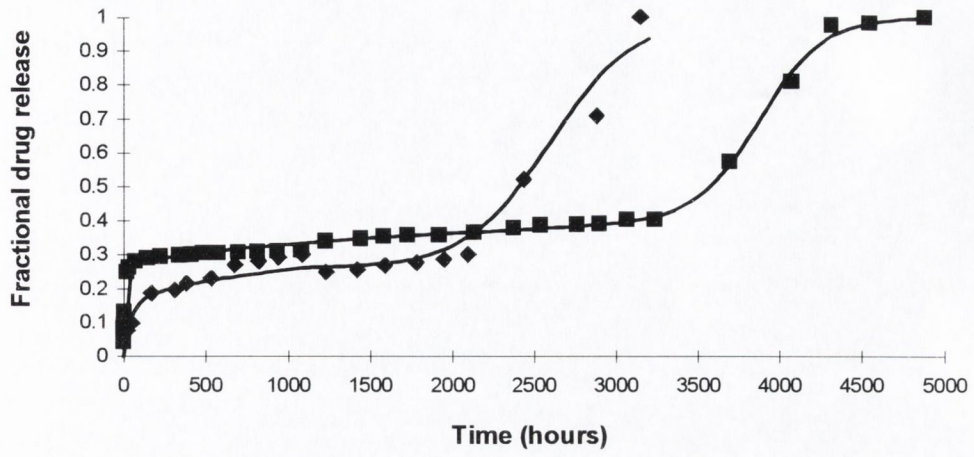

Figure 8.22. Drug release profiles of 20% (◆) and 40% (■) AMOX-H R 203 SE systems fitted to the three-term model, equation 3.20.

Table 8.16. Parameters and statistics obtained for drug release profiles of R 203 SE discs at 40% load, fitted to the two-term mathermatical model described by equation 3.19.

Fd_∞	0.33 ± 0.0073
k_r ($h^{-0.5}$)	0.0097 ± 0.0009
t_{max} (h)	3784 ± 38
k (h^{-1})	0.0037 ± 0.0004
r^2	0.9824
MSC	3.81

Table 8.17. Parameters and statistics obtained for drug release profiles of R 203 SE discs at 20% and 40% load, fitted to the three-term mathematical model described by equation 3.20.

	20%	40%
Fb_∞	0.13 ± 0.062	0.25 ± 0.0059
k_b (h^{-1})	0.021 ± 0.020	0.236 ± 0.022
Fd_∞	0.13 ± 0.065	0.16 ± 0.068
k_r ($h^{-0..5}$)	0.0019 ± 0.0005	0.0010 ± 0.0005
t_{max} (h)	2597 ± 46	3886 ± 53
k (h^{-1})	0.0039 ± 0.0005	0.0052 ± 0.00050
r^2	0.9812	0.9976
MSC	3.31	5.69

8.4.3. **Polymer mass loss studies with R 203 SE discs: drug-free and drug loaded**

Figure 8.23 shows the polymer mass loss profile of drug-free discs versus 20% drug loaded discs, fitted to equation 3.13. The mechanism of degradation appeared to differ in the presence and absence of the drug. After 300 hours of dissolution drug-free discs began to change their original cylindrical shape to a more spherical shape suggesting considerable swelling. Examination of the interiors revealed an inner liquid phase similar to the findings reported by Li et al. (1990) for PLA compacts. On examination of the discs at later times, a hollow interior was observed upon fracture of discs. Similar heterogeneous degradation, with differential mass loss between the surface and the center of the device was recently reported by Gallagher and Corrigan (1998) for PLA drug-free discs.

At 1100 hours there was evidence of mass loss from the drug-free discs (figure 8.23). In contrast, systems containing 20% drug load did not exhibit polymer loss at that stage. Solid material from the drug loaded discs was still present after 3200 hours of

dissolution. Table 8.18 lists the estimated parameters obtained with equation 3.13. There was an increase in the value of t_{maxP} in the presence of the drug. The value of the degradation rate constant k_P decreased from the drug-free to the 20% drug loaded system.

Mass loss profiles for 40% drug loaded discs were not performed. However, during drug release studies it was noticed that after circa 5000 hours of dissolution solid discs were still present.

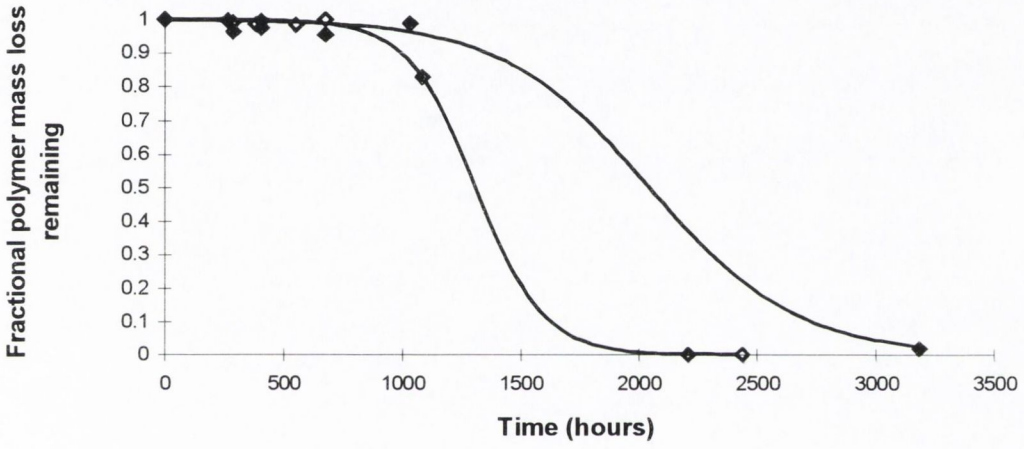

Figure 8.23. Fractional polymer remaining versus time plot for drug-free (◇) and 20% drug loaded (◆) R 203 SE discs.

Table 8.18. Parameters and statistics obtained for polymer loss profiles of drug-free and 20% drug loaded R 203 SE discs fitted to equation 3.13.

	drug-free	20% loaded
t_{maxP} (h)	1310 ± 39	2042 ± 211
k_P (h^{-1})	0.0069 ± 0.0012	0.0032 ± 0.00062
r^2	0.9997	0.9948
MSC	7.73	4.70

Gallagher and Corrigan (1998) estimated for drug-free R 203 SE discs that t_{max} was equal to 1353 hours and the degradation rate constant k was 0.00391 h^{-1}. In the terminology of the current work, such parameters correspond to t_{maxP} and k_P. The values reported are comparable to the results of table 8.18.

8.5. **CONCLUSIONS**

The initial release phase from RG 755 and R 203 systems appears to be controlled by dissolution and diffusion mechanisms, followed by polymer degradation in the final phase. The magnitude of each phase depends on processing and loading.

Drug release from RG 755 SE systems with AMOX-H loadings up to 30% showed bi-phasic release profiles, with predominance of square root of time kinetics followed by degradation dependent drug release. In contrast, at higher drug loadings (>40%) drug release was governed solely by dissolution and diffusion processes, with all the drug being released prior to commencement of polymer degradation.

Release profiles showed a prolongation of the onset of polymer degradation in the presence of the drug. Those systems releasing all the drug prior to onset of degradation (highly loaded RG 755 systems) also appeared to degrade over a longer period of time, as discs were still present beyond the dissolution time of the pure polymer discs.

Drug release profiles of R 203 systems indicated that the onset of degradation control was dependent on the initial drug load.

CHAPTER 9. STABILITY ASPECTS OF PLA AND PLGA FORMULATIONS CONTAINING AMOXYCILLIN

9.1. INTRODUCTION

Quantification of intact AMOX released from SE discs will be performed in detail in this chapter. Assessment of the chemical integrity of AMOX during drug release studies in Chapter 7 suggested that the stability of the drug depended upon the degradation of the polymer. Therefore, GPC and NMR studies will be undertaken to further explore stability aspects/interactions of the formulation components.

A recent review of biodegradable polymers by Göpferich (1996) stated that surface erosion does not typically occur with poly-alpha-hydroxy-aliphatic esters. Interestingly, this mechanism of degradation results in a decrease of the matrix dimensions such as that observed in the photographs shown in Chapter 7. At the end of this chapter, a surface erosion model will be used to fit the data.

9.2. STABILITY OF AMOXYCILLIN IN PLA/PLGA FORMULATIONS

9.2.1. Release profiles of intact Amoxycillin from RG 503, RG 504, RG 755 and R 203 SE discs containing 20% drug load

The release profiles of intact AMOX expressed as amount released (mg) versus time are shown in figure 9.1 for RG 503, RG 504, RG 755, R 203 SE discs at 20% drug loading. Discs prepared with RG 504 and RG 755 delivered greater quantity of intact AMOX than the equivalent systems formulated with the lower molecular weight polymers, RG 503 and R 203. From an original load of circa 24 mg, the overall release of intact drug reached approximately 12 mg for RG 504 and RG 755 systems and less than 5mg in the case of RG 503 and R 203 systems. Analysis of drug released in the

first day showed absence of degradation products. RG 504 and RG 755 delivered between 3-4 mg of intact drug in the first day. RG 503 and R 203 delivered between 1-2 mg in that time. The release of intact drug from the 20% loaded systems ceased after approximately 700 hours in all the cases.

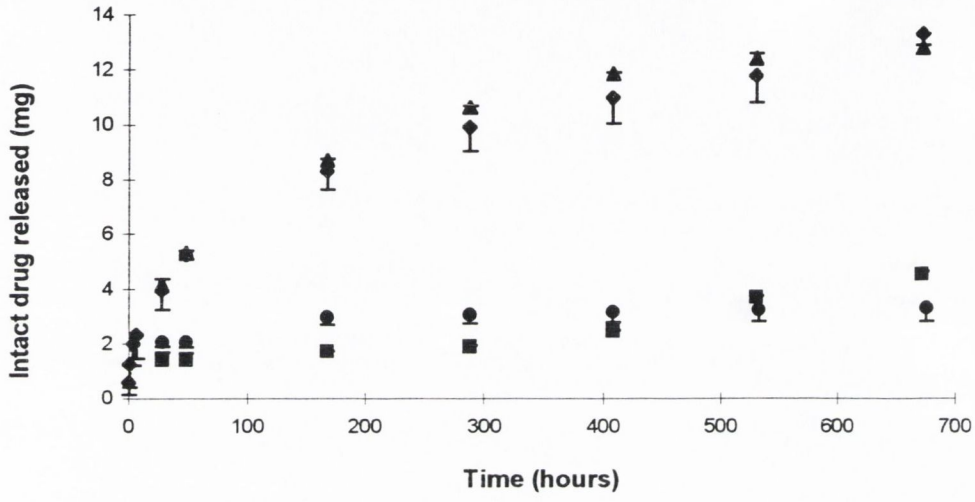

Figure 9.1. Drug release profiles (mg) of RG 503 (■), RG 504 (◆), RG 755 (▲) and R 203 (●) SE discs at 20% drug loading. Error bars show the range of the data.

Figure 9.2 shows the plot of fraction drug released versus time (I), for the discs of figure 9.1, and the equivalent simulations of total drug released (II). The latter were obtained from the data previously presented in Chapters 7 and 8. Similar release models to those previously used to fit the total drug release data were employed to fit the profiles of intact drug, as per the legend in the figure.

Between 70-80% of the overall intact AMOX released was delivered in the first 300 hours for RG 504, RG 755 (plot I). The data from RG 504 and RG 755 was described by a square root of time model (equation 3.10). Approximately 40% of the overall intact AMOX delivery in RG 503 systems occurred over the first 300 hours, the remaining 60% being delivered over the following 400 hours.

Degradation dependent release of intact AMOX was exhibited by the RG 503 formulation, which showed a bi-phasic profile consistent with equation 3.14. The relatively large proportion of *intact* drug available for release in the second phase of

RG 503 SE discs (plot I) is in agreement with the large fraction of *total* drug released in the second phase of this formulation (plot II). However, the R 203 formulation, which released a large fraction of the *total* drug delivered by a polymer degradation mechanism (plot II), showed lack of a degradation phase in the plot corresponding to *intact* drug (plot I).

I

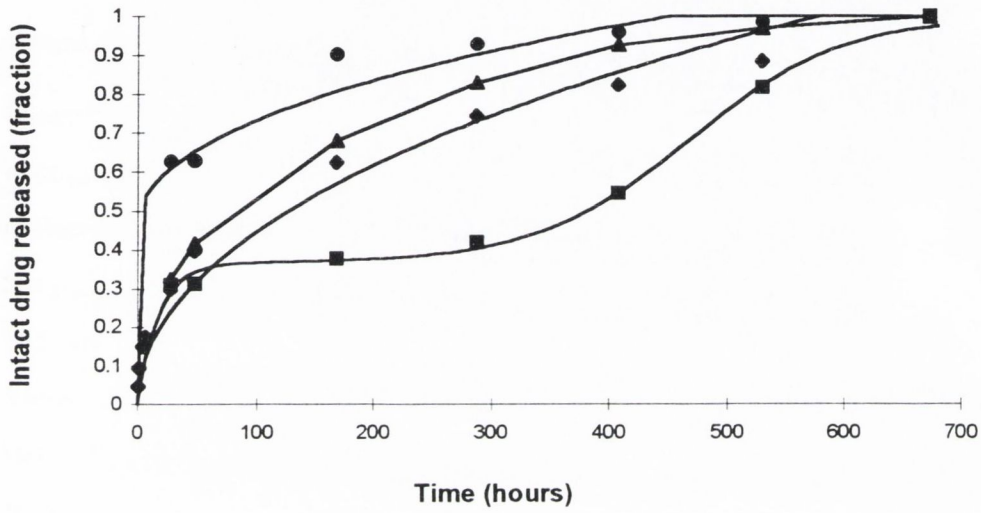

II

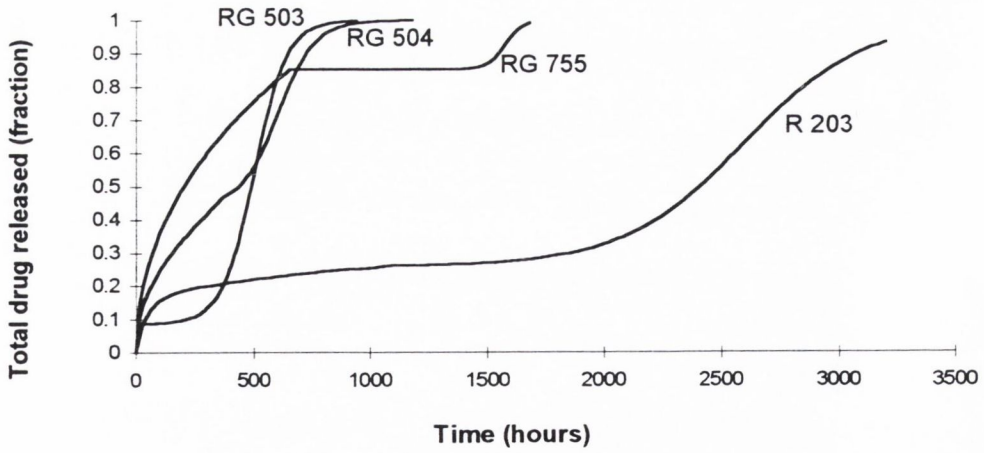

Figure 9.2. Release profiles of (I) intact Amoxycillin from 20% drug loaded SE discs prepared with RG 503 (■) fitted to equation 3.14, RG 504 (◆) fitted to equation 3.10, RG 755 (▲) fitted to equation 3.10, R 203 (●) fitted to equation 9.1, and (II) simulated data for total drug released obtained with equations 3.14 (RG 503), 3.19 (RG 504, RG 755) and 3.20 (R 203).

There was a greater proportion of AMOX degradation in the formulation prepared with the pure lactide polymer compared to the PLGA formulations. The profile of intact drug for R 203 (figure 9.2, I) was best described by a model accounting for an initial burst followed by a phase of slower release rate:

$$F_{tot} = Fb_{\infty}\left(1-e^{-k_b t}\right)+\left(1-Fb_{\infty}\right)\left(G_1 k_r t^{0.5}-G_2\left(k_r t^{0.5}\right)^2\right)+\left(G_3\left(k_r t^{0.5}\right)^3\right) \qquad \text{equation 9.1}$$

where the symbols have the same meaning as in equations 3.10 and 3.15.

Quantification of the fraction of intact drug released from each system is shown in the histogram of figure 9.3. Recovery of intact drug decreased in rank order with the molecular weight of the polymer used in the formulation, however the compositions of the polymers varied potentially contributing to the observed effect on the drug. RG 755 showed similar intact drug recovery to RG 504. The recovery of intact Amoxycillin from the formulation with RG 503 followed to that of RG 755 and RG 504. The formulation prepared with R 203 showed the lowest recovery of intact drug.

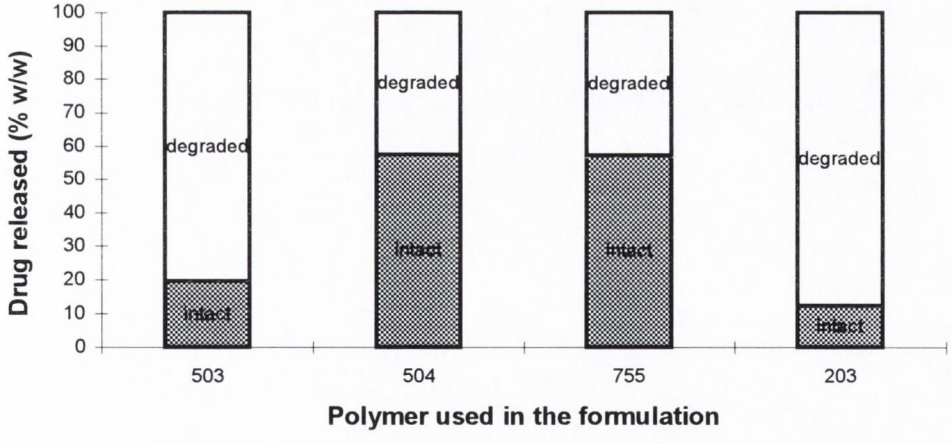

Figure 9.3. Histogram showing the fraction of intact drug released relative to the total drug released from RG 503, RG 504, RG 755, R 203 SE systems containing 20% drug loading.

The next sections concentrate on the quantification of intact drug for drug loadings other than 20%.

9.2.2. **Quantification of the amount of intact Amoxycillin released from RG 503 SE systems containing between 10% and 30% drug loading**

Figure 9.4 compares the amount of intact drug released (mg) from RG 503 SE discs containing 10% and 30% load. Figure 9.5 shows the fractional drug release profile of intact drug versus total drug. The profiles of total drug were simulated from data previously shown in Chapter 7. Similar to these simulations, the profiles of intact drug showed at least two phases. The data for intact drug was best fitted to equations 3.14 and 3.20, for the 10% and 30% drug loaded systems respectively. The overall release time for intact and total drug was approximately the same.

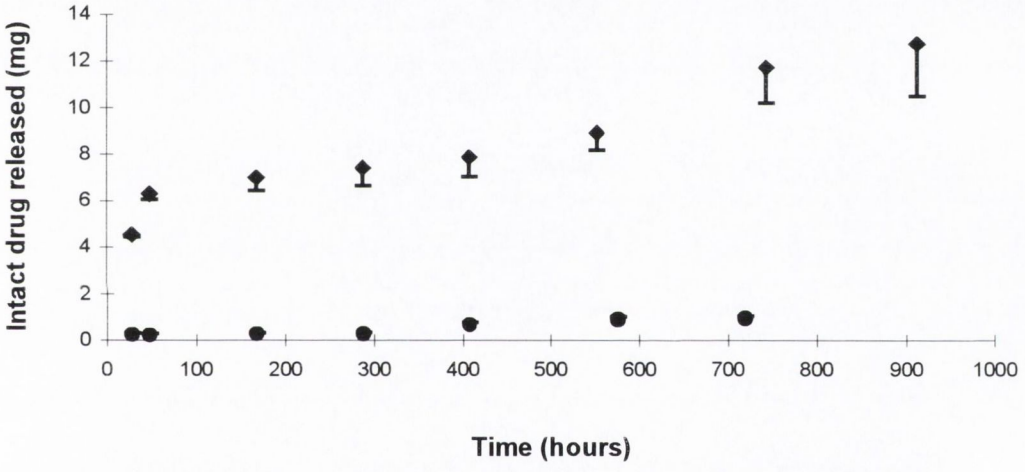

Figure 9.4. Intact Amoxycillin released (mg) from RG 503 SE discs containing 10% (●) and 30% (◆) drug loading. Error bars indicate the standard deviation of the data.

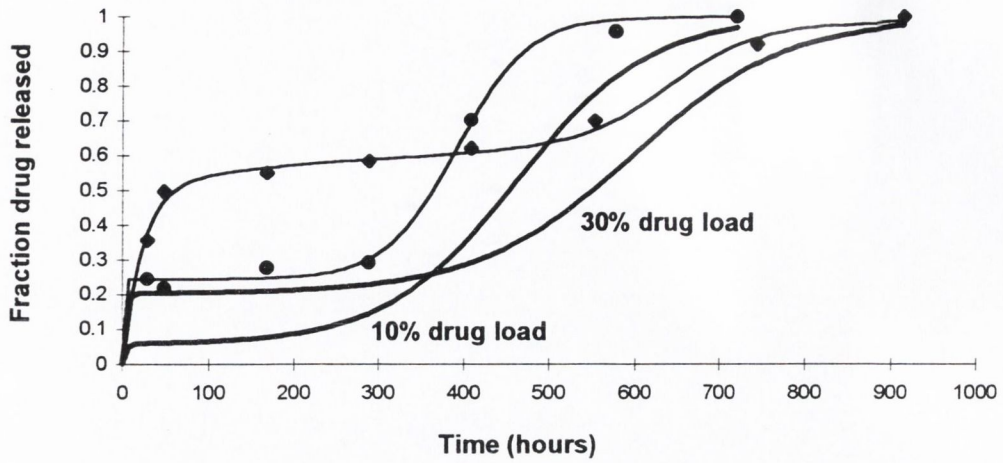

Figure 9.5. Fractional release profiles of *intact* Amoxycillin for RG 503 SE discs containing 10% (●) and 30% (◆) drug loading fitted to equations 3.14 and 3.20, respectively; simulated data (heavier lines) obtained with equation 3.14 for the corresponding *total* drug release profiles.

Figure 9.6 shows the histogram obtained when the % w/w of intact drug recovered from RG 503 SE discs loaded with 10%, 20%, 30% AMOX was plotted relative to the total drug released. The recovery of intact drug increased in rank order with the initial loading in the discs. At the 10% load most of the initial drug remains entrapped in the discs for a long period of time and is only released upon onset of polymer degradation. Drug which is released during polymer degradation is more vulnerable to chemical degradation. As the initial drug load increases there is a larger amount of drug released prior to onset of polymer degradation by dissolution and diffusion mechanisms. The drug released by a non-degradation dependant mechanism is not exposed to the acidifying effect of the polymer sub-units and therefore has a better change of remaining intact. The pH inside eroding PLA and PLGA systems can be as low as 2 (Göpferich, 1996) which may cause accelerated degradation of AMOX (Tsuji et al., 1978). The % w/w of intact drug recovered relative to the total drug released were 9, 20, 39 at 10%, 20%, 30% initial drug loading, respectively.

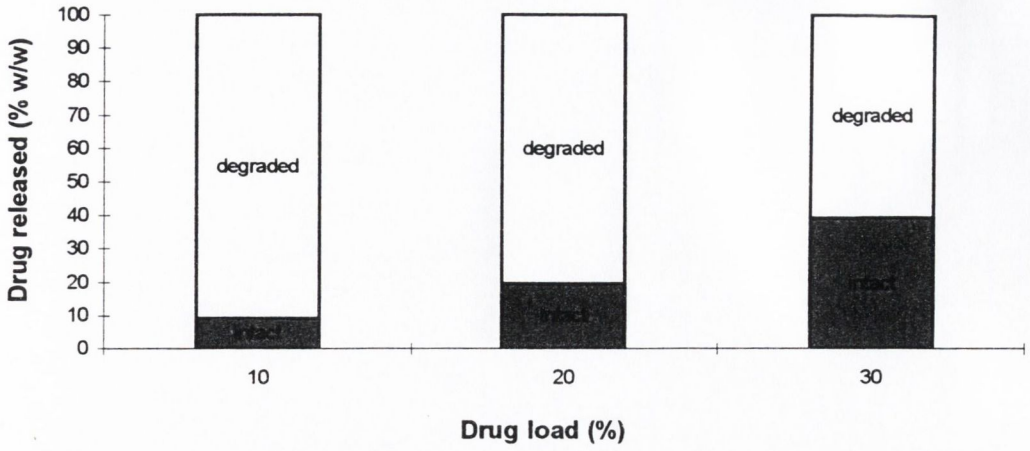

Figure 9.6. Histogram showing the overall % w/w of intact drug released from RG 503 SE discs containing 10%, 20% and 30% Amoxycillin load.

9.2.3. **Quantification of the amount of intact Amoxycillin released from RG 755 SE systems containing between 10% and 30% drug loading**

Figure 9.7 shows the profile for intact drug released (mg) from RG 755 SE discs containing 10% and 30% load. From an initial amount of approximately 12 mg less than 2 mg were recovered at the lower drug loading. Approximately 17 mg were recovered from the initial 30% loading. Release of intact drug ceased circa 100 hours and 700 hours for the 10% and 30% loadings respectively.

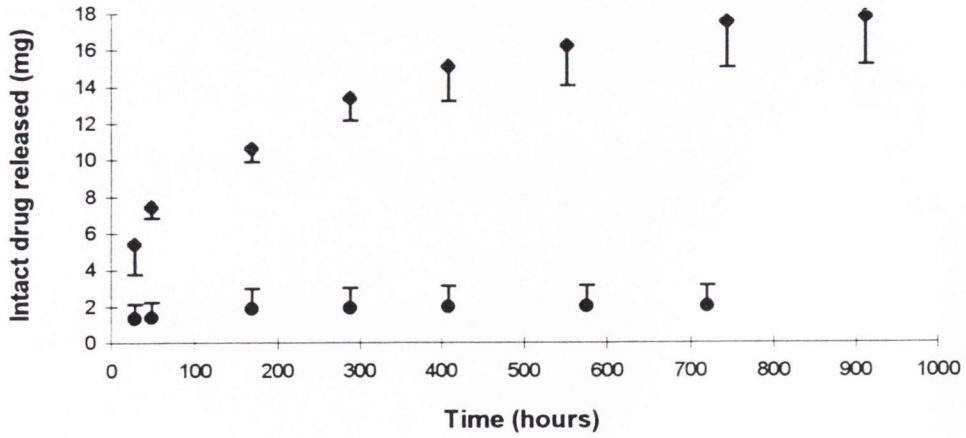

Figure 9.7. Intact Amoxycillin released from RG 755 SE discs at 10% (●) and 30% (◆) drug loading. Error bars indicate the standard deviation of the data.

Figure 9.8 shows the fractional drug release profiles of intact drug versus total drug. The profiles of total drug were simulated by means of equation 3.19 from the fractional drug release data previously shown in Chapter 8. The drug release data corresponding to intact drug was best fitted to equation 9.1.

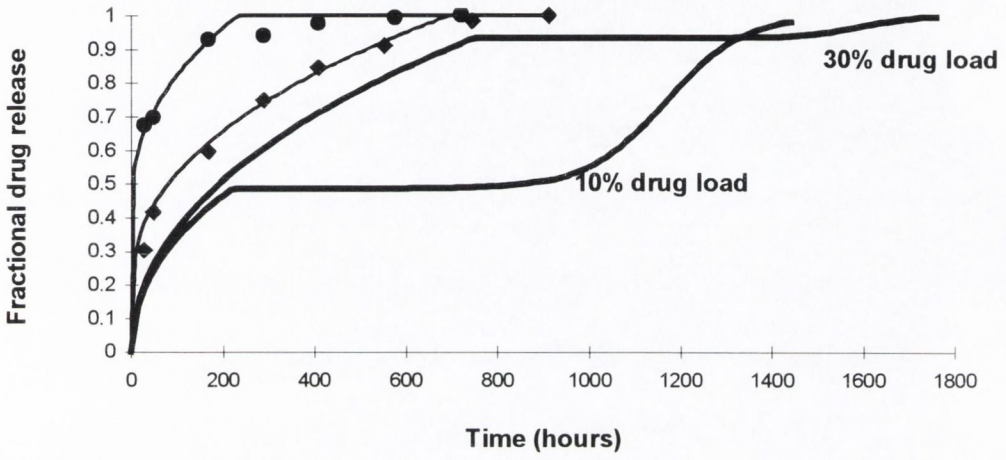

Figure 9.8. Fractional drug release profiles for *intact* AMOX from RG 755 SE discs containing 10% (●), 30% (◆) drug loading fitted to equation 9.1 and simulated data (heavier lines) obtained with equation 3.19 for the corresponding release profiles for *total* drug.

Figure 9.9 shows the histogram obtained when the fraction of intact drug recovered was plotted relative to the total drug released. Similar to RG 503 systems, the recovery of intact drug increased in rank order with the drug load. The % w/w of intact drug relative to the total drug released were 22, 57 and 64 at 10%, 20% and 30% loading, respectively.

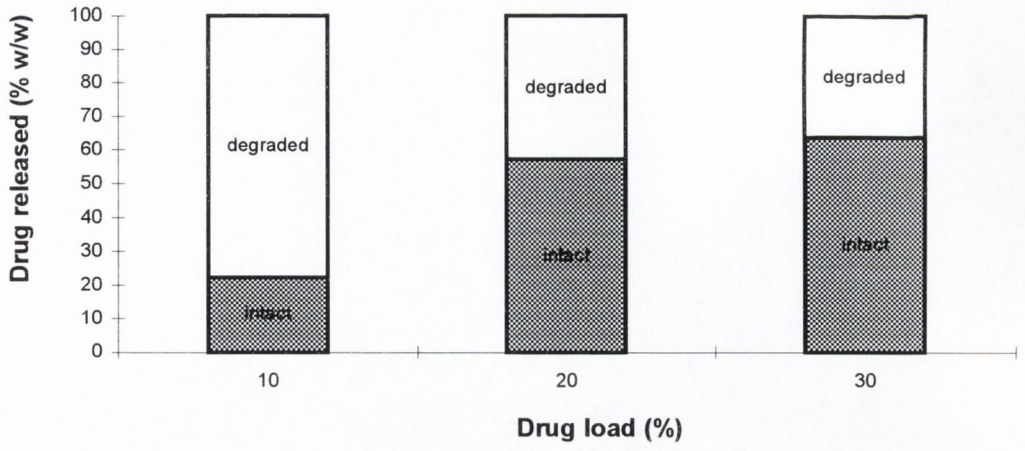

Figure 9.9. Histogram showing the overall % w/w of intact drug released from RG 755 SE discs containing 10%, 20% and 30% Amoxycillin load.

9.2.4. **Comparison of intact drug release profiles of RG 503 and RG 755 SE discs containing between 10% to 30% Amoxycillin load**

Figure 9.10 compares the fractional release profiles of intact drug obtained for RG 503 and RG 755 SE discs at 10% and 30% loading shown in the previous two sections.

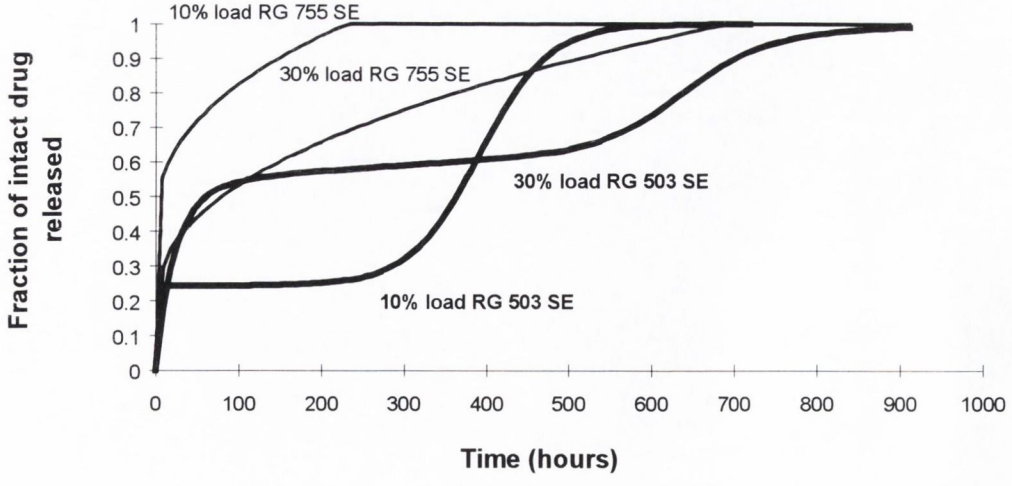

Figure 9.10. Comparison of the fractional drug release profiles obtained for *intact* drug released from RG 503 (heavier lines) and RG 755 SE discs at 10% and 30% drug load.

The profiles of RG 503 are sigmoidal, in agreement with a model which accounts for first-order kinetics followed by degradation control. RG 755 systems showed agreement with square root of time kinetics, without the contribution of degradation dependant drug release.

Figure 9.11 shows a histogram for the % w/w of intact drug recovered from RG 503 and RG 755 SE systems at 10%, 20% and 30% AMOX loading. The results show that the formulation prepared with RG 755 protected a higher fraction of drug compared to RG 503.

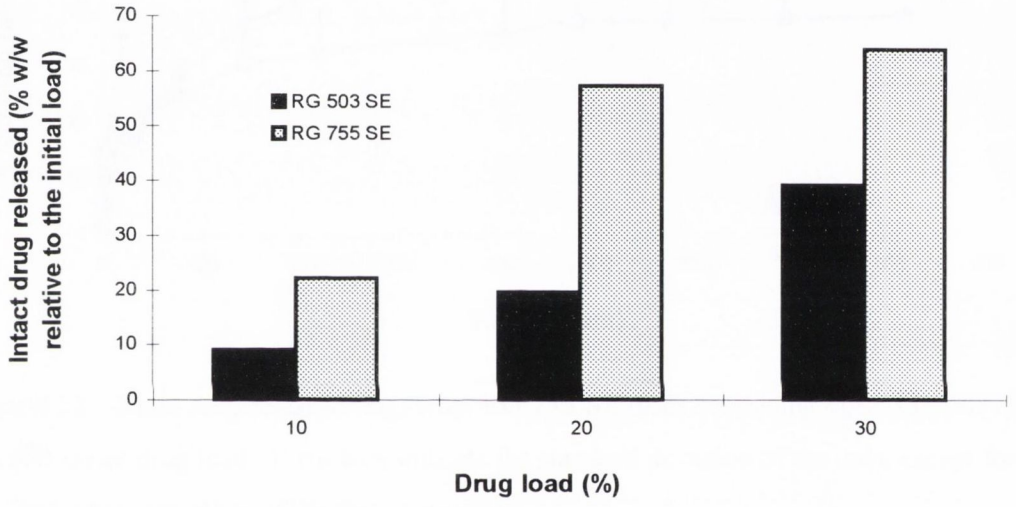

Figure 9.11. Histogram comparing the % w/w of intact drug recovered from RG 503 and RG 755 SE discs at 10%, 20% and 30% drug loading.

9.2.5. **Quantification of the amount of intact Amoxycillin released from RG 755 SE systems containing 40%, 50% and 60% drug loading**

Drug release profiles of RG 755 SE discs prepared at higher drug loadings showed minimal presence of degradation products from AMOX. Therefore, quantification of the drug released from these systems was only performed by HPLC analysis. Figure 9.12 compares the intact drug release profiles of 40%, 50% and 60% drug loaded systems, previously introduced in section 8.3.2. Release was completed in less than 600, 400 and 200 hours at 40%, 50% and 60% loading, respectively. Between 30-40

mg of intact drug are released from the 40% and 50% systems in the first 150 hours. The 60% drug loaded system releases that amount within the first day.

The recovery of intact drug was compared to the initial load of the systems. The resulting % w/w of intact drug recovered relative to the initial load is shown in figure 9.13 for the three loadings.

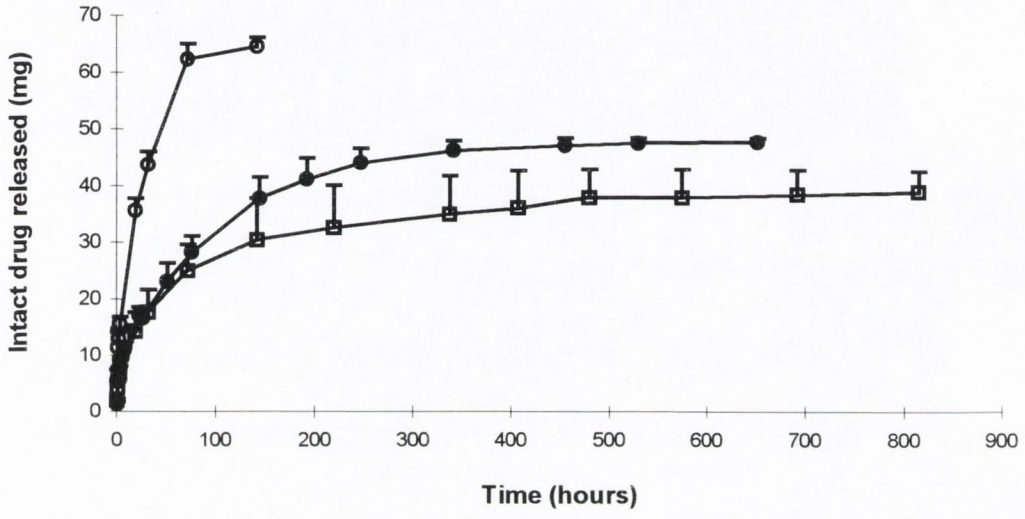

Figure 9.12. Intact drug released (mg) from RG 755 SE discs containing 40% (□), 50% (●), 60% (○) initial drug load. Error bars indicate the standard deviation of the data, except for the 50% load where the range of the data is specified.

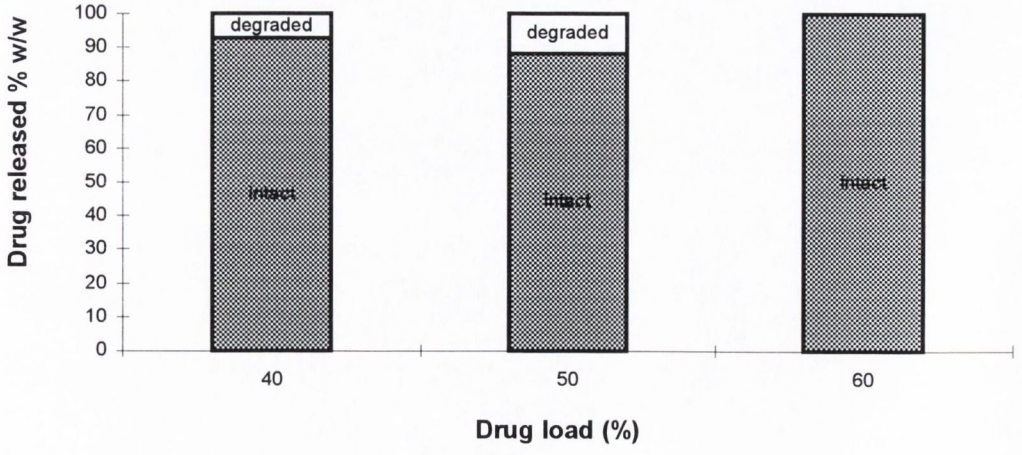

Figure 9.13. Histogram showing the %w/w of intact drug relative to the initial drug load for release profiles of RG 755 SE discs at 40%, 50%, 60% drug loading.

The histogram shows that at 40% and 50% loading approximately 90% of the drug loaded into the discs was released intact. At 60% drug load, degradation of AMOX released from RG 755 discs is highly improbable.

9.2.6. **Quantification of the amount of intact Amoxycillin released from R 203 SE systems containing 40% drug loading**

R 203 systems loaded with 40% AMOX resulted in lower recovery of intact drug than the corresponding RG 755 SE systems. Figure 9.14 compares the release profile of intact drug (mg) for these two systems. The overall release time with R 203 was much longer than with RG 755. However, the fraction of intact drug released from R 203 after the initial rapid phase was very small. Approximately 12 mg of intact AMOX were released from the R 203 formulation within the first 24 hours. This was followed by an induction period of approximately 4000 hours following which a small amount of drug, circa 2 mg, is then released, consistent with polymer degradation.

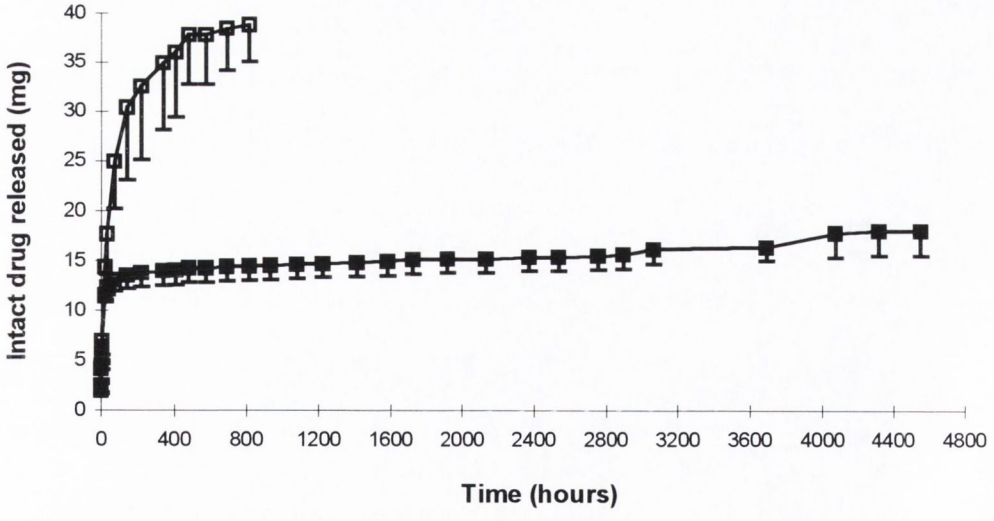

Figure 9.14. Release of intact Amoxycillin (mg) from SE discs at 40% drug load prepared with R 203 (■) and RG 755 (□). Error bars indicate the standard deviation of the RG 755 data and the range of the R 203 data.

The release profile of intact AMOX obtained with R 203 at 40% loading is compared to the corresponding profile of total drug (figure 9.15). The profiles were qualitatively

similar and quantitatively different. The larger fraction of intact drug was released in the initial rapid phase. Conversely, the larger fraction of total drug was released by a degradation controlled mechanism, after 3500 hours.

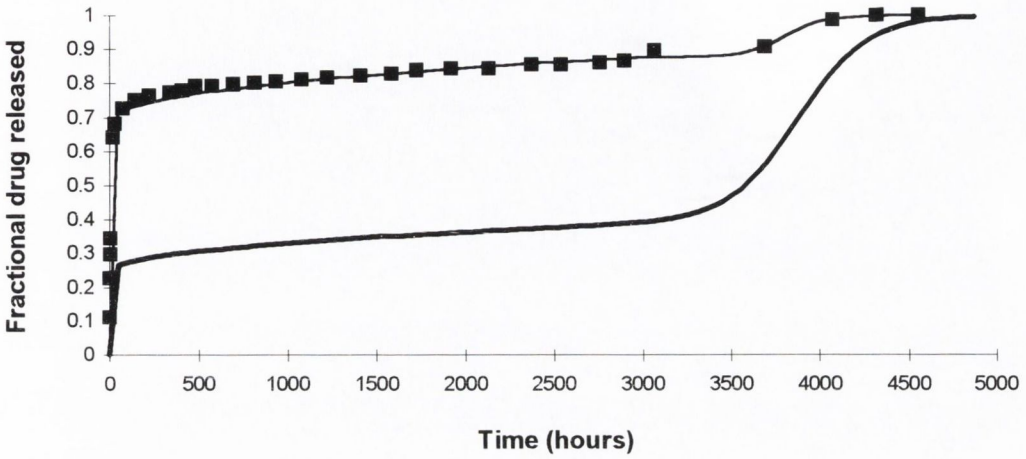

Figure 9.15. Release of intact Amoxycillin from 40% drug loaded R 203 SE discs fitted to equation 3.20 (■) versus simulated data (heavier line) obtained with equation 3.20 for the corresponding profiles of total drug.

Table 9.1 shows the parameters and statistics obtained for the release data of intact drug fitted to equation 3.20. The parameters related to the lag period, Fd_∞ and k_r, and the degradation parameters, t_{max} and k, were similar for both profiles (tables 8.17 and 9.1).

Table 9.1. Estimated parameters for the release of intact drug from R 203 SE systems at 40% drug load fitted to equation 3.20.

Fb_∞	0.69 ± 0.0098	t_{max}	3805 ± 107
k_b (h^{-1})	0.214 ± 0.012	k (h^{-1})	0.00981 ± 0.0061
Fd_∞	0.189 ± 0.0214	r^2	0.9929
k_r ($h^{-0.5}$)	0.0011 ± 0.00014	MSC	4.57

The % w/w of intact drug relative to the total drug released for R 203 SE discs is shown in figure 9.16. At 20% loading the recovery of intact drug was circa 10%. The 40% system released approximately 35 % of intact AMOX.

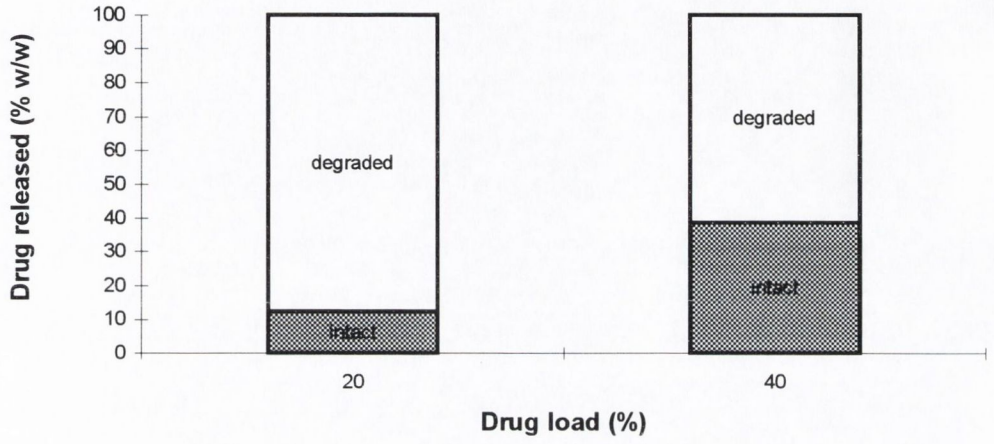

Figure 9.16. Histogram showing the % w/w of intact AMOX relative to the total drug released from R 203 SE discs at 20% and 40% loading.

9.2.7. **Drug stability inside poly-alpha-hydroxy-aliphatic esters during drug release studies**

It was shown in the previous sections that considerable degradation of drug occurred. This degradation could have occurred prior to release or in the dissolution media.

HPLC traces obtained for residual drug extracted from 20% drug loaded SE discs exposed to approximately 290, 410 and 1030 hours of drug release studies are shown in Appendix V. In these figures, discs prepared with RG 503 (a), RG 504 (b), RG 755 (c), R 203 (d) are compared. The drug peak to degradation peaks ratio decreases with time. By 290 hours of dissolution AMOX was found to be present inside each of the four systems (RG 503, RG 504, RG 755, R 203). Degradation peaks and/or byproduct peaks were also found in these systems. The intensities of these peaks were much lower than the AMOX peak. By 410 hours, the peaks obtained for RG 503 (a) and RG 755 (c) were of similar height. The corresponding degradation peaks in these

two systems were higher for RG 503. Therefore, it appeared that for a given amount of AMOX the formulation prepared with RG 503 had a greater amount of degradation products than the RG 755 formulation, by 410 hours of release. This was in agreement with the results obtained in the previous sections of this chapter which showed that the fraction of intact drug is lowest during the polymer degradation phase. RG 503 commences its degradation at approximately 400 hours (section 7.3.4), earlier than RG 755.

Samples of RG 503 and RG 504 were examined by 530 hours (not included in appendices). The chromatograms continued to show drug and degradation peaks; the number of peaks and the profiles were similar to those of the previous time point.

By 1030 hours of dissolution, only traces of AMOX were left in the RG 503 and RG 504 discs. The fraction of intact drug still entrapped in R 203 discs after 1030 hours was greater than in RG 755 discs. This was in agreement with the relative overall extent of drug release, approximately 1600 hours and 3000 hours for RG 755 and R 203, respectively.

The residual intact drug trapped in the discs was quantified at various time points. This is further discussed in the next chapter.

9.3. DEGRADATION OF PLA/PLGA DISCS IN THE PRESENCE AND ABSENCE OF AMOXYCILLIN

9.3.1. pH and colour changes during drug release studies

As was reported in section 7.5, colour changes were evident in the discs. These changes were also evident in the dissolution medium after considerable experimental time. The first colour changes observed in the dissolution media with 20% drug loaded SE discs occurred after 670 hours for the formulations with RG 503 and RG 504. The dissolution media had been last replaced 144 hours before the 670-hour sampling point. Table 9.2 lists the colour and pH values of the dissolution media

corresponding to this time point for the four polymers studied. The results are consistent with a degrading matrix at the observed time, in agreement with the mass loss profiles shown in Chapter 7.

The pH and colour of RG 755 and R 203 were not affected when examined after 670 hours of dissolution.

Table 9.2. Colour changes and pH values obtained for the 670-hour dissolution media samples from drug release experiments corresponding to RG 503, RG 504, RG 755 and R 203 SE discs loaded with 20% Amoxycillin. The values quoted correspond to two observations.

System	Colour	pH
Phosphate Buffer	clear	5.9
RG 503 (1)	green	4.3
RG 503 (2)	green	4.2
RG 504 (1)	light green	5.4
RG 504 (2)	light green	5.3
RG 755 (1)	clear	5.9
RG 755(2)	clear	5.9
R 203 (1)	clear	5.9
R 203 (2)	clear	5.9

9.3.2. **Effect of the addition of D,L-lactic acid to Amoxycillin solutions on the pH of the media**

Following the observations discussed in section 9.3.1, a series of tests were undertaken in order to reproduce the pH and colour changes observed during drug release studies.

A series of solutions (A, B, C, D) were prepared with AMOX-H and D,L-Lactic (section 5.5.7). The initial appearance of the solutions is described below:

A) Saturated solutions of AMOX-H in phosphate buffer pH 5.9: white powder in clear liquid.

B) Saturated solutions of AMOX-H in water: white powder in clear liquid.

C) Saturated solutions of AMOX-H in phosphate buffer pH 5.9 containing 1g of D,L-lactic acid: white powder in clear liquid.

D) 100 ml solutions of D,L-lactic acid in phosphate buffer pH 5.9 (1g in 100 ml): clear liquid.

The changes observed at various times are summarized in Appendix IV (Experiment 1). The results showed that the addition of free lactic acid considerably decreased the pH of the dissolution medium. These experiments also showed that after 150-200 hours of degradation, the presence of lactic acid was not required for a buffer solution containing pure AMOX to decrease its pH and change its colour. On this basis, it was possible to argue that the changes previously shown in table 9.2 related solely to the presence of drug in the medium. However, the changes were not observed during drug release prior to the indicated time (670 hours), which was a time point beyond the onset of mass loss from RG 503 systems.

It appears that the greenish coloration of the dissolution medium from RG 503 and RG 504 discs (table 9.2) was due to the presence of partly degraded AMOX, since coloration was also obtained during degradation studies of the pure drug, previously described in Chapter 6.

A greenish colouration was always accompanied by a sulphurous odor.

In addition to the above mentioned tests, one further experiment was performed. The material quantities chosen for this experiment were based on the maximum amount of free lactic acid calculated to be generated from dissolution in 25 ml of buffered media of 120 mg discs prepared with (50:50) PLGA and loaded with 20% drug. Therefore, to 50 ml of a saturated solution of AMOX in phosphate buffer pH 5.9, approximately 80 mg of D,L-lactic acid were added. The pH of the solution measured upon addition of the acid decreased from 5.6 to 3.93. After 144 hours at 37°C and 95 cpm, the pH of the solution was 3.88 and the color resembled that of (A) (yellow). Two days later, at 200 hours, no further changes were observed.

From the experiments above discussed it was concluded that the colour changes observed (yellows and greens) in the dissolution media (section 9.3.1) were associated with the presence of AMOX in the solutions.

9.3.3. **Gel Permeation Chromatography studies on polymer discs**

In the previous chapters it was shown that t_{maxP} (result obtained from mass loss profiles) for PLA/PLGA drug loaded discs was consistently higher than for equivalent polymer only discs. The estimated values of the degradation constant k were lower for the drug loaded discs compared to the equivalent drug-free discs. The effect of the drug on the polymer mass loss profiles of the different systems was such that t_{maxP} increased by 6% to over two fold. Similarly, the degradation rate constant was affected by a decrease between 7% to over three fold. To examine the effect of solvent-evaporation on the pure powder, a preliminary GPC analysis was undertaken with RG 503 SE drug-free systems. The resulting M_n, M_w and P for this sample were 22,008, 35,292 and 1.61, respectively. There appeared to be no significant difference when compared with the pure polymer powder. Table 9.3 shows the M_n, M_w and P obtained for various SE systems prepared with and without drug. Systems prepared with RG 503, RG 504, RG 755 and R 203, having undergone various stages of drug release, were compared to discs that had not been exposed to dissolution studies. The experimental time points, indicated on the table, were chosen on the basis of the polymer mass loss results previously referred to. The M_n and M_w values determined for the starting material were lower than those determined for the drug-loaded SE discs at

time zero, with the exception of RG 504 discs for which the values decreased upon processing with the drug.

Table 9.3. GPC determinations on RG 503, RG 504, RG 755, R 203 systems.

Sample	M_n	M_w (daltons)	P
RG 503 powder	22,136	35,610	1.62
RG 503 20% SE 0 h	24,740	36,686	1.48
RG 503 drug free SE 676 h	2,199	5,130	2.33
RG 503 20% SE 676 h	5,754	10,295	1.79
RG 504 powder	33,876	54,123	1.60
RG 504 20% SE 0 h	29,471	42,614	1.45
RG 504 drug free SE 676 h	770	1,474	1.91
RG 504 20% SE 676 h	9,293	16,385	1.76
RG 755 powder	39,560	72,525	1.85
RG 755 20% SE 0 h	43,361	76,938	1.77
RG 755 drug free SE 288 h	10,973	20,980	1.91
RG 755 20% SE 288 h	19,051	40,859	2.15
RG 755 drug free SE 1084 h	759	1,197	1.58
RG 755 20% SE 1084 h	15,071	25,851	1.72
R 203 powder	15,400	25,203	1.64
R 203 20% SE 0 h	17,266	26,541	1.54
R 203 drug free SE 1084 h	2,681	7,458	2.78
R 203 20% SE 1084 h	12,348	19,077	1.54

Systems having undergone drug release studies were also analyzed. GPC was performed on drug loaded discs in which degradation was suspected, on the basis of the polymer mass loss and/or drug stability profiles. The M_n and M_w of discs used in drug release experiments substantially decreased, with larger M_n and M_w reductions

observed for drug-free discs than for the equivalent 20% drug-loaded discs. Figure 9.17 shows a plot of M_n as a function of time for 20% drug loaded versus drug-free RG 755 SE discs having undergone different stages of drug release experiments. As previously mentioned, the initial M_n was greater for the drug loaded discs. The subsequent reduction of the initial M_n was faster for the drug-free systems. The other molecular weight average, M_w, followed a similar trend.

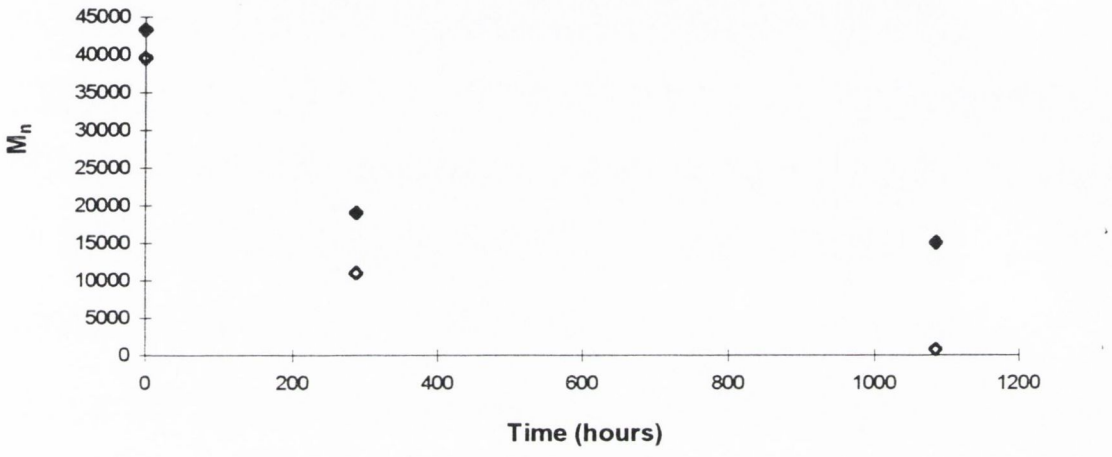

Figure 9.17. M_n reduction in 20% drug loaded (◆) versus drug-free (◇) RG 755 SE discs having undergone various stages of dissolution.

Comparison with the data from polymer mass loss (Chapter 8) shows that polymer degradation occurred earlier than mass loss, both for drug loaded and drug-free discs. The onset of mass loss for these systems was not earlier than 700 hours while there is at least a 50% reduction of the initial molecular weight by approximately 300 hours in the release medium.

RG 755 SE discs loaded with 50% AMOX-H were analysed after 1700 hours of dissolution studies. At this time, the discs were depleted of drug and a relatively large amount of polymer was still available for further dissolution. Interestingly, the M_n (8,925) and M_w (16,826) of these discs are comparable to those of drug-free SE discs when exposed to only 288 hours of dissolution studies.

In order to accentuate the influence of the presence of drug on the polymer molecular weight change, the molecular weight obtained in the presence of 20% drug (D.L.) was

divided by that obtained in the absence of drug (D.F.). The resultant ratios are summarized in table 9.4 for M_n and M_w data.

Table 9.4. M_n, M_w ratio for 20% drug loaded (D.L) and drug-free (D.F) systems prepared with RG 503, RG 504, RG 755 and R 203.

System	M_n D.L/ M_n D.F	M_w D.L/ M_w D.F
RG 503, 0 h	1.12	1.03
RG 503, 676 h	2.62	2.00
RG 504, 0 h	0.87	0.79
RG 504, 676 h	12.06	11.12
RG 755, 0 h	1.09	1.06
RG 755, 288 h	1.74	1.95
RG 755, 1084 h	19.86	21.60
R 203, 0 h	1.12	1.05
R 203, 1084 h	4.61	2.56

The M_n and M_w ratios in table 9.4 were greater than the unit in all cases except for RG 504 systems at the initial time point. In all the systems, the ratios obtained increased as a function of time. The increase in the ratio was in order of 12 fold for RG 504 after 676 hours and of the order of 20 fold for RG 755 after 1084 hours. Thus, the presence of drug had a dramatic effect on the molecular weight.

9.4. STUDIES PERFORMED TO EXPLORE THE OBSERVED EFFECT OF THE DRUG ON THE DEGRADATION OF THE POLYMER

9.4.1. Nuclear Magnetic Resonance studies

The results of ^{13}CNMR studies are shown in figure 9.18 for untreated polymer powder (top spectrum), drug-free SE discs having undergone 600 hours of dissolution (middle spectrum) and 20% drug loaded discs undergone 1000 hours of similar studies (bottom spectrum). Comparison of the results obtained with the NMR spectra reported by Shih et al. (1995) suggests that breakdown of the polymer backbone was greatest in the spectrum corresponding to drug-free SE discs (middle spectrum). The methyl group at approximately 16 ppm is considered to correspond to the lactic acid subunits in the polymer backbone. Chain scission with generation of free lactic acid is suggested by the methyl related peak displayed at approximately 21 ppm (20.2488 ppm, 20.3840 ppm and 20.4226 ppm). Similarly, it appears that at 70 ppm the methine groups of the polymer backbone displayed a signal which shifts to 67 ppm (66.4612 ppm and 66.7703 ppm) upon chain scission. Signals obtained at 175.0661 ppm and 177.5776 ppm are exclusive to the middle and bottom traces (drug loaded and drug-free discs used in dissolution studies), the middle trace displaying a significantly wider distribution of signals that suggests a higher degree of backbone breakdown in the drug-free discs compared to the 20% drug loaded systems.

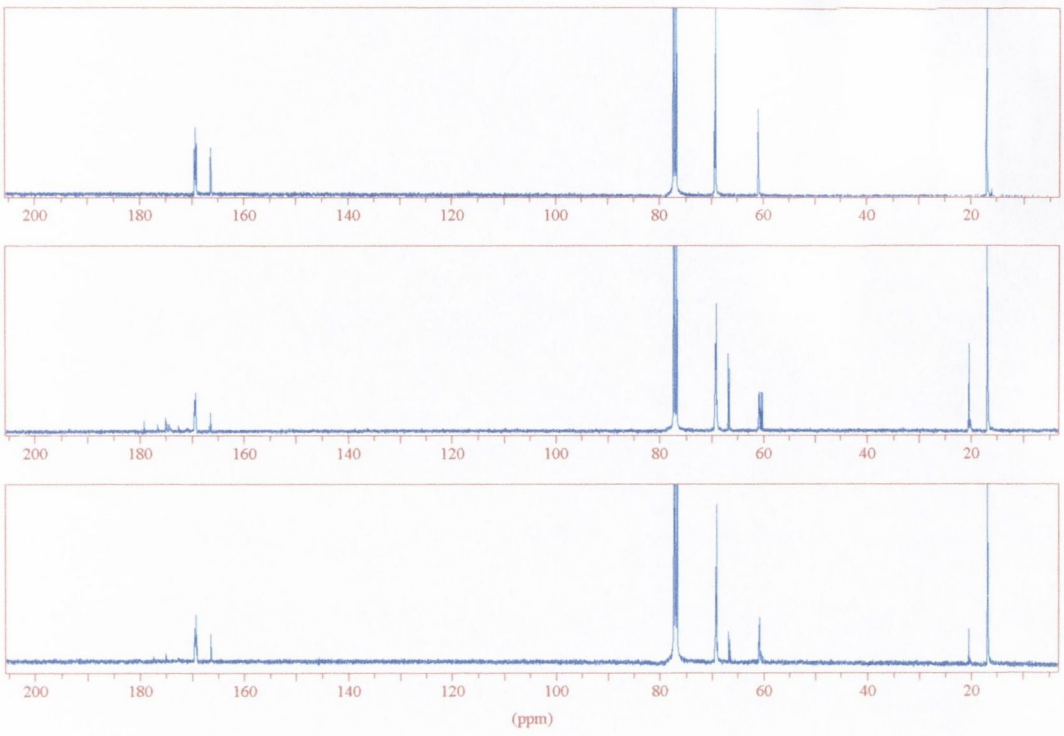

Figure 9.18. ^{13}C-NMR spectra from untreated RG 755 powder (top), RG 755 drug-free SE discs having undergone 600 hours of dissolution studies (middle) and 20% drug loaded RG 755 SE discs having undergone 1000 hours of similar studies (bottom).

Presence of the drug was not detected in the ^{13}C-NMR nor the ^{1}H-NMR analysis. The reason for this being the lack of solubility of the drug in the solvent employed in the preparation of the samples for NMR measurements ($CDCl_3$). The degradation products of the drug were also not detected under these experimental conditions.

Figure 9.19 shows ^{1}H-NMR measurements for the same samples described in the previous figure. The ^{1}H-NMR spectra were consistent with the results obtained by ^{13}C-NMR: increased polymer breakdown in drug-free discs compared to 20% drug loaded discs. In the ^{1}H-NMR spectra, drug loaded discs (bottom trace of figure 9.19) displayed two signals that were absent in the drug-free systems (top and middle traces of the same figure). As explained before, the drug can not be detected by this method and therefore the two new signals (2.3211 ppm and 5.0321 ppm) were initially thought to correspond to a possible interaction between the drug and the polymer.

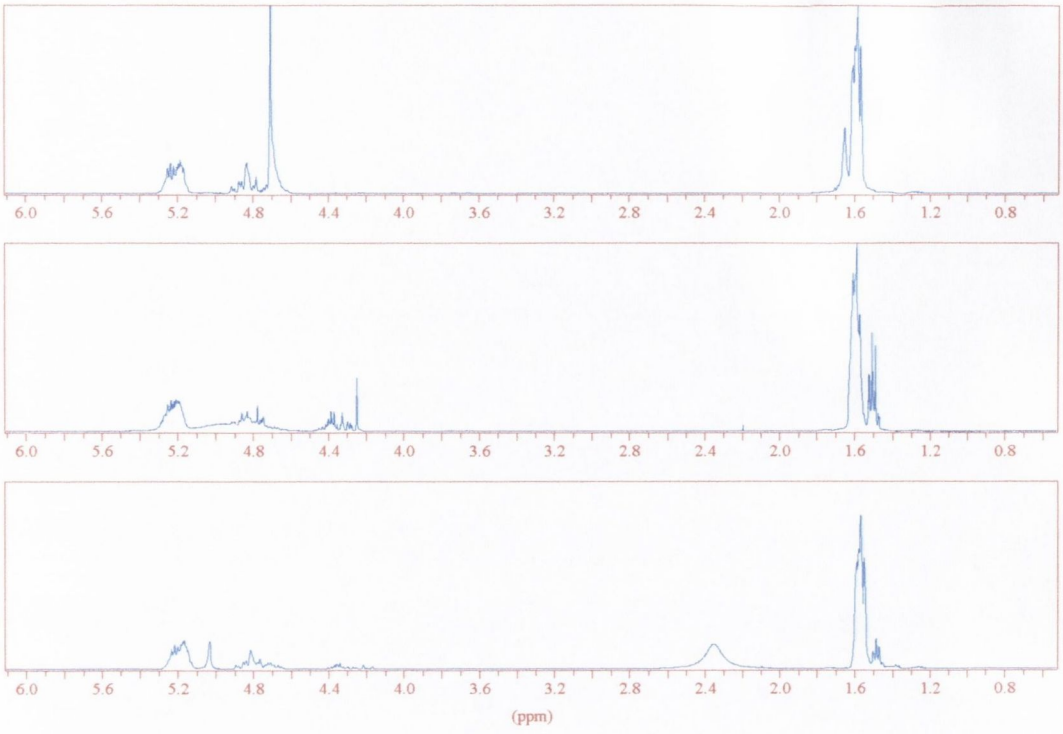

Figure 9.19. ^{1}H-NMR spectra from untreated RG 755 powder (top), RG 755 drug-free SE discs after 600 hours of dissolution studies (middle) and 20% drug loaded RG 755 SE discs after 1000 hours of similar studies (bottom).

However, the signal observed at approximately 2.3211 ppm may possibly be attributed to residual water in the sample (originating from the drug release studies). The signal at 5.0321 ppm was not attributable to any particular component.

9.4.2. **Effect of the drug on the pH of the medium**

It is widely recognized that poly-alpha-hydroxy aliphatic esters degrade under acidic and basic conditions (Göpferich, 1996), the pH inside PLA/PLGA eroding matrices having been found to be as low as 2 (Herrlinger, 1994). Preliminary pH measurements, described in Appendix IV, suggested that AMOX has the potential to reduce the acidity of an aqueous medium. It may be possible then that the drug inhibits the autocatalysis of the polymer by reducing the acidity generated upon release of lactic acid sub-units.

The quantities of the materials used were based on calculation of the likely amounts of free lactic acid generated from 120 mg discs prepared with (50:50) PLGA and loaded with 20% drug that would dissolve in the 25 ml of media, to simulate the case of drug release studies. The effect of the drug was firstly investigated in water. To 50 ml of water approximately 100 mg of D,L-lactic acid (Sigma) were added. The pH of this solution was 2.78. AMOX-H was then gradually added until saturation, the amounts of drug ranging between 10 mg and 200 mg. On saturation of the medium the pH increased to 2.92, an increase from the original pH of approximately 0.14 pH units. These results indicate that the drug does have an effect on the pH of the medium, decreasing its acidity.

In a subsequent experiment, 50 mg of D,L-lactic acid were placed in 50 ml of water. The pH changes obtained upon addition of AMOX-H are summarized in table 9.5, compiled with the values previously observed at the higher concentration of lactic acid. The results show that similar trends were obtained in both experiments.

Table 9.5. pH values obtained for solutions containing 100 mg of D,L-lactic acid (a) and 50 mg of D,L-lactic acid (b) in 50 ml of water upon addition of cumulative amounts of AMOX-H. The abbreviation n.s. denotes "no sample taken".

AMOX-H (mg)	pH measured (a)	pH measured (b)
0	2.78	2.90
10	2.74	2.86
20	2.74	2.86
50	2.78	2.90
100	2.85	2.96
150	2.87	3.02
200	2.92	n.s.
250	n.s.	3.04
300	2.92	n.s.
350	n.s.	3.04

Figure 9.20 shows the plot of pH versus amount of AMOX-H (mg) added to 50 mg and 100 mg of D,L-lactic acid to 50 ml of water. The overall change in the pH of the medium in both experiments was approximately 0.1 unit. It has been reported by Belbella et al. (1996) that poly-alpha-hydroxy-aliphatic esters are highly sensitive to a pH change in the region between 2 to 4. Faster degradation kinetics were reported at the lower pH values.

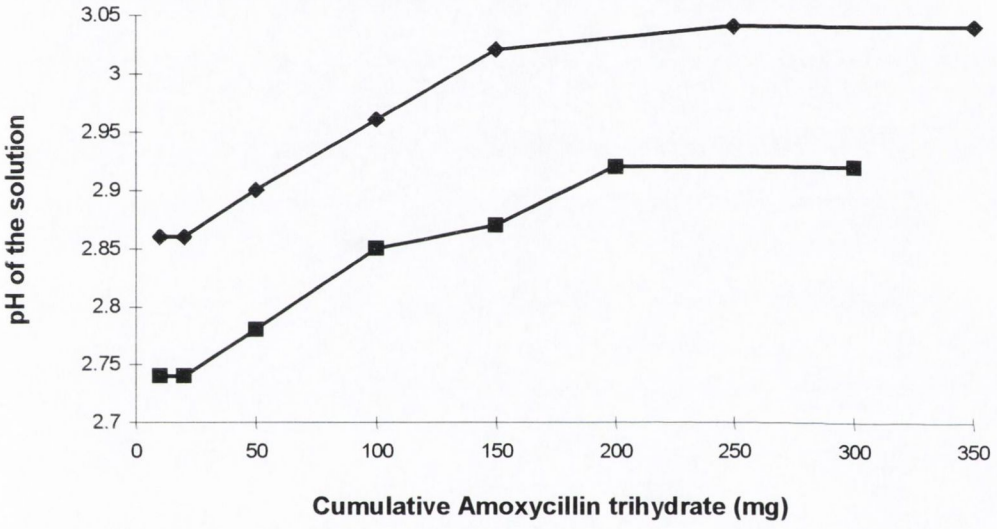

Figure 9.20. Plot of pH versus cumulative amounts of Amoxycillin trihydrate (mg) added to 50 ml of water containing 50 mg (◆) and 100 mg (■) dissolved D,L-lactic acid.

After observing the effect of the drug on the acidity of lactic acid solutions prepared in water, the next step taken was to investigate the pH changes when phosphate buffer was used instead of water. To 100 mg D,L-lactic acid (Sigma), 50 ml of phosphate buffer pH 5.9 were added with subsequent decrease of the pH to 3.49. Increasing amounts of AMOX-H were gradually added to this solution until saturation of the drug was reached. The amounts added ranged between 10 mg and 200 mg of AMOX-H. In contrast to the results obtained with water, the pH remained constant for all the additions made to the buffer and without changes from the initial value (3.49).

Despite the effect of the drug on the pH of the media being masked in phosphate buffer, the results presented show that AMOX may possibly compensate some of the acidity generated inside the eroding matrix. It has been reported by Li et al. (1990) that water uptake occurred faster for polymers in distilled water than in buffer as there were no osmotic effects preventing hydration. The observed osmotic effect suggests that the ions in the buffer may not penetrate into the matrix.

9.4.3 . **Swelling studies**

The results obtained from the NMR spectra failed to indicate the existence of a chemical interaction between the drug and the polymer. The observed effect of the drug on the pH of the medium does not seem to explain the degradation process in all the cases. For instance, systems that apparently released all the drug load prior to the onset of polymer degradation remained as solid discs beyond the dissolution time of the equivalent drug-free systems (Chapter 8). Therefore, with the aim to further explore the existence of an interaction between the drug and the polymer swelling studies were undertaken.

The rationale for performing a swelling study on Amoxycillin discs formulated with poly-alpha-hydroxy-aliphatic esters was to establish whether the observed retarded kinetics of polymer degradation might relate to crosslinking of the polymer matrix in the presence of the drug. Swelling studies reported by Sloop et al. (1994) showed that an increase in the degree of crosslinking of poly(ethylene oxide) and poly(oxymethylene-oligo(oxyethylene)) resulted in increased hydration of hydrophilic matrices.

Poly-alpha-hydroxy-aliphatic esters are hydrophobic polymers, therefore DCM was used as the solvent for swelling studies. On the basis of the GPC results presented earlier in this chapter, swelling studies were initially performed on dried discs previously used in drug release studies. The molecular weight determinations for these samples showed higher values for the drug loaded discs. This being the case, it was then expected that these discs would exhibit a greater degree of swelling than the equivalent drug-free discs.

The first swelling study was performed on RG 504 SE systems having undergone 290 hours of dissolution. Table 9.6 summarizes the series of observations made during the 12-hour length swelling study. The polymer only disc dissolved faster than the 20% drug-loaded disc, as indicated on the table. The drug-loaded disc showed a three-fold increase of height and maintained its original diameter after the 12-hour exposure to the organic solvent.

Table 9.6. Appearance of RG 504 discs during swelling studies performed in dichloromethane.

RG 504 System	Appearance
drug-free	
prior to swelling study	Opaque disc, 12.2 mm x 1.2 mm.
after 5 minutes in DCM	Starts to dissolve, resembles a clear gel.
after 20 minutes in DCM	Smaller and amorphous. Appears to increase its height.
after 30 minutes in DCM	Dissolution rate appears to accelerate.
after 12 hours in DCM	Practically all dissolved, some amorphous material left.
20% drug-loaded	
prior to swelling study	Opaque disc, yellowish, 12.2 mm x 1.1 mm.
after 5 minutes in DCM	Remains in one piece without changes in shape.
after 20 minutes in DCM	Gradual migration of drug particles (yellowish) into the solution. Some increase in the height, not quantified.
after 30 minutes in DCM	The disc decants to the bottom of the vial.
after 12 hours in DCM	The disc is still formed and has swollen, showing a diameter of approximately 13 mm and a height of approximately 3.0 mm.

At the end of the swelling study, this disc was removed from the solvent by filtering the contents of the glass vial through a 0.2 μm membrane with the aid of some additional DCM. A small debris of yellowish particles was collected on the membrane. The yellow colouration suggested the presence of drug (degraded) in the pieces. It was not clear, however, whether these pieces were composed of polymer. Therefore, the particles on the membrane were then washed with 200 ml of water in order to dissolve the residual drug. As a result of the washing procedure the material lost its yellow colouration, the size and shape of the particles remaining unchanged. This suggested that the material was composed of the original polymer.

On observation of a 20% drug loaded disc prepared by mechanical mixture of the drug and PLGA, the disc did not dissolve upon observation for 12 hours. This was expected due to the poor solubility of the drug in DCM. Swelling was not observed in this system, however there was leaching of white material from the surface which remained suspended in the surrounding solvent.

A short swelling experiment was subsequently performed with RG 503 SE discs having undergone 290 hours of drug release. The drug-free disc started to dissolve within 5 minutes of exposure to DCM, resulting in a semi-solid amorphous material. In contrast, the yellow-coloured disc still containing circa 10% of drug did not dissolve upon observation for 30 minutes in the solvent. Appendix IV shows a photograph of the 20% drug loaded disc (labelled as number 8) and the drug-free disc (labelled as number 9) taken 30 minutes after the start of the swelling study. A two-fold increase in the height of the drug-loaded disc was observed. The drug-free disc was practically dissolved.

Freshly manufactured discs, not exposed to drug release studies were then studied for swelling. The results obtained for these samples did not show any differences between the drug loaded and the drug-free discs, dissolution in DCM occurring within 5-10 minutes in all cases.

The results described in this section for discs exposed to the dissolution media are consistent with the GPC results obtained for similar samples. It still remains unknown whether the observed higher molecular weight of drug loaded discs versus equivalent

drug-free discs is the result of an inhibited polymer degradation in the presence of the drug or of a process in which, at some stage, the molecular weight of drug loaded discs increases. The latter would be the case of a system in which some polymer chains cross link to give longer chains, a covalent reaction mediated by the drug. This is addressed in the General Discussion (Chapter 10).

9.5. THE EROSION OF PLA/PLGA DISCS PREPARED WITH AMOXYCILLIN

Homogeneous bulk erosion is the process commonly reported to occur in eroding PLA/PLGA systems (Göpferich, 1996). However, in figure 7.48, the photograph of RG 503 and RG 504 20% drug loaded discs showed that the diameter of the discs decreases with time. The dimensions of these discs appeared to decrease while maintaining the original shape, consistent with a surface erosion mechanism such as that described by Hixson and Crowell (equation 3.23). In contrast to drug-free discs, it was observed that PLGA drug loaded discs, after varying and prolonged lag times, eroded consistently with surface erosion type mechanism.

The Hixson and Crowell model was therefore modified to take account of the lag phase. The weight loss profiles of discs were fitted to equation 9.2:

$$\left(\frac{W_d}{W_i}\right)^{1/3} = 1 - k_2\left(t_{elapsed} - t_{lag}\right) \qquad \text{equation 9.2}$$

where W_i is the initial weight of the system and W_d is the dried weight of the system after the elapsed dissolution time for a particular disc $t_{elapsed}$. t_{lag} is the induction period before onset of weight loss in any disc and k_2 is a rate constant. Appendix I shows the relevant model file corresponding to this equation.

Initially, the weight loss data of 20% drug loaded SE systems prepared with the four polymers was fitted to equation 9.2. The statistics obtained indicated poorer agreement with the model compared to the results of this equation when applied to the *polymer* mass loss data, previously introduced in Chapters 7 and 8. Figure 9.21 shows the cube root plot for the fraction undissolved polymer versus time obtained for RG 503, RG 504, RG 755, R 203 SE 20% drug loaded discs. All the profiles showed an initial induction period followed by a linear decay after onset of mass loss. Table 9.7 lists the statistics obtained, whereby the values of t_{lag} are in rank order with the known degradation times for the polymers.

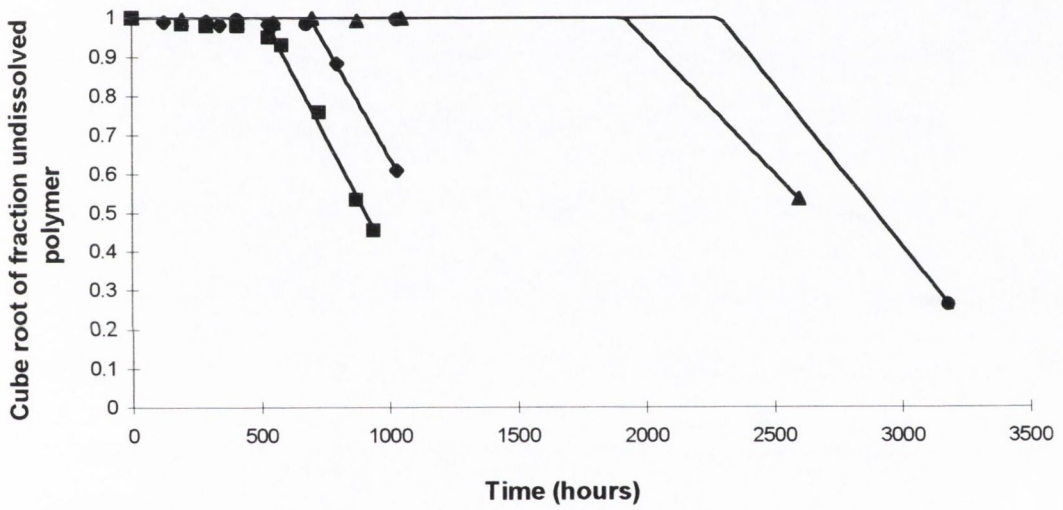

Figure 9.21. Cube root of undissolved polymer (fraction) versus time plot for RG 503 (■), RG 504 (◆), RG 755 (▲) and R 203 (●) SE 20% drug loaded discs. The data was fitted to equation 9.2.

Table 9.7. Parameters and statistics obtained for the cube root plot of polymer mass loss versus time for 20% drug loaded RG 503, RG 504, RG 755, R 203 SE discs fitted to equation 9.2. Estimated parameters were very uncertain for systems marked *, with large SD being returned.

System	k_2 (h^{-1}) x 10^4	t_{lag} (h)	r^2	MSC
RG 503 20% SE	13 ± 0.57	512 ± 12	0.9911	4.32
RG 504 20% SE	11,6 ± 0.82	692 ± 18	0.9888	4.09
RG 755 20% SE	6,8*	1917*	0.9957	4.99
R 203 20% SE	8,3*	2293*	0.9987	6.05

The number of data points available for RG 755 and R 203 defining the linear phases in figure 9.22 was very low. This is accounted for by the large standard deviations obtained for the relevant estimated parameters. A comparison of the statistical output from table 9.7 versus the corresponding statistics previously obtained for equation 3.13 (Chapters 7 and 8) is compiled in table 9.8. Higher r^2 and MSC values were obtained for RG 503 and RG 504 with equation 3.13. In contrast, RG 755 and R 203 showed better agreement with the cube root law (equation 9.2).

Table 9.8. Coefficients of determination (r^2) and model selection criterion (MSC) obtained for polymer mass loss data from 20% drug loaded RG 503, RG 504, RG 755, R 203 SE discs fitted to equations 3.13 and 9.2.

System	Equation 3.13		Equation 9.2	
	r^2	MSC	r^2	MSC
RG 503	0.9935	5.26	0.9911	4.32
RG 504	0.9922	4.45	0.9888	4.09
RG 755	0.9899	4.15	0.9957	4.99
R 203	0.9948	4.70	0.9987	6.05

Based on the Hixson Crowell laws Cobby et al. (1974) assummed that that the weight of drug remaining in the pellet was proportional to the volume (and hence to the cube of the radius) of the unreleased portion. They expressed this assumption as follows:

$$\frac{W_t}{W_i} = \frac{V_t}{V_i} = \left[\frac{r_t}{r_i}\right]^3 = 1 = f_t \qquad \text{equation 9.3}$$

where W_t, V_t, r_t are the weight, volume and radius of the unreleased portion at time t, W_i, V_i, r_i are the corresponding initial values, and f_t is the fraction of solute dissolved (released) at time t.

In the terminology of the present work, W_t / W_i corresponds to W_d / W_i. By substituting the first term of equation 9.2 with the radius equivalent according to equation 9.3, the following relationship should hold (Appendix I lists the model file):

$$\frac{r_t}{r_i} = 1 - k_2\left(t_{elapsed} - t_{lag}\right) \qquad \text{equation 9.4}$$

A plot of the ratio of the radius as a function of time will be linear after the lag period provided a surface erosion mechanism such as that described by Hixson and Crowell is operative. Figure 9.22 shows the results obtained for RG 503 and RG 504 SE 20% drug loaded systems when the radius data was fitted to equation 9.4. Also included in figure 9.22 are the simulated profiles obtained using equation 9.4 with the corresponding parameters from table 9.7. The plots of figure 9.22 parallel the cube root plots of figure 9.21. There was a linear decay observed after an initial lag period.

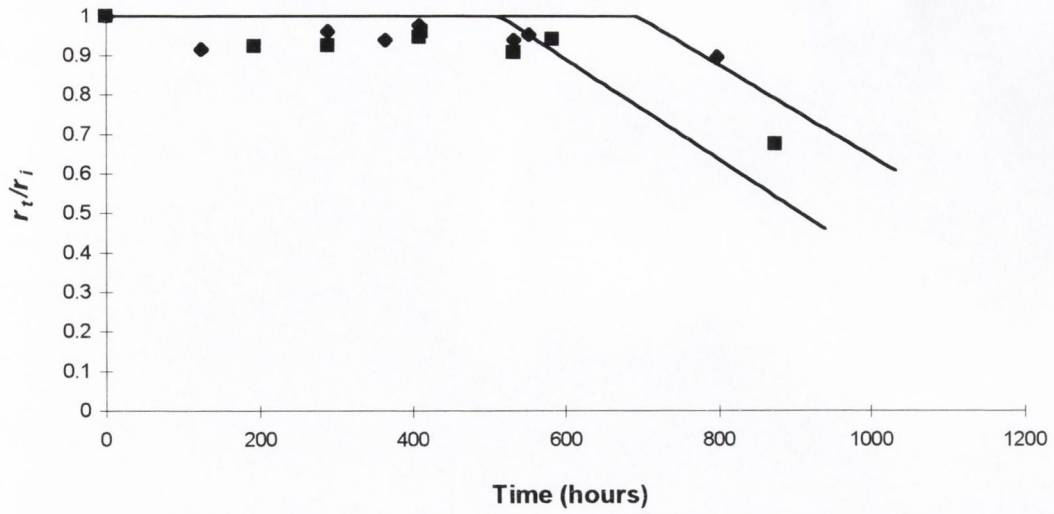

Figure 9.22. Ratio of final to initial radius plotted as a function of time for RG 503 (■), RG 504 (◆) SE 20% drug loaded discs. Simulated lines were obtained with the parameters listed in table 9.7 using equation 9.4.

Despite the limited and variable data, the radius changes observed with RG 503 and RG 504 20% drug loaded discs are consistent with the mass loss results obtained using the erosion related equation 9.2.

9.6. **CONCLUSIONS**

PLGA/PLA matrices can carry intact AMOX for over 1000 hours (42 days). The presence of degradation products, however, has been observed in these systems. The formulations prepared with RG 504 and RG 755 showed greatest drug stability, on the basis of the total relative proportion of intact drug recovered within each formulation. Conversely, the R 203 formulation, which showed the highest fraction of drug released by degradation control, displayed the lowest fraction of intact drug. Differences in surface/centre degradation rates in polymeric devices have been reported (Li et al., 1990) for systems composed of PLA, with increased entrapment of lactic acid in the centre of the devices. In the present work, this behavior was observed in drug-free

PLA discs (section 8.4.3). This may be related to the decreased recovery of intact AMOX obtained with R 203 systems.

M_n and M_w determinations obtained by GPC and swelling studies are in line with the mass loss profiles obtained in the previous chapters. Greater M_n and M_w were observed for drug-loaded systems compared to drug-free systems having undergone equivalent dissolution experiments. Similar information was obtained from the NMR spectra.

An effect of the drug on the pH of the dissolution media was observed, by which AMOX has the potential to decrease the acidity generated by free lactic acid. This observed effect may acquaint of the degradation mechanisms of poly-alpha-hydroxy-aliphatic esters in the presence of AMOX. Surface erosion may be playing a part in such mechanisms. A modification performed to the cube root equation to account for the lag-phase prior to onset of mass loss resulted in acceptable statistical output when the data of polymer mass loss profiles was fitted to the modified surface erosion model. The data corresponding to the change in dimensions of the discs was consistent with the cube root model.

CHAPTER 10. GENERAL DISCUSSION

10.1. INTRODUCTION

The previous chapters investigated four poly-alpha-hydroxy-aliphatic esters as possible delivery vehicles for amphoteric drugs such as Amoxycillin. The *total* drug released resulted in release profiles whose shape and duration depended on the processing method and the type of polymer employed. Such drug release profiles were fitted to physicochemical models consistent with homogeneous bulk erosion, as previously reported in this department for fluphenazine (Ramtoola et al., 1992), levamisole base (Fitzgerald and Corrigan, 1993) levamisole hydrochloride and albendazole (Gallagher and Corrigan, 1998).

Polymer degradation was compared in drug loaded and drug-free discs. The presence of the drug had an effect on the polymer resulting in retarded polymer degradation kinetics. In addition, at late dissolution times, a surface erosion (Göpferich, 1996) type mechanism contributed to the degradation of PLGA drug-loaded discs, in which the dimensions decreased maintaining the original shape of the discs.

The formulation of small amphoteric compounds using PLA/PLGA devices has precedent in the work of Min et al. (1995) who prepared ampicillin microspheres. Such work concentrated on clinical evaluations after *in vivo* administration of the devices. The results, however, were not interpreted from a mechanistic view point, i.e. polymer degradation kinetics and mathematical models describing drug release.

In the present work, HPLC studies performed on eroding systems were used to determine the proportion of *intact* Amoxycillin released from the discs versus the total drug released. These results will be discussed in the context of the formulation variables that may be adjusted to enhance the stability of the drug carried.

10.2. AMOXYCILLIN RELEASE FROM POLY-ALPHA-HYDROXY-ALIPHATIC ESTERS

Both diffusion and degradation mechanisms were found to be involved in the release of AMOX from poly-alpha-hydroxy aliphatic esters, the relative importance of each depending on the polymer characteristics, with variations for a given polymer depending on processing and loading.

10.2.1. Effect of the polymer molecular weight

The proportion of total drug released prior to the commencement of polymer degradation may be referred to as the non degradation controlled drug release fraction F_i. Figure 10.1 shows the plot of F_i against the molecular weight of the polymer carrier for 20% AMOX-H systems prepared using PLGA (50:50), PLGA (75:25) and PLA. There was a trend towards higher F_i values with increasing molecular weight of the polymer used in the preparation of the discs.

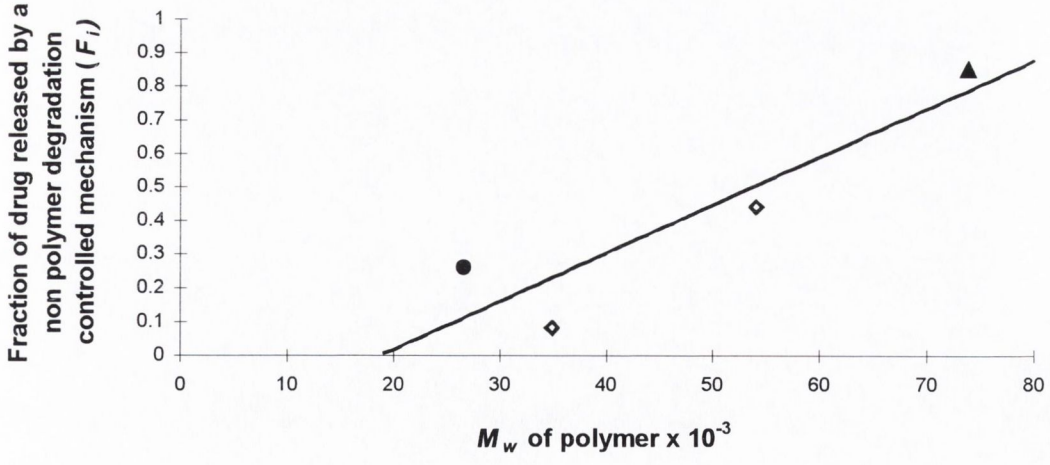

Figure 10.1. Non degradation controlled drug released fraction F_i from release profiles of 20% Amoxycillin loaded SE discs prepared using PLGA (50:50) (◇), PLGA (75:25) (▲) and PLA (●), plotted versus the corresponding polymer molecular weight values (r^2=0.8388; MSC=0.8254).

The plot in figure 10.1 suggested that, for systems prepared under the same experimental conditions, the following relationship holds:

as the molecular weight of a given polymer type increases a higher proportion of drug becomes available to percolate from the compact by a diffusion mechanism.

10.2.2. **Effect of the lactide to glycolide ratio**

The time for completion of total drug release increased with increasing lactide:glycolide ratio. This was in accordance with the findings of Sanders et al. (1986a) who observed an increasing duration of drug release and longer lag times before onset of degradation controlled drug release when the proportion of lactide content in polymer implants was higher. Comparison of the *in vitro* results obtained by Sanders et al. (1986b) for nafarelin loaded (44:56) PLGA microspheres with the results from Amoxycillin (50:50) PLGA SE discs, RG 503 and RG 504 systems, showed that the time for maximum rate of drug release in the polymer erosion related phase was similar. RG 503 and RG 504 systems containing Amoxycillin showed a release phase with maximum rate at 21 and 25 days, respectively. The maximum rate for nafarelin release in the polymer degradation dependant phase occurred at approximately 25 days.

Some additional trends were observed when comparing the four 20% drug loaded SE systems. The relative fractions of drug released by a non polymer degradation mechanism increased with increasing T_g. Figure 10.2 shows the relationship between F_i and the polymer T_g. Linearity was better than that previously obtained in figure 10.1. Since the glass transition temperature of a polymer is dependant on both the molecular weight and the lactide:glycolide ratio (Avoustakis and Nixon, 1991), the results of figure 10.2 indicated in turn that both the molecular weight and the ratio of lactide:glycolide played a part in defining the initial drug release phase of poly-alpha-hydroxy-aliphatic esters.

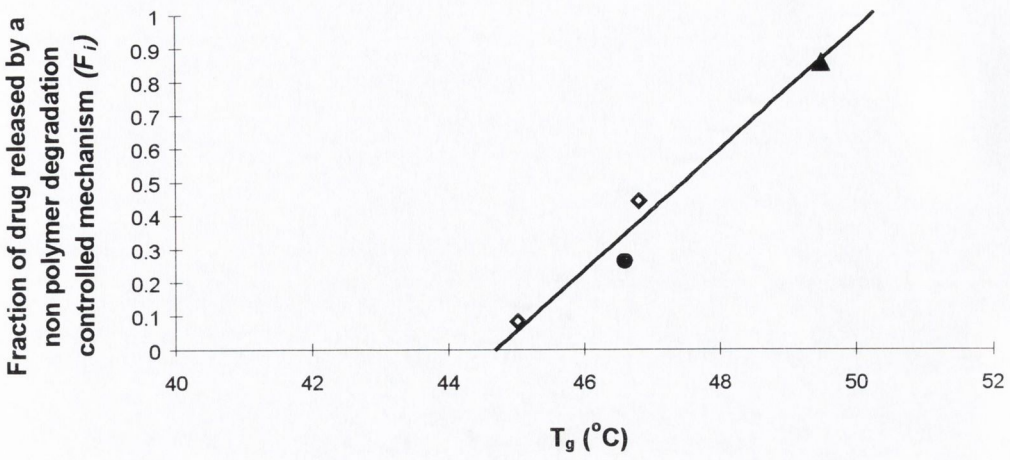

Figure 10.2. Fraction of non degradation controlled drug release F_i from 20% Amoxycillin loaded SE discs prepared using PLGA (50:50) (◈), PLGA (75:25) (▲) and PLA (●), plotted versus the corresponding glass transition temperature values; (r^2=0.9661; MSC=2.38).

The intercept on the ordinate axis of figure 10.2 was equal to 44.62 ± 0.38 °C, with a confidence interval equal to 42.99 - 46.25 °C, at the 95% level. Such temperature range includes the T_g value of RG 503. This was the only polymer whose release profile of 20% SE discs did not appear to be characterized by a square root of time mechanism, with release in the initial phase apparently only due to the drug present at the surface. These results were therefore consistent with the view that the proportion of drug available to percolate from the compacts may be controlled by the characteristics of the polymeric matrix employed, where those systems prepared with polymers showing a T_g below ≅ 46°C would have a minimal burst fraction.

10.2.3. **Effect of processing conditions**

Differences in the proportion of F_i between the four 20% drug loaded SE formulations discussed in the previous section could be reflecting a differential effect of the temperature applied (45°C) during manufacture of the discs. This temperature was considerably below the T_g of the highest molecular weight copolymer RG 755 which showed the greatest proportion of drug released prior to onset of the final phase,

probably due to a lower degree of fusion of the film pieces and, in turn, less entrapment of drug.

Comparison of the parameters estimated from the drug release profiles of RG 503 systems prepared using two manufacturing techniques, MM and SE Methods, showed differences in the parameter values obtained for the kinetics of drug release and the burst fractions. The effect of the manufacturing process was also exerted on the release profiles of RG 755 systems when the results of MM and SE Methods are compared.

Significantly lower Fb_{∞} values were obtained for RG 503 SE systems compared to MM systems. The values of t_{max} obtained for SE discs were lower than those of the equivalent MM RG 503 systems. In addition, there was a trend towards higher values of the final phase release rate constant k in SE discs, however the differences were not statistically significant.

In contrast to RG 503 systems, RG 755 discs showed a similar fraction of drug released prior to the polymer degradation phase both for the MM and SE preparative techniques. The values obtained for the square root of time rate constant k_r showed a tendency to decrease from MM to SE systems of equivalent drug loading.

The estimated values of t_{max} were of the same order in MM and SE RG 755 systems. The values of the polymer degradation related release rate constant k increased when the polymer was processed by SE, as previously described for RG 503.

10.2.4. **Effect of the drug loading**

Differences in drug loading within each preparative technique resulted in variations of the fraction of drug release in the initial phase.

Increasing the drug loading from 20% to 30% in RG 503 and RG 755 systems resulted in greater fractions of drug released in the initial phase, both for discs prepared by mechanical mixture and solvent evaporation. The rate of drug released by square root of time kinetics dramatically increased from 20% to 30% drug load in RG 755 MM discs.

In RG 503 systems, the values of the polymer degradation related parameter k, decreased from 20% to 30% drug loading while the values of t_{max} increased with an increase in the drug load, both for MM and SE. These results suggested that there was a slow down of the kinetics of polymer degradation with increasing AMOX-H loading.

10.3. DEGRADATION OF POLY-ALPHA-HYDROXY-ALIPHATIC ESTERS

10.3.1 Polymer degradation dependant drug release

Table 10.1 compares the drug and polymer degradation estimated parameters obtained for RG 503, RG 504, RG 755 and R 203 SE discs at 20% AMOX-H loading, using drug release and polymer mass loss data. There was a trend towards increasing t_{max} and t_{maxP} in the order RG 503< RG 504< RG 755< R 203. These results are quantitatively consistent with the data reported by Sanders et al. (1986a).

The values of k and k_P decreased following the order, RG 503> RG 504> RG 755> R 203.

Table 10.1. Comparison of the polymer degradation parameters estimated from drug release (t_{max} and k) and polymer mass loss (t_{maxP} and k_P) profiles of RG 503, RG 504, RG 755 and R 203 SE systems loaded with 20% Amoxycillin trihydrate.

System	From drug release profiles		From polymer loss profiles	
	k (h^{-1}) x 10^4	t_{max} (h)	k_P (h^{-1}) x 10^4	t_{maxP} (h)
RG 503 20%	146 ± 14	514 ± 8	98 ± 8	707 ± 10
RG 504 20%	127 ± 11	604 ± 9	82 ± 5	886 ± 10
RG 755 20%	*	1572 ± 26	34 ± 6	2099 ± 94
R 203 20%	39 ± 5	2597 ± 46	32 ± 6	2042 ± 211

* meaningful value not obtainable because of the negligible proportion of drug released in the final phase.

The values of t_{max} estimated for RG 503, RG 504, RG 755 systems from drug release data were smaller than the corresponding values obtained from polymer mass loss profiles (t_{maxP}). This showed that the fraction of AMOX still trapped in the discs after the initial diffusion phase, reached the maximum release rate at a time prior to the time for maximum rate of polymer mass loss ($t_{max} < t_{maxP}$). On calculation of the onset of mass loss, by subtraction of 4 half-lives from t_{maxP}, it was observed that the resulting values were lower than the corresponding values for the drug release parameter t_{max}. This showed that polymer degradation was a pre-requisite for the release of entrapped AMOX from the polymeric discs. It is possible then that the final phase of drug release was triggered by the commencement of polymer loss and further facilitated by an ingress of water into the system leading to an outflow of drug.

In the case of R 203, the value of t_{max} estimated from drug release profiles was higher than that estimated from polymer mass loss data (t_{maxP}), however the difference was not significant on the basis of the 95% confidence interval obtained for the parameter.

10.3.2. **The effect of the drug on the kinetics of polymer degradation**

Formulations of various drugs with poly-alpha-hydroxy-aliphatic esters (Ramtoola et al., 1992; Fitzgerald and Corrigan, 1993) released their active compound in a much shorter period of time than the discs presented here. In addition, drug-free PLA/PLGA discs dissolved in less time than equivalent AMOX-H loaded discs, as shown from polymer mass loss profiles and GPC studies.

Table 10.2 summarizes the polymer mass loss results obtained for 20% drug loaded and drug-free discs. In all the cases the presence of the drug resulted in higher t_{maxP} values and lower polymer degradation rate constants k_P.

Table 10.2. Parameters and statistics obtained for polymer mass loss profiles of 20% AMOX and drug-free SE discs prepared with RG 503, RG 504, RG 755, R 203.

System	k_P (h^{-1}) ± SD	t_{maxP} (h) ± SD	r^2	MSC
RG 503 drug-free	0.0105 ± 0.0008	669 ± 7	0.9945	4.76
RG 503 20% drug	0.0098 ± 0.0008	707 ± 10	0.9973	4.30
RG 504 drug-free	0.0123 ± 0.0014	674 ± 9	0.9941	4.64
RG 504 20% drug	0.0082 ± 0.0005	886 ± 10	0.9922	4.45
RG 755 drug-free	0.0116 ± 0.0017	993 ± 16	0.9824	3.68
RG 755 20% drug	0.0034 ± 0.0006	2099 ± 94	0.9899	4.15
R 203 drug-free	0.0069 ± 0.0012	1310 ± 39	0.9997	7.73
R 203 20% drug	0.0032 ± 0.00062	2042 ± 211	0.9948	4.70

The process of mass loss in 20% drug loaded discs was preceded by a considerable reduction of the M_w of the polymer, as was concluded from the data presented in table 9.3. A reduction of approximately 70% of the initial M_w occurred near to the onset of mass loss in PLGA 20% drug loaded systems (RG 504 and RG 755). In the 20% drug loaded PLA system, the M_w showed a 25% decrease by 1084 hours of dissolution, which is a time point earlier than the estimated onset of polymer mass loss for those discs. The decrease of M_w in the corresponding drug-free discs was considerably greater in all the cases investigated (table 9.3).

The magnitude of the effect of the drug on the retardation of polymer degradation appeared to increase both with increasing molecular weight and with increasing lactide content of the polymer. Table 10.3 shows the ratio of t_{maxP} from drug-free discs versus t_{maxP} from 20% drug loaded discs for each of the four polymers. The corresponding k_P ratios are also included in the table. In the case of RG 503 and RG 504, which are both (50:50) PLGA, the magnitude of the effect of the drug on the degradation kinetics of the polymer was greater for the higher molecular weight system (RG 504).

Comparison of RG 503 and R 203, which are the two systems of lowest molecular weight (26,613 and 34,896 respectively) suggests that the increase in lactide content resulted in an increase of the t_{maxP} ratio. On this basis, a higher t_{maxP} ratio for RG 755 systems compared to RG 503 and RG 504 systems was expected, as shown in the table. The results of the k_P ratios were consistent with the t_{maxP} ratios.

Table 10.3. Ratio of t_{maxP} and k_P for 20% drug loaded (D.L.) to drug-free (D.F.) SE discs prepared with RG 503, RG 504, RG 755 and R 203.

System	$\frac{t_{\max P} D.L.}{t_{\max P} D.F.}$	$\frac{k_P D.L.}{k_P D.F.}$
RG 503	1.058	0.93
RG 504	1.315	0.66
RG 755	2.114	0.293
R 203	1.559	0.464

For systems, the release profiles of which contained a polymer degradation mediated release phase, the polymer degradation related parameters t_{max} and k were compared for different drug loadings. Both PLA and PLGA showed increasing retardation of the kinetics of polymer degradation when the drug load increased. This effect was evident in RG 503, RG 504, RG 755 and R 203 systems. More recently Gallagher and Corrigan (1998) investigated the release of albendazole from RG 504 discs in 40% w/v 2-hydroxypropyl-β-cyclodextrin in phosphate buffer pH 7.4 as dissolution media. A retarding effect of the drug on the polymer degradation kinetics was reported on the basis of the polymer degradation related parameters estimated from the drug release profiles. The authors proposed that the retarding effect of the drug could relate to the hydrophobic nature of the drug, as previously reported by Zhang et al. (1995). Nonetheless, since two pKa values (3.89 and 10.40) were reported for albendazole (Gallagher and Corrigan, 1998), and in the light of the results obtained with

Amoxycillin, it is possible that the retarding effect of this drug on the kinetics of polymer degradation was related to the amphoteric nature of the compound.

A study presented by Miyajima et al. (1998) on the effect of basic drugs on the release profiles of low molecular weight (M_w 1500-4500) PLGA systems showed that increasing the proportion of the free bases verapamile and papaverine contained in the polymeric matrix resulted in lower *in vitro* percent release rates. These workers attributed such effect of the drug to a significantly larger number of polymer/drug interactions due to increased drug content, likely to give rise to an increase in the T_g of the polymer making the matrix more rigid. Higher T_g values were observed by these authors when the basic drugs were incorporated to the polymer.

10.3.3. **Surface Erosion of poly-alpha-hydroxy-aliphatic esters**

As mass loss proceeded, the observed changes in the dimensions of the discs indicated that, at later times, surface erosion was playing a part in the dissolution mechanism of PLGA/AMOX systems.

Aso et al. (1994) reported that when the drug release medium was maintained at temperatures above the T_g, degradation of PLA microspheres was a bulk process and drug release was a diffusion controlled process. In contrast, at temperatures below the T_g, degradation was restricted to the surface of the matrix and drug release was caused by matrix surface erosion.

The DSC results previously shown in this thesis, indicated that the inclusion of Amoxycillin did not reduce the T_g of the polymer. Since the glass transition temperatures remained above 40°C and the dissolution media employed in drug release studies was maintained at 37°C, the release of drug from PLA/PLGA systems containing Amoxycillin could be expected to partly occur by erosion mechanisms typical of other biodegradables (poly-ortho-esters and certain polyanhydrides), but not so common to poly-alpha-hydroxy-aliphatic esters (Göpferich, 1996). Gallagher and Corrigan (1998) reported that when levamisole base was incorporated into RG 504 the T_g of the polymer decreased to values below the temperature of the dissolution

medium (37°C), in all the cases investigated. To fit the data, they used a drug release model consistent with bulk erosion.

Gallagher and Corrigan (1998) also reported that the presence of water reduces the T_g of PLA and PLGA to below 37°C. In the current work, however, it is possible to argue that the water did not have a significant effect on Amoxycillin loaded discs, since surface erosion, reported to occur when the T_g values are above the temperature of the dissolution medium, took place.

Use of the Prout-Tomkins equation to describe drug release from bulk eroding polymers was previously placed on a theoretical footing by Fitzgerald and Corrigan (1993). The cube root law of Hixson and Crowell (1931) applies to tablets where dissolution takes place normal to the exposed surface area maintaining the initial geometric shape of the tablet at all times.

Polymer mass loss profiles of 20% Amoxycillin loaded PLA/PLGA discs were fitted (Chapter 9) to both the Prout-Tomkins and the modified Hixson-Crowell models (equations 3.13 and 9.2, respectively). The goodness of the fits obtained for 20% Amoxycillin loaded discs was similar for the bulk and the surface erosion models. However, from a visual inspection of the discs, the surface erosion mechanism appeared to prevail at late times. This was indicated by a decrease in the dimensions of the discs, which maintained their original shape.

To further investigate the contribution of surface erosion mechanisms to the degradation of poly-alpha-hydroxy-aliphatic esters, experimental data reported by Gallagher and Corrigan (1998) for the mass loss profiles of 10% levamisole hydrochloride RG 504 discs, prepared by a solvent-evaporation process, was fitted to equations 3.13 and 9.2. Figure 10.3 shows the relevant plots and tables 10.4 and 10.5 list the parameters estimated by equations 3.13 and 9.2, respectively. The fits obtained with levamisole discs were better using equation 3.13 than equation 9.2, consistent with the commonly reported bulk erosion mechanism for the degradation of PLGA systems.

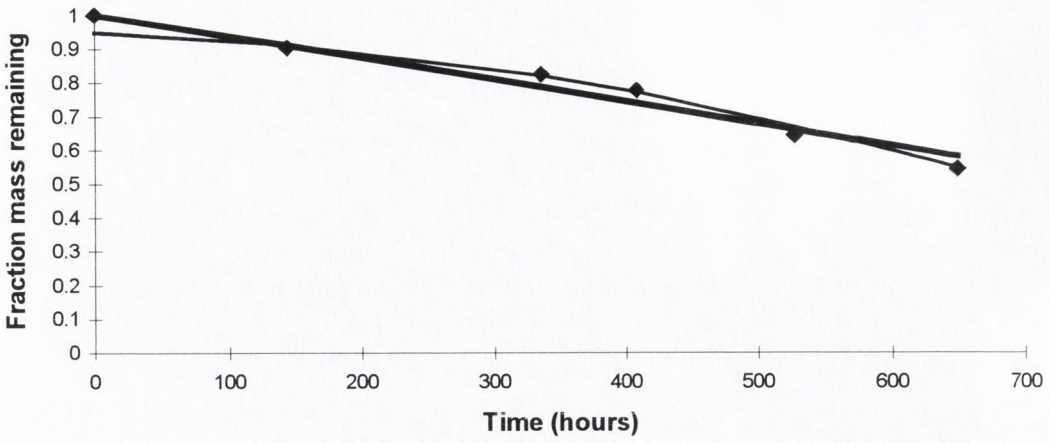

Figure 10.3. Fractional mass loss of 10% levamisole hydrochloride loaded RG 504 SE discs fitted to the Prout Tomkins model (equation 3.13) and the surface erosion related equation 9.2 (heavier line). The data fitted was taken with permission from Gallagher and Corrigan (1998), where the fractional mass loss was calculated for *total* mass loss (polymer and drug).

Table 10.4. Estimated parameters obtained with the bulk erosion related equation 3.13 for the mass loss profiles of RG 504 SE discs loaded with 10% levamisole hydrochloride reported by Gallagher and Corrigan (1998).

t_{max} (h)	k (h^{-1}) x 10^4	r^2	MSC
691.7 $\pm$ 26.9	42 $\pm$ 4.8	0.9763	3.07

Table 10.5. Estimated parameters obtained with the surface erosion related equation 9.2 for the mass loss profiles of RG 504 SE discs loaded with 10% levamisole hydrochloride reported by Gallagher and Corrigan (1998).

t_{lag} (h)	k_2 (h^{-1}) x 10^4	r^2	MSC
7.7 $\pm$ 59	6.5 $\pm$ 0.8	0.9676	2.76

The modified Hixson-Crowell equation (equation 9.2) resulted in better goodness of fit with Amoxycillin data than with levamisole data (comparing tables 9.7 and 10.5), supporting the view that a surface erosion mechanism played a part in the release of the amphoteric drug from poly-alpha-hydroxy-aliphatic esters.

10.4. **INTERACTION BETWEEN AMOXYCILLIN AND PLA/PLGA**

The results presented in the current work have shown that there is a potential interaction taking place between the drug, and/or its breakdown products, and the polymer. Based on the physical changes observed, such as for polymer mass loss and molecular weight, a few possible explanations are proposed in the next paragraphs.

10.4.1. **pH dependent degradation**

It is possible that the observed effect of Amoxycillin on the pH of an aqueous media (Chapter 9) compensated for the acidity generated upon dissolution of the polymer, decreasing the autocatalysed rate of polymer degradation.

The GPC chromatograms of D,L- PLA nanospheres dispersed in acidic medium (pH 2.2) for one month showed an intense broadening of the distribution of polymer chain lengths with a tail covering the low molecular weight area (Belbella et al., 1996). The authors reported that whatever the polymer and the starting pH, the pH of a nanospheres dispersion in unbuffered media rapidly dropped to values near the pKa of lactic acid, i.e. 3.8 at 25°C. The production of lactic acid increased considerably when decreasing the pH from 4 to 2. In contrast, at pH close to neutrality, only a small amount of lactic acid was produced.

The effect of the drug on the pH of the medium, however, does not explain the slowed polymer degradation kinetics observed in discs which were inspected for physical changes beyond the time when all the drug had apparently been released.

10.4.2. **Possible reaction between Amoxycillin and poly-alpha-hydroxy-aliphatic esters**

The chemical structures of Amoxycillin and that of PLA and PLGA are compared in figure 10.4. There is a range of possibilities for reaction both with the drug and its breakdown products.

Since the number of drug molecules per polymer molecule may be roughly estimated as between 60 to 200 depending on the polymer molecular weight of the polymer and loading of drug, only one in every 60-200 molecules of drug would be required to react with the polymer in a 1:1 stoichiometric reaction. NMR studies performed on drug loaded discs (Chapter 9) were carried out to determine a potential bond between the drug and the polymer. Since the signals related to the polymer backbone could mask the signals related to some potential drug-polymer interactions, such as amides or ester groups, the chances of detecting a new bond were dependant on the relative concentration of species. The results obtained with NMR did not suggest any novel groups, either because there was no interaction or the interaction was not detected.

Acid-base interactions were reported as responsible for the decrease of the degradation rate of gentamycin-containing PLA oligomers with respect to drug-free ones, on the basis that carboxylic end-groups catalyzing the hydrolytic degradation of PLA could be neutralized by the drug (Mauduit et al., 1993). It was postulated that, with basic drugs, there is a balance between "stabilization" of the matrix due to ionic interactions with consequent neutralization of end-groups, and "degradation" due to the basicity of the drug. For higher molecular weight polymers, base-catalyzed degradation would be favored over stabilization due to the decrease of the proportion of carboxylic end groups. In the current work, an acid-base reaction between Amoxycillin and the polymer would possibly result in a stabilizing effect (in contrast to a degradation catalysis) due to the amphoteric nature of the drug. Mauduit et al. (1993) postulated

that gentamycin chemically modified the PLA oligomer chains with the formation of ionic clusters known to crosslink the chains.

a)

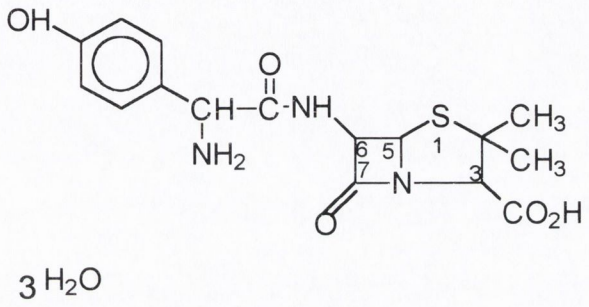

3 H_2O

b)

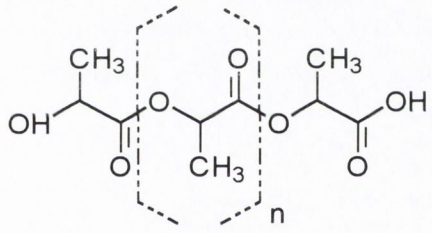

c)

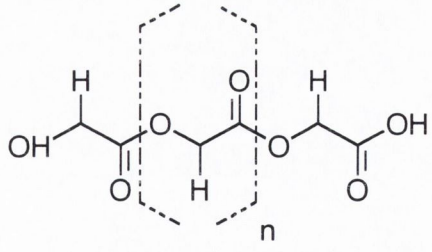

Figure 10.4. Comparison of the structures of a co-oligomer of Amoxycillin and penicilloic acid of Amoxycillin (a), PLA (b), PLGA (c).

The reported polymerization of Amoxycillin (European Pharmacopeia, 1998) may be a factor contributing to prevent the hydrolysis of the carboxylic bond of the polymer, for

the case that self-aminolysis occurred to a molecule of the drug which had reacted with the polymer. Access of water to the end-group ester bond could be more difficult if a tetramer of Amoxycillin was linked to this site. Shih et al. (1995) have shown that the scission of end-groups constitutes an important route of degradation for these polymers.

In Chapter 8, DSC analysis of RG 755 drug loaded systems appeared to indicate that a small proportion of the initial drug load dissolved in the polymer during the SE procedure. In contrast, this was not observed for RG 503, a polymer containing a lower proportion of D,L-lactic acid and which has been shown to be less affected by the presence of the drug.

10.5. THE DEGRADATION OF AMOXYCILLIN IN THE PRESENCE OF POLY-ALPHA-HYDROXY-ALIPHATIC ESTERS

10.5.1. Changes occurring in the discs and in the dissolution medium

PLA (R 203) systems exhibited AMOX degradation during the first phase of drug release. Such drug degradation was apparent from the increasing number of degradation peaks present in the HPLC traces as a function of time. Equivalent PLGA systems showed less proportion of degradation when examined in a similar release time. The effect of the pure PLA polymer on the stability of AMOX was consistent with the previously observed heterogeneous bulk erosion of drug-free R 203 discs (section 8.4.3), which swelled and exhibited a liquid centre. The latter was not observed with PLGA discs, in which the degradation of Amoxycillin resulted in lower fractional values compared to the PLA system (figure 9.3).

Residual Amoxycillin was extracted from PLA and PLGA discs in the course of release studies (section 9.2.7). The fraction of residual intact drug was plotted against time. Polymer and drug degradation in the discs together with the release of intact and total

drug into the dissolution media are represented in the profiles of figure 10.5 for RG 503 (first column) and RG 504 (second column) 20% Amoxycillin loaded SE discs. In the RG 503 solid (I, a), there was less than 20% reduction of the discs mass over the first 500 hours. This was accompanied by the loss of a small proportion of the polymer mass. The residual drug in the discs decreased markedly by the end of the initial 500 hour-period. The appearance of degradation products took place prior to such time. This was consistent with the view point that the onset of polymer degradation triggered degradation of the drug. At approximately 1000 hours, the systems existed as small pieces of material.

The changes of the drug in the RG 503 solid are expanded in (I, b). At approximately 300 hours, the *intact drug* release curve commenced to depart from the curve of *total drug*. The quantity of degradation products in the discs was maximum at approximately 400 hours, after which time the amount of degradation begun to decrease as a result of the release of the compounds into the dissolution medium. Delivery of intact Amoxycillin took place for up to approximately 700 hours (I, c), the drug still trapped at that stage being delivered in a degraded form thereafter.

The second column of figure 10.5 shows the changes occurring in RG 504 discs. There was a gradual loss of 20% discs mass over the first 600 hours of release together with a small loss of polymer (II, a). The drug loss in this period was gradual, with very little generation of degradation products in the discs (II a, b). The discs were depleted of drug by circa 800 hours and pieces of the initial polymer discs were still present by 1100 hours. After released, the drug in solution degraded resulting in substantially different profiles for *total* and *intact drug* (II, c).

The degradation of the drug and polymer in the discs together with the release of intact and total drug from RG 755 and R 203 are represented in figure 10.6. The first column shows the changes occurring in RG 755 discs. Approximately 20% of the discs mass was lost over the first 800 hours (I, a). Polymer loss was not evident in the first 1100 hours of exposure to the dissolution medium. The profiles of drug changes in the in the discs (I, a and b) reflected that the proportion of degradation products was relatively small in this system. The drug released into the dissolution medium (I, c) was partly intact up until 800 hours, after which time the remaining drug was released in a degraded form.

In the second column of figure 10.6, the changes in the R 203 solid are displayed. The mass of the discs slightly decreased over this period (II, a), in accordance with the small proportion of drug that was released in the first 200 hours. Similar to RG 755, polymer mass loss was not evidenced during the first 1100 hours. Analysis of the drug in the discs showed that by 300 hours of dissolution a substantial proportion of drug degradation products was already present in the matrices, which resulted in a larger fraction of degradation by 1000 hours (II, b). The difference between the *total drug* in solution and the *intact drug* in solution was greatest with the R 203 systems compared to the PLGA systems. At 2300 hours, the rate of drug release accelerated (II, c).

In summary, RG 503 discs (figure 10.5, I) were the only systems that delivered intact drug beyond the onset of polymer mass loss, in accordance with the large proportion of total drug still available for release in the final phase of these systems. Nonetheless, R 203 systems (figure 10.6, II), which also delivered a large proportion of drug via polymer degradation, did not show any contribution from intact Amoxycillin in the final phase. Degradation of the drug in the PLA system occurred significantly earlier than polymer mass loss, in contrast to PLGA systems. The overall fraction of degraded drug was greatest in the PLA systems. RG 504 and RG 755 (figures 10.5, II and 10.6, I respectively) were the systems which released the greatest proportion of *intact drug*. The formulation prepared with RG 504 showed the lowest proportion of drug degradation products, in the discs.

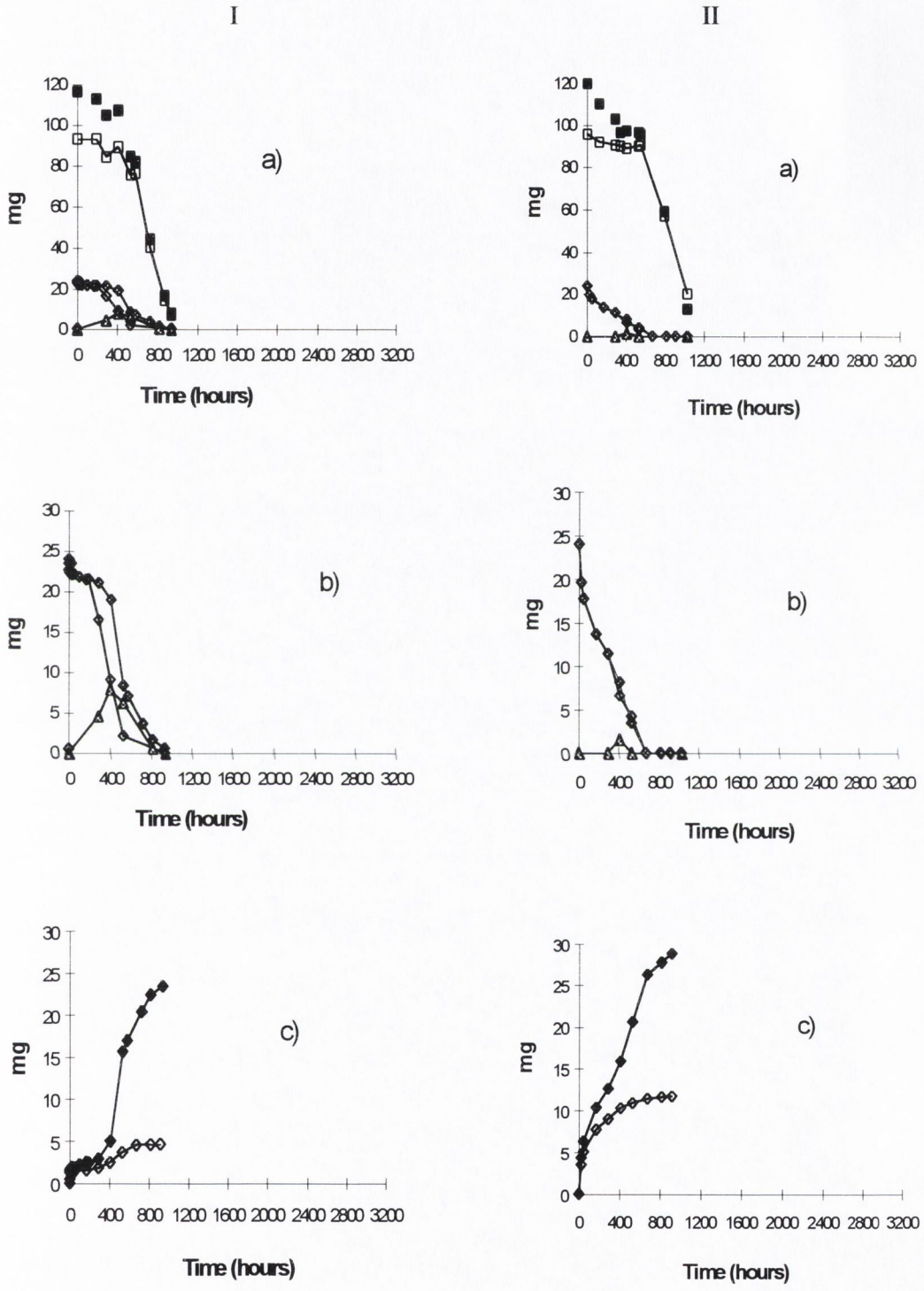

Figure 10.5. Amount versus time plots for RG 503 (I) and RG 504 (II) SE systems showing the changes occurring in the solid (a, b) and in the dissolution medium (c). Key: (■) disc mass loss, (□) polymer mass remaining, (◆) total drug remaining in the discs, (◇) intact drug remaining in the discs, (▲) degradation products formed in the discs, (◆) total drug released, (◇) intact drug released.

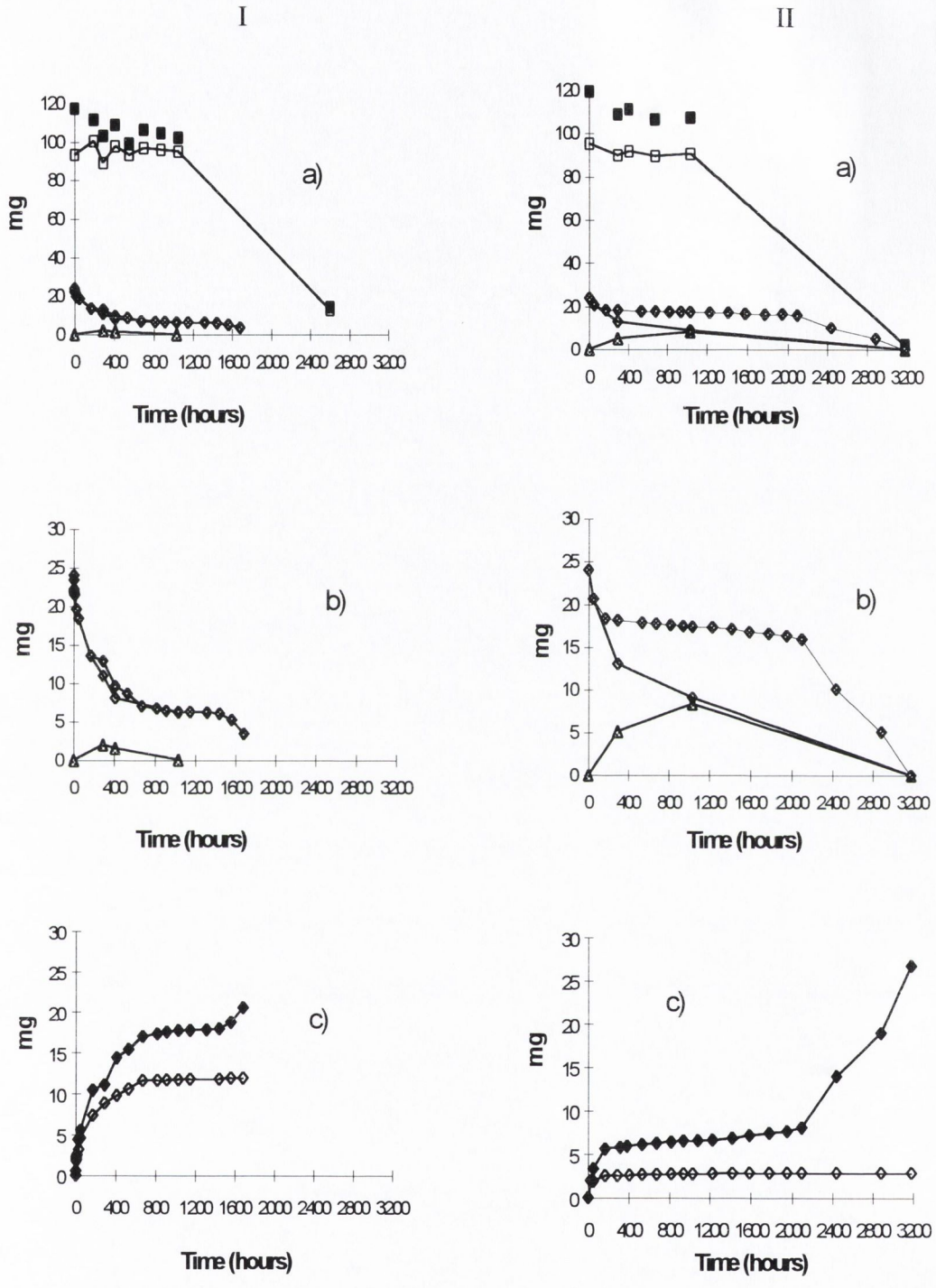

Figure 10.6. Amount versus time plots for RG 755 (I) and R 203 (II) SE systems showing the changes occurring in the solid (a, b) and in the dissolution medium (c). Key: (■) disc mass loss, (□) polymer mass remaining, (◆) total drug remaining in the discs, (◇) intact drug remaining in the discs, (▲) degradation products formed in the discs, (◆) total drug released, (◇) intact drug released.

10.5.2. **The prediction of intact drug released**

Due to the instability of the drug in solution, the proportion of intact drug measured in the dissolution media may be expected to be lower than the proportion of intact drug released from the discs. To obtain a better estimate of the proportion of drug released intact, a mathematical model that accounts for the degradation of the drug following release from the discs was necessary. For the burst phase, the rate of fractional total drug released $\frac{dF_b}{dt}$ may be obtained by differentiation of equation 3.15. The rate is then given by equation 10.1:

$$\frac{dF_b}{dt} = F_{b\infty} . k_b . e^{-k_b t} \qquad \text{equation 10.1}$$

Equation 10.1 was validated by comparing the least squares parameter optimization obtained for a given data set versus the fit obtained with the integrated form of the model (equation 3.14). The results were comparable, as judged by the values of the parameters, their standard deviations and the relevant statistical output, r^2 and MSC.

The rate of change of the concentration of intact drug in solution $\frac{df_b}{dt}$, in the initial burst, will be given by

$$\frac{df_b}{dt} = F_{b\infty} . k_b . e^{-k_b t} - k_{\text{deg}} . f_b \qquad \text{equation 10.2}$$

where f_b is the fraction of intact drug in solution arising from the burst phase and k_{deg} is the degradation rate constant of the pure drug in the dissolution medium.

Equations 10.2 may be combined with equation 3.21 (an equivalent model for the polymer degradation related phase) to obtain the change of total drug concentration in solution $\frac{df_{TOTAL}}{dt}$, arising from the burst and the polymer degradation controlled phases, where degradation of the overall drug in solution occurs by a first-order process with rate k_{deg}:

$$\frac{df_{TOTAL}}{dt} = F_{b\infty}.k_b.e^{-k_b t} - k_{\deg}.f_b + \left(1 - F_{b\infty}\right)k.x\left(1 - \frac{x}{x_{tot}}\right) - k_{\deg}.f_P \qquad \text{equation 10.3}$$

In equation 10.3 (Scientist model file listed in Appendix I), the degradation constant of the pure drug in solution k_{deg} was assumed to be the same for drug released by either an exponential or a polymer dependant mechanism. In the current work, the dissolution medium being frequently replaced, this seemed to be a reasonable assumption since pH changes throughout the release process were kept to a minimum.

The equivalence between the differential equation 10.3 and its related integrated form equation 3.14 was confirmed by fitting the data from *total* drug release (RG 503 SE 20% loaded discs) to the differential form using initial parameter estimates from table 7.14, obtained with equation 3.14, and a value of k_{deg} for the pure drug of 1.43 x 10^{-3} h^{-1} (Chapter 6) which has no bearing in the calculation of *total drug*. The resulting optimized parameters were comparable to the values shown in table 7.14, i.e. equations 3.14 and 10.3 resulted in drug release parameters that were not significantly different in the statistical sense. Appendix III lists the parameters together with the relevant plot.

A simulation of the fractional *intact drug* released from RG 503 20% drug loaded SE discs, relative to *total drug* released, was subsequently generated using equation 10.3 and the parameters obtained for *total drug* (table 7.14). Figure 10.7 shows the resulting plot superimposed to the plot of total drug. As previously discussed, equation 10.3 assumes that there is a cumulative amount of dissolved drug which continuously degrades, i.e. A→ B→ C kinetics, without taking into account the replacement of the dissolution medium. Therefore, upon completion of drug release (depletion of A), the model predicts that the concentration of intact drug in solution (B) will decay, as shown by the lower curve of figure 10.7 towards the end of the experimental time.

Up until the first 400 hours, there was good agreement between the simulated data and the experimental data. In contrast, in the polymer degradation controlled phase the simulated line showed higher values than the experimental line. This appeared to indicate that the degradation of the drug in solution was governed by different rates in the initial and the final drug release phases, possibly due to degradation of drug

occurring in the matrix microenvironment, prior to drug release into the dissolution medium, during the polymer degradation controlled phase. These results support the view point that degradation of Amoxycillin *dissolving* in the solid is triggered by the conversion of the polymer into its acidic constituent sub-units. Once the dissolved drug is released into the dissolution medium, it is likely that the degradation rate constant of the pure drug applies.

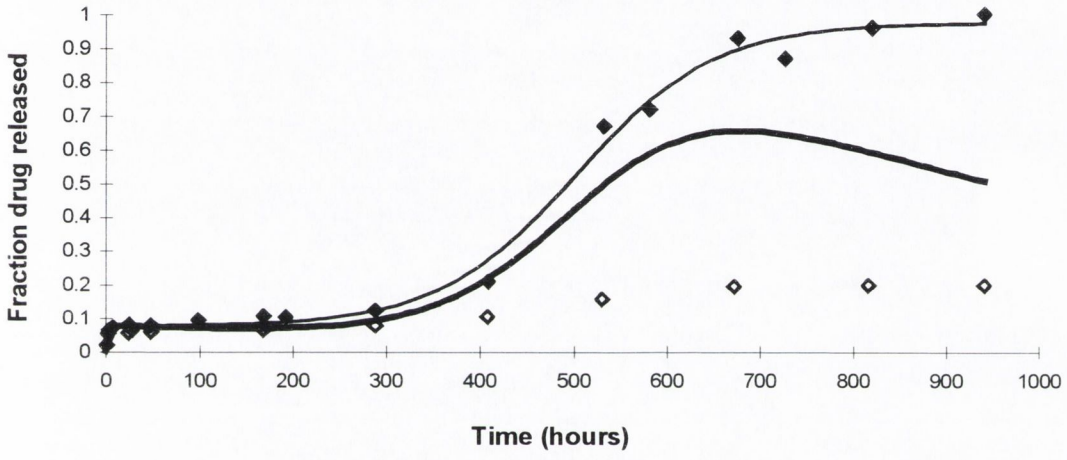

Figure 10.7. Fraction of total and intact drug determined in the release medium for RG 503 20% drug loaded SE discs fitted to equations 3.14 and simulated with equation 10.3 (heavier line), respectively.

The degradation of the drug in the RG 503 solid, also illustrated in the first column of figure 10.5 (b), can be estimated from figure 10.7 as the difference between the experimental and the simulated data.

Figure 10.8 shows the fractional *intact drug* from 10%, 20% and 30% drug loaded SE systems prepared with RG 503 and the corresponding simulated data obtained with equation 10.3. The parameters used were based on the estimates previously obtained with equation 3.14 (table 7.14) for the *total drug* release data. A value of 1.43×10^{-3} h^{-1} was used for k_{deg}, calculated in Chapter 6 for the pure drug.

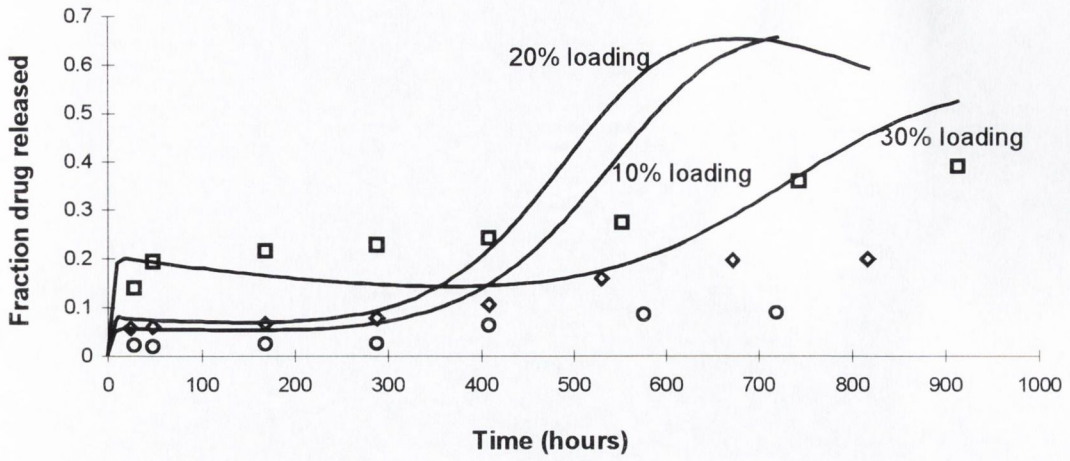

Figure 10.8. Fraction of *intact* drug determined in the release medium of RG 503 10% (O), 20% (◇) and 30% (□) drug loaded SE discs as a function of time. Simulations were obtained with equation 10.3 and parameter estimates from *total* drug release data; k_{deg} was taken from the degradation rate of the pure drug in solution.

As with the 20% drug loading, equation 10.3 predicted for the 10% drug loaded system excessive levels of intact drug, shown by the simulated line, in the final polymer degradation controlled release phase. The 30% drug loaded system, in contrast, showed better agreement between the experimental and the simulated curves.

The difference between the predicted and the experimental values was in inverse rank order with the drug loading, with greatest stability of Amoxycillin in the system containing 30% drug. These results indicated that degradation of the drug in the solid was greatest at the 10% drug loading. For this system, the predicted curve showed values up to 6 fold greater than the experimental values. This is due to the larger burst fraction shown with an increase in the drug loading, resulting in more drug released by a non-polymer degradation mechanism.

To estimate the acceleration of the degradation rate of the drug due to the acidification of the matrix by polymer degradation, different Amoxycillin degradation rate constants for the burst and final release phases were subsequently rendered. Equation 10.3 was modified by means of incorporating k_{degb} as the rate constant governing the degradation of the drug in solution released in the burst (f_b), and k_{degP} as the rate constant that controls the degradation of drug in solution released in the polymer dependant phase (f_P). Thus, equation 10.3 becomes:

$$\frac{df_{TOTAL}}{dt} = F_{b\infty}.k_b.e^{-k_b t} - k_{\deg b}.f_b + \left(1 - F_{b\infty}\right)k.x\left(1 - \frac{x}{x_{tot}}\right) - k_{\deg P}.f_P \qquad \text{equation 10.4}$$

The data of figure 10.8 was then fitted to equation 10.4 to estimate the new parameter k_{degP}. Figure 10.9 shows the new predicted lines for the 10%, 20% and 30% drug loaded systems, which are closer to the experimental data.

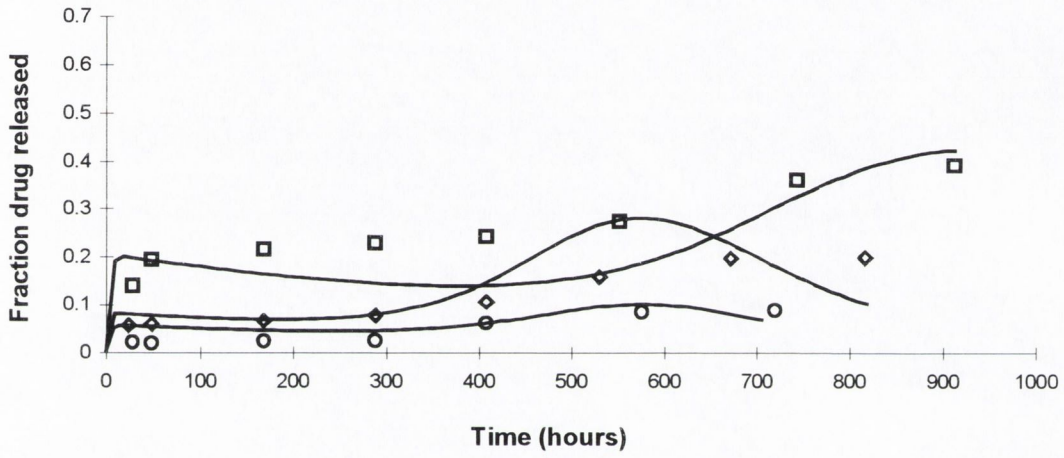

Figure 10.9. Fraction of *intact* drug determined in the release medium of RG 503 10% (O), 20% (◇) and 30% (□) drug loaded SE discs as a function of time. Simulations were obtained with equation 10.4 and parameter estimates from *total* drug release data; k_{degb} was taken from the degradation rate of the pure drug in solution and k_{degP} was allowed to float.

Table 10.6 gives the values of the rate constants for the degradation of Amoxycillin in eroding PLGA matrices k_{degP}, obtained by least squares regression. The rate was greater than the value in phosphate buffer pH 5.9 (0.00143 h^{-1}) in all the systems investigated. An inverse rank order between k_{degP} and the drug loading was found, i.e. the highest value corresponding to the lower loading.

The results shown in table 10.6 provided an estimate of the acceleration of the degradation rate of Amoxycillin in the presence of eroding PLGA. A ratio of 26, 7 and 2 was found for the increase in the degradation rate (relative to the pure drug dissolved in buffer pH 5.9) for 10%, 20% and 30% Amoxycillin loading.

Table 10.6. Estimated rate constants for the degradation of Amoxycillin in eroding PLGA matrices, for 10%, 20% and 30% drug loaded SE discs.

RG 503 SE system	k_{degP} (h^{-1})
10% loading	0.03713 ± 0.01078
20% loading	0.01022 ± 0.00262
30% loading	0.00276 ± 0.00101

10.6. **CONCLUSION**

The preparation of Amoxycillin controlled release discs with poly-alpha-hydroxy-aliphatic esters can be performed by compressing a mechanical mixture of the drug and polymer or by filmcasting a suspension of the drug in a polymer solution. The release characteristics of the discs prepared by these two methods differ significantly. Mechanically mixed discs resulted in *in vitro* release profiles with significant drug release for the first 48 hours only. In contrast, two significant release phases, an initial burst and a second phase at long and variable times, may be obtained with systems prepared by solvent evaporation.

The drug loading is an important factor determining the shape of the profile and the duration of release. Profiles with an initial burst and a polymer degradation controlled phase of drug release, are obtainable with SE discs at low drug loading, for instance 10% loading. However, in these systems the stability of the drug is compromised in the final phase, due to acidification of the matrix upon degradation of the polymer. PLGA SE systems containing 40%, 50% and 60% drug loading release all the drug in a single phase over a time period that can vary between 4 to 8 days (RG 755 SE discs). The stability of the drug is enhanced where release is solely controlled by matrix diffusion, such as with highly loaded discs.

The release profiles of a given drug loading vary depending on the type of polymer and the processing method employed. Increasing the proportion of lactide in the polymer resulted in longer duration of drug release. Discs prepared from mechanical mixtures released practically all the drug within the first 48 hours from the commencement of release.

An unexpected finding was the retarding effect of the drug on the degradation kinetics of high molecular weight poly-alpha-hydroxy-aliphatic esters. Drug-free discs eroded in a shorter period of time and at a faster rate than drug-loaded discs, in contrast to the erosion of similar systems loaded with basic drugs reported by other workers (Fitzgerald and Corrigan, 1993; Gallagher and Corrigan, 1998). Furthermore, a proportional decrease in dimensions after prolonged dissolution times was observed, which is consistent with the Hixson-Crowell cube root law for surface erosion not commonly reported for these polymers. An interaction between the drug and the polymer appeared to be taking place.

The stability of the drug carried in these matrices is dependant on the type of polymer and the preparation method used. The drug loading indirectly plays a part in the degradation of the drug. Those systems releasing a larger proportion of the loading prior to the onset of polymer mass loss resulted in higher levels of overall intact drug. RG 504 and RG 755 systems released the greatest proportion of intact drug.

This work shows that intact Amoxycillin may be delivered for a period of up to 700 hours by a single polymer disc prepared with poly-alpha-hydroxy-aliphatic esters, such as the case of 20% drug loaded RG 504 systems which showed the lowest proportion of degradation products in the solid state analysis (figures 10.5 and 10.6). Mathematical models applied to the release of Amoxycillin (equations 3.14, 3.19 and 3.20) can aid the formulator in predicting the release of more complex amphoteric compounds, i.e. peptides. A model was proposed (equations 10.3) to predict the proportion of intact drug in solution from the measurement of total drug. The model was modified (equation 10.4) to estimate the acceleration of the rate of drug degradation in the microenvironment of the PLGA matrix.

The delivery of therapeutically active Amoxycillin over a period of a week may find possible applications in the veterinarian field. RG 755 SE discs loaded with 50% Amoxycillin release intact drug over approximately 10 days. When the drug loading is reduced to 30% and the formulation is prepared with RG 503, the release of intact drug is extended to approximately 40 days. A combination of PLGA systems in a single product also has potential application in the treatment of human osteomyelitis for which continuous antibiotic treatment over 4 to 6 weeks is recommended.

REFERENCES

Asano, M., Yoshida, M., Kaetsu, I., *Biodegradability of a Hot-Pressed Poly(Lactic Acid) Formulation with Controlled Release of LH-RH Agonist and its Pharmacological Influence on Rat Prostate*, Macromolecular Chemistry Rapid Communication, 6 (1985), 509-516.

Aso, Y., Yoshioka, S., Terao, T., *Effects of Storage on the Physicochemical Properties and Release Characteristics of Progesterone-Loaded Poly(l-lactide) Microspheres*, International Journal of Pharmaceutics, 93 (1993,) 153-159.

Aso, Y., Yoshioka, S., Po, A. L. W., Terao, T., *Effect of Temperature on Mechanisms of Drug Release and Matrix Degradation of Poly(dl-Lactide) Microspheres*, Journal of Controlled Release, 31 (1994), 33-39.

Avgoustakis, K. and Nixon, J. R., Biodegradable Controlled Release Tablets 1: *Preparative Variables Affecting the Properties of Poly(Lactide-Co-Glycolide) Copolymers as Matrix Forming Material*, International Journal of Pharmaceutics, 70 (1991), 77-85.

Batycky, R.P., Hanes, J., Langer, R., Edwards, D.A., *A Theoretical Model of Erosion and Macromolecular Drug Release from Biodegrading Microspheres,* Journal of Pharmaceutical Sciences, 86 (12) (1997), 1464-1477.

Belbella, A., Vauthier, C., Fessi, H., Devisaguet, F.P, *In vitro degradation of nanospheres from poly(D,L-lactides) of different molecular weights and polydispersities,* International Journal of Pharmaceutics, 129 (1996), 95-102.

Benoit, J.P., Courteille, F., Thies, C., *A Physicochemical Study of the Morphology of Progesterone-Loaded Poly (d,l-Lactide) Microspheres*, International Journal of Pharmaceutics, 29 (1986), 95-102.

Bhattacharyya, P.K. and Cort, W.M., Analytical profiles of drug substances, vol. 7, Ed: Florey, K., Academic Press, New York (1978), 19-41.

Bodmer, D., Kissel, T. and Traechslin, E., *Factors influencing the release of peptides and proteins form biodegradable parenteral depot systems,* Journal of Controlled Release, 21 (1992), 129-138.

Bonny, J.D., Leuenberger, H., *Matrix Type Controlled Release Systems I: Effect of Percolation on Drug Dissolution Kinetics*, Pharmaceutica Acta Helvetica, 66 (5-6) (1991), 160-164.

British Pharmacopeia (1993).

Calhoun, J. H. and Mader, J. T., *Treatment of Osteomyelitis with a Biodegradable Antibiotic Implant,* Clinical Orthopaedics and Related Research, 341 (1997), 206-214.

Cha, Y. and Pitt, C. G., *The Acceleration of Degradation-Controlled Drug Delivery from Polyester Microspheres*, Journal of Controlled Release, 8 (1989), 259-265.

Chandrashekar, G. and Udupa, N., *Biodegradable Injectable Implant Systems for Long Term Drug Delivery Using Poly(Lactic-co-glycolic) Acid Copolymers,* Journal of Pharmacy and Pharmacology, 48 (1996), 669-674.

Chu, C.C. and Campbell, N.D., Journal of Biomedical Materials Research, 16 (1982), 417.

Cobby, J., Mayershon, M. and Walker, C., *Influence of Shape Factors on Kinetics of Drug Release from Matrix Tablets I: Theoretical*, Journal of Pharmaceutical. Sciences, 63 (5) (1974), 725-732.

Concannon, J., Lovitt, H., Ramage, M., Hoon Tai, L., McDonald, Ch., Sunderland, B., *Stability of aqueous solutions of amoxicillin sodium in the frozen and liquid states,* American Journal of Hospital Pharmacy, 43 (1986), 3027-3030.

Conti, B., Pavanetto, F., Genta, I., *Use of polylactic acid for the preparation of microparticulate drug delivery systems,* Journal of Microencapsulation, 9 (2) (1992), 153-166.

Corrigan, O.I., Gallagher, K.M., Fitzgerald, J.F., "*Mechanistic Aspects of The Release of Levamisole Hydrochloride from a Biodegradable Polymer*", in Proceedings of the 16th Pharmaceutical Technology Conference, Athens, April (1997).

Corrigan, O.I. and Holohan, E.M., *Amorphous spray-dried hydroflumethiazide-polyvinylpirrolidone systems: physicochemical properties,* Journal of Pharmacy and Pharmacology, 36 (1984), 217-221.

De Luca, P.P., Mehta, R.C., Hausenberger, A.G., Thanoo, B.C., *Biodegradable Polyesters for Drugs and Polypeptide Delivery in Polymeric Delivery Systems*, in 'Polymeric Delivery Systems', American Chemical Society, C 4 (1993), 53-79.

Doff, D.H., Brownen, F.L, Corrigan, O.I., *Determination of α-Impurities in the β-Polymorph of Inosine Using Infrared Spectroscopy and X-ray Powder Diffraction,* Analyst, vol. III February (1986), 179-182.

Eenink, M.J.D., Feijen, J., Olijslager, J., Albers, J.H.M., Rieke, J.C., Geidanus, P.J., *Biodegradable Hollow Fibres for the Controlled Release of Hormones,* Journal of Controlled Release, 6 (1987), 225-247.

Ellis, M. and Corrigan, O.I. (Supervision), M.Sc. thesis submitted at Trinity College Dublin (1994).

European Pharmacopeia (1998).

Fitzgerald, J. F. and Corrigan, O. I., *Mechanisms Governing Drug Release From Poly α Hydroxy Aliphatic Esters, Diltiazem Base Release From Poly-Lactide-co-Glycolide Delivery Systems*, in 'Polymeric Delivery Systems', American Chemical Society (1993), 311-326.

Fitzgerald, J.F. and Corrigan, O.I., *Investigation of the Mechanisms Governing the Release of Levamisole from Poly-Lactide-co-Glycolide Delivery Systems*, Journal of Controlled Release, 42 (1996), 125-132.

Floy, B. J., Visor, G. C. and Sanders, L. M., *Design of Biodegradable Polymer Systems for Controlled Release of Bioactive Agents*, in 'Polymeric Delivery Systems', American Chemical Society, (1993), 155-167.

Ford, J.L. and Timmins, P., *The use of thermal analysis in polymeric drug delivery systems* in 'Pharmaceutical Thermal Analysis, Techniques and Applications', Ellis Horwood Ltd., Chichester (1989).

Frazza, E.J. and Schmitt, E.E., *A New Absorbable Suture*, Journal of Biomedical Materials Research, 1 (1971), 43.

Fukuzaki, H., Yoshida, M., Asano, M. and Kumakura, M., *Synthesis of Copoly(D,L-Lactic Acid) With Relatively Low Molecular Weight and In Vitro Degradation*, European Polymer Journal, 25 (10) (1989),1019-1026.

Fukuzaki, H., Yoshida, M., Asano, M. Kumakura, M., Mashimo, T., Yuasa, H., Imai, K., Yamanaka, H., *In Vivo Characteristics of High Molecular Weight Copoly(l-Lactide/Glycolide) with S-Type Degradation Pattern for Application in Drug Delivery Systems*, Biomaterials, 12 (1991), 433-437.

Furr, B. J. A. and Hutchinson, F.G., *A biodegradable delivery system for peptides: preclinical experience with the gonadotrophin-releasing hormone agonist Zoladex®,* Journal of Controlled Release, 21 (1992), 117-128.

Gallagher, K. and Corrigan, O.I. (Supervision), Ph.D. thesis submitted at Trinity College Dublin (1998).

Gido, C., Langguth, P., and Mutschler, E., *Predictions of in Vivo Plasma Concentration from in Vitro Release Kinetics: Application to Doxepin Parenteral (I.M) Suspensions in Lipophilic Vehicles in Dogs,* Pharmaceutical Research, 11 (6) (1994), 800-809.

Gilding, D.K. and Reed, A.M., *Biodegradable polymers for use in surgery_polyglycolic/poly(lactic acid) homo and copolymers: 1,* Polymer, 20 (1979), 1459-1464.

Gilding, D.K. and Reed, A.M., *Biodegradable polymers for use in surgery_polyglycolic/poly(lactic acid) homo and copolymers: 2,* Polymer, 22 (1981), 494-498.

Göpferich, A., *Review: Polymer Degradation and Erosion: Mechanisms and Applications,* European Journal of Pharmaceutics and Biopharmaceutics, 42 (1) (1996), 1-11.

Göpferich, A., Langer, S., *Modeling of polymer erosion in three dimensions-rotationally symmetric devices,* AIChE Journal, 41 (1995), 2292-2299.

Graham, P.D., Brodbeck, K.J., McHugh, A.J., *Phase inversion dynamics of PLGA solutions related to drug delivery,* Journal of Controlled Release, 58 (1999), 233-245.

Hausberger, A.G., Kenley, R.A., De Luca, P.P., *Gamma Irradiation Effects on Molecular Weight and in Vitro Degradation of Poly(D,L-Lactide-Co-Glycolide) Microparticles,* Pharmaceutical Research, 12 (6) (1995), 851-856.

Heller, J., Helwing, R.F., Baker, R.W. and Tuttle, M.E., *Controlled release of water-soluble macromolecules from bioerodible hydrogels,* Biomaterials, 4 (1983), 262-266.

Heller, J., *Polymers for controlled parenteral delivery of peptides and proteins,* Advanced Drug Delivery Reviews, 10 (1993), 163-204.

Herrlinger M., In vitro Polymerabbau and Wirkstofffreigabe von poly-DL-Laktid-Formlingen. PhD thesis, University of Heidelberg, Germany (1994).

Higuchi, T., *Rate of Release of Medicaments from Ointment Bases Containing Drugs in Suspension*, Journal of Pharmaceutical Sciences, 50 (10) (1961), 874-875.

Higuchi, T., *Mechanism of Sustained-Action Medication*, Journal of Pharmaceutical Sciences, 52 (1963), 1145-1149.

Hixson, A.W. and Crowell, J.H., *Dependence of Reaction Velocity upon Surface and Agitation,* Industrial and Engineering Chemistry, 23 (1931), 923-931.

Hou, J.P. and Poole, J.W., *The Amino Acid Nature of Ampicillin and Related Penicillins,* Journal of Pharmaceutical Sciences, 58 (12) (1969), 1510-1515.

Hutchinson, F. G. and Furr, B. J. A., *Biodegradable carriers for the sustained release of polypeptides,* Tibtech., 5 (1987), 102-106.

Hutchinson, F.G. and Furr, B. J. A., *Biodegradable Polymer Systems for the Sustained Release of Polypeptides*, Journal of Controlled Release, 13 (1990), 279-294.

Hydranal Manual, Riedel de Haen, 1988.

Iwata, M. and McGinity, W., *Preparation of multi-phase microspheres of poly(D,L-lactic acid) and poly(D,L-lactic-co-glycolic acid) containing a W/O emulsion by a multiple emulsion solvent evaporation technique,* Journal of Microencapsulation, 9 (2) (1992), 201-214.

Iwata, M. and McGinity, W., *Dissolution, Stability, and Morphological Properties of Conventional and Multiphase Poly(DL-Lactic-Co-Glycolic Acid) Microspheres*

Containing Water-Soluble Compounds, Pharmaceutical Research, 10 (8) (1993), 1219-1227.

Jalil, R. and Nixon, J.R., *Biodegradable Poly(Lactic Acid) and Poly (Lactide-Co-Glycolide) Microcapsules: Problems Associated with Preparative Techniques and Release Properties,* Journal of Microencapsulation, 7 (1990a), 297-235.

Jalil, R. and Nixon, J.R., *Microencapsulation Using Poly(D,L-Lactic Acid) III: Effect of Polymer Molecular Weight on Release Kinetics,* Journal of Microencapsulation, 7 (1990b), 357-374.

Jalil, R. and Nixon, J.R., *Microencapsulation Using Poly(L-Lactic Acid) IV: Release Properties of Microcapsules Containing Phenobarbitone,* Journal of Microencapsulation, 7 (1990c), 53-66.

Kim, J.H., Kwon, I.C., Kim, Y.H., Shon, Y.T., Jeong, S.Y., *The modified solvent extraction method on the preparation of poly(L-lactic acid) microspheres,* Proceedings of the International Symposium on Controlled Release of Bioactive Materials, 24 (1997), 549-550.

Langer R., Peppas, N., *Chemical and physical structure of polymers as carriers for controlled release of bioactive agents: A review,* J. Macromol. Sci. - Rev. Macromol. Chem. Phys., C23 (1983) 61-126.

Lashev, L.D., Pashov, D.A., *Interspecies variations in plasma half-life of ampicillin, amoxycillin, sulphadiamide and sulphacetamide related to variations in body mass,* Research in Veterinary Science, 53 (1992) 160-64.

Ledwidge, M. and Corrigan, O.I. (Supervision), Ph.D. thesis submitted at Trinity College Dublin (1997).

Lee, P.I., *Diffusional Release of a Solute from a Polymeric Matrix_Approximate Analytical Solutions,* Journal of Membrane Science, 7 (1980), 255-275.

Le Ray, A.M., Vert, M., Benoit, J.P., *Synthesis of Radiolabeled Poly(α-hydroxy acid). Preparation and In Vivo Studies of ^{14}C-Poly(d,l-lactide-co-glycolide) Nanoparticles,* Proceedings of the International Symposium on Controlled Release of Bioactive Materials, 18 (1991), 461-462.

Li, S.M., Garreau, H., Vert, M., *Structure-Properties Relationships in the Case of the Degradation of Massive Aliphatic Poly-(α-Hydroxy Acids) in Aqueous Media, Part 2*, Journal of Materials Science: Materials in Medicine, 1 (1990), 123-130.

Li, S.M., Garreau, H., Vert, M., Therin, M., Christel, P., *In vivo degradation mechanism of massive aliphatic polyesters derived from lactic and glycolic acids, In: Vert, M., Feijen, J., Albertson, A., Scott, G., Chiellini, E. (Eds.),* Biodegradable Polymers and Plastics. Redwood Press Ltd., Melksham, UK, (1992), 7-20.

Li, S., Girod-Holland, S., Vert, M., *Hydrolytic Degradation of Poly(dl-Lactic Acid) in the Presence of Caffeine Base*, Journal of Controlled Release, 40 (1996), 41-53.

Makino, K., Masayuki, A., Kondo, T., *Preparation and in Vitro Degradation Properties of Polylactide Microcapsules,* Chemical and Pharmaceutical Bulletin, 33 (1985), 1195-1201.

Makino, K., Oshima, H., Kondo, T., *Mechanism of Hydrolytic Degradation of Poly(l-Lactide) Microcapsules: Effects of pH, Ionic Strength and Buffer Concentration,* Journal of Microencapsulation, 3 (1986), 203-212.

Makino, K, Oshima, H., Kondo, T., *Effects of Plasma Proteins on Degradation Properties of Poly(l-lactide) Microcapsules,* Pharmaceutical Research, 4(1) (1987), 62-65.

Martin, A. M., *Physical Pharmacy*, Lea and Febiger, Philadelphia, London (1993).

Martindale, The Extra Pharmacopoeia, 30th Edition, Reynolds, J.E.F. (Ed.), The Pharmaceutical Press, London (1993).

Mauduit, J., Bukh, N. and Vert, M., *Gentamycin/poly(lactic acid) blends aimed at sustained release of local antibiotic therapy administered per-operatively. I. The case of gentamycin base and gentamycin sulphate in poly(DL-lactic acid) oligomers,* Journal of Controlled Release, 23 (1993) 209-220.

Maulding, H.V., *Prolonged Delivery of Peptides by Microcapsules*, Journal of Controlled Release, 6 (1987), 167-176.

Mc Donald, C., Sunderland, V.B., Lau, H., Shija, R., *The Stability of Amoxycillin Sodium in Normal Saline and Glucose (5%) Solutions in the Liquid and Frozen States,* Journal of Clinical Pharmacy and Therapeutics, 14 (1989), 45-52.

Mendez, R., Alemany, M.T., Jurado, C., Martin, J., *Study on the Rate of Decomposition of Amoxycillin in Solid State using High-Performance Liquid Chromatography,* Drug Development and Industrial Pharmacy, 15 (8) (1989), 1263-1274.

Mettler Toledo STARe Thermal Analysis System version 5.1 User Manual (1998).

Miller, R.A., Brady, J.M., Cutright, D.E., *Degradation Rates of Oral Resorbable Implants (Polylactates and Polyglycolates): Rate Modification with Changes in PLA/PGA Copolymer Ratios,* Journal of Biomedical Materials Research, 11 (1977), 711-719.

Min, Y.G., Kim, Y.K., Choi, Y.S., Shin, J.S., Kuhun, S.K., *Mucociliary Activity and Histopathology of Sinus Mucosa in Experimental Maxillary Sinusitis: A Comparison of Systemic Administration of Antibiotic and Antibiotic Delivery by Polylactic Acid Polymer,* Laryngoscope, 105 (1995), 835-842.

Miyajima, M., Koshika, A., Okada, J., Kusai, A., Ikeda, M., *The effects of drug physico-chemical properties on release from copoly (lactic/glycolic acid) matrix,* International Journal of Pharmaceutics, 169 (1998), 255-263.

Painter, P.C. and Coleman, M.M., *Fundamentals of Polymer Science, An Introductory Text,* 1994.

Park, T.G., Lu and W., Crotts, G., *Importance of In Vitro Experimental Conditions on Protein Release Kinetics, Stability and Polymer Degradation in Protein Encapsulated Poly(d,l-Lactic-Co-Glycolic Acid) Microspheres,* Journal of Controlled Release, 33 (1995), 211-222.

Paul, M., Fessi, H, Laatiris, A., Boulard, Y., Durand, R., Deniau, M., Astier, A., *Pentamidine-loaded poly(D,L-lactide) nanoparticles: physicochemical properties and stability work,* International Journal of Pharmaceutics, 159 (1997), 223-232.

Pharmaceutical Handbook, 19th Ed., A. Wade (Ed.), The Pharmaceutical Press, London (1980).

Phillips, M. and Gresser, J.D., *Sustained-Release Characteristics of a New Implantable Formulation of Disulfiram,* Journal of Pharmaceutical Sciences, 73 (12) (1984), 1718-1720.

Pitt, C.G., Gratzl, M.M., Kimmel, G.L., Surles, J. and Schindler, A., *Aliphatic polyesters II. The degradation of poly(DL-lactide), poly(ε-caprolactone) and their copolymers in vivo,* Biomaterials, 2 (1981), 215-220.

Pitt, C.G. and Schindler, A., *The Design of Controlled Drug Delivery Systems Based on Biodegradable Polymers*, in 'Biodegradable and Delivery Systems for Contraception', vol. 1, Hafez, E.S.E., van Os, W.A.A. Eds, MTP Press Ltd., Lancaster, England (1980), 17-46.

Prout, E.G., Tompkins, F.C., *The Thermal Decomposition of Potassium Permanganate,* Transactions of the Faraday Society, 40 (1994), 488-498.

Ramtoola, Z., Corrigan, O.I. and Barrett, J.C., *Release Kinetics of Fluphenazine from Biodegradable Microspheres*, Journal of Microencapsulation, 9 (4) (1992), 415-423.

Ramtoola, Z., Corrigan, O.I. and Bourke, E., *Characterization of Biodegradable Microspheres Containing Dihydro-Iso-Androsterone*, Drug Development and Industrial Pharmacy, 17 (1991), 1857-1873.

Redmon, M.P., Hickey, A.J., De Luca, P.P, *Prednisolone-21-Acetate Poly(Glycolic Acid) Microspheres: Influence of Matrix Characteristics on Release,* Journal of Controlled Release, 9 (1989), 99-109.

Ries, R. and Moll, F., *Matrix Formation of Polyglycolic Acid Tablets by Annealing,* European Journal of Pharmaceutics and Biopharmaceutics, 40 (1) (1994), 14-18.

Ritger, P.L. and Peppas, N.A., *A Simple Equation for the Description of Solute Release I. Fickian and non-Fickian Release from Non-Swellable Devices in the Form of Slabs, Spheres, Cylinders or Discs,* Journal of Controlled Release, 5 (1987a), 23-36.

Ritger, P.L. and Peppas, N.A., *A Simple Equation for the Description of Solute Release II. Fickian and anomalous Release from Swellable Devices,* Journal of Controlled Release, 5 (1987b), 37-42.

Sah, H. and Chien, Y. W., *Effects of H^+ liberated from Hydrolytic Cleavage of Polyester Microcapsules on their Permeabiltiy and Degradabiltiy*, Journal of Pharmaceutical Sciences, 84 (11) (1995), 1353-1359.

Sanders, L.M., Kent, J.S., Mc Rae, G.I., Vickery, B.H., Tice, T.R., Lewis, D.H., *Controlled Release of Luteinizing Hormone-Releasing Hormone Analogue from Poly(d,l-lactide-co-glycolide) Microspheres,* Journal of Pharmaceutical Sciences, 73 (9) (1984), 1294-1297.

Sanders, L.M., Kell, B.A., Mc Rae, G.I. Whitehead, G.W., *Prolonged Controlled-Release of Nafarelin, a Luteinizing Hormone-Releasing Hormone Analogue, From Biodegradable Polymeric Implants: Influence of Composition and Molecular Weight of polymer*, Journal of Pharmaceutical Sciences, 75 (1986a) 356-360.

Sanders, L.M., Mc Rae, G.I., Vitale, K.M., Kell, B.A., *Controlled Delivery of an LHRH Analogue from Biodegradable Injectable Microspheres,* Journal of Controlled Release, 2 (1986b), 187-195.

Sato, T., Kanke, M., Schroeder, H.G., DeLuca, P.P., *Porous Biodegradable Microspheres for Controlled Drug Delivery. I. Assessment of Processing Conditions and Solvent Removal Techniques,* Pharmaceutical Research, 5 (1) (1988), 21-30.

Schartel, B., Volland, C.H., Li, Y.X., Wendorff, J.W., Kissel, T., *Dielectric and thermodynamic properties of biodegradable poly(D,L-lactide-co-glycolide) and the effect on the microencapsulation and release of captopril,* Journal of Microencapsulation, 14 (4) (1997), 475-488.

Schlicher, E.J.A.M., Postma, N.S., Zuidema, J., Talsma, H. and Hennik, W.E., *Preparation and Characterization of poly(D,L-lactic-co-glycolic acid) microspheres containing desferrioxamine,* in 'Drug Delivery Approaches in Malaria Treatment', Utrecht University, The Netherlands (1997).

Schmitt, E.E., Epstein, M., Polistina, R.A., *Process for polymerizing a glycolide,* U.S. Patent, 3422871 (1969).

Schmitt, E.A., Flanagan, D.R., Linhardt, R.J., *Degradation and Release Properties Of Pellets Fabricated From Three Commercial Poly(D,L-Lactide-Co-Glycolide) Biodegradable Polymers*, Journal of Pharmaceutical Sciences, 82 (1993), 326-329.

Schwartz, J. B., Simonelli, A. P. and Higuchi, W.I., *Drug Release from Wax Matrices I: Analysis of Data with First-Order Kinetics and with the Diffusion-Controlled Model,* Journal of Pharmaceutical Sciences, 57 (2) (1968), 274-277.

Scientist User Handbook, Micromath Scientific Software, Utah, U.S.A (1995).

Shih, C., *Chain-End Scission in Acid Catalyzed Hydrolysis of Poly(D,L-Lactide) in Solution*, Journal of Controlled Release, 34 (1995), 9-15.

Shively, M.L., Coonts, B.A., Renner, W.D., Southard, J.L., Bennett, A.T., *Physico-chemical characterization of a polymeric injectable implant delivery system,* Journal of Controlled Release 33 (1995), 237-243.

Siegel, R., *Modelling of Drug Release in Porous Polymers* in 'Controlled Release of Drugs: Polymers and Aggregate Systems', Rosoff, M. (Ed.), VCH Publishers, N.Y., (1989), 1-51.

Siegel, R. and Langer, R., *Mechanistic Studies of Macromolecular Drug Release from Macroporous Polymers. II. Models for the Slow Kinetics of Drug Release.* Journal of Controlled Release, 14 (1990), 153-167.

Singh, M., McGee, J.P., Li, X-M., Koff, W., Zamb, T., Wang, C.Y., O'Hagan, D.T., *Biodegradable Microparticles with an Entrapped Branched Octameric Peptide as a Controlled-Release HIV-1 Vaccine,* Journal of Pharmaceutical Sciences, 86 (11) (1997), 1229-1233.

Statistics, An Introduction, Mason, R.D., Lind, D.A., Marchal, W.G. (1998).

Suzuki, K. and Price, J.C., *Microencapsulation and Dissolution Properties of a Neuroleptic in a Biodegradable Polymer, Poly(d,l-lactide),* Journal of Pharmaceutical Sciences, 74 (1) (1985), 21-24.

The Data Sheet Compendium, (1995-1996), Ed: Irish Pharmaceutical Healthcare Association.

The Merck Index, 12th Edition, Ed. S. Budavari (1996) Merck, New Jersey.

Thomasin, C., Corradin, G., Men, Y., Merkle, H.P., Gander, B., *Tetanus Toxoid and Synthetic Malaria containing Poly(Lactide)/Poly(Lactide-Co-Glycolide) Microspheres: Importance of Polymer Degradation and Antigen Release for Immune Response,* Journal of Controlled Release, 41 (1996), 131-145.

Tsuji, A., Nakashima, E., Shoichiro, H., Yamana, I., *Physicochemical Properties of Amphoteric β-Lactam Antibiotics I: Stability, Solubility, and Dissolution Behavior of*

Amino Penicillins as a Function of pH, Journal of Pharmaceutical Sciences, 67 (8) (1978), 1059-1066.

USP XXIII, 1995.

Van Krimpen, P.C., Bult, A., Review articles: *Penicillins and cephalosporins: Physicochemical properties and analysis in pharmaceutical and biological matrices,* Pharmaceutisch Weekblad Scientific Edition, 9 (1987), 1-23.

Wagner, J., *Interpretation of Percent Dissolved-Time Plots Derived From In Vitro Testing of Conventional Tablets and Capsules*, Journal of Pharmaceutical Sciences, 58 (10) (1969), 1253-1257.

Wakiyama, N., Juni, K., Nakano, M., *Preparation and Evaluation In Vitro of Polylactic Acid Microspheres Containing Local Anaesthetics*, Chemical and Pharmaceutical Bulletin, 29 (1981), 3365-3368.

Young, R.J., Lovell, P.A., Introduction to Polymers, 2nd Edition, Chapman and Hall, London (1991).

Zhang, X., Wyss, U.P., Pichora, D. and Goosen, M.F.A., *Biodegradable Controlled Antibiotic Release Devices for Osteomyelitis: Optimization of Release Properties*, Journal of Pharmacy and Pharmacology, 46 (1994), 714-724.

APPENDIX I (SCIENTIST MICROMATH MODEL FILES)

Micromath model file for equation 3.10 (square root of time diffusion, with shape factor)

IndVars: T

DepVars:ftot

Params: KR

fd := 18.25*KR*T^0.5-33.5*(KR*T^0.5)^2+16.25*(KR*T^0.5)^3

ftot=ifgtzero(fd-1,1,fd)

Micromath model file for equation 3.14 (exponential burst, degradation control)

IndVars: T

DepVars: ftot

Params:k,tmax,fbin,k1

fb=fbin*(1-exp(-k1*t))

1=fbin+f

ln(x/(1-x))=k*t-k*tmax

fdeg=f*x

ftot=fdeg+fb

//constraints

0.0<x<1

Micromath model file for equation 3.19 (square root of time diffusion, degradation control)

IndVars: T

DepVars: ftot

Params:kr,fdin,k,tmax

fd=18.25*kr*(t^0.5)-33.5*((kr*(t^0.5))^2)+16.25*((kr*(t^0.5))^3)

flag=unit(1-fd)

fdtot=(fd*flag)+(1*(1-flag))

fdif=fdin*fdtot

1=fdin+f

ln(x/(1-x))=k*t-k*tmax

fdeg=f*x

ftot=fdeg+fdif

//constraints

0.0<x<1

Micromath model file for equation 3.20 (exponential burst, square root of time diffusion, degradation control)

IndVars: T

DepVars: ftot

Params:kr,fdin,k,tmax,fbin,k1

fd=18.25*kr*(t^0.5)-33.5*((kr*(t^0.5))^2)+16.25*((kr*(t^0.5))^3)

flag=unit(1-fd)

fdtot=(fd*flag)+(1*(1-flag))

fdif=fdin*fdtot

fb=fbin*(1-exp(-k1*t))

1=fdin+f+fbin

ln(x/(1-x))=k*t-k*tmax

fdeg=f*x

ftot=fdeg+fb+fdif

//constraints

0.0<x<1

Micromath model file for equation 9.1 (exponential burst, square root of time diffusion)

IndVars: T

DepVars: ftot,fb,fdif

Params:kr,fbin,k1

fd=18.25*kr*(t^0.5)-33.5*((kr*(t^0.5))^2)+16.25*((kr*(t^0.5))^3)

fdtot=IFGTZERO(fd-1,1,fd)

fdif=f*fdtot

fb=fbin*(1-exp(-k1*t))

ftot=fb+fdif

//constraints

1=f+fbin

0.0<f<1

Micromath model file for equation 9.2 (Surface Erosion Model)

IndVars:tlaps

DepVars:y

Params:k2,tlag

t=tlaps-tlag

x^0.3333=1-k2*(t)

xtot=1*(x^0.3333)

y=IFLEZERO(tlaps-tlag,1,xtot)

Micromath model file for equation 10.3 (change of the concentration of drug in solution released by exponential burst and polymer degradation)

IndVars: t

DepVars: F, f, d, x, fp, dp, fb, fbint, db

Params: k, xtot, kdeg, fbin, kb

F'=(k*x*(1-(x/xtot)))* (1-fbin)+(fbin*kb)*(exp(-kb*t))

f'=(k*x*(1-(x/xtot)))*(1-fbin)-kdeg*fp+(fbin*kb)*(exp(-kb*t))-kdeg*fb

d'=kdeg*fp+kdeg*fb

x'=(k*x*(1-(x/xtot)))*(1-fbin)

fp'=(k*x*(1-(x/xtot)))*(1-fbin)-kdeg*fp

dp'=kdeg*fp

fb'=(fbin*kb)*(exp(-kb*t))

fbint'=(fbin*kb)*(exp(-kb*t))-kdeg*fb

db'=kdeg*fb

//Initial conditions

t=0

F=0.002

f=0.002

d=0.000

x=0.001

fp=0.001

dp=0.000

fb=0.001

fbint=0.001

db=0.000

Micromath model file for equation 10.4 (change of concentration of drug in solution released by exponential burst and polymer degradation, accounting for drug degradation occurring in the microenvironment of the releasing matrix)

IndVars: t

DepVars: F, f, d, x, fp, dp, fb, fbint, db

Params: k, xtot, kdegb, kdegp, fbin, kb

F'=(k*x*(1-(x/xtot)))* (1-fbin)+(fbin*kb)*(exp(-kb*t))

f'=(k*x*(1-(x/xtot)))*(1-fbin)-kdegp*fp+(fbin*kb)*(exp(-kb*t))-kdegb*fb

d'=kdegp*fp+kdegb*fb

x'=(k*x*(1-(x/xtot)))*(1-fbin)

fp'=(k*x*(1-(x/xtot)))*(1-fbin)-kdegp*fp

dp'=kdegp*fp

fb'=(fbin*kb)*(exp(-kb*t))

fbint'=(fbin*kb)*(exp(-kb*t))-kdegb*fb

db'=kdegb*fb

//Initial conditions

t=0

F=0.002

f=0.002

d=0.000

x=0.001

fp=0.001

dp=0.000

fb=0.001

fbint=0.001

db=0.000

APPENDIX II

amoxycillin trihydrate sigma lot84ho450

Lens: 100mm
Background: Cyclohexane.

R

2615 pil 1m00294

High Size	Under %	High Size	Under %	High Size	Under %	High Size	Under %	High Size	Under %	High Size	Under %	Span 2.81
188	100	84.5	99.2	38.0	93.4	17.1	74.1	7.69	39.1	3.46	9.4	D[4,3] 14.58µm
175	100	78.6	98.9	35.4	92.4	15.9	71.4	7.15	35.7	3.21	7.8	
163	100	73.1	98.6	32.9	91.3	14.8	68.7	6.65	32.4	2.99	6.4	
151	100	68.0	98.3	30.6	90.0	13.7	65.8	6.18	29.2	2.78	5.3	D[3,2] 6.90µm
141	100	63.2	97.9	28.4	88.5	12.8	62.8	5.75	26.2	2.59	4.3	
131	99.9	58.8	97.4	26.4	86.9	11.9	59.7	5.35	23.3	2.40	3.5	
122	99.9	54.7	96.9	24.6	85.2	11.1	56.4	4.97	20.5	2.24	2.9	D[v,0.9] 30.64µm
113	99.8	50.8	96.4	22.9	83.3	10.3	53.1	4.62	17.9	2.08	2.4	
105	99.7	47.3	95.8	21.3	81.2	9.56	49.6	4.30	15.5	1.93	1.9	
97.8	99.6	44.0	95.1	19.8	79.0	8.89	46.1	4.00	13.2			D[v,0.1] 3.55µm
90.9	99.4	40.9	94.3	18.4	76.6	8.27	42.6	3.72	11.2			

Source = :Sample	Beam length = 14.3 mm	Model indp	D[v,0.5] 9.63µm
	Log. Diff. = 2.450		
Focal length = 100 mm	Obscuration = 0.1669	Volume Conc. = 0.0029%	
Presentation = pil	Volume distribution	Sp.S.A 0.8693 m^2/cc.	

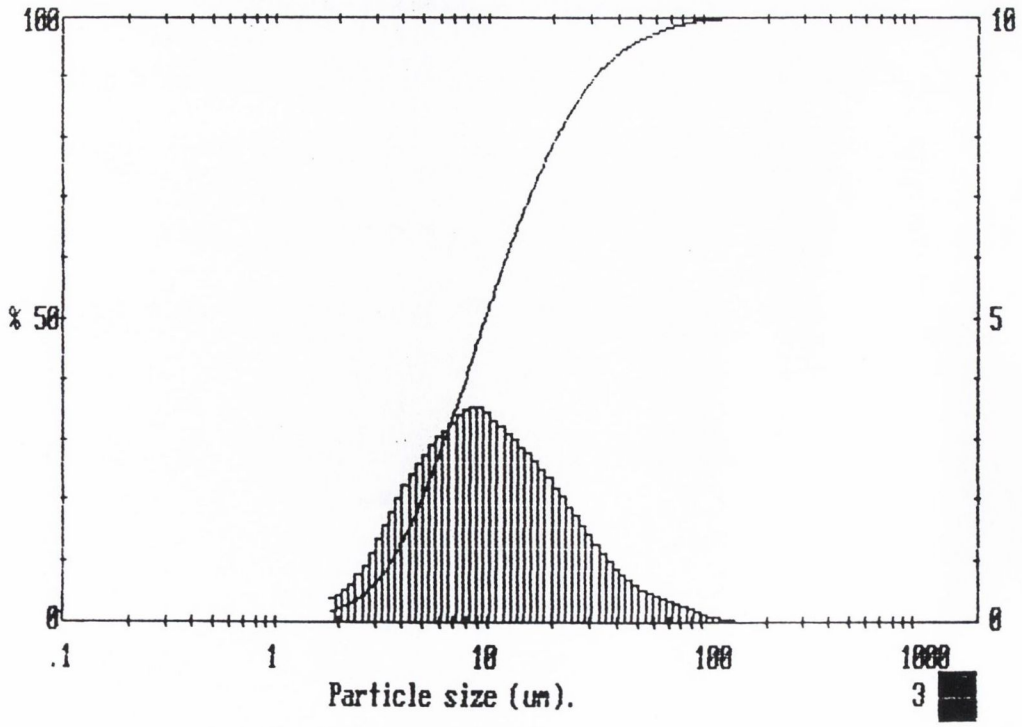

Figure 1. Particle size distribution obtained for Amoxycillin trihydrate by Laser Diffraction.

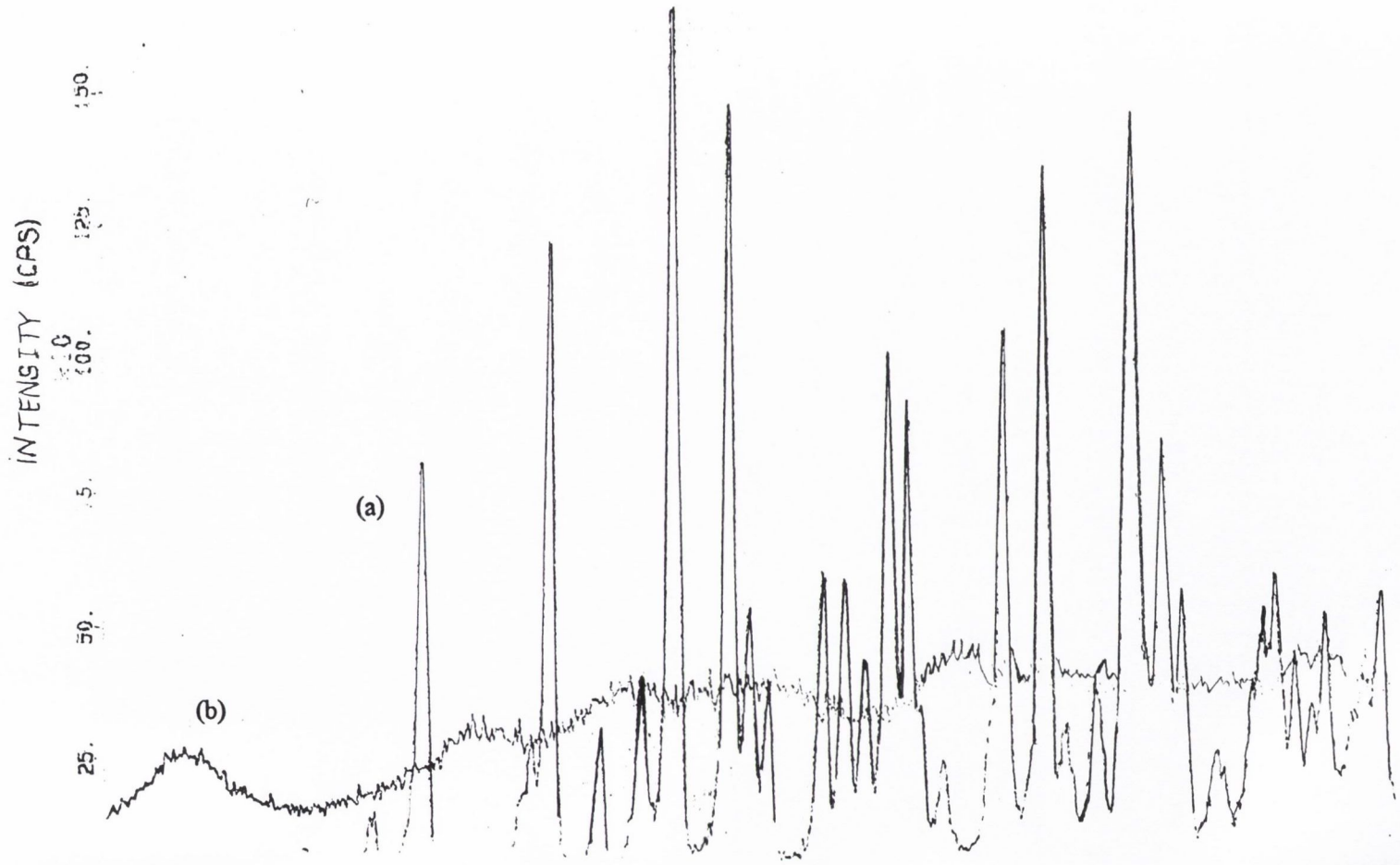

Figure 2. XRD of Amoxycillin trihydrate (a) before and (b) after treatment with Methanol.

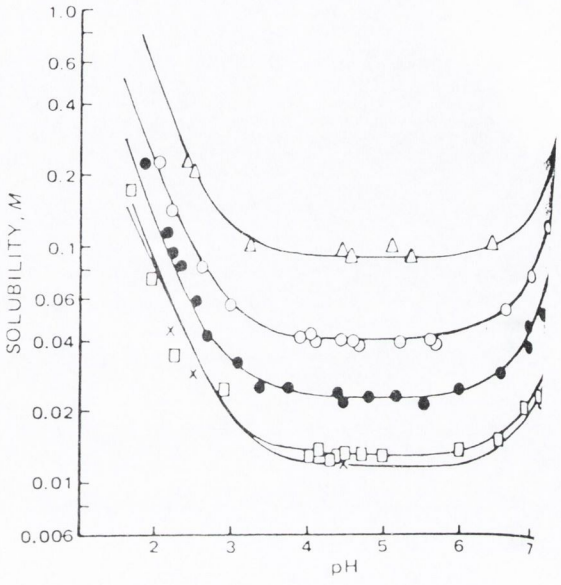

Figure 3. Solubility data in aqueous media for Amoxycillin trihydrate (□) and other alpha-amino penicillins, from Tsuji et al. (1978).

DSC EVALUATIONS

Glass transition temperatures were calculated as the STAR^e midpoint. This point is defined as the intersection between the bisector angle and the measuring curve, where the bisector angle goes through the intersection point of the baselines before and after transition (Mettler Toledo STAR^e Software User Manual, 1998). A descriptive scheme is shown in figure 4.

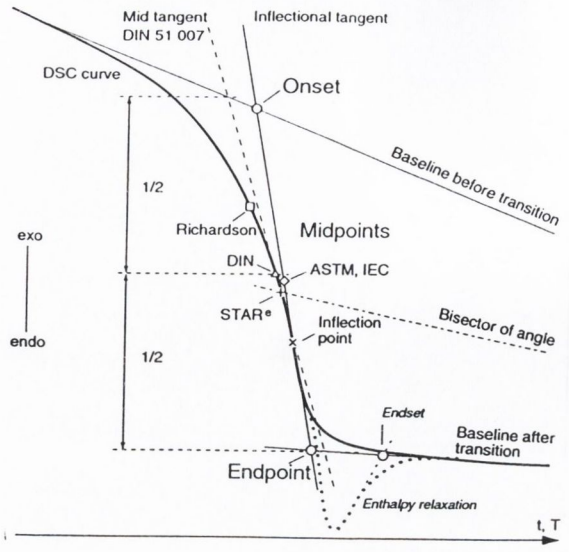

Figure 4. Determination of T_g by the STAR^e midpoint method.

^exo

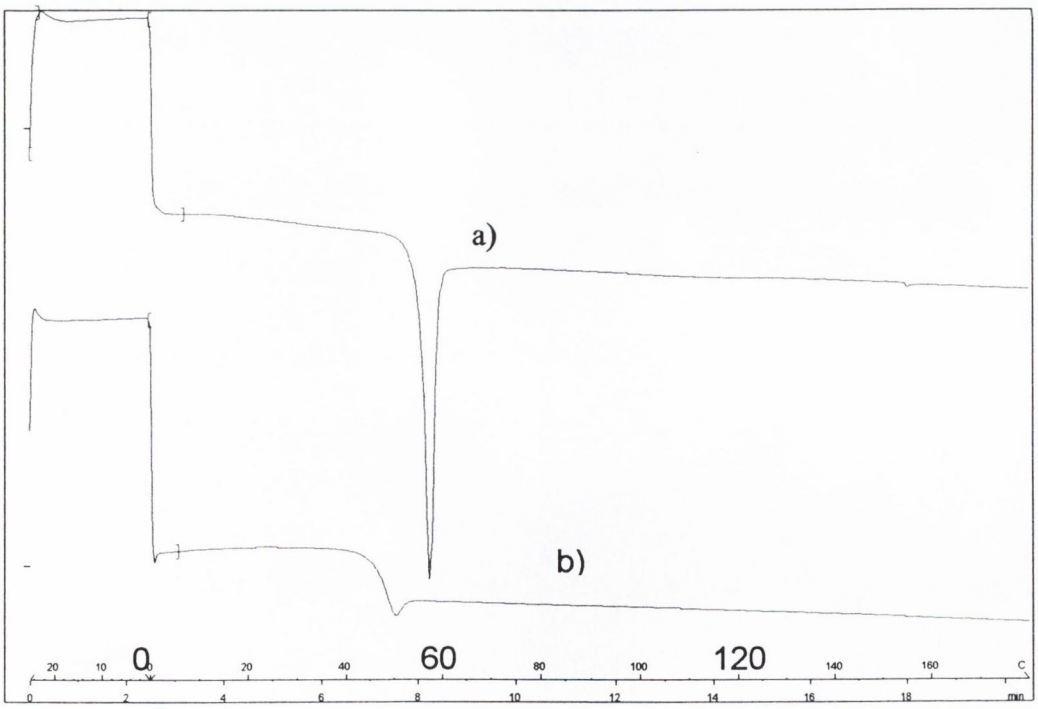

Figure 5. DSC of first (a) and second (b) scan of RG 504 powder.

SEM OF POLYMER POWDERS

(a)

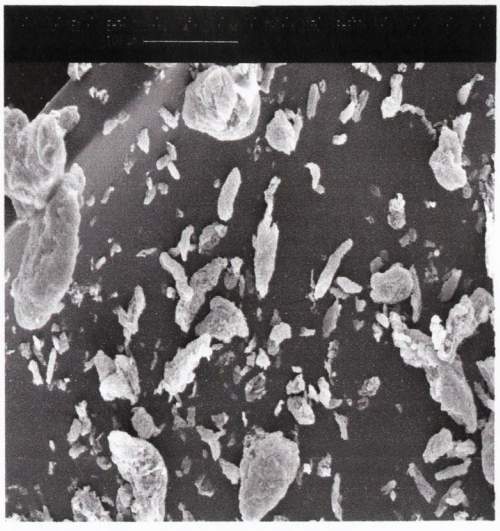

(b)

Figure 6. SEM images of RG 503 powder showing (a) large aggregations and (b) particles smaller than 50 μm, magnified 235 times.

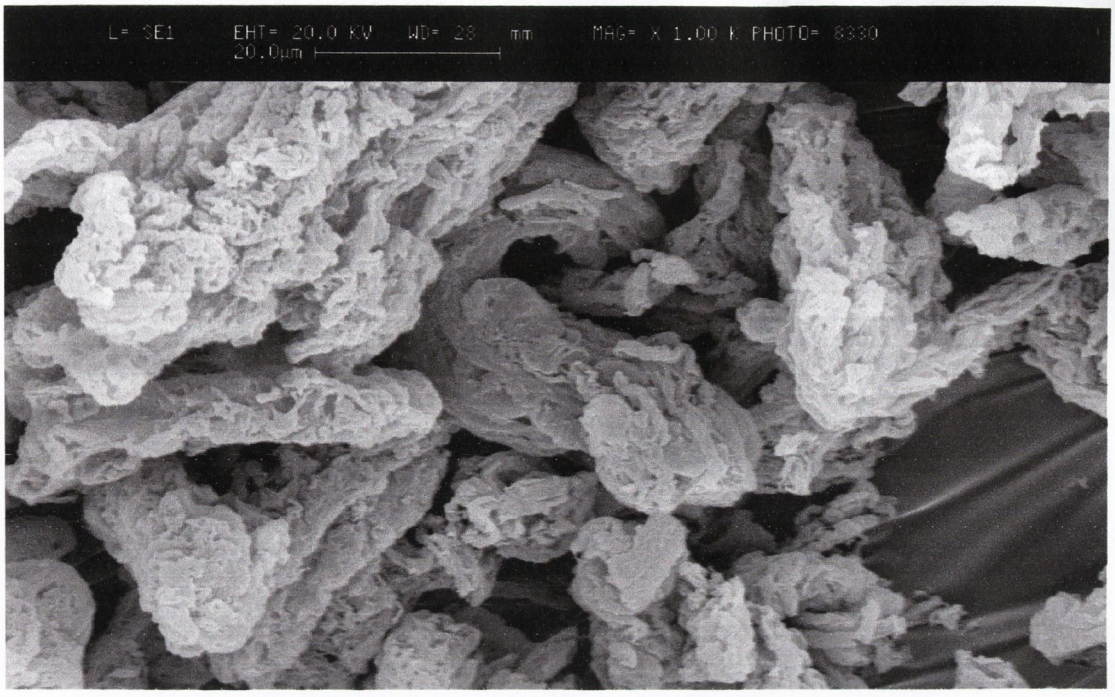

Figure 7. SEM of RG 504 powder at a magnification of X 1K.

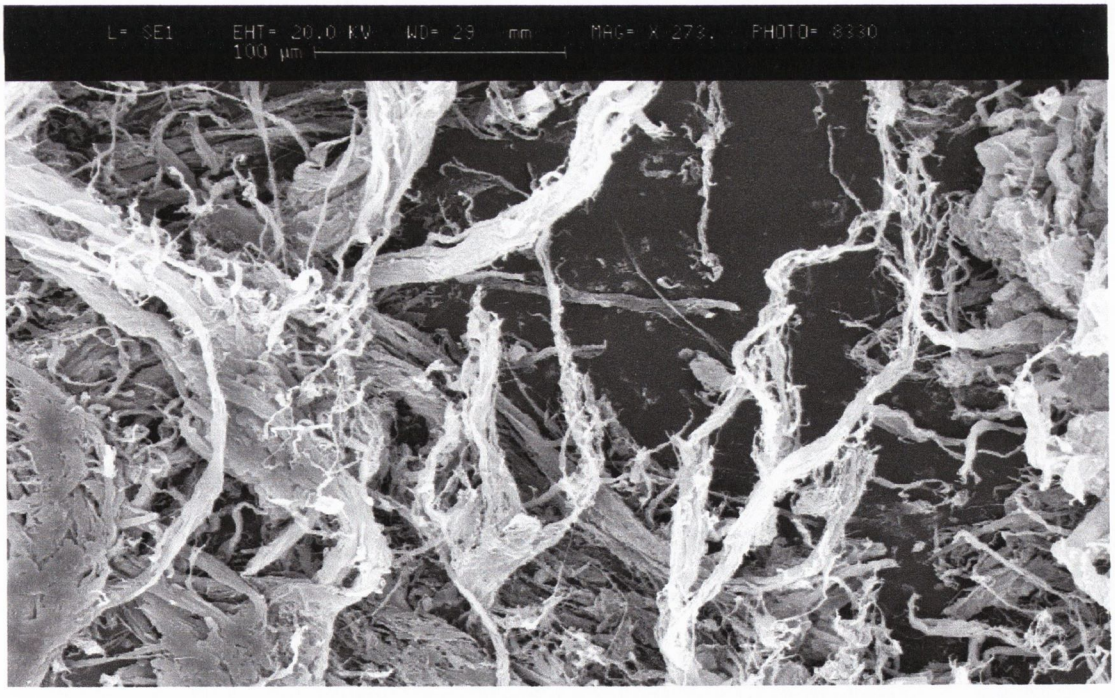

Figure 8. SEM image of RG 755 powder at a magnification of X 235.

APPENDIX III (Statistics)

Table 1. Estimated parameters and statistics obtained for drug release from RG 503 SE discs containing 20% AMOX-H fitted to equation 3.14. Two similar experiments are compared.

k_b (h^{-1})	■0.28 ± 32	0.38 ± 0.086
Fb_∞	0.086 ± 0.017	0.103 ± 0.006
k (h^{-1})	0.0144 ± 0.0014	0.0219 ± 0.0010
t_{max} (h)	501 ± 7	515 ± 4
r^2	0.9977	0.9994
m.s.c.	5.20	6.59

■ this experiment contained less number of points in the first phase of the release profile than the experiment it is being compared with. The large uncertainty observed in the first k_b is related to this.

Table 2. Summary of the XRD intensity data used in the Student t-test performed for RG 755 MM and SE discs (section 8.3.1). The test showed that there were no significant differences to indicate a phase transformation of the drug during the filmcasting procedure.

	SE discs	MM discs	Differences (d)
XRD Intensity at 20% loading	486	795	309
XRD Intensity at 30% loading	572	944	372
Mean	529	869.5	304.5
s	60.8	105.4	44.54

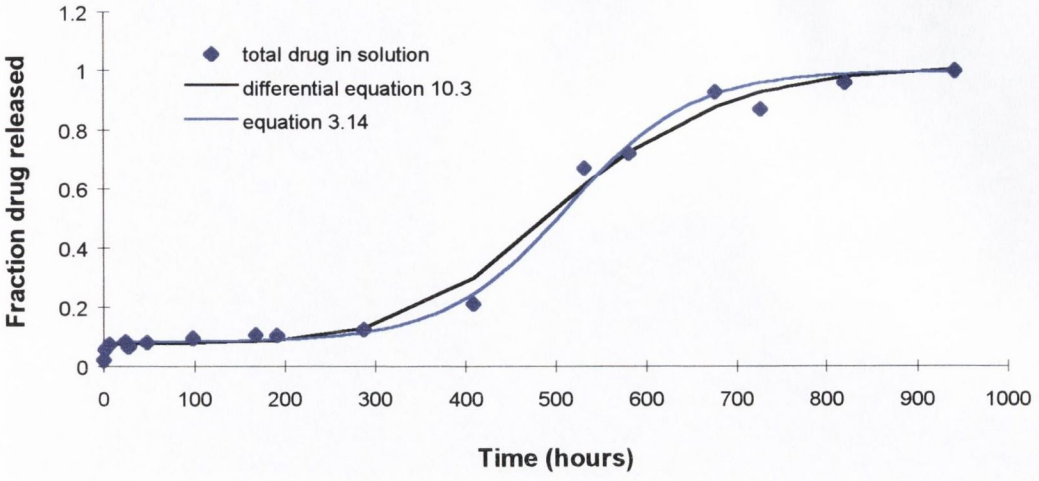

Figure 1. Plot obtained for the total drug release profiles of RG 503 20% drug loaded SE discs fitted to equation 3.14 versus the differential equation 10.3.

Table 3. Comparison of the estimated parameters obtained with (I) equations 3.14 and (II) 10.3 for the total drug release profiles of RG 503 20% drug loaded SE discs.

Drug loading (%)	(I) Equation 3.14	(II) Equation 10.3
k_b (h^{-1})	0.49 ± 0.51	0.54 ± 0.51
Fb_∞	0.081 ± 0.015	0.076 ± 0.012
k (h^{-1})	0.0146 ± 0.0014	0.0146 ± 0.00025
t_{max} (h)	514 ± 8	n.a.
x_{tot}	n.a.	0.89 ± 0.022
r^2	0.9920	0.9940
MSC	4.42	4.68

APPENDIX IV (STABILITY ASPECTS OF THE FORMULATIONS)

EXPERIMENT 1: pH studies

Following the observations discussed in section 9.3.1, a series of tests were undertaken (section 5.5.7) in order to reproduce the pH and colour changes observed during drug release studies. The results obtained are tabulated below:

Experiment 1. pH values obtained for saturated solutions of AMOX-H in phosphate buffer pH 5.9 (A), saturated solutions of AMOX-H in water (B), saturated solutions of AMOX-H in phosphate buffer pH 5.9 containing D,L-lactic acid (C) and solutions of D,L-lactic acid in phosphate buffer pH 5.9 (D) as a function of time, maintained at 37°C and 95 cpm.

Time (h)	sample A	sample B	sample C	sample D
3	5.6	4.1	2.9	2.8
26	5.5	4.0	n.s.	n.s.
150	5.1 yellow	3.6 lime-green	3.0 dark yellow*	2.8 clear
200	4.9 yellow-green	3.5 dark-green	3.0 yellow brownish*	2.8 clear
480	4.3 orange-green*	3.7 dark-green*	3.1 orange**	n.s. clear

*denotes sulphurous smell and evolution of gas, samples "C" presenting the strongest smell (**). When "no sample was taken" this is indicated by n.s.

These experiments indicated that addition of D,L-lactic acid to solutions of AMOX considerably decreased the pH of the medium. The colour changes observed (yellows and greens) are associated with the presence of AMOX in the solutions.

EXPERIMENT 2: Swelling Studies

PLGA discs were placed in dichloromethane (DCM) with the purpose of examining their swelling potential. The samples used were 20% drug loaded and drug-free RG 503 SE systems having undergone 290 hours of drug release studies. The drug loaded disc is still intact after 30 minutes while the drug-free disc has completely dissolved in the organic solvent.

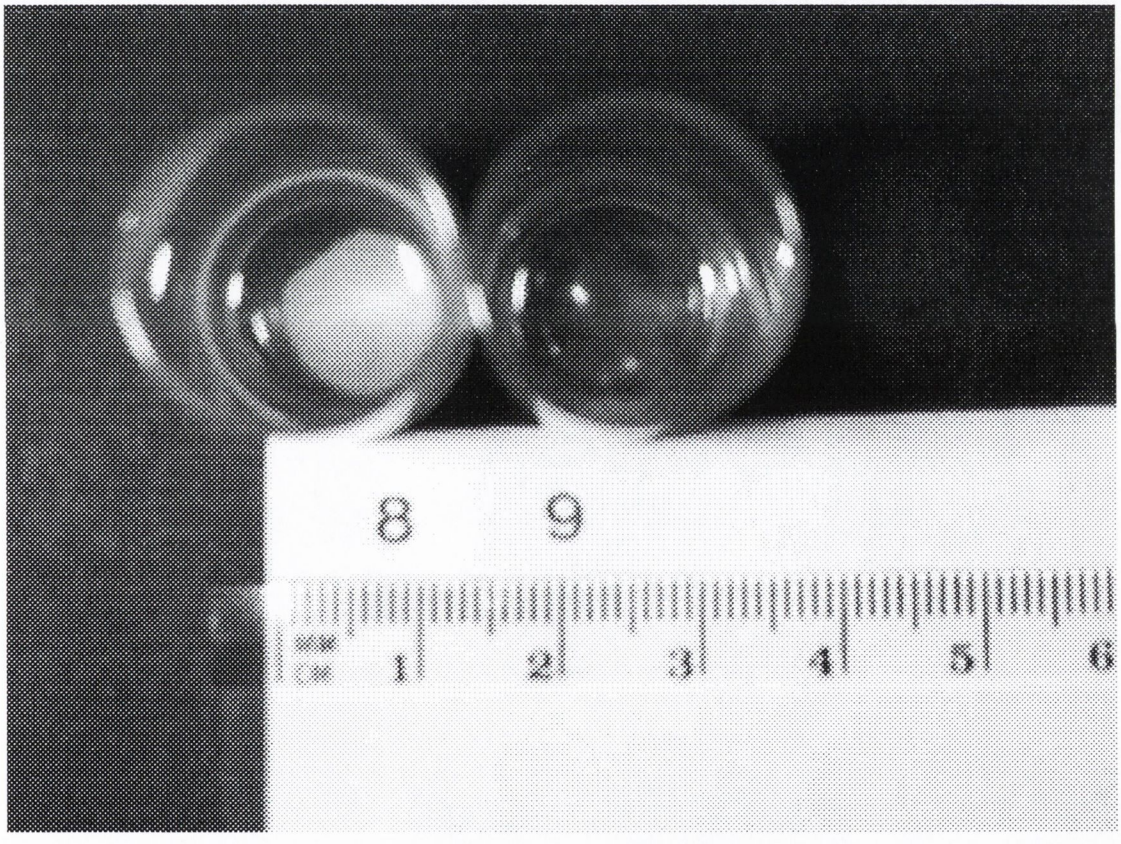

Photograph of 20% Amox-tri (number 8) and drug-free (number 9) RG 503 SE discs undergone 290 hours of drug release experiments taken 30 minutes after the samples were placed in glass vials containing 2 ml of DCM. Scale in mm and cm.

APPENDIX V (HPLC chromatograms)

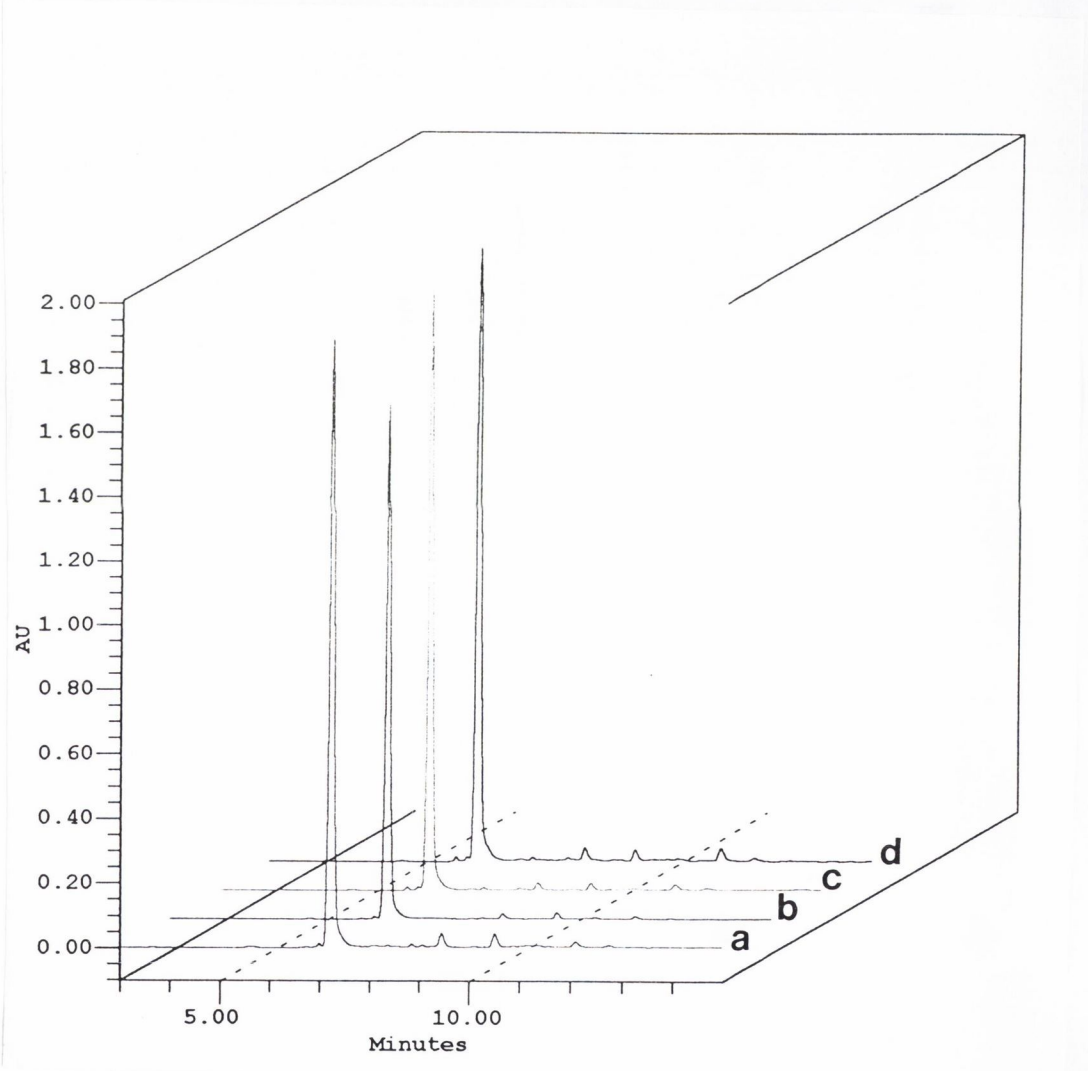

Figure 1. HPLC traces obtained for drug extracted from 20% drug loaded RG 503 (a) , RG 504 (b), RG 755 (c), R 203 (d) SE discs having undergone 290 hours of release studies.

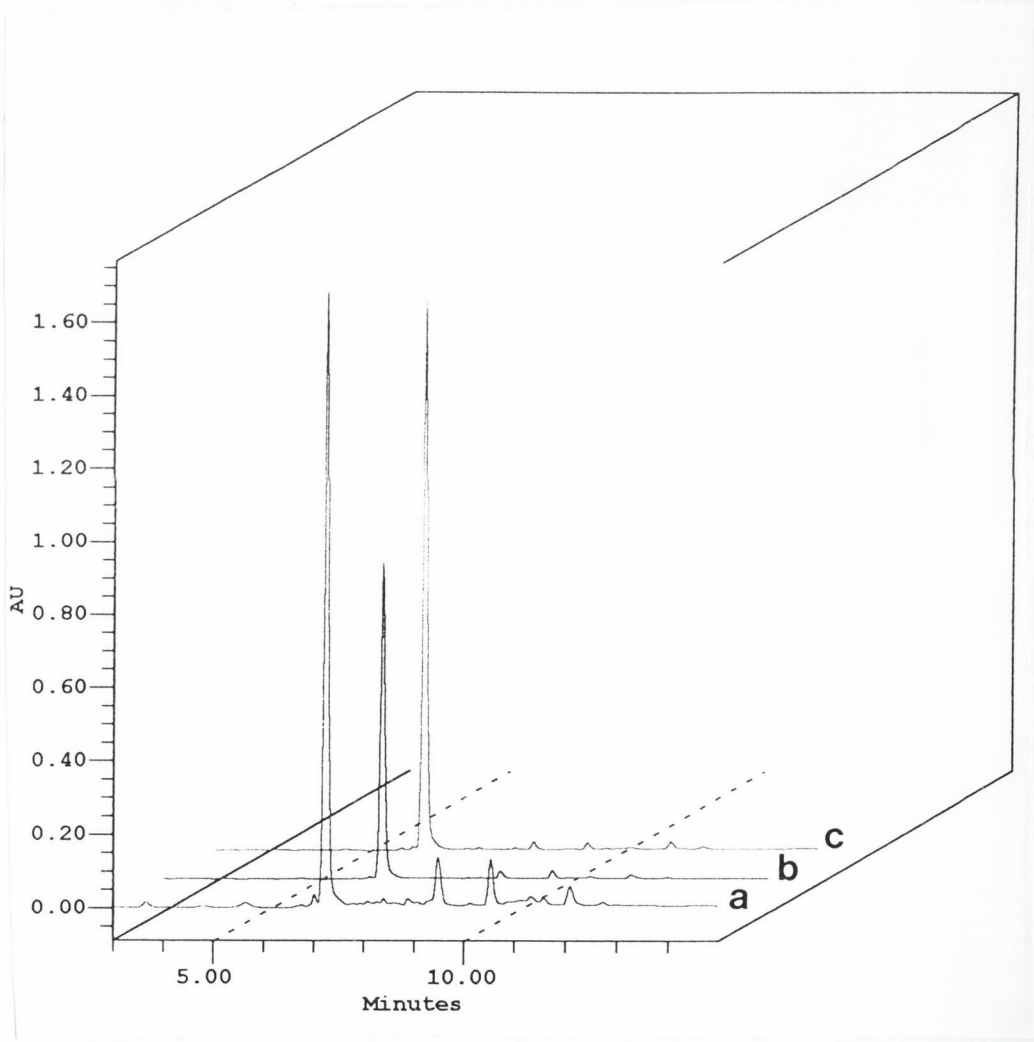

Figure 2. HPLC traces obtained for drug extracted from RG 503 (a), RG 504 (b), RG 755 (c) 20% drug loaded SE discs having undergone 410 hours of dissolution studies.

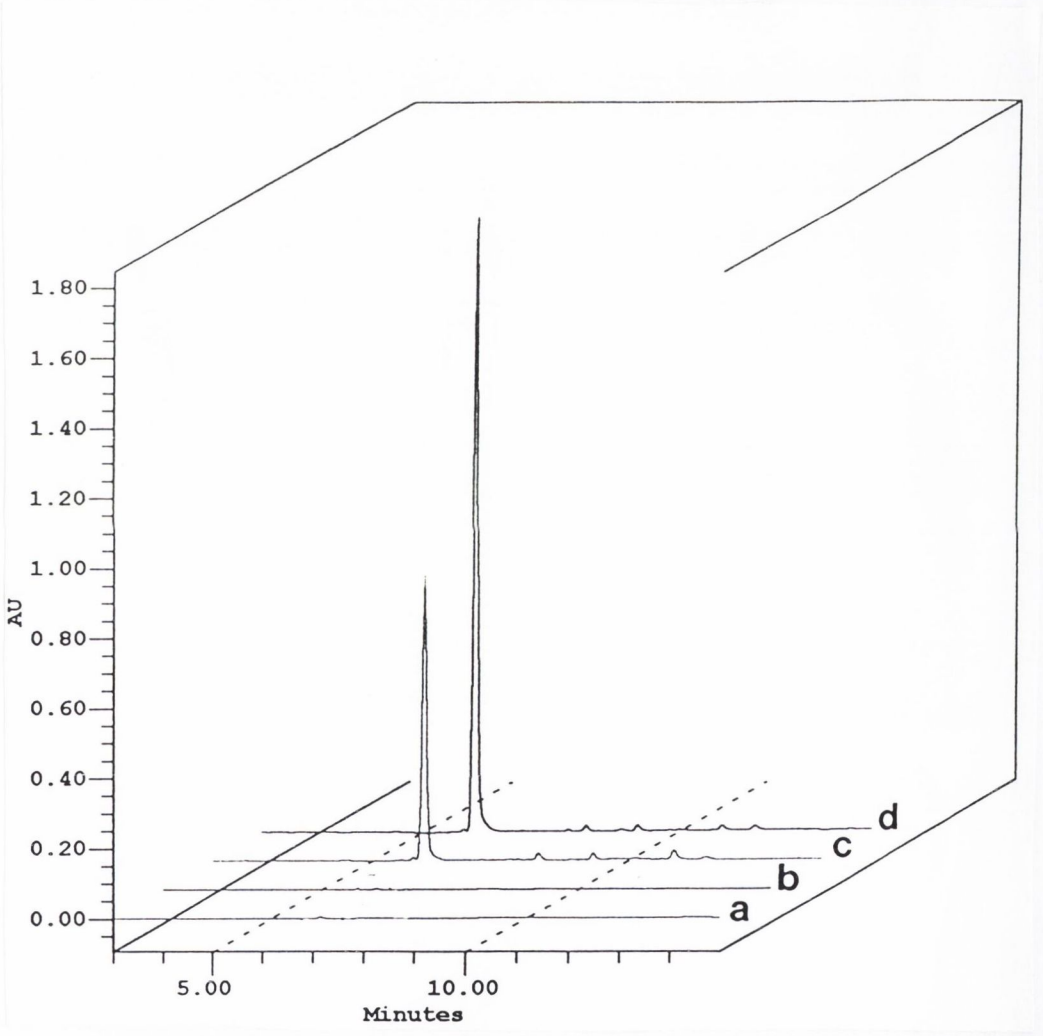

Figure 3. HPLC traces obtained for drug extracted from RG 503 (a), RG 504 (b), RG 755 (c) and R 203 (d) 20% drug loaded SE discs having undergone 1030 hours of dissolution studies.